POLITECNICO DI TORINO

Dipartimento di INGEGNERIA STRUTTURALE, EDILE E GEOTECNICA (DISEG)

Master's degree Thesis

BIM and Geotechnical Analysis for shallow Tunnel Settlement evaluation

Case Study: 2nd Line of Metropolitan in Turin

Supervisor

Prof.ssa Maria Migliazza

Co-Supervisor

Prof. Renato Cosentini

Candidate

Akbarkhon Maksudov

31 march 2026

Благодарности

В рамках профессионально - научного содержания данной работы, в первую очередь хочу поблагодарить своих научных руководителей: Мария Рита Мильяцца и Ренато Мария Косентини, я считаю это большой удачей работать со специалистами, которые поддерживают твои идеи, воспринимают их всерьёз и содействуют на пути к их осуществлению. К счастью, именно таким определением я могу описать прошедшие 7 месяцев работы с моими руководителями. Также данный проект был бы невозможен без практических навыков, полученных мной во время работы в компаниях, поэтому я бы хотел поблагодарить руководителей и коллег, каждый раз это больше чем коллектив, это команда, где навыки каждого совершенствуются в сотрудничестве, речь идёт о: ARCHIQUAD Group, INFRATRASPORTI.TO S.R.L, Nemesis & Icon Ingegneria S.R.L.

Отдельную и особенную благодарность я хочу выразить своей маме Г.М., хочу сказать, что я ценю все усилия, что она прикладывает для моего становления, мне очень повезло расти в атмосфере безусловной любви и искренней заботы и принципиального благородства. Все мои труды и достижения в жизни я буду всегда посвящать ей, как главному человеку в моей жизни. Спасибо моему брату Т. М., который был здесь со мной во время работы над данным проектом, может он не всегда мог сказать, но я всегда чувствовал его неуклонную веру в меня. В целом я очень благодарен всем родным за поддержку, любовь и веру, находясь сейчас не рядом с ними, особенно понимается ценность семейных связей.

И последнюю, но не менее важную благодарность я бы хотел выразить своим друзьям, людям, которые стали мне практически семьёй здесь, я мог бы долго перечислять всех, но я уверен, что, читая это, каждый из их понимает, что речь идёт о нём/ней. Кого-то я знаю дольше, кого-то меньше, но я точно могу сказать, что горжусь людьми, которыми окружён, что действительно вижу в них хороших людей, полных благородия, доброты и трудолюбия. Спасибо вам за помощь, поддержку и веру.

Acknowledgements

In light of the academic and professional nature of this work, I would first and foremost like to thank my academic supervisors: Maria Rita Migliazza and Renato Maria Cosentini. I consider it a great privilege to work with experts who support your ideas, take them seriously and help you bring them to fruition. Fortunately, this is precisely how I can describe the past seven months of working with my supervisors. Furthermore, this project would not have been possible without the practical skills I acquired whilst working in companies, so I would like to thank my managers and colleagues; more than just a group of people, this is a team where everyone's skills are honed through collaboration. I am referring to: ARCHIQUAD Group, INFRATRASPORTI. TO S.R.L, Nemesis & Icon Ingegneria S.R.L.

I would like to express my special and heartfelt thanks to my mother, G.M. I want to say that I appreciate all the effort she has made for my development; I have been very fortunate to grow up in an atmosphere of unconditional love, sincere care and principled nobility. I will always dedicate all my work and achievements in life to her, as the most important person in my life. Thank you to my brother T. M., who was here with me whilst I was working on this project; he may not always have said so, but I always felt his unwavering faith in me. Overall, I am very grateful to all my family for their support, love and faith; now that I am not with them, I particularly appreciate the value of family ties.

Last but not least, I would like to express my gratitude to my friends - the people who have practically become family to me here. I could go on and on listing everyone, but I'm sure that as they read this, each of them will know I'm talking about them. I've known some of you for longer, others for less time, but I can say with certainty that I'm proud of the people around me; I truly see in them good people, full of nobility, kindness and hard work. Thank you for your help, support and faith.

INDEX

Chapter I: Introduction

Building Information Modeling (BIM) has emerged as a comprehensive digital methodology for the creation, management, and exchange of information throughout the lifecycle of built assets. By integrating three-dimensional geometry with semantic information related to materials, structural properties, and construction processes, BIM enables enhanced data consistency, interoperability, and collaboration among stakeholders. As the purpose of the thesis, BIM has been explored not only as a design and construction tool, but also as a platform for advanced engineering analyses and performance-based assessments.

In the scope of given study, BIM technologies in combination with parametric modelling technologies are used for analysis of settlements induced by shallow tunnels. In underground construction, particularly in urban tunneling projects, excavation-induced ground movements can significantly affect existing buildings. These movements may result in structural damage, serviceability issues, or long-term degradation of building performance. Reliable assessment of building damage due to tunnel excavation is therefore a critical component of risk management and urban infrastructure development. There are existing methods for damage analysis such as empirically – theoretical methods and/or numerical models (explained in Introduction; 1.3 Work objective; Page 7), but each of them has disadvantages by sense of results precision or time of execution. In contrast, this study proposes an alternative method for analyzing and assessing the level of damage to buildings caused by tunnel excavations, using BIM as the central analytical and data management framework. The method exploits BIM's capacity to integrate geometrical data within the regression models which describe the shape of settlement basin with decent precision and automatically links soil deformations to building damage assessment. By linking damage indicators and assessment parameters directly to BIM elements, the proposed approach facilitates automated data flow, improved traceability, and consistent evaluation across different damage scenarios.

Furthermore, the BIM-based methodology allows for intuitive visualization of damage distribution within three-dimensional building models, supporting clearer interpretation of results and more effective communication between geotechnical engineers, structural engineers, and project stakeholders. The proposed framework aims to enhance the accuracy, transparency, and practicality of building damage assessment in tunneling projects, thereby contributing to improved risk evaluation and decision-making in urban underground construction.

1.1. Problem statement

Geotechnical projects which are concerning direct soil manipulation usually have spreading effect on the soil mass around it described by elastic-plastic behavior and phenomenon of volume loss. This work is directed on analysis of settlements induces by shallow tunnel excavation in urban areas, since in uninhabited areas some surface deformations can be ignored. However in the urban areas, it is crucially important to analyze deformations and damage caused by future geotechnical projects. Everything that in the common form can be called urban environment (including infrastructures; buildings and communications) are directly influenced by the dynamics of the soil they are located on (or inside in some cases), physical movement of soil is taking the structure on the same direction, with a less amplitude, as the weight of the structure is always directed on the vertical (gravitational vector), but during the analysis of structure, its movement is assumed to be the same as movement of the soil, because the amplitude of difference of displacement between soil and structure has big amount of variable factors, such as weight of the structure, friction between building material and soil, variable loads in the moment of soil manipulation, mentioned factors are also variating from one structure to another one, and also depends on the type of soil (which is actually is taken into account), so with an aim to reduce the calculation time and be on the safety side, physical movements of the structures are assumed to be the same as soil dynamical displacements.

The occurrence of structural damage due to ground deformation cannot be explained solely by comparing the elastic limits of soil and construction materials. While soils, particularly cohesive and saturated ones, are capable of undergoing relatively large deformations without reaching a failure state, the response of structures is governed by their limited ability to accommodate imposed displacements.

Construction materials such as concrete and masonry are generally characterized by brittle or quasi-brittle behavior, with low tensile strength and limited deformation capacity prior to cracking. However, the primary cause of structural damage is not the absolute magnitude of soil strain, but the development of differential settlements, which induce distortions within the structure.

When the ground deforms non-uniformly, the structure is forced to adapt to these imposed displacements. Due to its stiffness and continuity, this adaptation results in the generation of internal stresses, particularly tensile stresses. Since materials like masonry and concrete perform poorly in tension, even relatively small differential movements can lead to cracking and, in severe cases, loss of serviceability or structural integrity.

Therefore, structural damage is more accurately attributed to the incompatibility between ground deformations and the deformation capacity of the structure, rather than to a simple difference in elastic or plastic behavior between soil and construction materials.

1.2. Case study introduction

Project of second line of subway in Turin was proposed in the late 2010's, facing significant number of changes on the way from Preliminary phase to the Phase of detailed design, caused by administrative and engineering decisions. The current plan of subway alignment is possible to see on Figure 1.1

The line starts in the district of Borgata Vittoria, which is located on North – West part of Turin city, afterwards, alignment is moving towards East in the crossing the district of Barrier di Milano, going South it is crossing Aurora district going to Centro. Intersection with the first subway line will be done in the in the station Porta Nuova, which is one of the most important stations of Metro Linea 1 and also one of 2 the most important passenger transferring Train Stations. The end of Metro Linea 2 is taking place near university – Politecnico di Torino.

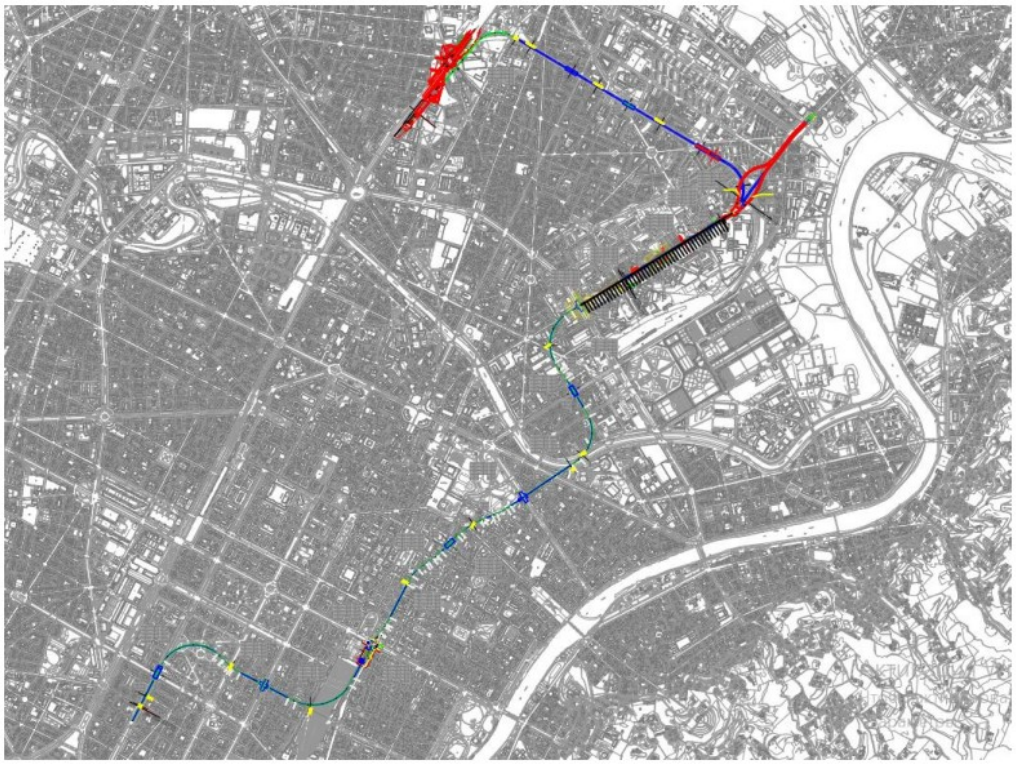

Figure 1.1. Horizontal alignment of Metro Linea 2 plotted on the map of city Turin. [INFRATRASPORTI.TO S.R.L 01_MTL2T1A2DPRCG00R001-0-1]

Stations, as far as they require total excavation from the level of ground till intersection with the tunnel (also about 2 meters of concrete foundation), they are located rather on the squares rather on the intersections of big roads, such locations are explained by reducing as much as possible the influence of civil works on the existing urban environment of the city.

Biggest challenge in case of urban environment is the historical center of city Turin – Region Centro. Buildings in the area are characterized by high vulnerability to civil works including vibrations or/and soil deformations, it is explained in the means of high buildings damage with relatively negligible levels of environment condition changing, buildings are characterized with significant age, and material properties are worse compared to initial conditions. Therefore, a lot of numerical models are created to estimate the influence of tunnel excavations and open excavations carefully

and precisely on historical buildings.

When it comes to the methodology of excavations, by the current plan, from Borgata Vittoria to Cimarosa station, excavation of tunnel sand stations is going to be done conventionally by top down excavation, afterwords, for the tunnel until station Politecnico Earth pressure balance TBM will be used, while the stations will be excavated by top down cut and cover methodology.

1.3. Work objective

From the explanation of case study project and problem statemen, the objective comes to the solid form of analyzing effect of tunnel excavation on urban environment in the city of Turin. Analysis is included in the project state of risk evaluations, several methods are used to analyze the distribution of settlements during the geotechnical works:

- Theoretical – empirical method using simplified models for analyzing the settlements induces by tunnel excavation. The method has a big advantage in the case for time of execution; the calculation indicates maximum settlements (which is caused by soil vertical displacement) and horizontal displacements for the long section of tunnel excavation. Inputs for this method are usually represented by the geometrical data of the tunnel (or any other construction interacting with the soil such as retaining walls or slab/footing/pile foundations) and assumptions for the dynamics and characteristics of soil. Data of the soil is not directly applied in the calculations, but assumptions for calculations are made according to the basic soil properties, such as soil type based on the particles size (clay, silt, sand, gravel); another basic input is the soil loss percentage, which is theoretically described as loss of the air voids between the particles of soil, the per cent is usually assumed as 1 or 0,5; but more precise per cent (only applied for similar soil types) can be assumed according to real case previous experiences (through back calculations knowing already the soil deformations done by civil works).
  Disadvantage of the given method is that specific soil properties which directly affect the settlement are not taken into the account, the results are dependent mostly on engineering assumptions. By the end they are usually significantly exaggerated, which keeps the urban environment on safety side, but as the negative consequence, financial and labor efforts are put in the areas of potential damage, which in the end does not happen because real values of soil dynamics come out significantly smaller than the ones given by manual calculations.

- Numerical modelling constitutes one of the principal approaches for analysing soil–structure interaction problems, enabling the estimation of stress distribution and deformation within both the ground and the structure. These methods are typically based on discretization techniques such as the Finite Element Method (FEM), the Finite Difference Method (FDM), and, less frequently, the Boundary Element Method (BEM). In all cases, the continuous medium is divided into smaller elements or zones, whose mechanical behaviour is defined by appropriate material models, while their interaction is governed by equilibrium and compatibility conditions.
  Depending on the level of interaction considered between soil and structure, numerical analyses can be broadly classified into uncoupled and coupled approaches. In uncoupled analyses, soil and structural responses are evaluated separately, and the interaction is introduced in a simplified manner, typically through imposed boundary conditions or

prescribed displacements. This approach is computationally efficient but may neglect important interaction effects. In contrast, coupled analyses simulate soil and structure within a unified model, allowing for direct transfer of stresses and deformations between them. Although more accurate, coupled methods require greater computational effort and more detailed input data.

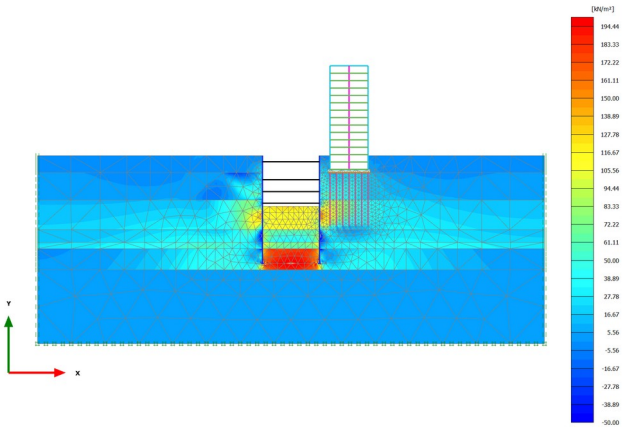

Figure 1.2. FEM analysis example in 2D [Plaxis 2D]

Numerical models can also be developed in either two-dimensional (2D) or three-dimensional (3D) space. Two-dimensional models are commonly used to represent plane strain or plane stress conditions, providing a simplified representation of the problem through a representative cross-section. Their main advantage lies in reduced modelling time and computational cost, making them suitable for preliminary analyses. However, they inherently neglect variations along the third dimension, which may lead to inaccuracies in cases involving complex geometries, non-uniform loading, or significant longitudinal effects.
Three-dimensional models, on the other hand, allow for a more realistic representation of soil and structural behavior by accounting for spatial variability in all directions. This enables a more accurate assessment of deformation patterns and stress redistribution, particularly in problems involving irregular geometries or localized effects. Nevertheless, 3D analyses are significantly more demanding in terms of modelling effort, computational resources, and data requirements.

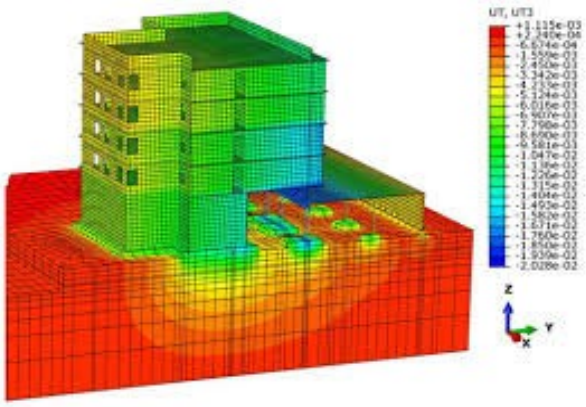

Figure 1.3. FEM analysis example in 3D [Plaxis 3D]

It is understandable through method descriptions that the analysis is not taking the compromise between reliability of results (output deformations and stresses), time of analysis execution and size of area of analysis.

The work described in this thesis is aimed at demonstrating alternative method to analyze the soil deformation and also apply it to the existing urban environment.

The method is established the way to analyze 3 - dimensional deformation of the soil deformation, so it takes the best feature of 3D FEM analysis to demonstrate soil dynamics both in longitudinal and transversal directions of the structure, however, as in vantage in compare to 3D FEM model, the time of execution will be reduced only till process of entering coordinates of the structures and terrains, and the mainly, as it is important for engineers, results of analysis in sense of displacements are as similar as possible to the ones given by 3D FEM analysis.

The model is based on BIM technologies and methods, relying on parametric modelling while the parameters themselves are derived through the data flow, which reduces the risks of human factor mistakes. As the aim of the work, the delivery of dynamic models of tunnel, terrain and buildings, is established. The definition of dynamic model in the scope of given project is given in the following passage.

This thesis encompasses the development of a Building Information Modeling (BIM) methodology and its practical application to a specific tunneling case study. The research is structured as follows: Chapter 2 establishes the theoretical framework for estimating settlements induced by shallow tunneling, incorporating foundational empirical theories such as Peck (1969) and O'Reilly & New (1982). This chapter also details the Finite Element Method (FEM) analyses that serve as the basis for the regression models developed to align subsequent analytical results with numerical simulations.

In Chapter 3, the core principles of BIM theory and existing tunneling workflows are evaluated. Building upon this theoretical base, Chapter 4 describes the development of a parametric tunnel model and the generation of dynamic terrain within the Autodesk Dynamo environment. Chapter 5 provides a comprehensive description of the case study, including specific geotechnical characteristics and geometrical data.

The integration of these elements occurs in Chapter 6, where the dynamic model is applied using case study data and FEM-based regression models. This chapter further explores methodologies for mapping settlement distribution to assess the degree of potential structural damage to adjacent buildings. Finally, the results are compared against data provided by INFRATRANSPORTI.TO S.R.L. to validate the accuracy and reliability of the proposed BIM-based method

Chapter II: Settlement analytical theory and FEM project background

The starting chapter will be dedicated to the initial ideas and theoretical approaches that lay on the core of development of the method that will be described.

The first part is explaining the reasons and classification of buildings damages, after - theoretical formulas that were developed to describe settlement values, depending on assumptions, that take into consideration the soil characteristics, and exact geometrical data of soil interaction structures. Those theories are usually used for the first method of analysis (introduction Page 6.), simplified forms of settlement basins described by mathematical functions taking distance as the variable value.

As part of method modernization, chapter describes the analysis of FEM (Finite elements model), the results of which were used to derive complex regression equations describing the settlement basin variation in a more precise way compared to theoretical formulas based on soil assumptions

2.1. Building's damage caused by earthworks: definition and classification.

First two sub passages are describing the phenomenon of ground deformation, the sources of it during the tunnel excavation, physical background and concept of volume loss. Starting from the third sub passage, the link between soil deformations and buildings is described. Finelly, passage arrives to the definition of building damages and their classification. [J. N. Franzius; 2003]

2.1.1 Soil movement in the excavation phase

The primary cause of ground movements induced by tunnelling is the disturbance of the initial in situ stress state within the soil mass. Prior to excavation, the soil is in a condition of equilibrium, where stresses generated by the self-weight of the overlying layers and any external loads are balanced.

Tunnel excavation involves the removal of material and, consequently, the elimination of the stresses previously carried by that volume of soil. This results in a reduction of radial stress at the excavation boundary and a loss of confinement in the surrounding ground. In response, the stress field is redistributed around the cavity, leading to the development of new equilibrium conditions.

A key feature of this process is the formation of stress concentration zones around the tunnel perimeter, commonly referred to as the arching effect. Through this mechanism, part of the load previously carried by the excavated soil is transferred to the surrounding ground. However, this redistribution is inevitably accompanied by deformation, as the soil mass adjusts to the new stress conditions

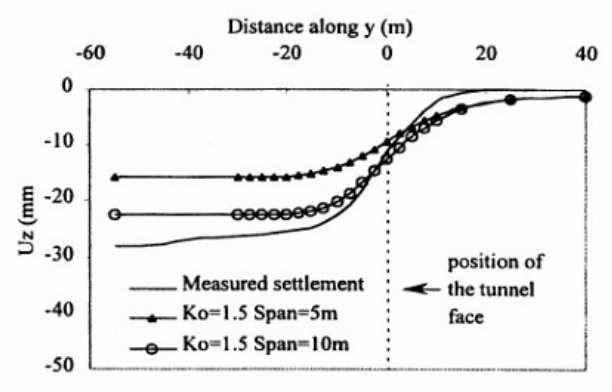

Figure 2.1. Longitudinal settlement profiles obtained for different excavation lengths Lexc (after Tang et al., 2000).

The reduction in confinement causes the ground to deform towards the excavation, generating convergent displacements around the tunnel. These deformations propagate through the soil mass and may extend to the ground surface, where they manifest as settlement. The magnitude and distribution of these movements depend on several factors, including soil properties, depth of the tunnel, and excavation method.

In mechanized tunnelling, such as with Tunnel Boring Machines (TBMs), support measures including face pressure, shield confinement, and segmental lining installation are used to control stress changes and limit ground deformation. Nevertheless, these measures do not entirely prevent stress redistribution, and some degree of ground movement is unavoidable.

2.1.2 Ground loss definition. Main reasons

During tunnel excavation, ground loss refers to the net reduction in ground volume around the tunnel compared with the original in-situ condition. This loss arises from the inevitable stress relief and deformation of the ground as material is excavated and support is installed. Ground loss is a fundamental mechanism governing surface and subsurface movements induced by tunnelling.

Several sources contribute to ground loss during tunnel construction:

- Over-excavation may occur due to limitations in excavation control, tool wear, or intentional allowances made to facilitate tunnel advance.

- Face deformation results from inadequate support pressure at the tunnel face, leading to inward movement of the surrounding ground.

- In mechanized tunnelling, a shield tail void is created between the tunnel lining and the excavated ground; if this void is not completely and promptly filled by grouting, additional ground loss can develop. In soft ground conditions, volume changes within the soil mass, such as consolidation or stress-induced compression, may further increase the total ground loss.

Although the magnitude of ground loss is typically small, often in the range of 0.5–2% of the excavated tunnel volume, its effects can be significant. Even such limited volume losses are sufficient to generate measurable ground movements, which propagate upward and outward from the tunnel and

may manifest as surface settlement. These movements form the basis of the settlement trough observed above tunnels and represent the primary cause of tunnelling-induced damage to overlying structures.

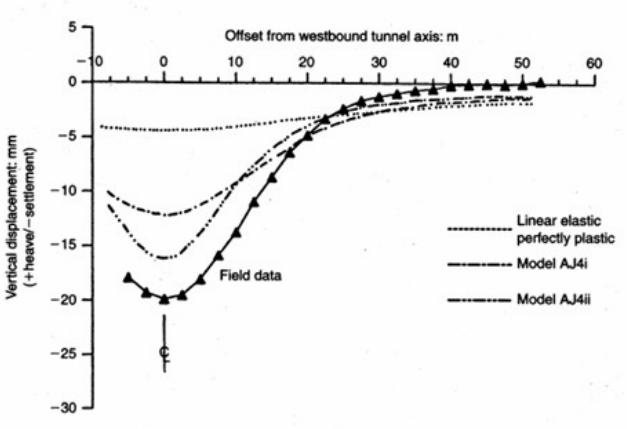

Figure 2.2. Surface settlement troughs obtained from different anisotropic soil models (after Addenbrooke et al., 1997).

2.1.3 Effect of above-mentioned factors on buildings

Ground movements induced by soil deformation influence the entire building system, affecting both the substructure and the superstructure. The response of a structure depends primarily on how these movements are transferred to the foundation level and subsequently redistributed within the structural system.

The type of foundation plays a key role in this process. Shallow foundations, such as strip or isolated footings, interact directly with near-surface soil layers and therefore tend to follow ground deformations more closely. As a result, any spatial variability in settlement is more readily transmitted to the structure. Deep foundations, such as piles, transfer loads to deeper and often stiffer strata, which can reduce total settlement and modify the pattern of deformation imposed on the building. However, even in such cases, differential movements may still develop due to variability in soil conditions or pile response.

It is well established that absolute settlement alone is not a reliable indicator of structural damage. Instead, damage is primarily associated with differential settlement, which causes distortion of the building geometry. When different parts of a structure experience unequal vertical displacements, the system is subjected to bending and rotation, leading to the development of internal stresses.

These distortions are commonly quantified using parameters such as angular distortion or deflection ratios, which provide a measure of relative displacement over a given distance. When these values exceed the deformation capacity of structural or non-structural elements, damage occurs.

The most typical form of damage in buildings subjected to ground movements is cracking, particularly in materials with low tensile strength such as masonry, concrete, and plaster. These materials are unable to accommodate significant tensile strains, and therefore even moderate structural distortions can lead to visible cracking. In contrast, more flexible structural systems may tolerate larger deformations without severe damage.

Uniform settlement, in which all parts of the structure undergo similar vertical displacement, generally results in limited internal stress and is less likely to cause structural damage. However, even in such cases, serviceability issues may arise, particularly in relation to utilities, connections to adjacent structures, or architectural elements.

The occurrence and severity of building damage depend on the interaction between the magnitude and distribution of ground movements, the type of foundation, and the stiffness and deformation capacity of the structure. Therefore, the assessment of damage risk requires consideration of structural distortion and strain compatibility, rather than settlement magnitude alone.

2.1.4 Critical strain concept

Burland and Wroth (1974) demonstrated that tensile strain is the fundamental parameter governing the onset of cracking in buildings subjected to ground movement. Rather than correlating damage directly with settlement magnitude or structural displacement, they showed that cracking is controlled by the level of strain induced in the structural elements.

Their conclusions were based on a synthesis of results from a number of large-scale experimental studies on masonry panels and walls subjected to different deformation patterns, including bending, shear, and combined modes. By examining the deformation at which cracking first became visible, they observed that cracking consistently occurred when the average tensile strain in the masonry reached a particular threshold value.

A key finding of their work was that this threshold strain was relatively independent of the mode of deformation. Whether the masonry element was subjected primarily to curvature, differential vertical displacement, or shear distortion, the onset of visible cracking occurred at approximately the same value of average tensile strain. This indicated that tensile strain provides a more reliable and physically meaningful indicator of damage than displacement-based measures alone.

Burland and Wroth (1974) defined this threshold as the critical strain, denoted as ε_{crit}. The critical strain was measured as an average tensile strain over a representative gauge length, typically taken as 1 m or greater, in order to filter out highly localized effects and capture the strain relevant to visible cracking at the structural scale.

The concept of critical strain is significant because it provides a direct link between ground-induced deformation and structural damage. It allows building response to settlement to be assessed in terms of strain compatibility, rather than absolute movement, and forms the basis for later damage classification frameworks and serviceability criteria for structures affected by ground movements.

The values of critical strain are determined taking into account individual behavior of construction materials, referring to their elastic deformation dominions, most relevant values are:

ε_{crit} for the brick masonry structures is 0.05% - 0.1%

ε_{crit} for the concrete structures is 0.03% - 0.05%

Those values are defined by Burland and Wroth (1974), also it was noted that those values are larger than the local tensile strain corresponding with tensile failure.

In 1977, Burland et al. replaced the notation $\varepsilon_{crit}$with $\varepsilon_{\lim ¿¿}$, which they defined as the limiting tensile strain, in order to account for differences in construction materials and the relevance of serviceability limit states. This refinement recognised that acceptable strain levels vary depending on material behaviour and the performance requirements of the structure. Building on this concept, Boscardin and Cording (1989) further developed the limiting tensile strain framework by correlating specific strain levels with observed building damage derived from case studies of excavation-induced subsidence. Their work provided an empirical basis for relating calculated strains to expected damage levels in practice. Derived limitations are demostrated in table 2.1 and summarised in table 2.2.

2.1.5 Background of Burland (1977) observation. Damage criteria

During the 1960s and 1970s, experience from case histories involving settlement, excavation, and tunnelling-induced ground movements showed that traditional indicators such as crack width or calculated tensile strain were insufficient to fully describe the extent and significance of building damage. Buildings exhibiting similar crack widths were often observed to perform very differently in practice. In some cases, cracking was largely cosmetic and affected only the appearance of the structure, while in others it led to functional problems such as jamming of doors and windows, leakage in services, or loss of usability of internal spaces. In more severe situations, ground-induced deformations compromised the load-carrying capacity of structural elements, posing a risk to overall stability and safety.

In response to these observations, Burland et al. (1977) proposed that building damage should not be assessed solely on the basis of structural response parameters, but rather through a broader framework that accounts for multiple performance criteria. Their approach emphasized the need to distinguish between aesthetic damage, serviceability impairment, and structural instability, recognizing that these forms of damage occur at different deformation levels and have different engineering and practical implications. This multi-criteria assessment enabled more consistent communication of damage severity, supported rational decision-making regarding the necessity and urgency of repairs, and clarified the distinction between serviceability-related damage and damage that threatens structural safety. The concepts introduced by Burland et al. subsequently formed the basis for widely adopted building damage classification systems, including those relating crack width and tensile strain to observable damage categories.

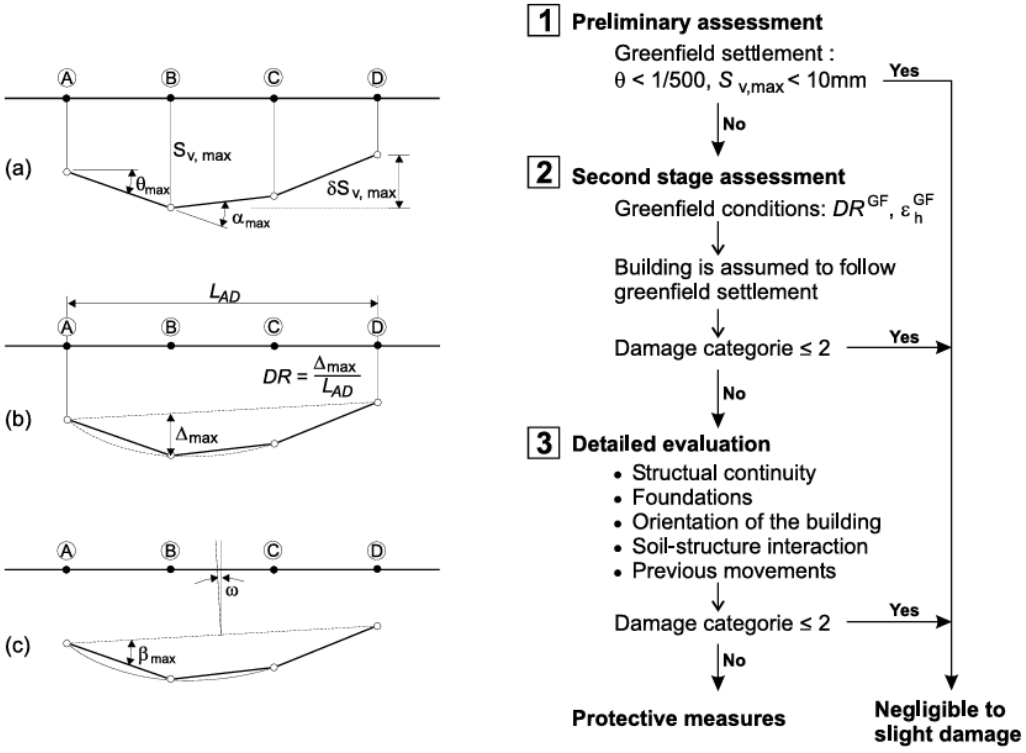

Figure 2.3. Definition of building deformation (after Burland, 1995 and Schematic diagram of three stage approach for damage risk evaluation).

In the following passages, every criterion underlined by Burland (1977) is described:

1. Visual appearance: Aesthetic damage

Visual appearance, or aesthetic damage, refers to changes in the appearance of a building that do not significantly affect its structural integrity or functional performance. This type of damage commonly includes hairline cracking in plaster or masonry, cracking around openings such as doors and windows, minor spalling or deterioration of surface finishes, and slight distortions or tilting that may be noticeable to occupants. Although aesthetic damage is generally cosmetic in nature and the building remains safe and usable, it is nevertheless important because it often causes concern to owners and occupants. Such damage can negatively affect the perceived quality and value of a building and is frequently the primary trigger for complaints or damage claims, particularly in projects involving ground movement or nearby construction activities.

Typical characteristics

- Hairline cracks in plaster or masonry
- Cracks around doors, windows, or corners
- Minor spalling of finishes
- Uneven surfaces or slight tilting noticeable to occupants

2. Serviceability or/and functional damage

Serviceability or functional damage occurs when building movements or deformations impair the ability of the structure to perform its intended function, even though overall structural stability may not be compromised. Typical manifestations include jamming or misalignment of doors and windows, cracking that leads to water pressure, damage or misalignment of services such as pipes and drains, and uneven floors that hinder normal use of internal spaces. In this case, the building remains structurally safe but does not operate satisfactorily, and remedial measures are usually required to restore usability. Serviceability damage is particularly significant because it often develops at relatively low levels of strain or deformation and therefore governs many design and assessment criteria aimed at limiting unacceptable performance long before structural failure is reached.

Typical characteristics:

- Doors or windows that jam or won't close
- Cracked or broken pipes and drains
- Water ingress due to cracking
- Uneven floors affecting usability
- Damage to finishes that affects hygiene or comfort

3. Stability: Structural damage

Stability, or structural damage, refers to damage that affects the load-carrying capacity and overall safety of a building. This form of damage is characterized by severe cracking through load-bearing elements, crushing or failure of masonry, excessive rotation or displacement of structural components, and in extreme cases, partial or total collapse. Unlike aesthetic or serviceability damage, stability-related damage poses a direct risk to life and property and represents an ultimate limit state condition. When such damage is identified, immediate intervention, such as structural strengthening, temporary support, or evacuation, may be required. Consequently, maintaining structural stability is the most critical criterion in building damage assessment and must be ensured under all normal design and operational conditions.

Typical characteristics:

- Wide, through-thickness cracks in load-bearing elements
- Crushing or cracking of masonry piers
- Loss of support or excessive rotation
- Risk of partial or total collapse

Burland's damage classification indicates that the visual appearance of a building may begin to be

affected when structural elements experience deviations of approximately 1/250 from the vertical or horizontal. At larger deviations, on the order of 1/100, or when deflection ratios reach about 1/250, such distortions become readily apparent to observers. Burland et al. (1977) emphasized, however, that visual damage is inherently difficult to quantify because it depends largely on subjective judgement, which can vary between occupants, owners, and inspectors.

To address this limitation, they proposed a practical system of building damage categories based on the ease with which the observed damage can be repaired rather than solely on measured deformations or crack widths. This approach provided a more consistent and meaningful basis for assessing damage severity, as it linked observable effects to the level of intervention required, ranging from minor cosmetic repairs to major structural remediation. By focusing on repairability, the classification system helped bridge the gap between engineering measurements and the practical implications of damage for building owners and users. Categories are visualized and described Iin the following table2.1:

Category of damage	**Normal degree of severity**	**Description of typical damage** (Ease of repair is printed *italic*) **Note:** Crack width is only one factor in assessing category of damage and should not be used on its own as a direct measure of it
0	Negligible	Hairline cracks less than about 0.1 mm
1	Very Slight	*Fine cracks which are easily treated during normal decoration.* Damage generally restricted to internal wall finishes. Close inspection may reveal some cracks in external brickworks or masonry. Typical crack widths up to 1 mm.
2	Slight	*Cracks easily filled. Re-decoration probably required. Recurrent cracks can be masked by suitable linings.* Cracks may be visible externally and *some repointing may be required to ensure weathertightness.* Doors and windows may stick slightly. Typical crack width up to 5 mm.
3	Moderate	*The cracks require some opening up and can be patched by mason. Repointing of external brickwork and possibly a small amount of brickwork to be replaced.* Doors and windows sticking. Service pipes may fracture. Weathertightness often impaired. Typical crack widths are 5 to 15 mm or several up to 3 mm.

4	Severe	*Extensive repair work involving breaking-out and replacing sections of walls, especially over doors and windows.* Windows and door frames distorted, floor sloping noticeably[1]. Walls leaning[1] or bulging noticeably, some loss of bearing in beams. Service pipes disrupted. Typical crack widths are 15 to 25 mm but also depends on the number of cracks.
5	Very severe	*This requires a major repair job involving partial or complete rebuilding.* Beams lose bearing, walls lean badly and require shoring. Windows broken with distortion. Danger of instability. Typical crack widths are greater than 25 mm but depends on the number of cracks.

Table 2.1. Classification of visible damage to walls with particular reference to ease of repair of plaster and brickwork masonry (after Burland, 1995).

Category of damage	**Normal degree of severity**	**Limiting Tensile strain** [%]
0	Negligible	0 - 0.05
1	Very slight	0.05 - 0.075
2	Slight	0.075 - 0.15
3	Moderate*	0.15 - 0.3
4 to 5	Severe to Very Severe	>0.3

*__Note:__ Boscardin & Cording (1989) describe the damage corresponding to the tensile strain in the range 0.015 - 0.3%. as 'moderate to severe'. However, none of the cases quoted by them exhibit severe damage for this range of strains. There is therefore no evidence to suggest that tensile strains up to 0.3% will result in severe damage.

Table 2.2. Relation between category of damage and limiting tensile strain (after Boscardin & Cording, 1989 and Burland (1995)).

2.1.6 Angular distortion

Angular distortion is a measure of the relative rotation or change in slope between two points of a structure caused by differential vertical displacement. It is commonly defined as the ratio of differential settlement between two points to the horizontal distance separating them. Unlike uniform settlement, which generally results in rigid-body movement without significant internal distress, angular distortion induces bending and tensile strains within structural elements. These strains may lead to cracking in masonry, distortion of frames, and damage to finishes and services. Angular distortion is therefore a more meaningful indicator of potential building damage than absolute settlement when assessing the effects of tunnelling.

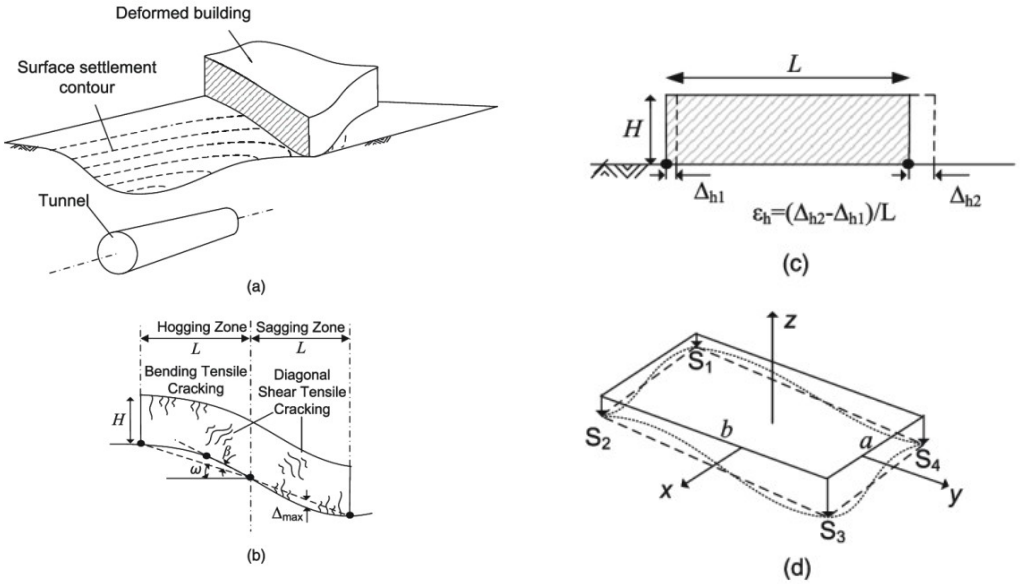

Figure 2.4. Angle of distortion visual representation [E. Namazi1 and H. Mohamad; 2013]

The primary reason for adopting angular distortion as a damage indicator is that buildings are typically more sensitive to *differential* movement than to overall vertical displacement. Tunnel excavations generate settlement troughs with varying curvature, meaning that different parts of a building may experience different magnitudes of settlement. This non-uniform movement leads to internal deformation that cannot be captured by total settlement alone. Angular distortion provides a simple yet effective means of relating ground movement to structural response, allowing engineers to assess the likelihood of cracking and functional impairment. Furthermore, angular distortion can be estimated from predicted settlement profiles, making it a practical parameter for both design and risk assessment during tunnelling projects.

The effects of angular distortion on buildings depend on several factors, including the magnitude of distortion, building stiffness, construction material, foundation type, and structural configuration. At low levels of angular distortion, damage is typically limited to aesthetic effects such as hairline cracking in plaster or minor cracking in masonry. As angular distortion increases, serviceability problems may arise, including jamming of doors and windows, cracking that permits water ingress, and misalignment or failure of services.

At higher levels, angular distortion can induce significant tensile and shear strains in load-bearing elements, leading to wider cracks, separation of structural components, and, in extreme cases, loss of structural stability. Masonry buildings are particularly vulnerable due to their low tensile strength, whereas framed structures may tolerate larger distortions but still experience damage to infill panels and non-structural elements. Consequently, angular distortion plays a central role in damage classification systems and is closely linked to limiting tensile strain concepts used in building damage assessment.

Angular distortion can be evaluated using both predictive and observational approaches. In the design stage, it is typically estimated from calculated or empirically derived settlement troughs associated with tunnel excavation. By determining the expected settlement at key points along a building footprint, the differential settlement and corresponding angular distortion can be calculated. Analytical methods, empirical correlations, and numerical modelling techniques such as finite

element analysis are commonly used to predict settlement profiles and associated distortions.

During construction, angular distortion may be assessed through monitoring data, including precise levelling surveys, inclinometers, and structural monitoring of buildings. Measured settlement data allow for the calculation of actual differential movements, enabling comparison with predicted values and predefined damage thresholds. This observational approach supports the implementation of mitigation measures if distortions exceed acceptable limits.

2.2. Applied method for 2nd line of metro in Turin and regulations for buildings damage predictions

A significant limitation of the damage classification methods proposed by John Burland (1977; 1995) is that they are primarily based on observations made after damage has already occurred. For example, aesthetic damage, such as cracks around window and door frames, can only be assessed once it becomes visible. In more advanced cases, detailed numerical analyses, such as finite element models, are required to evaluate stress concentrations and strain levels that may exceed the strength of construction materials.

However, such approaches are not practical for large-scale urban assessments involving a high number of buildings. The development of detailed numerical models for each structure requires substantial time, computational effort, and financial resources.

For this reason, predictive methods for risk assessment are preferred. These methods rely on parameters that can be estimated prior to excavation and before any damage occurs. The approaches discussed in this section are based on methodologies applied in the INFRATRASPORTI.TO S.R.L. project for the construction of the second metro line in Turin, where extensive urban areas with dense building distributions are affected. All the listed tables and references can be found in the report of INFRATRASPORTI.TO S.R.L - 01_MTL2T1A2DPRCG00R001-0-1

2.2.1 Buildings characteristics

Characteristics of the buildings that are important to understand how significant terrain deformation for them is taken from METROPOLITANA AUTOMATICA DI TORINO PROGETTO DEFINITIVO LINEA 2 research. Important data is:

- Material of the buildings structural part – Masonry or Concrete (or also combined), those materials are characterized with different maximum tensile strength (which in case of both of the materials is ~ 10 times smaller than the compressive strength, so orientation is done on tensile strength).

- Width & Length of the building (depending on the position of the building with respect to tunnel alignment). It identifies the distance between buildings maximum and minimum settlement which creates the angle of inclination of the building.

- Height of the building – identifies the inclination of façade, which leads to the tensile stress on the vertical structure (which's limits depend on the material of structure – referring to the first property).

- Age of the building – materials are losing its original properties during the service lifetime of the building.

All the listed characteristics are summed into the unit representation of the tendency of the building to deform, which is **Vulnerability Index**:

It is described by two numbers referring to the immediate reaction of the building to the terrain deformation, and also reaction over time. With the specific boundaries of vulnerability, limits of deformation – damage classification is identified for each building separately.

2.2.2 Methodology characteristics

The methodology for assessing the risk of damage to structures, buildings and public services follows the specifications of the ITA (International Tunneling Association) following three levels of assessment and in-depth analysis based on the results estimated at each level. The methodology is summarized below.

Phase 1 (Stage 1) of the assessment is based on the calculation of subsidence under free-field conditions (greenfield) and the angular distortion of existing buildings based on the zoning of the surface deformation. Buildings with subsidence below limit values (slight damage) can be considered with a negligible risk of damage and will be excluded from further studies. Buildings that reach the limit values, on the other hand, will be subject to the second assessment phase. The following table defines the admissible values considered for subsidence and angular distortion for phase 1 of the assessment, when no vulnerability is considered (buildings in good condition without initial defects):

Categoria di danno	Massimo cedimento [Smax (mm)]	Massima distorsione angolare [1/β]
0 - 1 Trascurabile a molto lieve	<10 mm	< 1/500
2 Lieve	10 – 50 mm	1/200 – 1/500
3 Moderato	50 – 75 mm	1/50 – 1/200
4 Severo	> 75 mm	1/50 – 1/200
5 Molto grave	> 75 mm	> 1/50

Table 2.3. First stage of classification based on Massimo cedimento [maximum settlement] and Massimo distorsione angolare [maximum distortion angle]

The classification must be corrected to suit the actual conditions of the buildings by varying the maximum values of subsidence and angular distortion for each damage category according to the values of the vulnerability index. The following table defines the permissible values of subsidence and angular distortion for phase 1 of the assessment, when the vulnerability index is taken into consideration.

Categoria di danno	Edifici normali in condizioni standard (Iv<75)		Edifici sensibili (Iv>75, edifici protetti e patrimonio, edifici pubblici, etc)	
	S_{max} (mm)	1/β	S_{max} (mm)	1/β
0 – 1	<10	< 1/500	<5	< 1/1000
2	10–50	1/200 – 1/500	5–25	1/400 – 1/1000
3	50–75	1/50 – 1/200	25–37.5	1/100– 1/400
4	>75	1/50 – 1/200	>37.5	1/100– 1/400
5	>75	> 1/50	>37.5	> 1/100

Table 2.4. First stage of classification including the Vulnerability index

The second stage (Stage 2) of the analysis is based on the calculated maximum tensile stresses for each building that falls into a damage category ranging from “slight” (2) to “very severe” (5). The methodology for estimating tensile stresses in buildings follows the equivalent beam approach Burland & Worth (1974) and Burland et al (1977)]. This model represents the building as a simple rectangular, elastic, weightless beam subject to deformation modes with the part resting on the ground assuming a concave or convex shape . This approach easily gives an idea of the cracking mechanisms and allows the calculation of the critical tensile strain, which is the maximum between the tensile strain due to bending (εb) and the tensile strain due to shear (Subsequently, Boscardin and Cording (1989) proposed a modification of the model to take into account the horizontal tensile strain εh by adding it to εb and εd. Depending on the position of the building with respect to the yield curve, angular deformations will develop (positive for upward concavity - sagging - and negative for downward concavity - hogging).

Categoria di danno	Massima deformazione di trazione (%)
0 Trascurabile	< 0.05
1 Molto lieve	0.05 - 0.075
2 Lieve	0.075 - 0.15
3 Moderato	0.15 - 0.3
4 - 5 Grave a molto grave	> 0.3

Table 2.5. Second stage of classification based on deformation percent

The maximum deformation values will be compared with the limit values (refer to Table 2.5 and Table 2.6); in this way a damage category is provided for each building. The table shows the damage category for phase 2 in case the vulnerability index is not considered (for buildings in good condition without initial defects).

The classification must be corrected to suit the actual conditions of the buildings by varying the limit tensile strain values for each damage category according to the values of the vulnerability index. The damage category for phase 2 is shown below when the vulnerability index is taken into account.

Vulnerabilità	Edifici normali in condizioni standard (Iv<75)		Edifici sensibili (Iv>75, edifici protetti e patrimonio, edifici pubblici, etc)	
Categoria di danno	$\varepsilon_{lim\ min}$ (%)	$\varepsilon_{lim\ max}$ (%)	$\varepsilon_{lim\ min}$ (%)	$\varepsilon_{lim\ max}$ (%)
0	0	0.050	0	0.025
1	0.050	0.075	0.025	0.038
2	0.075	0.150	0.038	0.075
3	0.150	0.300	0.075	0.150
4-5	>0.300		>0.150	

Table 2.6. Second stage of classification including vulnerability index

Third stage is performed for buildings that do not meet, i.e. exceed, the defined damage criteria in the second step of the risk assessment analysis. Notwithstanding the results of the risk assessment, buildings with foundations very close to the tunnel (with a distance of less than one diameter from the tunnel) must undergo the third stage of the risk assessment in order to identify whether appropriate mitigation measures are needed. At this stage, each building has to be considered on its own and requires a detailed structural investigation and FEM analysis considering the construction sequence, geotechnical and geometric conditions, structural type of buildings, foundation type, subsidence history, water level variation, etc. If the results of the analysis still show high damage on existing buildings, consolidation treatments will be proposed.

2.2.3 Classification used for case study

In the table 2.6 is visible only one vulnerability index gradation used for damage classification, for buildings with vulnerability more than 75 and less than 75, following table 2.7 is taking into account more gradations in case of buildings vulnerability indexes and also takes into account buildings maximum settlement point, grade of inclination and horizontal strain. Indeed, different deformation and displacement characteristics can be located in different criterions of damage, for this case, the worst which means the biggest damage classification according to the parameter showing the most significant result is taken for whole building. Tabe is taken from INFRATRASPORTI.TO S.R.L

company's archives, it is also used in the second stage before turning to FEM analysis for the buildings with the highest damage characteristics:

		Buildings vulnerability index									
		IRRILEVANTE		BASSO		MEDIO		ALTO		ELEVANTO	
		0<Iv<20		20<Iv<40		40<Iv<60		60<Iv<80		80<Iv<100	
Categorie di Rischino	1 MOLTO LIEVE	Smax [mm] <10	βlim [-] <0.002	Smax [mm] <8	βlim [-] <0.0016	Smax [mm] <6.7	βlim [-] <0.0013	Smax [mm] <5.7	βlim [-] <0.0011	Smax [mm] <5	βlim [-] <0.001
	2 LIEVE	Smax [mm] 10-50	βlim [-] 0.005	Smax [mm] 8-40	βlim [-] 0.004	Smax [mm] 6.7-33.3	βlim [-] 0.003	Smax [mm] 5.7-28.6	βlim [-] 0.0028	Smax [mm] 5-25	βlim [-] 0.0025
	3 MODERATO	Smax [mm] 50-70	βlim [-] 0.02	Smax [mm] 40-60	βlim [-] 0.016	Smax [mm] 33.3-50	βlim [-] 0.013	Smax [mm] 28.6-42.9	βlim [-] 0.011	Smax [mm] 25-37.5	βlim [-] 0.01
	4 GRAVE	Smax [mm] >75	βlim [-] >0.02	Smax [mm] >60	βlim [-] >0.016	Smax [mm] >50	βlim [-] >0.013	Smax [mm] >42.9	βlim [-] >0.011	Smax [mm] >37.5	βlim [-] >0.01

Table 2.7. Applied classification with several damage characteristics including vulnerability index

In the table of final classification above, on the columns buildings are classified by their vulnerability indexes:

From 0 to 20 – Irrelevant

From 20 – 40 – Low

From 40 – 60 - Medium vulnerability

From 60 – 80 – High

From 80 – 100 – Extremely high

2.3. Theoretical background of settlement distribution evaluation

The Peck method (1969), is a widely used approach to assess and predict ground settlement caused by tunnel excavation, especially in urban environments. It provides an opportunity to estimate the impact of tunneling on the surface and sub-surface structures, which is crucial for construction projects that involve underground work.

Key Aspects of the Peck (1969) and O'Reilly & New (1982) Method :

1. Ground Movement Profiles: The Peck method emphasizes that tunneling induces a characteristic ground movement profile, which typically resembles a bell-shaped curve. Settlement tends to increase as the distance from the tunnel increases until it reaches a peak directly above the tunnel. Beyond a certain distance, the settlement decreases.
2. Factors Influencing Settlement: The method considers several factors that influence ground movement, including:
   - Tunnel Depth: Deeper tunnels generally result in less surface settlement.
   - Tunnel Diameter: Larger tunnels can lead to increased settlement due to the larger disturbed zone.
   - Soil Properties: Different soil types (clays, sands, silts) have varying responses to tunneling. Cohesive soils may behave differently from granular soils.
   - Construction Method: The method of tunnel excavation (open face, shielded, etc.) affects ground movement.

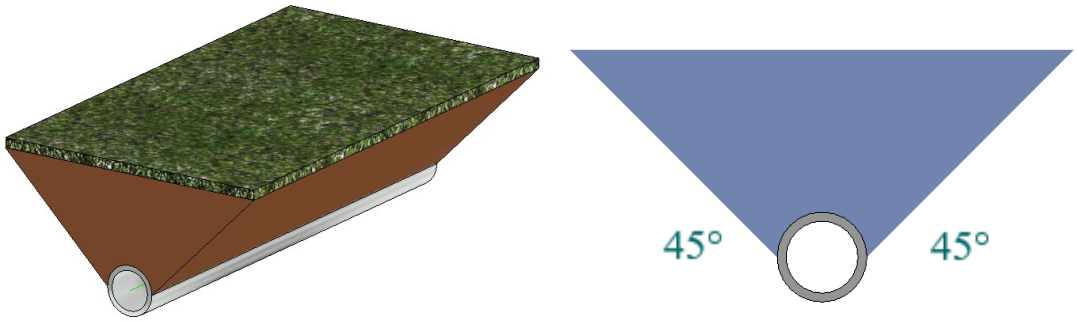

Figure 2.5. Volume of soil influenced by tunnel excavation (in case of maximum settlement)

3. The zone of influence for tunnel excavation by both TBM and conventional method is commonly defined as that between the tunnel and a cone to the surface that opens at 45° (based on the theory of Attewell and Yeates, 1984)

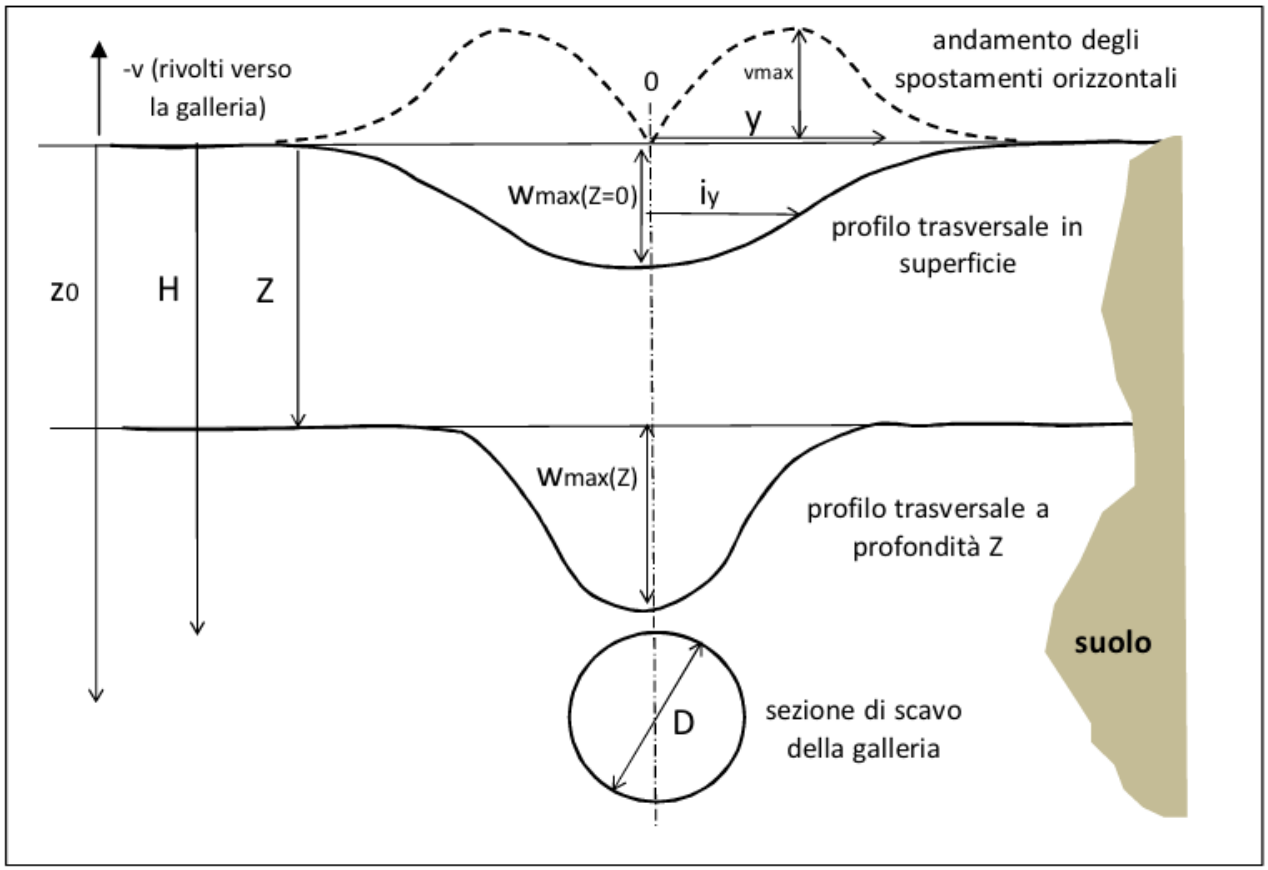

Figure 2.6. Soil deformation following Gaussian distribution [F. Nemorini; 2010]

Regardless of the ground conditions and type of excavation method, the development of subsurface subsidence in a section perpendicular to the tunnel axis can be represented by a Gaussian curve (since the shape of subsidence can be well represented by a Gaussian or normal distribution curve) with the expression (Peck 1969):

$$S = Smax * e^{\left(-\frac{y^2}{2*|i|^2}\right)} \qquad [1]$$

where S is the vertical subsidence of a point at a vertical (z) and horizontal (y) distance from to the tunnel axis.

According to Attewell and Farmer (1974), Burland et Al. (1977), Burland, O'Really and New (1991), Mair, Taylor and Burland (1996), the above hypothesis (the Gaussian shape of the subsidence line) is duly confirmed by field measurements.

To estimate the distance 'i' of the bend point of the curve from the axis of the tunnel, several formulas have been proposed in the literature (Schmidt, 1969; Peck, 1969). The deflection point 'i' is the amplitude of the deflection curve, which represents the distance of the bend point from the axis (corresponding to a standard deviation of the curve of normal distribution) and is determined by the ground conditions as described below.

O'Reilly & New (1982) showed that, for a larger tunnel diameter coverage, a direct proportionality relationship can be assumed between 'i' and the depth of the tunnel z-axis according to the formula:

$$i = K * z \quad [2]$$

'K' is a coefficient that depends on the conditions and the type of subsoil; it defines the shape of the subsidence surface and can be considered constant with depth. (Referring to the geological analysis with boreholes).

The total volume of the subsidence curve ΔV can then be obtained by integrating the generalized subsidence formula over z and is equal to:

$$\Delta V = \sqrt{2\pi} * S_{max} * K * z \quad [3]$$

The Smax value can be obtained by assuming the expected value ΔV, referred to as "lost volume":

$$S_{max} = \frac{\Delta V}{\sqrt{2\pi} * K * z} \quad [4]$$

The lost volume (ΔV) is calculated as a percentage of the theoretical excavation volume V_L (%) on one meter of advancement for a circular tunnel with a radius R:

$$\Delta V = V_L * \pi * R^2 \quad [5]$$

Then, knowing the volume lost, the type of soil and the tunnel cover, one can calculate the maximum subsidence and all points of the hypothetical subsidence curve at ground level for a circular tunnel:

$$S_{max} = \frac{\pi * R^2 * V_L}{\sqrt{2\pi} * K * z} \quad [6]$$

2.4. FEM analysis: Predictive models establishment

Free-field settlements induced by shallow tunnel excavations can be effectively evaluated using numerical modelling techniques, which allow for the simulation of soil behaviour and stress redistribution during the excavation process. Among these approaches, the Finite Element Method (FEM) is widely used due to its ability to represent complex soil–structure interaction and to provide detailed predictions of ground deformation.

In this context, F. Nemorini (2010) proposed a three-dimensional FEM analysis for the simulation of metro tunnel excavation, taking into account realistic soil conditions and construction phases. The results obtained from this study form the basis for the development of the dynamic characteristics of the method proposed in the present work.

The applicability of these results is supported by the similarity between the soil conditions adopted in the referenced model and those encountered in the urban environment of Turin, particularly in relation to the Metro Line 2 project. As demonstrated later in Chapter 5, a detailed soil comparison confirms that the free-field simulations performed for Milan soils can be considered applicable to the Turin site.

2.4.1 Model and considered characteristics

Analyses were done using the commercial software ABAQUS (Simulia Corp.), with an objective of evaluating the deformations caused by the excavation of shallow tunnel by use of TBM EPB (Earth Pressure Balance), main steps of modeling include:

1. Soil mass discretized by smaller pieces in the tunnel face and around the face, on this level check of geostatic pressure was also done.
2. Cancelation of elements on the tunnel volume alignment with an application of pressure to the circular cross section to simulate the action of EPB.
3. Creation of tunnel ring elements along within the movement of EPB face on every stage of excavation.

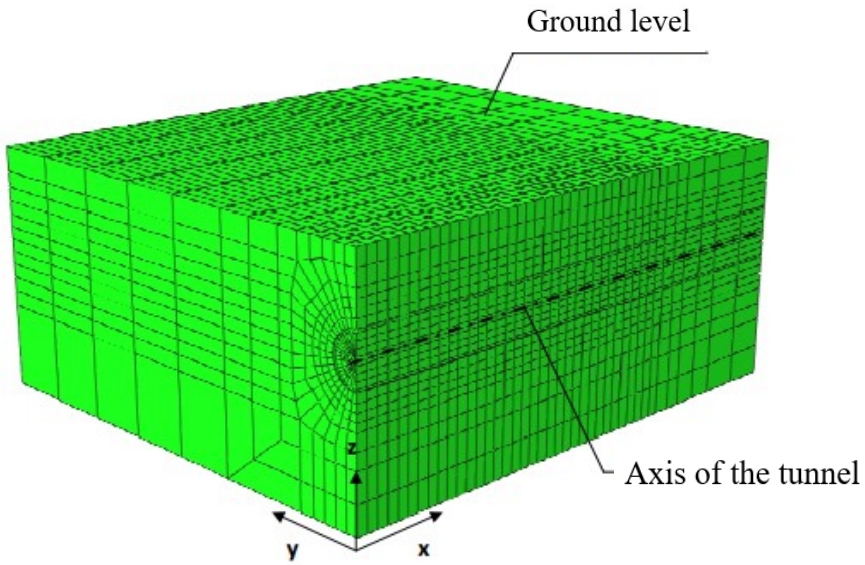

Figure 2.7. Geometry Model Abaqus 6.8.1 viewer [F. Nemorini; 2010]

Basic model, which was used for parametric analysis, consists of 14760 connections and 15049 elements, which together create parallelepiped with sizes 67.6 x 60 x 29.5 meters correspond to axis x, y and z. (Figure 3.1. Geometry Model Abaqus 6.8.1 viewer), only half of tunnel with soil mass was modeled as it is assumed that on another half effects and deformations are symmetric.

Shield support of EPB was designed as system of springs on the periphery of tunnel boring machine, which take the infinite rigidity when surrounding elements come in contact with springs, this scenario is taking into account the physical support of shield as maximum possible vertical and horizontal deformation inside of tunnel volume, here, the system of supports can be described on every stage of excavation:

- On the first stage support is characterized by lower layers of the soil, outer parts of the model are characterized by rigid supports, so soil creates geostatic pressure on every element below, the excavation is not presented on this stage.
- At the stages of excavation, the support is represented by systems of springs as it was described above.
- Concrete rings represent the final stage of tunnel stability with a backfilling between the extrados of rings and periphery left by TBM cutter head.

Materials which are inserted in the numerical model are soil and conglomerates. Their characteristics form the core of mechanical properties of the model such as strength, ductility and deformability. Model elements that represent the soil are programmed as simplified nonviscous material in dried conditions, isotropic and homogeneous, respecting the Mohr-Columb strength criterions and ideal elastic – plastic behavior following the link of stress and strain.

Materials used as tunnel construction ones do not overcome the elastic deformation area of elastic plastic deformation curve, the link of stress and strain is remaining in linear relation.

CHARACTERISTICS OF THE SOIL						
Cohesion (KPa)	Shear strength Angle (^{0})	Angle of dilatancy (°)	Thrust coefficient at rest (/)	Specific Weight [kN/m^3]	Young Modulus [MPa]	Poisson coefficient (/)
c	Φ	ψ	K_0	γt	Et	νt
0.1	35	10	0.43	18	75	0.3

CHARACTERISTICS OF THE TUNNEL MATERIALS				
Elements of the project	Thickness [m]	Specific weight [kN/m3]	Young Modulus [MPa]	Poisson coefficient (/)
#	Δ	γg	Eg	νg
Backfilling Cement Solution	0.1	25	0.9	0.2
Concrete Rings Reinforced concrete	0.3	25	25000	0.2

Table 2.8. Material mechanical characteristics

For the objectives of parametric analysis, the properties of the materials were always remaining as the ones mentioned in Table 2.8., however there were also three other models created, where the variable factor is the depth of the tunnel, and also taking into account its radius – overburden.

Model A: Overburden H = 1.23D

Model B: Overburden H = 2D

Model C: Overburden H = 3D

Model D: Overburden H = 4D

Simulation of excavation was done in a way that dimensions and pressure of EPB were considered and applied on the face of excavation, deleting elements every 1.4 meters on area of excavation of 33,18 m^2, which in total is equal to 46.45 m^3, total excavation length is 40m which is equal to 29 stages of excavation.

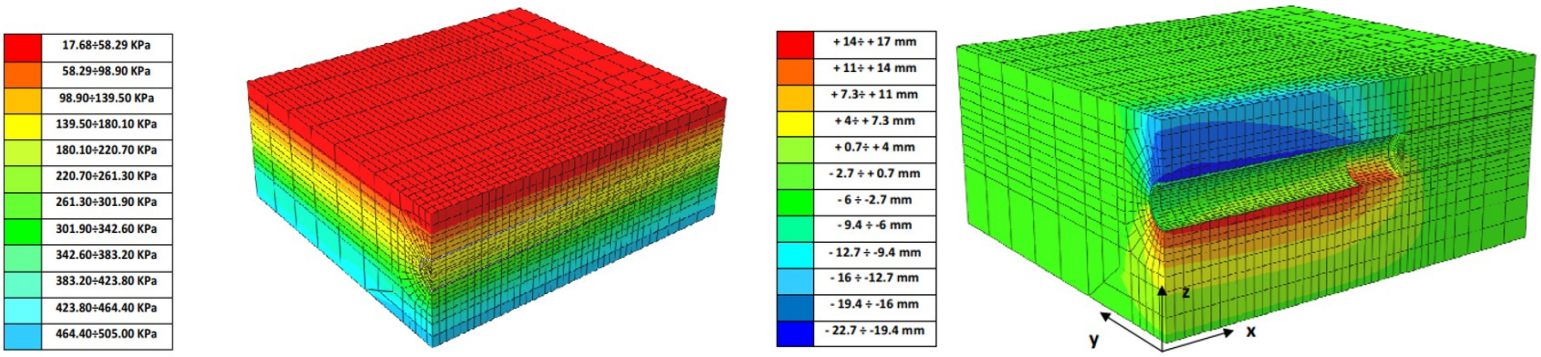

Figure 2.8. Geostatic pressure distribution before tunnel excavation & Pressure distribution in 40 m of excavated tunnel with support of concrete rings [F. Nemorini; 2010]

2.4.2 Simulation Results; Predictive models

The software processes the information contained in various 'input' files prepared for analysis and, after a while, outputs the results of the calculation process, which are grouped into one or more 'output' files. The commercial code ABAQUS® (Simulia Corp.) summarizes the results of the processes in text files that specify the values of the variables of interest. In this case, the variables that need to be determined are the displacement components of the nodes contained on the edges shown earlier. By processing these values in a spreadsheet, it was possible to reconstruct the dynamics of the movements caused by the change in parameters. In particular, for each factor analyzed, the following were obtained: Values of vertical soil displacement caused by soil excavation, on the surface and at depth, in cross-sections.

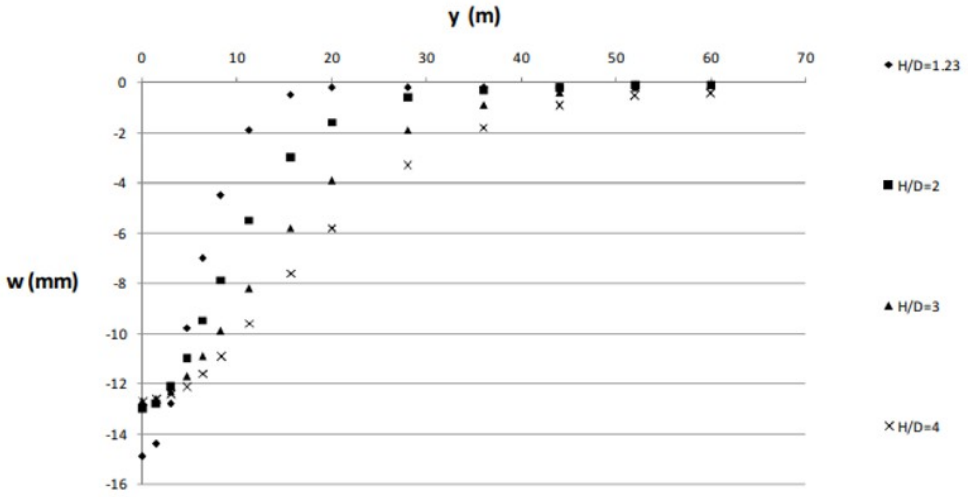

Figure 2.9. Values of Maximum vertical displacement and displacement distribution along section of width 'y'; according to different H/D ratios [F. Nemorini; 2010]

Four models were analyzed under the influence of soil weight and TBM pressure, on the basis of surface vertical displacements graphs that can be visible in Figure 2.9 were constructed, variable 'y' represents the distance on the perpendicular transversal section on the axis of tunnel, initial point where the settlement reaches the maximum value, represents the axis right above the tunnel. From the

graphs is understandable that the maximum settlement respect to the depth of the tunnel is reached when tunnel comes close to the ground surface, in this same time, this scenario leads to the smallest influence length, however the dependence of maximum settlement to the influence cannot be called linearly inverse proportional, because in other 3 models when ratio of overburden and tunnel diameter take higher values, the maximum settlements remains approximately the same, however the angle of inclination of settlement distribution is showing significant expanding of influence zone as tunnel goes deeper respect to ground surface.

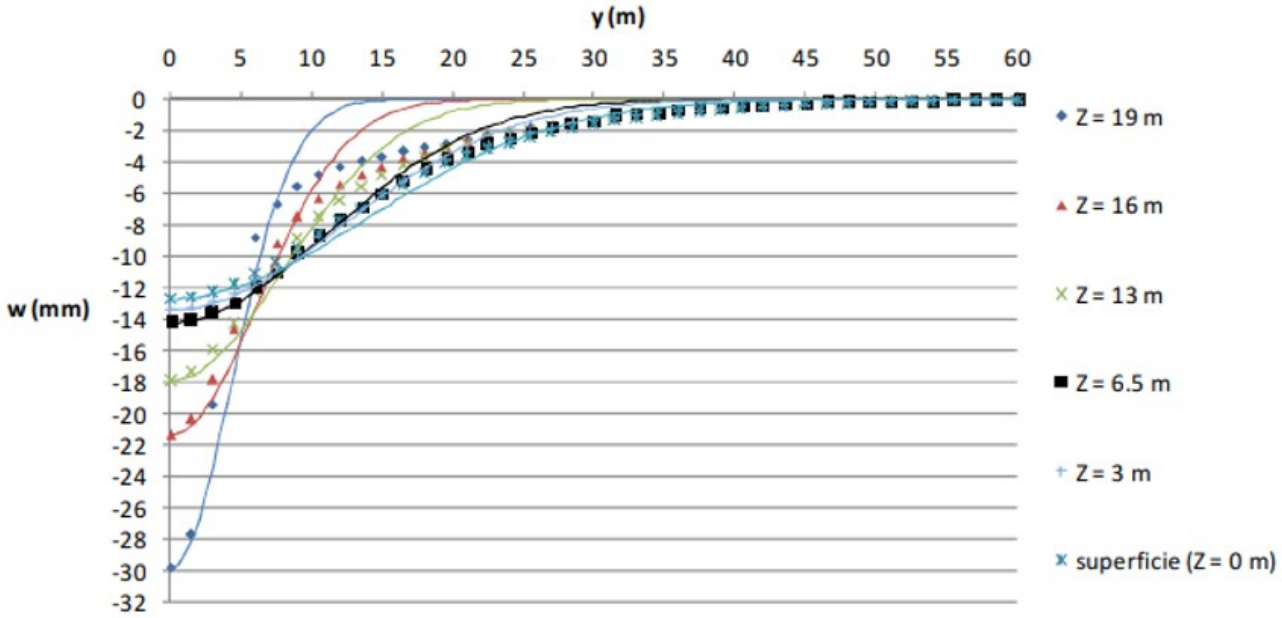

Figure 2.10. Values of Maximum vertical displacement and displacement distribution along section of width 'y'; 'Z' represents different levels of underground [F. Nemorini; 2010]

To analyze underground movements, horizontal lines were established, from which profiles were extracted using the SURFER® program (Golden Software Inc.). The use of SURFER® was necessary due to the irregular arrangement of nodes on the transverse edges. To extract intermediate displacement values, the program uses a grid interpolation method, which is superimposed on the area of input node values.

The kriging method was used, which treats displacement values as a random variable in accordance with geostatistical theory. As the reference model for the analysis, from the point of maximum settlement is visible that H/D = 3 was chosen, because firstly, the maximum settlement in this depth is taking the value which is approximately equal to ones of H/D = 2 and H/D = 4, taking the middle value between them, even though the differences are almost negligible, and secondly, the angle of inclination which represents the settlement distribution along 'y' variable distance is taking the middle values between the distributions around it.

The aim of graph plotting was to represent the change of maximum settlement and settlement distribution in the lower layers of soil, trying to construct the function that would take the depth itself as the variable, and the function itself would work for the cases with different H/D ratio, depending on the surface deformation function and, once again, taking the depth of analysis as a variable.

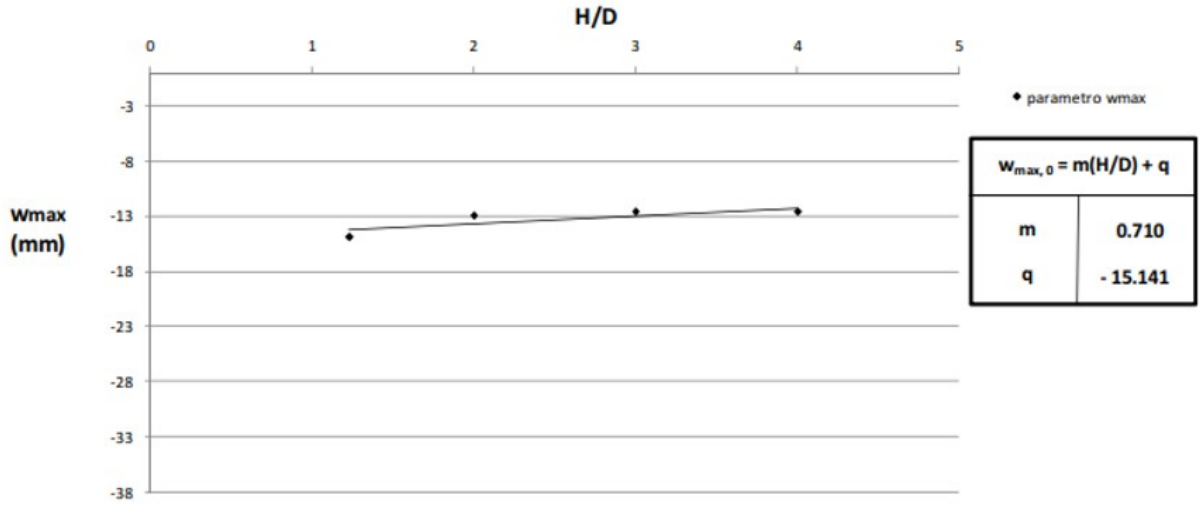

Figure 2.11. Linear function representing the dependance of maximum settlement on Tunnel geometrical properties [F. Nemorini; 2010]

Inputting the values from Figure 2.11. into the table of depending on values, where only w_{max} was taken as the output and geometrical parameters of the tunnel are the variables, the table of depended values was established and using the data in the table the line of trend was plotted to evaluate the coefficients of the function, that describes dependence of maximum settlement according to the depth of the tunnel, such function permits the approximate (but significantly more precise than theory based) results of maximum settlement in the same soil or soil with similar properties for different inputs in case of soil geometry.

Final regression model: $w_{max,0} = 0.71 * (H/D) - 15.141$

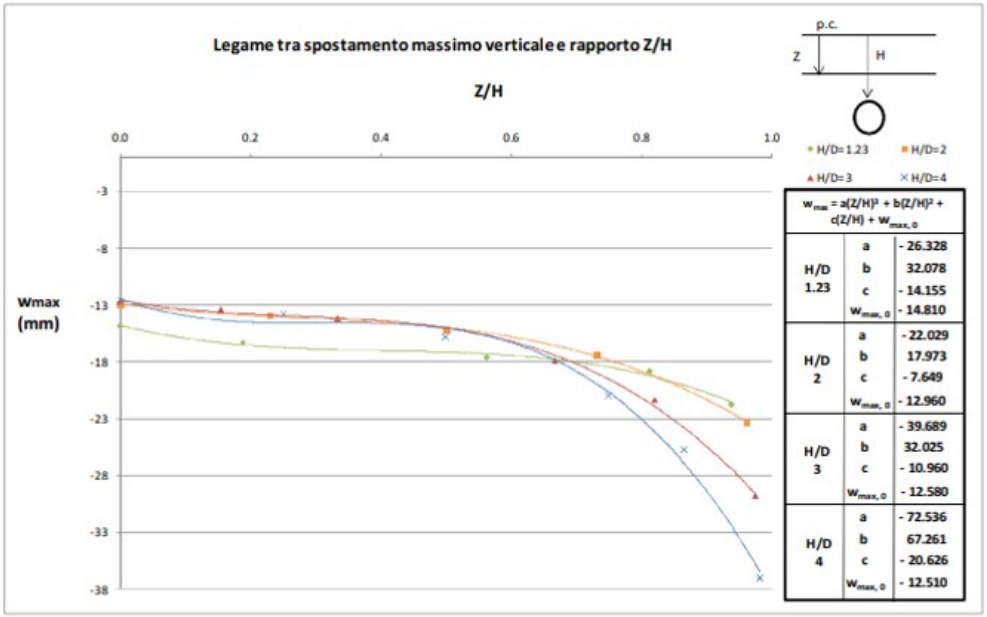

Figure 2.12. Cubic function representing the dependance of maximum settlement on Tunnel geometrical properties along the different vertical depth levels [F. Nemorini; 2010]

Set of functions were plotted for prediction models referring to the maximum settlement in the deeper layers of the ground. As it can be visible on Figure 2.12, the unit function that takes into variable value only the level 'z' inside of soil was not possible, as the behavior of inner soil layers are different depending on the depth of the tunnel, minimum power of the function for each analyzed model (H/D =

1.23; 2; 3; 4) was the cubic function, as it gets close enough to the data points got from the FEM analysis. Important remark here is, that until the ratio of Z/H close to the value of 0.7, it means that the interest depth of analysis is 70 per cent from the depth (overburden) of the tunnel, the functions belonging to the depth of tunnel H/D equal to two, three and four, are getting almost the same values of maximum settlement change, functions can be called superimposed to each other, it is an important point for predicting models, because rarely there are structures on such a significant depth (70 per cent from tunnel excavation depth), so it means that for the tunnel depth that exceeds two times its diameter, it is possible to use approximate union cubic function which will take only 'z' depth of analysis value as the variable.

Function corresponding to H/D = 2 can be used as it takes the average values between others in the region, or to be kept on the safe side, H/D = 3, as it takes the highest change in settlement.

Final regression model (H/D = 3): $w_{max} = -39.689*(Z/H)^3 + 32.025*(Z/H)^2 - 10.96*(Z/H) + w_{max,0}$

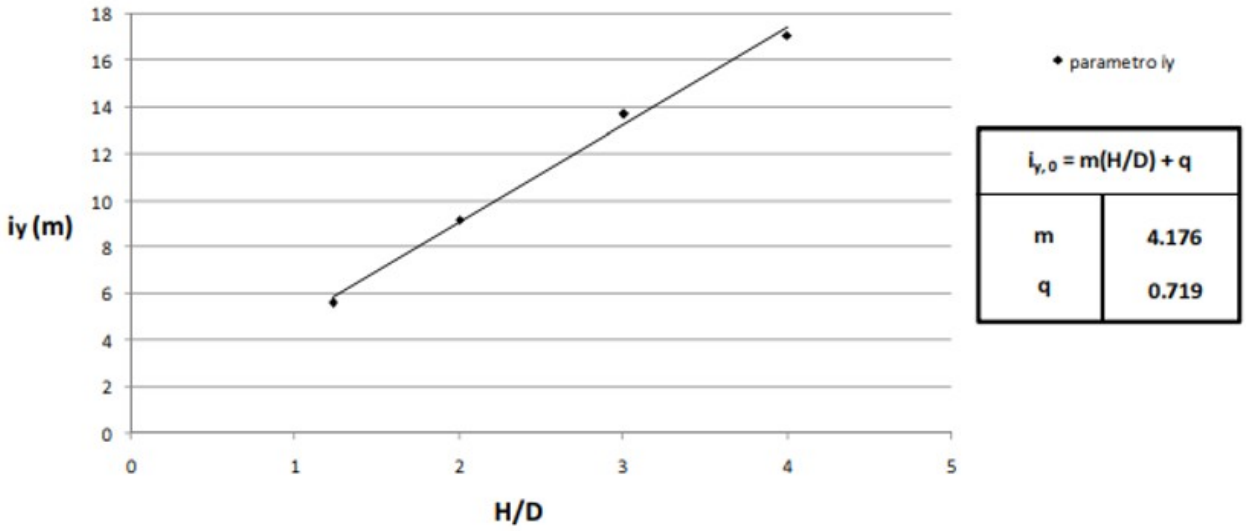

Figure 2.13. Linear function representing the dependance of settlement inclination angle on Tunnel geometrical properties [F. Nemorini; 2010]

Situation with parameter "i_y" is taking the opposite functional behavior in compare to the maximum settlement function, both functions were taken assuming the ratio of overburden to the diameter of tunnel, from Figure 2.12 – the closer tunnel alignment comes to the ground surface, the bigger is the value of maximum settlement.

In addition to the explained phenomenon, Figure 2.13, demonstrates, that the deeper is the settlement point, the shorter distance in the transversal cut is needed to absorb the effect of the settlement, so if the line of reference is taken horizontally on the point of maximum settlement and angle of settlement distribution is taking the origin in the point of w_{max}, angle of distribution is less as less is the maximum settlement, so it takes bigger distance on the surface to reach the 0 value, in contrary, the higher is the settlement, the higher is the angle of distribution angle, so in total the settlement basin takes a sharper shape, leaving significant, but small in case of area of influence effect on the surface.

Regression model: $i_{y,0} = 4.176*(H/D) + 0.719$

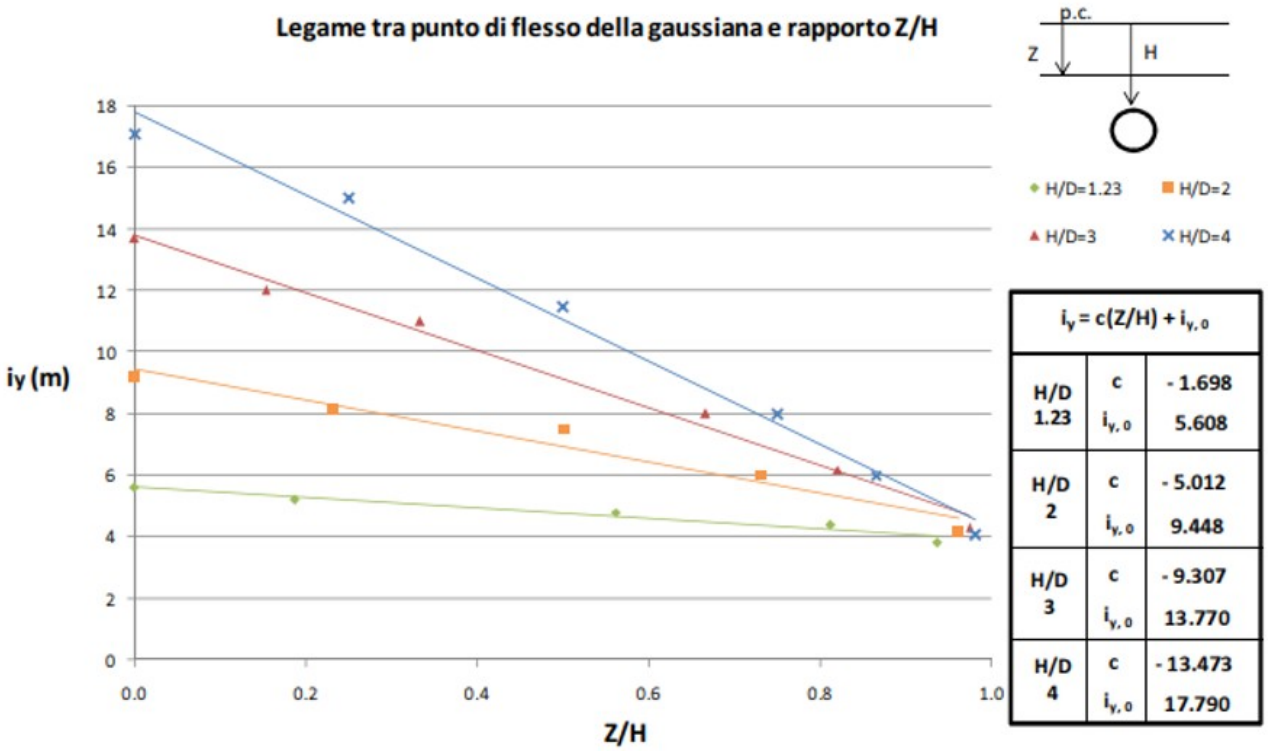

$i_y = c(Z/H) + i_{y,0}$		
H/D 1.23	c	- 1.698
	$i_{y,0}$	5.608
H/D 2	c	- 5.012
	$i_{y,0}$	9.448
H/D 3	c	- 9.307
	$i_{y,0}$	13.770
H/D 4	c	- 13.473
	$i_{y,0}$	17.790

Figure 2.14. Linear function representing the dependance of settlement inclination angle on Tunnel geometrical properties along the different vertical depth levels [F. Nemorini; 2010]

Final function that is used for the objectives of this thesis, as creating the dynamic visual and data – full model for settlement predictions – is the variability of settlement distribution angle along the depth from the surface. In compare to the progression of maximum settlement deeper in the layers of soil that becomes larger as level of analysis coming closer to the tunnel crown, the influence area is becoming smaller so the shape of settlement basin taking the sharper angle.

As in the Figure 2.14, where the variation of maximum settlement is demonstrated, the function of inclination angle gave different behavior characteristics for different analyzed models, making the function depend on "Z-Depth of analysis" only in the case of unique transversal section, where depth of excavation [being more precise H/D] stays constant. Comparing the behavior of functions in different depth excavations, it is visible that the closer level of analysis is to the tunnel crown, less are the differences of settlement angles, finally they arrive on the same point when level of analysis is reaching the level of excavation.

Final regression model (H/D=3) = -9.307*(Z/H) + $i_{y,0}$ = -9.307*(Z/H) + 4.176*(H/D) + 0.719

Chapter III: BIM core concept and application to tunnelling

The paradigm of Building Information Modeling (BIM) has fundamentally shifted the focus of underground construction from 2D drafting to multidimensional information management. In tunneling, the method of BIM is usually used for design with high LOD, which also takes into account the geographical position with a help of direct data flow which includes topographical data and geo coordinates data, but in the given work will concentrate on automatic calculation abilities of the BIM, which minimize the error because of direct data flow, and distance estimation in the working space. Referring to Fabozzi S. et al, 2021.

3.1. The role of parametric modeling in subsurface design

Unlike traditional CAD, where a change in tunnel alignment requires a manual redrawing of all cross-sections and geotechnical profiles, Parametric Modeling treats the project as a system of variables and constraints. By defining the tunnel geometry through parameters—such as the alignment curvature (R), the ring width (w), and the segment thickness (t)—the model becomes an intelligent, reactive entity.

Extending BIM with Visual Programming: Dynamo and Revit

While standard BIM platforms like Autodesk Revit offer robust tools for vertical construction, they often lack the native flexibility required for the complex, linear, and curved geometries of tunnels. This gap is bridged by Autodesk Dynamo, a visual programming interface that extends Revit's capabilities.

Dynamo allows engineers to move beyond the limitations of the standard user interface by writing scripts using "node-based" logic. For a tunneling thesis, Dynamo's value lies in three specific areas:

1. Algorithmic Alignment: Dynamo can ingest coordinate data from surveyors (CSV or Excel) and generate a smooth 3D "NURBS" curve that serves as the tunnel's centerline.

2. Automated Component Placement: Instead of placing tunnel segments manually, a Dynamo script can iterate through the entire length of the alignment, placing and rotating rings to match the precise orientation required by the TBM's path.

3. Data Bridge for Soil Dynamics: Dynamo acts as the computational engine that extracts geometric data from Revit and reformats it for geotechnical analysis software. It can automate the generation of the "influence zone" the volume of soil affected by the excavation—which is critical for setting up a dynamic simulation.

3.1.2 Software Interoperability and Data Flow

The core challenge of research simulating soil dynamics depends on a high-fidelity Data Flow. Information must travel through a multi-stage ecosystem without losing its "intelligence":

- The Authoring Stage (Revit + Dynamo): The physical tunnel and its segments are defined parametrically.

- The Translation Stage (JSON/XML/API): Data regarding the structural mass and the excavation sequence is exported. Visual programming scripts ensure that the mesh density in the simulation matches the critical areas of the BIM model.

- The Simulation Stage (FEM/DEM Software): Numerical solvers (like PLAXIS 3D or Midas GTS NX) receive the parametric geometry to perform the dynamic analysis, calculating stress-strain behavior and ground vibrations during the TBM's advancement.

Research Significance: By utilizing Dynamo to link Revit with geotechnical solvers, the workflow moves from a "Static BIM" (a snapshot in time) to a "Dynamic BIM" (a predictive tool). This allows for the simulation of scenarios: for instance, how the soil dynamic response changes if the TBM's advance rate increases, also in case of change of alignment geometry or tunnel radius, different scenarios of backfilling thickness can be also taken into account.

3.2. Defining the Level of Development (LOD)

In any BIM-based research, the Level of Development (LOD) is a critical metric that defines the reliability and "maturity" of the digital elements. LOD is a composite of the Level of Geometry (LOG) and the Level of Information (LOI), ensuring that all stakeholders understand the intended use of a specific model component.

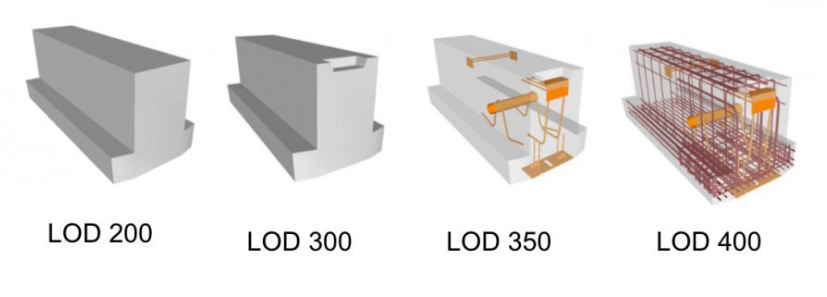

Figure 3.1. Visual different LOD demonstration

LOD Framework for Tunneling and Soil Simulation

The progression of LOD in a tunnel project dictates the depth of the dynamic soil analysis:

- LOD 100 – 200 (Conceptual to Schematic): The tunnel is represented as a volumetric mass. Geotechnical information is limited to broad stratigraphy. While useful for initial route planning, the data at these stages is insufficient for complex dynamic simulations.

- LOD 300 (Detailed Design): This represents the "Numerical Analysis Baseline." At this stage, the model contains precise geometry and defined material properties (E, c, γ, θ, φ). The material properties also include the materials of the tunnel, difference in Young Modulus of concrete from which the rings are done (solid) and the one used for backfilling (liquid) should

be considered.

- LOD 350 (Interfacial Coordination): This level introduces the modeling of joints and the specific interfaces between the tunnel lining and the surrounding soil. This is essential for accurately capturing the "soil-structure interaction" during a dynamic event or excavation phase.

- LOD 400 – 500 (Fabrication to As-Built): These stages incorporate high-fidelity details such as reinforcement bars and grout ports. While critical for construction, for the purposes of soil dynamic modeling, this level of detail is often "simplified" back to LOD 300/350 to maintain computational efficiency during the simulation.

3.3. BIM tunnelling workflow

Developed BIM tunnel model must include the model of soil mass where tunnel excavated, first phase of the work is taking the geometry of topography, for a purpose to correctly reconstruct topographical surface, several methods can be used:

- Most reliable are the GIS empowered software that requires from the user only the geographical location of the project, boundaries of land are usually given by default limitation settings of the software but can be also manipulated by users in enlarged settings. The coordinate systems of the given software are usually taking into account the world's central geographical system considering the beginning of coordinates in the intersection of equator with a main meridian and sea level is taken as reference for 'z' coordinate. LOD of the developed topographic models can be taken as a maximum one, it is justified by high topography geometry precision, because it is constructed with significant amount of coordinate points and also every point from which topography consists of contains its numerical coordinates, which brings the model on the high level also from informative point of view.
- Total station physical observation input.
  Requires field analysis, amount of observed points depends on researchers' decisions, but by the field analysis requirements they must be enough to reconstruct the topography with lowest and highest points.
  Geometrical data about the points location can be imported from the Total station to CAD 3D space, where it can be digitally reconstructed, precision in case of topography geometry is lower than in case of GIS software, but in case of small fields, the method becomes financially cheaper than commercial GIS subscriptions, however the method of physical observation by Total station is rarely used in infrastructure construction (at least at the design stage), because projects of infrastructures are taking large area sizes.
- Manual inserting of the ground vertical coordinates using the 'Topography' tool in Revit working space, the method can be characterized as the least precise, because the x - y coordinated are basically chosen visually and the level of 'z' is inserted by hand, as a big advantage of the method can be mentioned time of execution as it does not require data flow, observations and topography plane can be created with low number of coordinate point. Another advantage that other above-mentioned methods cannot provide from foundational point of view – flexible reference level, in global system vertical coordinate is taken by the reference to sea level, so the coordinates of the project itself (infrastructure or/and building) must be projected with the reference to sea level, in case of Revit Topography tool, reference

level can be, for example, chosen as ‘0 level’ of the infrastructure, so this way, amount of ground soil works will be visually determined, also it will use less operational capacity so the program runs faster.

In case of tunnel project, the shape of the top surface is not the level where the drawings are executed, so the 3D modelling requites the design of inner soil masses with all necessary inputs in case of layers geometry and mechanical properties, both of the inputs are taking role not as much as in producing engineering drawings, but for physical analysis of soil deflections and pressures that Tunnel Buring machine must apply:

The geometrical forms of soil layers combining with tunnel alignment and transversal tunnel section data give the clear understanding of TBM path through soils and it is visible which types of soils are entered, knowing the mechanical properties of every soil layer, the pressure that TBM should apply can be estimated, it can be linear if TBM goes through 1 type of soil or multi linear if TBM goes through several soil layers combining on one phase.

The methods for estimating the soil geometry are usually boil down to borehole analysis, which are the kind of ‘on site’ observations. Boreholes have relatively small diameters, and their depth is estimated by the level of interest, for tunnel projects they are done along the tunnel projected alignments, the differences of soil on each borehole give the idea of inner structure of soil masses. Also, the water table level should be estimated, as it directly reacts to the applied pressure by face of TBM, in comparison to soil, water does not have any friction angle, so the pressure by water which is applied horizontally is equal to the vertical one.

As soon as the topography form with inner soil layers are constructed, the geometry of tunnel can be integrated, depending on LOD, the model of tunnel can consist of different amount and kind of elements, law level of details includes only the alignment of the tunnel and radius/diameter of TBM (if this is the methos that is used), higher levels of details can include tunnel rings, backfilling, still pipe umbrella (if they are used), steel arches (usually used for conventional method) and etc. Higher levels of development are used for excavational management of the tunnel (fabrication or as-build stage), while for understanding the soil dynamics and risks, the law level of details which includes only tunnel alignment and diameter is enough, as it gives the correct estimation of excavation volumes for the soils, however the soil masses modelling requite high details level as it should combine, as it is mentioned above, correct geometrical shape of the layers (as correct as site observation with boreholes and layer modelling can provide), so not only the total volume of the soil is estimated but individual volumes of different types of soils.

Above mentioned steps lead to the obtaining of developed 3D model with high Level of details for geometry, especially the ground surface terrain geometry, and Level of details for information inserted, as different types of soils are characterized with different mechanical properties. Such a model can be transferred to the software working on FEM (Finite element model) basis for structural and geotechnical analysis of the section.

In the context of tunneling and underground infrastructure, the BIM-to-FEM transition faces unique complexities due to the soil-structure interaction (SSI) and the sequential nature of excavation. The interoperability process must bridge the gap between a static geotechnical BIM and a time-dependent numerical analysis.

Discretization of the Soil-Structure Interface:

A critical stage in the tunneling workflow is the definition of the interface between the lining and the ground.

- Interface Elements: The interoperability protocol must automatically generate interface elements at the extrados of the tunnel lining. These elements account for friction and potential slippage, which are mathematically represented in FEM but often only implicitly defined in a BIM environment.

- Meshing Transitions: Interoperability scripts often manage "Graded Meshing," ensuring a high density of finite elements near the tunnel face where stress gradients are high, and a coarser mesh toward the far-field boundaries.

In tunneling, BIM-FEM interoperability shifts from a structural focus to a geo mechanical focus. The process is not merely a transfer of geometry but a transfer of state variables and construction sequences. For a thesis, it is essential to highlight that the "Analytical Model" in tunneling must include the volume of the excavated ground and the surrounding stress field, making it a significantly more data-intensive exchange than traditional building interoperability.

4D BIM: Temporal Analysis and Construction Sequencing:

4D BIM involves the synchronization of the 3D geometric model with the construction schedule (e.g., Primavera P6 or MS Project). In tunneling, this is critical because the structural stability of the excavation is time dependent.

- Sequential Excavation Simulation: For methods like NATM (New Austrian Tunneling Method), the 4D model visualizes the lag between excavation and support installation. This allows for the verification of "stand-up time" and ensures that the FEM analysis reflects the actual construction stages (e.g., top heading → bench → invert).

- Logistical Conflict Resolution: Tunneling often occurs in constrained environments with single-entry points. 4D analysis simulates the movement of the TBM (Tunnel Boring Machine), segment delivery, and muck removal, identifying spatial-temporal "bottlenecks" where equipment or personnel schedules overlap.

- Settlement Monitoring Integration: High maturity 4D models link real-time sensor data (e.g., total stations or piezometers) to the timeline. This allows engineers to compare "predicted vs. actual" ground subsidence at specific timestamps, triggering safety protocols if thresholds are exceeded.

5D BIM: Automated Quantity Take-Off (QTO) and Cost Control:

5D BIM integrates cost data into the 4D-linked model, allowing for real-time financial forecasting based on the geometric and temporal progress of the tunnel.

Chapter IV: Development of a parametric BIM model for tunnel and terrain representation

Following chapter is dedicated to obtaining the dynamic parametric modelling (Definition of dynamic model look at Chapter 1: introduction; Passage 1.3: Work objectives). During the case study execution two methods were used to create the dynamic tunnel model:

First method: Importing the three-dimensional tunnel model from Revit to Dynamo

Second method: Inserting the coordinates using AutoCAD alignment into code blocks of Dynamo

As it can be noticeable from methods descriptions, the platform for model definitions was Revit's visual programming Plug-in – Dynamo, version Dynamo 2.13, which is default version integrated in Revit version 2023.

4.1. Software definition and application for tunnel modelling

Dynamo is a visual programming environment integrated into Autodesk Revit, designed to extend and automate BIM workflows through parametric and algorithmic modeling. It allows users to create scripts by connecting graphical nodes that represent functions, data inputs, and logical operations, without the need for traditional text-based programming languages. Dynamo operates directly on Revit elements, enabling the creation, modification, and management of BIM objects based on rules, parameters, and external data.

One of the main advantages of Dynamo is its ability to manage parametric relationships between geometric, structural, and geotechnical variables. In the context of tunnel modeling, this capability is particularly relevant, as tunnels are linear infrastructures characterized by repetitive geometry, strong dependency on alignment data, and continuous interaction with surrounding ground and surface structures. Dynamo allows tunnel geometry—such as axis alignment, depth, diameter, and lining thickness—to be generated and updated automatically based on input parameters, ensuring consistency throughout the model.

Furthermore, Dynamo facilitates the integration of external datasets into the BIM environment. Geotechnical parameters, settlement profiles, or analytical results can be imported from spreadsheets or calculation tools and directly linked to Revit elements. This feature is especially beneficial for tunnelling projects, where soil stratigraphy, ground movement predictions, and structural response must be continuously correlated with spatial and geometric data. By using Dynamo, these relationships can be formalized into a repeatable and transparent workflow.

Another significant benefit of Dynamo for tunnel modeling is its capability to automate repetitive tasks and reduce modeling errors. The generation of tunnel segments, lining rings, or excavation stages can be automated along the tunnel alignment, while maintaining control over parameter variations. This is particularly useful when assessing multiple scenarios or when applying analytical methods along extended tunnel sections, as is often required in settlement and damage assessment studies.

In addition, Autodesk Dynamo supports the creation of custom analytical outputs within the BIM model. Parameters such as maximum settlement, angular distortion, or damage classification indices can be calculated externally and then assigned to building or tunnel elements within Revit. This enables a direct link between numerical analysis and BIM-based visualization, improving result interpretation and supporting decision-making processes.

In summary, Dynamo enhances Revit's capabilities by introducing parametric control, automation, and data integration, making it a powerful tool for tunnel modeling within a BIM framework. Its use is particularly suitable for urban tunnelling projects, where complex interactions between tunnel geometry, settlement distribution, and existing buildings must be analyzed in a structured, efficient, and reproducible manner. For these reasons, Dynamo represents an effective platform for implementing and validating the BIM-based methodology proposed in this thesis.

4.2. Tunnel modeling

4.2.1 Tunnel central axis

The most important geometrical data that must be available in Dynamo space is the central alignment axis of the tunnel, as all the theoretical formulas proposed in passage 2.3 theoretical background are based on the depth of the when the reference is taken from the central axis of the tunnel, furthermore, making the parametric model based on the coordinates of central axis is giving user all control on design parameters of the tunnel such as geometrical shape and diameter of the tunnel as distance from the central axis to periphery.

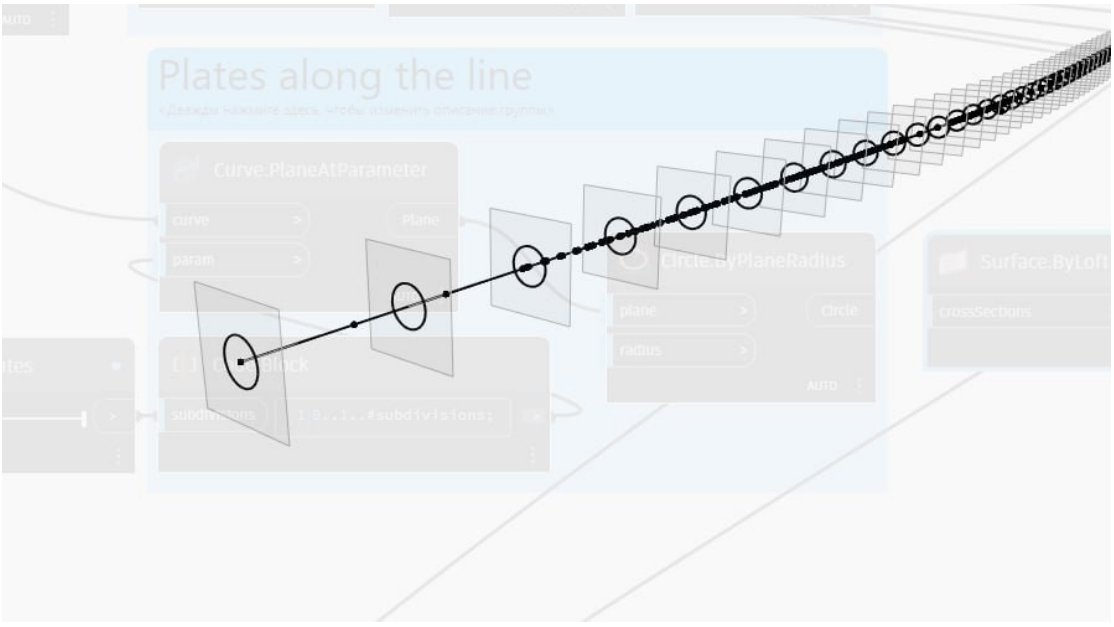

Figure 4.1. Central axis of the tunnel in Dynamo space

Modeling a tunnel by relying on its central axis (alignment) represents a practical and efficient approach for both geometric definition and analytical consistency. The tunnel axis constitutes the

primary reference element of the infrastructure, as all geometric, structural, and construction-related characteristics of the tunnel are defined with respect to this line.

From a geometric standpoint, the central axis allows the tunnel to be modeled as a parametric linear element, along which cross-sectional properties such as diameter, lining thickness, or excavation profile can be generated and repeated. This approach simplifies the creation of the tunnel geometry, particularly for long underground infrastructures, as it avoids manual modeling of individual sections and ensures continuity and coherence along the entire tunnel length. Any modification to the alignment—such as changes in depth, curvature, or gradient—can be propagated automatically to the entire tunnel model. Relying on the tunnel axis is also advantageous from an engineering and analytical perspective. Ground movements induced by tunnelling, including vertical settlements and horizontal displacements, are commonly evaluated as functions of the distance from the tunnel centerline. Settlement trough formulations, angular distortion calculations, and damage assessment methods are all intrinsically referenced to the tunnel axis. Therefore, defining the tunnel geometry based on its central axis ensures direct compatibility between the BIM model and the analytical models used for ground–structure interaction assessment.

In addition, the use of a central axis facilitates the integration of geotechnical and structural data. Soil stratigraphy, geotechnical parameters, and predicted settlement profiles can be projected or evaluated at specific chainages along the tunnel alignment. This allows a consistent correlation between longitudinal tunnel position, subsurface conditions, and surface building response, which is essential for damage classification in urban environments.

From a modeling workflow perspective, an axis-based approach improves model clarity, flexibility, and computational efficiency. The tunnel can be discretized into segments or chainages along the axis, enabling automated generation of tunnel components, excavation stages, and analytical outputs. This is particularly beneficial when implementing parametric or BIM-based methods, as it supports repeatability, scenario analysis, and future model updates with minimal manual intervention.

4.2.2 Revit → Dynamo Tunnel model interoperability

As input geometry for the dynamic parametric model, a 3D tunnel model in Revit format was provided by INFRATRASPORTI.TO S.R.L. It is important to note that, initially, the coordinate system of the tunnel model can be arbitrary. However, to ensure consistency, all additional elements —including terrain, existing buildings, and other infrastructures—must conform to the same coordinate system and origin. This ensures that the complete model of the urban environment, together with the future tunnel, is aligned within a unified spatial reference, allowing meaningful spatial and structural analyses. Upon opening the provided *.rvt* file, a corresponding Dynamo workspace was created. Using the *Select Model Elements* node, any geometry in solid form can be transferred into the Dynamo environment.

At this stage, the tunnel model exists as a static solid geometry, which is suitable for visualization but lacks the dynamic parametric properties required for advanced analyses. Specifically, central axis coordinates of the tunnel are essential for modeling soil–structure interaction and for evaluating potential impacts on surrounding buildings. Therefore, a procedure was developed to extract the tunnel's central axis and convert the model from a static representation into a dynamic, parametric form.

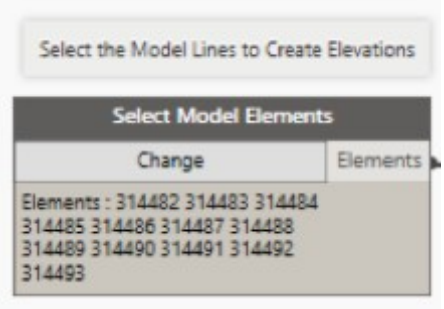

Figure 4.2. Select Model Elements node

The procedure is as follows:

1. Geometry Decomposition – The *Geometry.Explode* node is applied to the solid tunnel geometry. This operation decomposes the model into its constituent elements, providing the alignment of individual construction rings.

2. Bounding Box Generation – The *Box.ByGeometry* node is first applied to enclose the entire tunnel in a single bounding box. While this provides a global reference, it is not yet useful for dynamic alignment. By applying *Box.ByGeometry* a second time, separate bounding boxes are generated for each construction ring.

3. Center Point Extraction – Using the *BodyCenter* node, the mass centers of each ring's bounding box are computed. These points approximate the central axis of the tunnel.

4. Axis Construction – The *NurbsCurve.ByPoints* node connects the extracted center points, resulting in a continuous curve that precisely represents the tunnel's central axis.

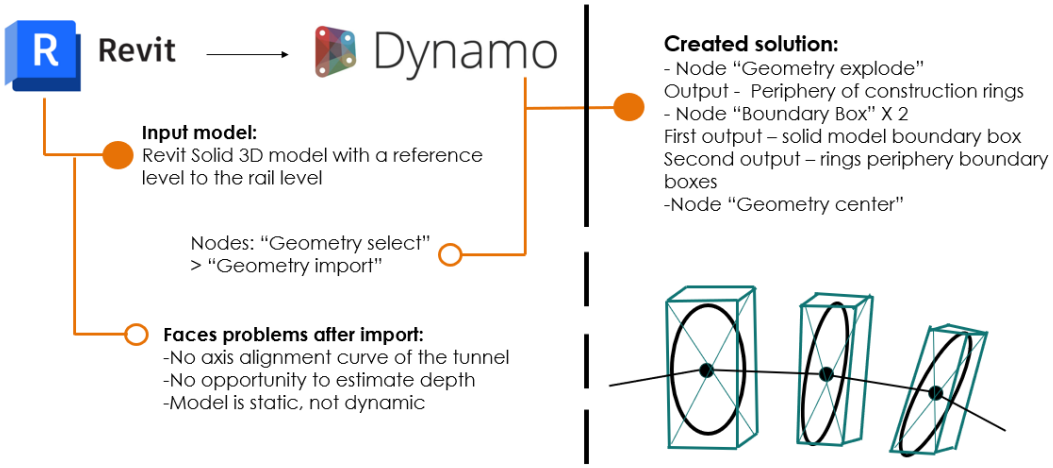

Figure 4.3. Recap of interoperability process

At this stage, the main output—the tunnel central axis—is fully integrated within the Dynamo environment and available for parametric manipulation. To facilitate discretization suitable for user-defined analyses, *the EqualChordLength* node is applied to the central axis, creating a series of evenly spaced points along its length. A perpendicular plane is then defined at each discretized point, allowing the tunnel diameter to be assigned as a dynamic parameter that can be adjusted according to the designer's input. Consequently, the transversal size of the tunnel becomes fully parametric and responsive to user-defined modifications.

During the implementation, it was observed that the obtained model became too computationally heavy for the operational capacity of the PC. The *Geometry.Explode* node generated approximately 150,000 individual elements, significantly affecting performance and usability. To address this, a strategic decision was made to reconstruct the tunnel using only the already known coordinates of the centroids, which provided almost 100% accuracy. Instead of processing all 150,000 elements, only four key points—corresponding to locations where the tunnel changes geometric direction—were used. All subsequent steps, including discretization along the axis, creation of perpendicular planes, and assignment of tunnel diameter as an input parameter, were maintained exactly as before. This approach ensured that the dynamic parametric behavior of the tunnel model was preserved while drastically improving computational efficiency. All nodes used in this procedure will be presented and described individually in the following sections:

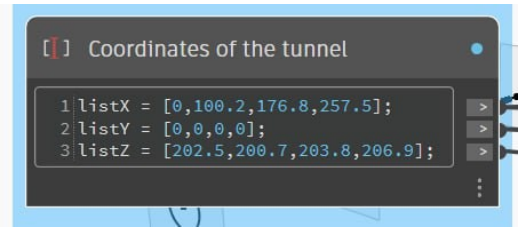

Figure 4.4.Code Block. Principal coordinates input

In Dynamo, a Code Block is a versatile node that allows users to write short scripts or expressions in DesignScript, Dynamo's native scripting language. Unlike standard nodes, which often require multiple inputs and outputs, a Code Block can execute complex mathematical operations, define variables, create lists, or generate geometrical data with a compact syntax. Its flexibility makes it particularly useful for parametric modeling tasks where repetitive or patterned operations are required.

One common application of a Code Block in tunnel modeling is for coordinate input. Coordinates of key points—such as the centroids of tunnel rings or points where the tunnel alignment changes—can be manually entered or generated in a Code Block as numeric values. For example, a simple Code Block may define three points along the X, Y, and Z axes:

X = [0, 100.2, 176.8, 257.5];

Y = [0, 0, 0, 0];

Z = [202.5, 200.7, 203.8, 206.9];

These lists represent the coordinates of points in 3D space, which can then be converted into actual point geometry using the *Point.ByCoordinates* node.

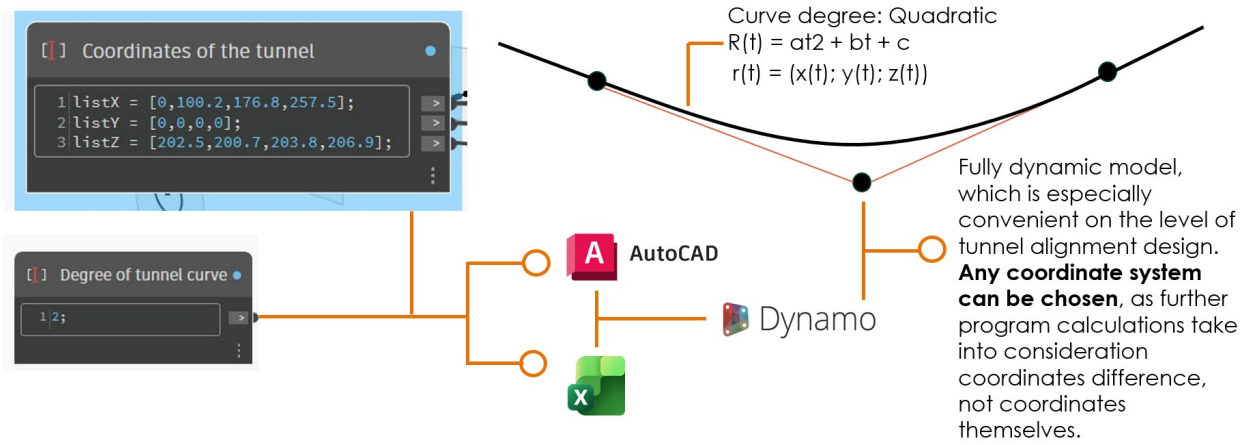

Figure 4.5.Tunnel alignment construction recap

Why Coordinates Are Divided into Lists:

In Dynamo, coordinates are often divided into separate lists for X, Y, and Z components because geometric nodes like *Point.ByCoordinates* expect each coordinate axis to be provided as a list or a single value. By separating the axes:

- Correspondence is maintained: The first element of each list corresponds to the X, Y, and Z components of the first point; the second elements define the second point, and so on.
- Flexibility in data manipulation: Operations such as scaling, offsetting, or transforming points can be applied independently along each axis.
- Compatibility with list management nodes: Nodes like *List.Map* or *List.Combine* require structured input, and separating coordinates into lists allows efficient parametric control and automation.

4.3. Applied code nodes workflow

In the context of tunnel modeling, dividing coordinates into lists enables the construction of the tunnel axis from a minimal set of key points, allows easy discretization along the axis, and ensures that parametric modifications (e.g., shifting the tunnel in any direction) can be applied efficiently while preserving alignment accuracy.

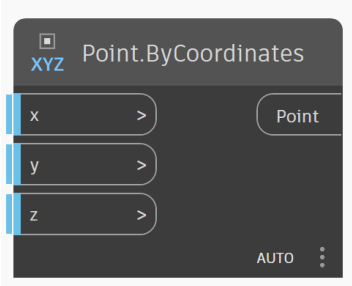

Figure 4.6. Points.ByCoordinates Node

In Dynamo, the *Point.ByCoordinates* node is fundamental for constructing geometrical points in 3D space. This node allows users to convert numerical coordinate values into actual physical points that exist in the Dynamo modeling environment, bridging the gap between abstract data and a visible geometric representation. In other words, it is the node where the model transitions from purely numerical inputs (lists of X, Y, and Z values) to a physical, manipulable geometry within the parametric workspace.

Inputs

The node accepts the following inputs:

1. X – The X-coordinate of the point, which can be a single numeric value or a list of values.
2. Y – The Y-coordinate of the point, similarly either a single value or a list corresponding to X values.
3. Z – The Z-coordinate of the point, also either a single value or a list corresponding to X and Y.

When lists are provided for X, Y, and Z, each corresponding element across the three lists defines a unique point in 3D space. This ensures that the first elements of X, Y, and Z create the first point, the second elements create the second point, and so on.

Outputs:

- Point – The output is one or more Dynamo Point objects, which are now physical geometrical entities in the Dynamo environment. These points are visible in the workspace, can be referenced by other nodes, and can be used to generate further geometry such as lines, curves, surfaces, or parametric frameworks.

Significance:

The *Point.ByCoordinates* node is crucial in parametric modeling because it transforms raw numerical data—such as lists of centroids or key tunnel alignment points—into tangible points that can drive the geometry of the tunnel, discretization planes, and other dynamic elements. Once points are created, they can be connected using nodes like *NurbsCurve.ByPoints* to form curves or axes, thereby enabling the construction of a fully parametric, manipulable 3D tunnel model.

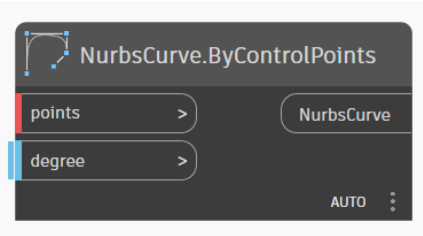

Figure 4.7. NurbsCurve.ByControlPoints Node

In Dynamo, the *NurbsCurve.ByControlPoints* node is used to create smooth, continuous curves that pass near or through a series of defined points. Unlike a simple polyline, which connects points with straight segments, a NURBS (Non-Uniform Rational B-Spline) curve provides a flexible and mathematically smooth representation, making it particularly suitable for modeling curved alignments such as tunnels, roads, or pipelines in a parametric environment.

Inputs:

The node requires the following inputs:

1. Points – A list of points that act as control points for the curve. These points influence the shape of the NURBS curve but are not necessarily located exactly on the curve. The curve's smoothness and shape are mathematically determined by the positions of these points.

2. Degree – The degree of the curve, which determines the polynomial order of the NURBS function and directly influences the smoothness of the curve. A higher degree results in a smoother curve that better approximates complex geometries, while a lower degree produces a simpler, less flexible curve.

Output:

- Curve – The output is a NURBS curve in the Dynamo workspace. This curve exists as a physical, manipulable geometry and can serve as the central axis for the tunnel model or as a guiding alignment for further parametric operations, such as discretization, plane creation, or cross-section placement.

The *NurbsCurve.ByControlPoints* node is essential for translating the discrete points along the tunnel alignment into a continuous, parametric axis. This axis serves as the backbone of the dynamic tunnel model, allowing further operations—such as discretization and diameter assignment—to be applied consistently along its length.

In addition, the degree of the curve must be specified as an input. For the scope of this project, a degree of 2 was chosen. This provides sufficient smoothness to accurately represent the tunnel's alignment, including its directional changes, while maintaining computational efficiency within the Dynamo environment.

Second-Degree NURBS Curves and Their Application in Tunnel Alignment:

In the context of NURBS (Non-Uniform Rational B-Spline) curves, the degree of a curve defines the polynomial order used to interpolate or approximate the curve between its control points. A second-degree (quadratic) curve uses a polynomial of order two, which produces a curve that is continuous, smooth, and capable of representing gentle bends with minimal inflection.

Second-degree curves are particularly advantageous for modeling tunnel alignments for several reasons:

1. Smoothness and Flexibility – Quadratic curves provide a smooth transition between control points while remaining computationally efficient. They allow for gradual changes in both horizontal and vertical directions, which is consistent with the design requirements of most urban tunnels.

2. Consistency with conventional design practices – Even in traditional, manual tunnel design, both horizontal and vertical alignments are typically defined using quadratic equations. For example, horizontal curves often use circular or parabolic transition segments to connect straight sections, and vertical profiles are designed with parabolic arcs to ensure smooth gradients. By using second-degree NURBS curves in Dynamo, the parametric model naturally mirrors these conventional design principles.

3. Adequate Approximation of Alignment Geometry – A quadratic curve is sufficient to capture all the primary directional changes of the tunnel without overcomplicating the model. Higher-degree curves, while mathematically smoother, are not necessary for typical tunnel geometries and may increase computational load without meaningful improvement in accuracy.

By selecting a degree of 2 in the *NurbsCurve.ByControlPoints* node, the tunnel alignment in Dynamo achieves a balance between accuracy, smoothness, and computational efficiency. This ensures that the central axis accurately reflects both the horizontal curvature and the vertical profile of the tunnel, while remaining fully parametric and adaptable for discretization, plane creation, and other modeling operations.

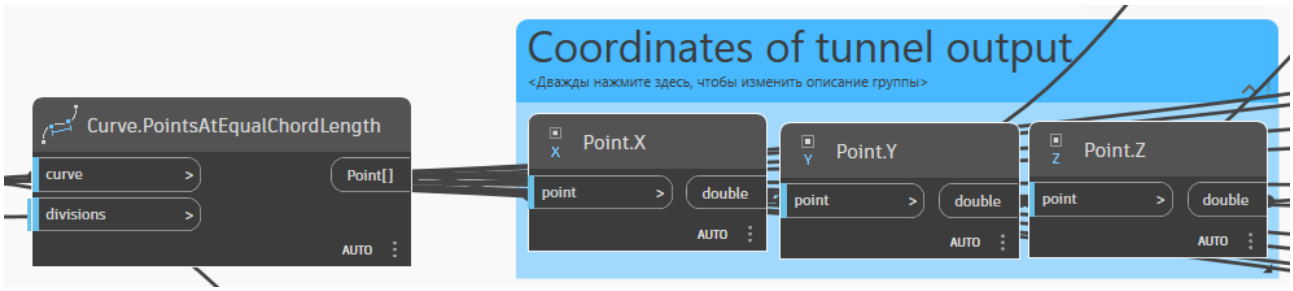

Figure 4.8. Curve.PointAtEqualChordLength Node and Coordinate parameters separate data

Once the tunnel's central axis is established as a continuous NURBS curve, it is often necessary to discretize the alignment into points spaced at regular intervals. This allows the model to be used for parametric operations such as cross-section placement, plane creation, or numerical simulations of soil and structural behavior. In Dynamo, this is achieved using the *Curve.PointAtEqualChordLength* node.

Curve.PointAtEqualChordLength

The *Curve.PointAtEqualChordLength* node takes a curve as input and generates a series of points along its length such that the distance between consecutive points (chord length) is constant. This process ensures uniform discretization, which is essential for parametric modeling and numerical analysis.

- Input:
    - Curve – The NURBS curve representing the tunnel central axis.
    - ChordLength – The user-defined distance between points along the curve. This parameter allows the designer to control the resolution of the discretization, balancing accuracy with computational efficiency.
- Output:
    - Points – A list of points evenly distributed along the curve, each representing a specific location along the tunnel alignment.

This node effectively converts the continuous alignment into a discrete set of points that can be further processed in parametric or numerical analyses.

Extraction of Individual Coordinates

Once the points along the alignment are obtained, it is often necessary to separate their X, Y, and Z components for numerical simulations, finite element analyses, or other computational procedures. Dynamo provides the nodes *Point.X*, *Point.Y*, and *Point.Z* for this purpose:

- Point.X – Extracts the X-coordinate of each point in the list, producing a numerical list of X-values.
- Point.Y – Extracts the Y-coordinate of each point in the list, producing a numerical list of Y-values.
- Point.Z – Extracts the Z-coordinate of each point in the list, producing a numerical list of Z-values.

By separating the coordinates into independent numerical sets, designers and engineers gain full control over parametric or numerical operations. Each coordinate axis can be processed individually, transformed, or used as input for simulations of settlement prediction, or structural response. Moreover, this approach allows seamless integration with finite element models, regression models, or other computational frameworks that require numerical coordinate input rather than geometrical points.

In summary, the combination of *Curve.PointAtEqualChordLength* for uniform discretization and the Point.X, Point.Y, and Point.Z nodes for coordinate extraction enables the transition from a continuous parametric tunnel axis to fully usable numerical datasets for simulation and engineering analysis

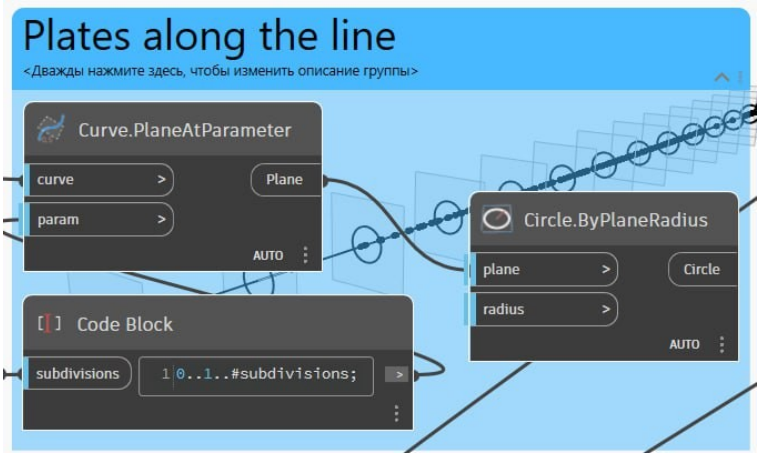

Figure 4.9. Curve.PlaneAtParameter node

Following the definition of the tunnel alignment through surveyed coordinate points and the generation of a *Nurbs.Curve* representing the axis with quadratic curvature behavior, the subsequent stage of the modeling workflow involves the creation of local reference planes along this spatial trajectory. This operation is performed using the *Curve.PlaneAtParameter* node in Autodesk Dynamo, which enables the transformation of the alignment curve into a geometrically controlled framework suitable for cross-sectional development.

The fundamental principle underlying this node is the evaluation of the curve's differential properties in order to determine its instantaneous direction. At any selected location along the curve, the tangent vector is computed, representing the local directional vector of the alignment. This tangent vector defines the normal direction of the constructed plane. Consequently, the generated plane is always perpendicular to the curve at the evaluated point. Since the tangent vector continuously adapts to changes in curvature, the orientation of the plane dynamically follows both horizontal and vertical deviations of the alignment.

This behavior ensures that the reference planes remain orthogonal to the tunnel axis regardless of spatial complexity. Whether the curve bends in plan, changes elevation, or exhibits combined three-dimensional curvature, the resulting planes maintain consistent perpendicularity to the direction of travel. This geometric relationship is essential in tunnel modeling, where cross sections must be aligned precisely with the axis to avoid distortions in subsequent solid generation.

From a modeling perspective, these planes establish a sequence of local coordinate systems distributed along the tunnel alignment. Each plane provides a stable geometric workspace in which cross-sectional profiles can be constructed. Because their orientation is directly derived from the directional properties of the alignment curve, they guarantee coherence between the global path of the tunnel and the local geometry of its sections.

Thus, the application of *Curve.PlaneAtParameter* constitutes a critical step in the parametric development process. It creates the geometric foundation required for the accurate definition of tunnel

cross sections and ensures that the evolving three-dimensional model remains fully consistent with the spatial behavior of the alignment curve.

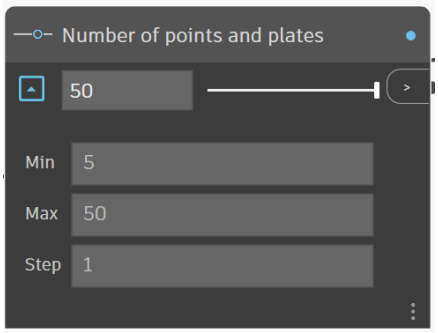

Figure 4.10. Number Slider node

Within the parametric modeling environment of Autodesk Dynamo, the *Number Slider* node represents one of the fundamental tools for controlled variable input. In contrast to fixed numerical values, the Number Slider introduces an adjustable parameter that can be interactively modified while remaining constrained within predefined limits. This functionality makes it particularly suitable for parametric tunnel modeling, where geometric relationships must remain both flexible and rigorously controlled.

The convenience of the Number Slider lies in its structured definition through several key inputs: minimum value, maximum value, step size, and the current numerical value determined within those bounds. By defining the minimum and maximum boundaries, the designer establishes a controlled numerical domain within which the parameter is allowed to vary. This prevents unintended or geometrically invalid values from being introduced into the model, thereby enhancing stability and computational reliability. In tunnel development, such constraints are essential when defining parameters such as section spacing, lining thickness, radius values, or offset distances, where exceeding logical bounds could compromise model integrity.

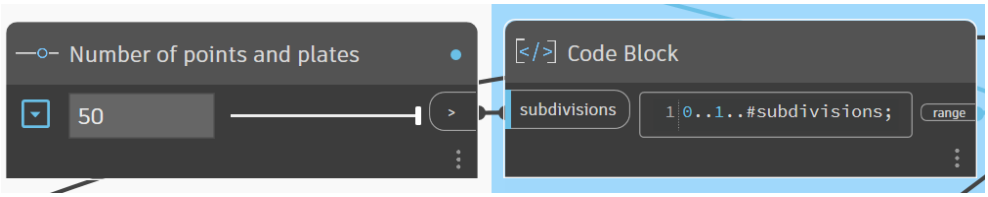

Figure 4.11. Subdivisions connected to Slider node

Following the generation of perpendicular reference planes along the tunnel alignment using *Curve.PlaneAtParameter* and the introduction of parametric control through the Number Slider, the next step in the modeling process involves establishing a systematic discretization of the tunnel axis. This discretization enables the controlled distribution of section planes along the entire length of the alignment.

In Autodesk Dynamo, this operation is implemented through a Code Block expression written as:

0..1..#subdivisions

This expression applies Dynamo's range syntax to generate a sequence of parameter values. The interval 0..1 represents the normalized domain of the previously defined Nurbs.Curve, where 0 corresponds to the beginning of the tunnel alignment and 1 corresponds to its end. By operating within this normalized parameter space, the discretization remains independent of the actual geometric length of the curve, ensuring proportional and scalable subdivision regardless of alignment modifications.

The term #subdivisions specifies the number of equally distributed values within this interval. The hash symbol indicates that the sequence is defined by the total number of divisions rather than by a fixed step size. Consequently, the output is a list of evenly spaced parameter values covering the entire domain of the curve.

The variable subdivisions is connected directly to a Number Slider, allowing interactive control over the density of discretization. By adjusting the slider, the user modifies the number of generated parameter values, which directly influences the number of planes created along the alignment. A higher subdivision value increases the number of reference planes, resulting in a finer geometric resolution of the tunnel model. Conversely, a lower value produces a coarser distribution suitable for preliminary modeling stages or conceptual analysis.

When this generated list of parameter values is supplied to the *Curve.PlaneAtParameter* node, Dynamo evaluates the curve at each value in the sequence and produces a corresponding series of perpendicular planes. This establishes a structured array of local coordinate systems distributed continuously along the full extent of the tunnel axis.

This step forms a critical connection between parametric control and geometric generation. The combination of normalized range syntax and slider-driven subdivision introduces scalability, adaptability, and precision into the modeling workflow. It ensures that the tunnel alignment can be discretized consistently and efficiently, providing the geometric framework necessary for subsequent cross-sectional definition and three-dimensional solid development.

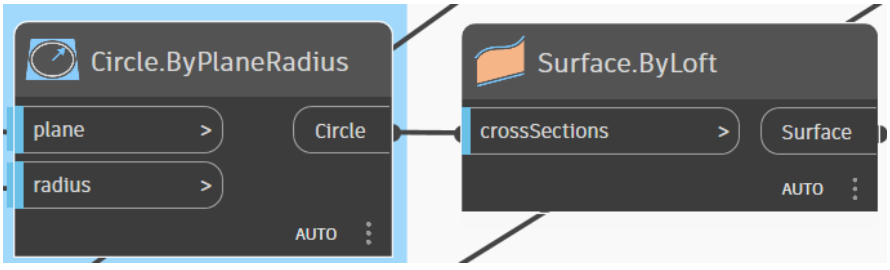

Figure 4.12. Circle.ByPlaneRadius connected to Surface.ByLoft

After establishing the discretized system of perpendicular reference planes along the tunnel axis, the next stage of the modeling process involves the definition of the tunnel cross-sectional geometry. In the case of mechanized excavation using an Earth Pressure Balance Tunnel Boring Machine (EPB TBM), the cross section can be reasonably approximated as circular, with a radius equal to the cutterhead radius of the boring machine.

Within the standard node library of Autodesk Dynamo, several predefined geometric constructors allow the creation of planar profiles directly on reference planes. Examples include *Rectangle.ByPlane*, *Triangle.ByPlane*, and *Polygon.ByPlane*, which enable the generation of basic and more complex planar geometries. For tunnel modeling under EPB TBM conditions, however, the appropriate node is *Circle.ByPlaneRadius*, which generates a circular profile constrained to a given plane with a specified radius.

This node requires two principal inputs. The first input is the set of perpendicular planes previously generated along the tunnel alignment. These planes define the spatial orientation and position of each cross section and are distributed according to the user-controlled subdivision density. The second input is the radius value corresponding to the TBM cutterhead. This parameter is connected to a Number Slider configured with a step increment of 0.10 m (10 cm), allowing controlled yet sufficiently precise variation of the excavation diameter.

Because the model is fully parametric, any change in the TBM radius propagates automatically through the geometric definition of the tunnel. As a result, subsequent operations—such as surface generation, solid modeling, or interaction analysis—are updated in real time. This dynamic responsiveness is particularly valuable during the design phase, where rapid evaluation of different excavation diameters may be required. For example, adjustments to the cutterhead radius can immediately influence calculated excavation volume, lining geometry, and predicted surface deformation responses.

Thus, the integration of *Circle.ByPlaneRadius* with user-controlled plane distribution and radius input establishes a robust parametric framework for tunnel cross-section generation. It enables efficient exploration of design alternatives and supports performance-based decision-making within the digital modeling environment.

In the final stage of the parametric tunnel modeling process, the individually generated circular cross sections are integrated into a continuous geometric entity representing the excavation envelope. This operation is performed using the *Surface.ByLoft* node in Autodesk Dynamo. The node connects a sequential set of planar curves—here, the circles distributed along the tunnel alignment—into a unified surface that visually and mathematically represents the tunnel shell within the Dynamo workspace.

The fundamental principle of *Surface.ByLoft* is the interpolation of a surface between multiple cross-sectional profiles arranged in a defined order. The node generates a smooth transitional geometry that passes through each input curve, preserving their relative orientation and position in space. Because the circular sections have been constructed on planes perpendicular to the tunnel axis, the resulting lofted surface follows the exact spatial trajectory of the alignment while maintaining geometric continuity between sections.

In general, Dynamo provides several alternative methods for surface generation. For example, *Surface.ByPatch* can create a surface from a single closed boundary curve, making it suitable for planar or isolated surface definitions. *Surface.BySweep* generates a surface by extruding a profile along a guiding curve, while *Surface.ByRevolve* produces rotational surfaces around a specified axis. Additionally, surfaces may be constructed through NURBS-based definitions or by stitching together multiple surface patches. Each of these methods serves specific geometric purposes depending on the structural logic of the modeled object.

However, for tunnel design based on discretized cross sections along a three-dimensional alignment, *Surface.ByLoft* represents the most appropriate solution. Unlike sweep operations, which assume a single guiding path and a profile that may not adapt automatically to complex spatial curvature, lofting directly connects the already oriented and distributed sections. Since the perpendicular planes were generated according to the tangent direction of the alignment curve, each circular profile is precisely aligned with the local tunnel axis. The loft operation therefore ensures a smooth and continuous envelope that accurately reflects both horizontal and vertical curvature without requiring additional geometric transformations.

Moreover, the lofting process maintains full parametric dependency. Any modification to the alignment curve, subdivision density, or TBM radius automatically updates the individual cross sections and, consequently, the resulting surface. This associative behavior is essential in parametric tunnel design, where iterative adjustments and scenario testing are integral to the engineering workflow.

Therefore, the application of *Surface.ByLoft* constitutes the logical culmination of the modeling sequence. It transforms discrete sectional geometry into a coherent three-dimensional surface model, providing both accurate spatial representation and dynamic responsiveness to design modifications. In the context of mechanized tunnel excavation modeling, lofting ensures geometric continuity, computational efficiency, and design adaptability, making it the most suitable surface-generation method for this specific application.

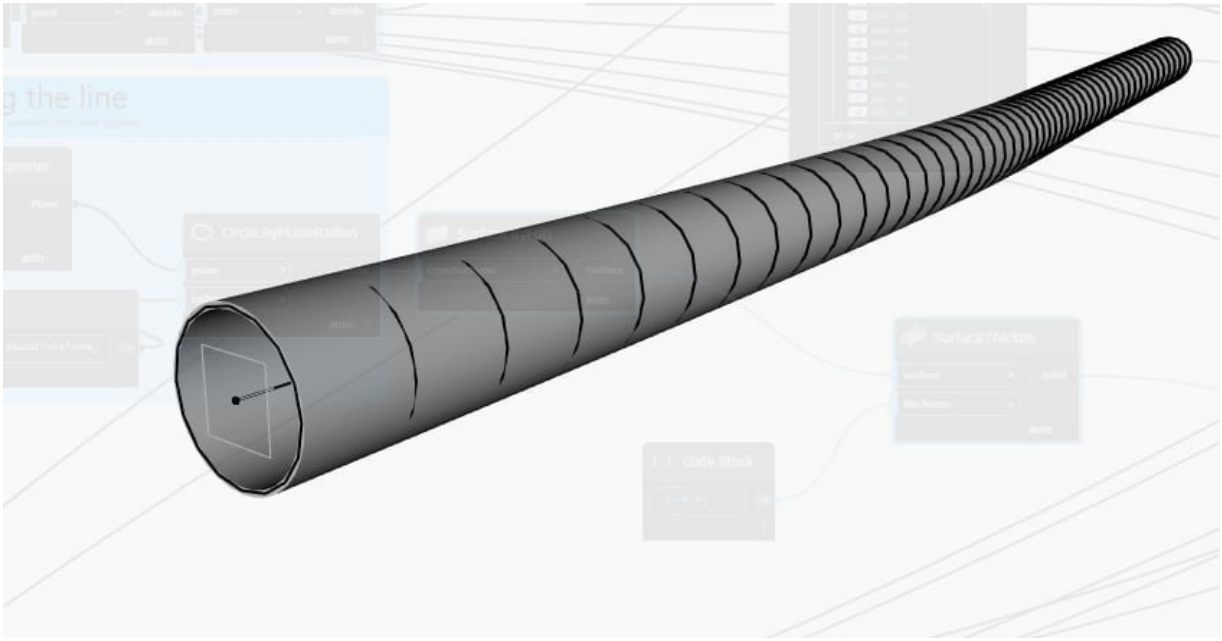

Figure 4.13. Dynamic Parametric model of Tunnel in Dynamo

As a final outcome of the described workflow, a fully parametric and geometrically consistent tunnel model is obtained within the environment of Autodesk Dynamo. The model integrates alignment definition, sectional geometry generation, discretization control, and surface creation into a single associative system in which all principal geometric parameters remain user-controlled.

The tunnel radius, representing the cutterhead radius of the TBM, is directly governed by a Number Slider, allowing immediate geometric updates in response to dimensional adjustments. Simultaneously, the alignment of the tunnel is defined through clustered coordinate points structured in the X, Y, and Z directions. These coordinates are fully accessible and modifiable by the user, ensuring complete control over the spatial configuration of the Nurbs.Curve that represents the central axis. Any modification to these coordinate values results in automatic recalculation of the alignment curve, the perpendicular planes, the circular cross sections, and ultimately the lofted tunnel surface.

The level of alignment discretization is likewise parameterized. By linking the subdivision variable to a Number Slider, the density of reference planes—and therefore the resolution of the resulting geometry—can be dynamically adjusted. This enables the model to function efficiently in both preliminary conceptual stages (with lower subdivision density) and more detailed geometric analyses (with higher subdivision density), without restructuring the underlying logic.

An additional advantage of this parametric framework lies in its interoperability. The generated model can be transferred directly into Autodesk Revit, enabling integration within a Building Information Modeling (BIM) environment. From there, or through CAD export procedures, the geometry can be further transferred into Autodesk AutoCAD, where it can be represented in three-dimensional form as well as in derived two-dimensional documentation such as planimetric views, longitudinal profiles, and transverse sections. This ensures compatibility with conventional engineering drafting workflows and facilitates multidisciplinary coordination.

Furthermore, the clustered coordinate data defining the alignment can be easily copied and transferred into spreadsheet software such as Microsoft Excel for numerical processing, statistical evaluation, or additional analytical operations. This bidirectional exchange between geometric modeling and numerical computation strengthens the analytical robustness of the design process.

Consequently, the final result is a fully adaptable parametric tunnel model that combines geometric accuracy, user-controlled flexibility, and interoperability across major design platforms. The system supports iterative design development, analytical evaluation, and documentation production within an integrated digital workflow, thereby fulfilling both engineering precision requirements and practical implementation standards

The subsequent chapter addresses the modeling of terrain within Autodesk Dynamo, with the principal objective of establishing a dynamic and fully parametric surface capable of responding to geometric modifications and deformation analysis. Since tunnel-induced settlements must be evaluated relative to the original ground configuration, the terrain model must provide both geometric accuracy and numerical accessibility of elevation data.

4.4. Terrain geometry creation in Autodesk Revit

The terrain geometry is initially generated in Autodesk Revit using the *Toposurface* tool (Toposolid in Revit 2026). This tool constructs a three-dimensional ground surface based on a set of spatial coordinate points. The modeling procedure is grounded in the definition of discrete points positioned in the horizontal (x–y) plane within the planimetric view, while their vertical position (z-coordinate) is assigned as a numerical input corresponding to the adopted coordinate reference system. In most engineering applications, elevations are defined relative to sea level or another standardized vertical datum.

From a geometric standpoint, the minimum number of points required to generate a surface is three, as three non-collinear points define a plane. However, while this represents the theoretical minimum, practical terrain modeling requires a substantially larger dataset. Increasing the number of input points enhances the resolution and fidelity of the triangulated surface generated by the Toposurface tool. A denser distribution of points allows for more accurate representation of natural terrain irregularities, slopes, and local variations.

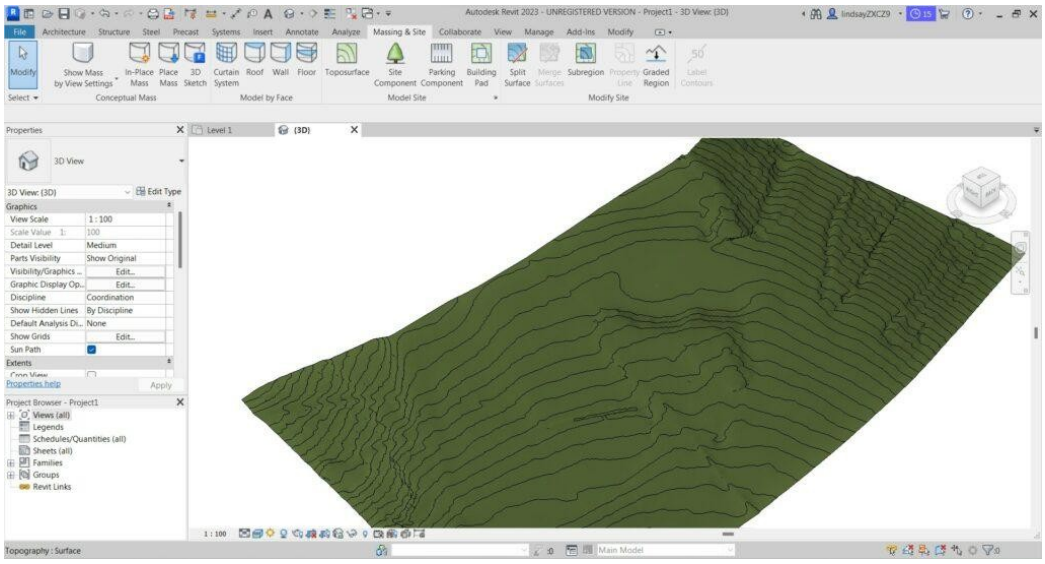

Figure 4.14. Terrain model in Autodesk Revit 2023

4.4.1 Automatic boundary generation

When points are inserted, Revit automatically determines the outer boundary of the terrain surface. This boundary is generated by computing the convex hull of the outermost points in the dataset. The convex hull represents the smallest enclosing polygon that contains all inserted points.

If no explicit boundary is defined by the user, Revit assumes that the terrain extends across the full convex envelope of the point cloud. However, the boundary can later be refined or constrained using subregions or building pads, which modify the triangulated mesh locally.

4.4.2 Surface Interpolation and Elevation Continuity

Between defined vertices, elevation is interpolated linearly across each triangular face. This means that within a single triangle, the surface is mathematically described by a planar equation derived from its three vertices. While this approach does not create a smooth curvature across triangles, the approximation becomes increasingly accurate as point density increases.

Therefore, the geometric precision of the terrain depends directly on:

- The number of elevation points
- Their spatial distribution
- The representation of terrain breadlines (if manually introduced)

A denser and strategically distributed point network results in smaller triangles and improved fidelity of terrain representation.

4.4.3 Importance of Geometric Precision for Deformation Analysis

The requirement for high geometric precision becomes critical in the context of deformation assessment. The ultimate objective of the parametric model is to evaluate vertical displacements induced by tunnel excavation. This is achieved by comparing the original elevation of a terrain point (z_initial) with its displaced elevation after simulation or geometric modification (z_final). The settlement value is defined as:

$$\Delta z = z_{initial} - z_{final}$$

Thus, the reliability of calculated deformation values depends directly on the accuracy of the original terrain model. Any geometric simplification or insufficient point density may introduce deviations that propagate into settlement calculations, potentially compromising analytical validity.

4.5. AutoCAD terrain model interoperability. CAD_link & CAD_import

In infrastructure design workflows, terrain data is frequently developed in Autodesk AutoCAD or related civil engineering platforms before being transferred into a Building Information Modeling environment. The interoperability between AutoCAD and Autodesk Revit therefore represents a critical stage in establishing a reliable and geometrically accurate terrain model intended for parametric processing. This transfer is primarily facilitated through the CAD Link and CAD Import functionalities within Revit, each of which provides distinct advantages depending on the project requirements.

In AutoCAD, terrain information is typically represented through 3D points containing explicit X, Y, and Z coordinates, contour polylines assigned with elevation values, 3D polylines, or triangulated meshes derived from survey data. These elements encode spatial information in a coordinate system that must remain consistent during transfer to Revit. Particular attention must be given to units, origin positioning, and vertical datum reference (commonly elevation above sea level), as inconsistencies at this stage may introduce systematic geometric deviations affecting subsequent deformation analyses.

The CAD Link tool enables the external DWG file to be referenced into the Revit project without embedding it permanently into the model database. In this configuration, the terrain geometry remains stored externally, while Revit maintains a dynamic connection to the source file. Any modifications made to the DWG file in AutoCAD—such as adjustments to elevation points or contour refinement—can be updated within Revit by reloading the link. This approach preserves file efficiency and supports iterative workflows, particularly in early project stages when survey data may undergo revision. Furthermore, linking allows control over insertion positioning, including origin-to-origin or shared coordinate placement, ensuring spatial alignment between the CAD terrain dataset and the BIM environment.

Alternatively, the CAD Import tool embeds the DWG file directly into the Revit project, converting the external data into a static internal reference. In this case, subsequent modifications to the original AutoCAD file do not automatically propagate into the Revit model, and any update requires manual re-import. Although this increases project file size, it eliminates dependency on external references and may be advantageous once terrain data has been finalized and validated.

Following either linking or importing, Revit enables the generation of a Toposurface directly from the CAD-based elevation data. During this process, 3D points or contour lines can be selected as input for terrain creation. Revit extracts their coordinate information and uses it to construct a triangulated surface model based on an internal triangulated irregular network (TIN) algorithm. Once the Toposurface is generated, the underlying CAD geometry can be hidden or removed, as the resulting terrain becomes a native Revit element fully integrated into the BIM environment.

4.6. Autodesk Revit to Dynamo Terrain model transfer and discretization

4.6.1 Terrain import technique

The subsequent and most critical stage of the workflow involves transferring the terrain model from Autodesk Revit into Autodesk Dynamo, where the parametric tunnel model has already been developed. At this stage, geometric consistency between the terrain and tunnel datasets becomes essential, as any discrepancy in spatial reference or scale may compromise the validity of deformation analysis and spatial coordination within the urban context.

The first and most fundamental requirement concerns the coordinate system. The coordinate reference framework used for designing the tunnel alignment must be identical to that employed for generating the terrain model. This includes consistency in origin definition, orientation of axes, and vertical datum reference. If the tunnel was modeled relative to shared coordinates or a specific survey benchmark, the terrain must be referenced within the same system. Failure to ensure this alignment would result in spatial displacement of the tunnel relative to the ground surface, leading to incorrect interpretation of depth, cover thickness, and interaction with surrounding infrastructure. Therefore, before transferring geometry into Dynamo, verification of shared coordinates and project base points in Revit is mandatory.

The second essential control parameter is scale consistency. The scale factor applied in both the tunnel and terrain models must be identical to prevent dimensional distortion. This requirement is directly linked to the definition of project units. Units of length—typically meters or millimeters in infrastructure projects—must coincide across both models. Any mismatch in units (for example, meters in one model and millimeters in another) would result in significant geometric misalignment, affecting distances, elevations, and calculated deformation values. Consequently, verification of project units in Revit prior to Dynamo integration is a critical validation step.

Once coordinate systems and unit settings are confirmed to be consistent, the terrain Toposurface can be accessed within Dynamo and integrated with the parametric tunnel model. At this point, both geometries coexist within a unified spatial framework, ensuring that the tunnel is positioned accurately beneath the terrain surface and within its surrounding urban environment. This spatial coherence forms the foundation for reliable settlement analysis, geometric intersection operations, and subsequent numerical evaluation of vertical displacements.

The transfer of terrain geometry from Autodesk Revit into Autodesk Dynamo represents a critical step in establishing a unified parametric environment in which both the tunnel and the surrounding ground surface coexist and interact. In a standard workflow, the terrain—created in Revit using the Toposurface tool—is referenced in Dynamo using the Select Model Element node. This node enables direct selection of the Toposurface as a native Revit element. Subsequently, the SelectElement.Geometry node is applied to extract the geometric representation of the terrain into the Dynamo workspace.

At this stage, the terrain is typically interpreted as a unified poly mesh or composite geometric object. Although geometrically accurate, this representation is static and lacks internal parametric structure within Dynamo. It does not inherently maintain a dynamic relationship with the tunnel model, nor does it provide immediate access to logically structured elevation data required for deformation analysis. Consequently, further geometric processing is necessary to transform the imported terrain into a dynamically controllable surface model.

The first transformation step involves applying the *Geometry.Explode* node to the extracted terrain geometry. This operation decomposes the composite object into its constituent geometric elements, which may include faces, edges, or boundary curves depending on the internal structure of the Topo surface. However, the resulting elements are returned as an unordered list, without hierarchical or elevation-based organization.

At this point, direct application of *Surface.ByLoft* is not feasible. Loft operations require a logically ordered sequence of curves to generate a coherent and continuous surface. Since the exploded geometry lacks inherent ordering, Dynamo cannot determine the correct sequence for surface reconstruction. Therefore, list management operations must be introduced to establish geometric structure.

To achieve this, representative elevation data are extracted from the decomposed elements. For instance, a point can be evaluated along each curve using *Curve.PointAtParameter*, and its vertical coordinate can be obtained via Point.Z. These elevation values serve as sorting keys in the *List.SortByKey* node, which organizes the curves according to their vertical position. Through this procedure, the dataset is structured into a coherent sequence corresponding to terrain elevation progression.

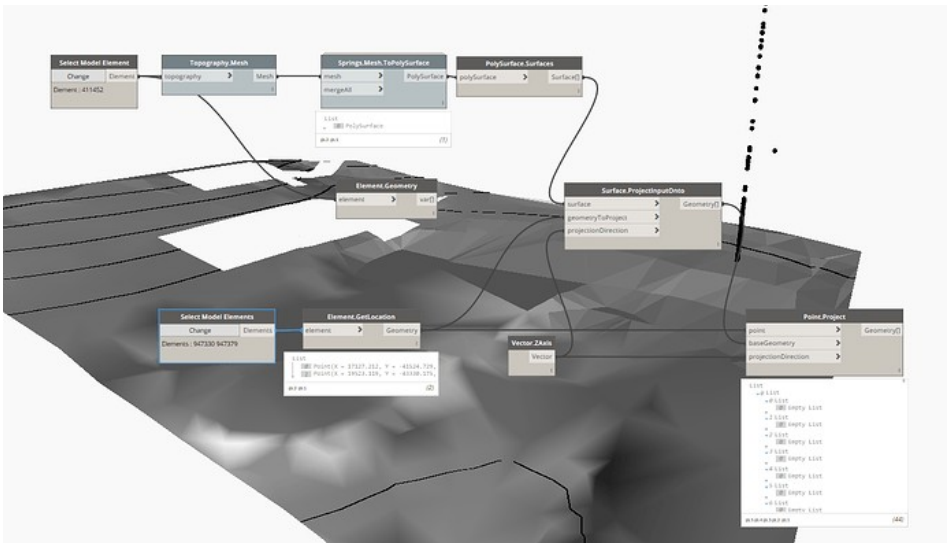

Figure 4.15. Example of terrain model in Dynamo

Once properly ordered, the curves can be supplied to the *Surface.ByLoft* node. The loft operation interpolates a continuous surface through the sequential curves, reconstructing the terrain geometry directly within Dynamo. Unlike the initially imported static poly mesh, the loft-generated surface is derived from explicitly organized geometric inputs and therefore becomes integrated into the parametric workflow. Any modification of elevation data, curve definition, or related parameters can propagate through the loft operation, enabling dynamic updates of the terrain model.

It should be noted that when the original Topo surface is based on a triangulated irregular network (TIN), complete geometric equivalence may not always be achieved through lofting contour curves alone. In such cases, alternative strategies—such as working directly with mesh faces—may provide a more accurate representation. Nevertheless, the described procedure establishes a logically structured and dynamically responsive terrain model within Dynamo.

Through this transformation—from static imported geometry to an internally reconstructed parametric surface—the terrain becomes fully integrated with the tunnel model. This integration ensures geometric coherence, analytical accessibility, and the capacity for subsequent deformation simulations within a unified digital modeling framework.

From a theoretical and methodological perspective, alternative techniques exist for generating a dynamic terrain model directly within Autodesk Dynamo. In addition to the standard node library, several specialized packages developed by the Dynamo community include nodes explicitly dedicated to terrain and topography processing. These nodes often contain terms such as *Terrain* or *Topography* in their naming conventions and are designed to interact more directly with Revit Toposurface elements.

Examples of such specialized nodes include *Topography.ExtractPoints*, *Terrain.MeshFromPoints*, *Topography.SmoothSurface*, and *Terrain.FromPoints*, which provide advanced functionality for meshing, extracting elevation points, converting Toposurfaces into structured mesh representations, or directly reconstructing surfaces suitable for analytical operations. These nodes allow for automated workflows that simplify the creation of a parametric terrain model, eliminating the need for manual decomposition of geometry and ordered list management. For instance, *Terrain.MeshFromPoints* can generate a continuous mesh directly from a set of elevation points, while *Topography.ExtractPoints* facilitates direct access to the vertices of a Revit Toposurface for parametric manipulation.

However, these advanced terrain-processing nodes are not part of the default Dynamo installation. They require the installation of external libraries or custom packages through the Dynamo Package Manager. The availability and compatibility of such packages depend on the specific Dynamo version integrated with Revit. In the present study, working within the Dynamo environment associated with Autodesk Revit 2023, the required terrain-specialized libraries were either unavailable or incompatible with the software version used. This limitation restricted the possibility of employing dedicated terrain nodes for direct parametric manipulation of the Toposurface.

Consequently, the procedure described in the previous section—based on selecting the model element, extracting geometry, decomposing it using *Geometry.Explode*, organizing elements through list management operations, and reconstructing the surface via *Surface.ByLoft*—was developed as an alternative solution. Although more methodologically explicit and requiring additional geometric structuring, this approach ensured full control over the reconstruction process and maintained compatibility with the standard node library available in the working environment.

The adoption of this custom reconstruction workflow therefore reflects both technical constraints and methodological rigor. By relying exclusively on universally available nodes, the developed approach guarantees reproducibility, version independence, and long-term applicability, while still achieving a fully dynamic and parametrically integrated terrain model within the Dynamo environment

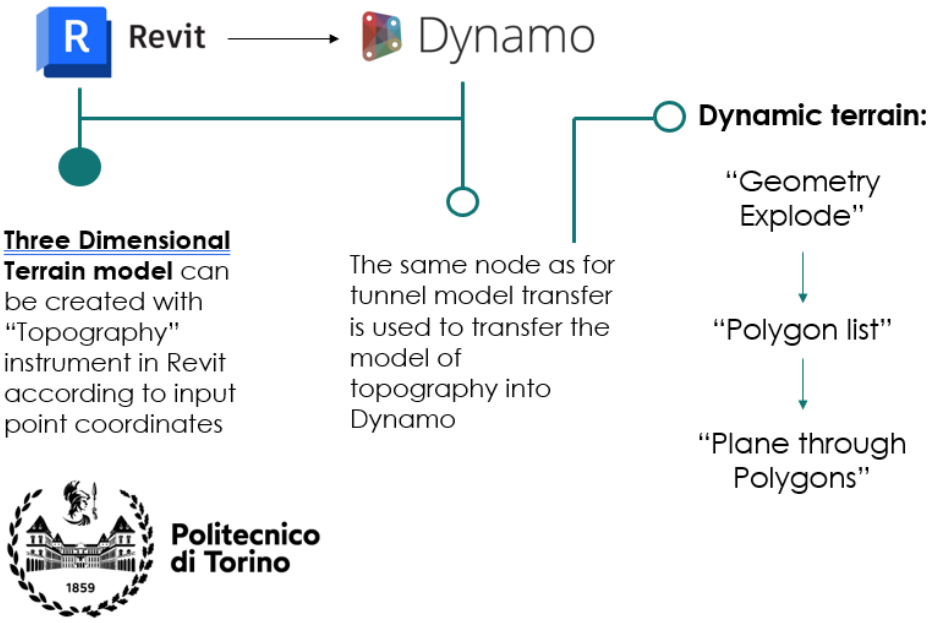

Figure 4.16. Dynamo Terrain Modeling Recap

4.6.2 Dynamo terrain model tunnel connected discretization

Once the terrain surface was reconstructed using the *Surface.ByLoft* node, the next essential step was to integrate it with the tunnel model, thereby forming a unified analytical system in which both the tunnel alignment and the surrounding ground surface could interact. The methodology developed relies on projecting the discretized tunnel axis onto the terrain surface, ensuring that the tunnel alignment respects the actual topography in planimetric coordinates while simultaneously accounting for the vertical elevation of the ground.

As a preliminary step, the tunnel axis was discretized into a series of points along its length. In the presented case study, the alignment was divided into fifty points; however, this number is adjustable and can be controlled dynamically via a Number Slider node. Each point of the discretized axis carries its X, Y, and Z coordinates, corresponding to the parametric definition of the tunnel alignment. For the purpose of projecting the tunnel onto the terrain, only the X and Y coordinates were retained, while the Z coordinate was assigned a constant value positioned above the highest point of the terrain.

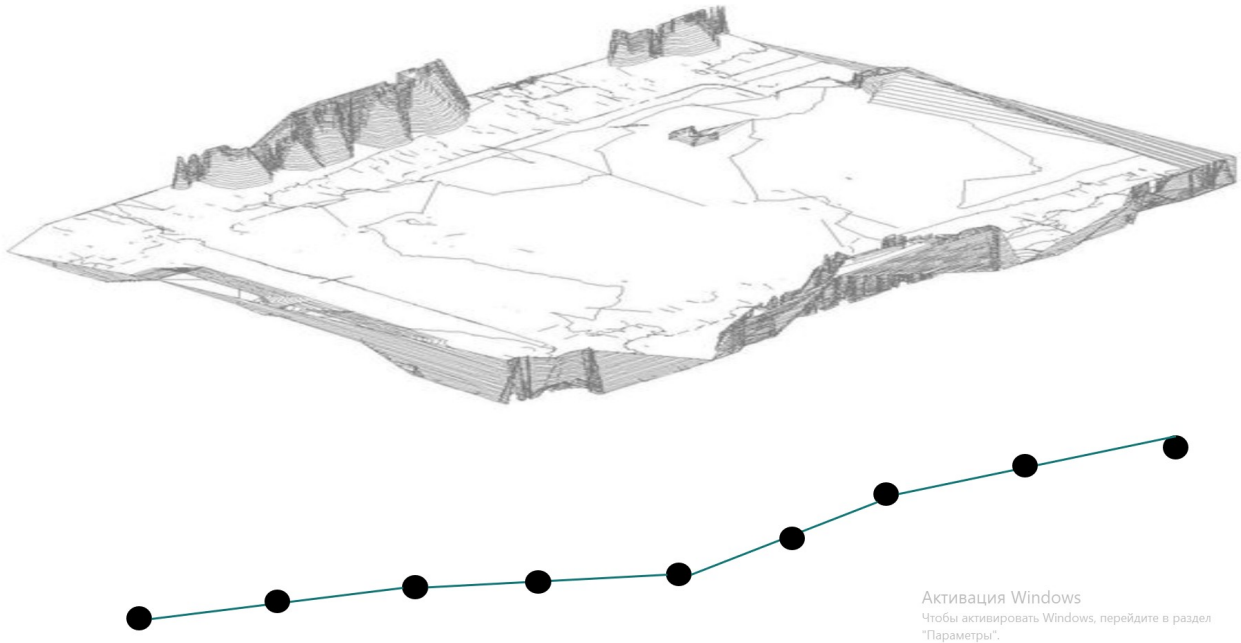

Figure 4.17. Tunnel axis discretization points under the terrain model [Symbolic Representation]

In the case study, the terrain elevation ranged between 230 and 240 meters above sea level, and the Z-coordinate for the projected points was set at 400 meters, providing a vertical offset of approximately 160 meters above the surface. This step ensured that all points were initially positioned above the terrain, avoiding intersection ambiguities.

Following this, the *Line.ByStartPointEndPoint* node was employed to connect each discretized tunnel point to its corresponding elevated point, effectively creating fifty vertical lines penetrating the terrain surface. These lines served as geometric probes for determining the exact intersection of the tunnel alignment with the surface.

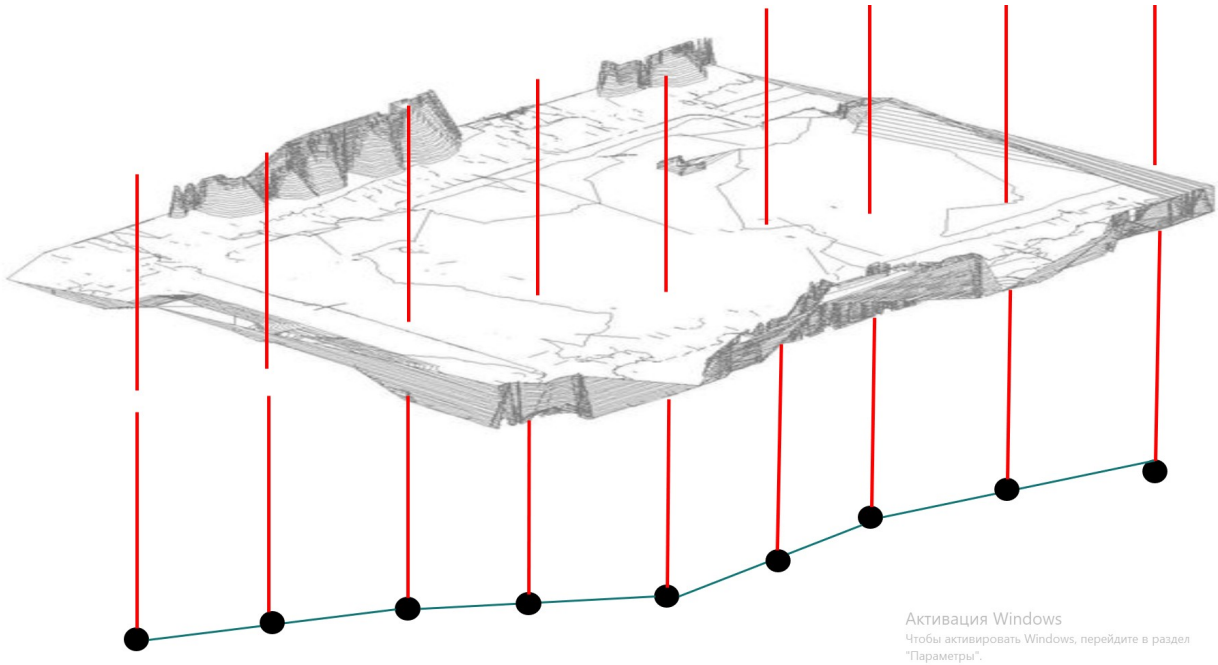

Figure 4.18. Connection of tunnel points to corresponding ones above terrain level [Symbolic Representation]

Subsequently, the *Geometry.Intersect* node was applied, taking as input the terrain surface and the vertical lines. The output consisted of points where each line intersected the surface, thereby providing precise X, Y, and Z coordinates corresponding to the topographic distribution of the terrain.

Finally, the resulting intersection points were used to reconstruct the tunnel axis in direct correspondence with the terrain. This was achieved through the *NurbsCurve.ByControlPoints* node, specifying a degree of one to ensure a piecewise-linear connection. By doing so, the reconstructed curve exactly coincides with all intersection points, maintaining both the horizontal planimetric alignment and vertical correspondence with the terrain surface.

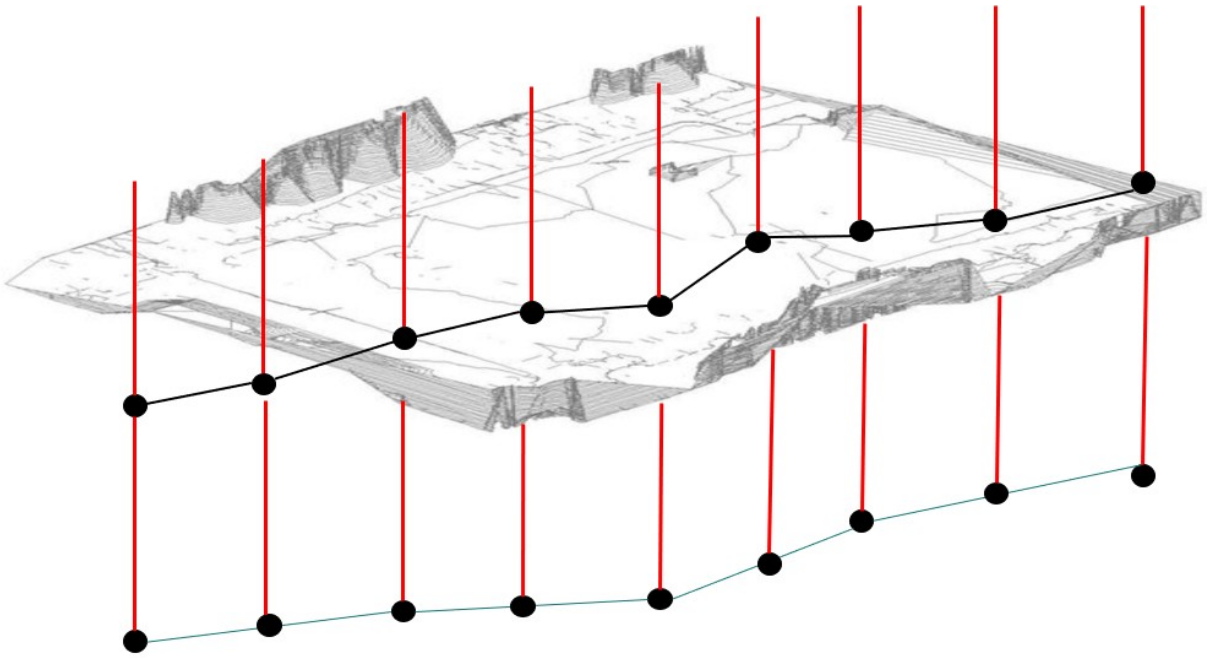

Figure 4.19. Output of Geomtry.Intersect node [Symbolic Representation]

This methodology establishes a fully parametric and analytically consistent relationship between the tunnel alignment and the surrounding topography. It allows the tunnel model to respond dynamically to changes in terrain geometry while preserving the discretization and structural characteristics of the original alignment. Moreover, the approach is fully compatible with parametric modifications in Dynamo, such that adjustments to the number of points, terrain surface, or tunnel alignment automatically propagate through the system, maintaining geometric coherence and analytical validity.

In the context of tunnel-induced ground deformation analysis, a fundamental requirement arises from the nature of both theoretical and empirical models of settlement distribution. The majority of existing models—whether derived from analytical solutions, numerical simulations, or empirical observations—are designed to represent deformation around a tunnel cross-section that is strictly perpendicular to the tunnel axis. This principle stems from the fact that soil displacement and stress distribution are inherently three-dimensional phenomena, but their variation along the tunnel alignment is often relatively smooth. Consequently, analytical and empirical formulations focus on the response of soil elements relative to the local tunnel cross-section, assuming a plane normal to the axis as the reference for evaluating vertical and horizontal displacements.

When integrating a tunnel model with a parametric terrain surface, this requirement introduces a significant geometric and computational challenge. The terrain surface itself is defined independently of the tunnel alignment and is represented as a lofted or meshed surface derived from contour lines or triangulated irregular networks. Its geometric structure is dictated primarily by topographic features such as slopes, valleys, and undulations, rather than by the orientation of the tunnel. As a result, the native discretization of the surface—based on surface vertices, faces, or loft-generated grid points—does not inherently conform to the local orientation of the tunnel axis. The spacing and orientation of mesh elements on the surface are often uniform in planimetric directions or follow terrain curvature, which generally does not align with the perpendicular planes required by soil deformation models.

Therefore, a direct application of standard surface discretization to tunnel-soil interaction analysis is

inappropriate. If points or mesh elements on the surface were used without adjustment, the resulting cross-sectional slices would not be perpendicular to the tunnel axis, violating the assumptions of classical soil mechanics models. Such misalignment can produce significant errors in both analytical and numerical simulations. For instance, vertical settlement profiles, lateral displacement fields, or stress distributions derived along non-perpendicular planes may underestimate or overestimate actual deformation, leading to inaccurate predictions of tunnel-soil interaction, ground settlements, and potential surface damage.

This issue is particularly critical when the tunnel alignment is curved or when the topography exhibits substantial variations. In these cases, the deviation between the terrain-based discretization and the perpendicular planes increases progressively along the tunnel axis. Consequently, any attempt to model soil deformation using a mesh or point set that follows the surface rather than the tunnel orientation would fail to satisfy the fundamental assumption of cross-sectional normality, rendering the analysis invalid for engineering purposes.

The solution to this problem requires the construction of a dedicated discretization system that is directly linked to the tunnel alignment. Each discretized plane must be oriented perpendicular to the local tangent of the tunnel curve at its corresponding point. Only by doing so can the deformation analysis at each cross-section accurately represent the local soil response. This approach necessitates a parametric workflow in which the tunnel alignment serves as the guiding geometry for generating perpendicular planes and projecting them onto the terrain, ensuring that subsequent calculations of settlement, displacement, and stress distribution remain consistent with the theoretical foundations of tunnel-soil interaction.

4.6.3 Vector system discretization

To generate tunnel-perpendicular planes along the alignment, a rigorous understanding of vector mathematics is essential, particularly the concept of the vector cross product, which provides a fundamental tool for determining spatial orientation and constructing orthogonal geometries. In three-dimensional space, a vector is defined as a quantity possessing both magnitude and direction, commonly represented by its components along the X, Y, and Z axes. Vectors are used in computational design software, such as Dynamo, to describe directions of edges, tangents of curves, or orientations of planes in a parametric environment.

The cross product is a binary operation between two vectors, denoted as A × B, which produces a third vector that is perpendicular to both input vectors. Mathematically, for two vectors $A=[A_x, A_y, A_z]$ and $B=[B_x, B_y, B_z]$, the cross product is defined as:

$$A \times B = \begin{bmatrix} A_y B_z - A_z B_y \\ A_z B_x - A_x B_z \\ A_x B_y - A_y B_x \end{bmatrix}$$

The resulting vector has a magnitude equal to $|A|\ |B| \sin\theta$, where θ is the angle between vectors A and B. Importantly, the direction of the resulting vector follows the right-hand rule, which establishes a consistent orientation in three-dimensional space.

The cross product has specific geometric interpretations depending on the relationship between the

two input vectors:

1. Perpendicular Vectors: If vectors A and B are perpendicular ($\theta = 90^{\circ}$), the sine term reaches its maximum value ($\sin 90^{\circ} = 1$), and the magnitude of the cross product equals the product of the magnitudes of the two vectors. The resulting vector is fully defined in direction and magnitude, forming an axis orthogonal to the plane spanned by A and B. This property is exploited in parametric modeling to construct planes perpendicular to a given direction, such as the tangent to a tunnel axis.

2. Parallel Vectors: If vectors A and B are parallel or anti-parallel ($\theta = 0^{\circ}$ or $\theta = 180^{\circ}$), the sine term equals zero ($\sin 0^{\circ} = \sin 180^{\circ} = 0$), and the cross product is the zero vector. This indicates that no unique perpendicular direction exists between the two vectors, a situation that must be avoided when generating orthogonal planes. In parametric workflows, special handling is required to prevent undefined orientations in the cross-product calculation.

3. Vectors at an Arbitrary Angle: When vectors A and B intersect at an angle θ that is neither zero nor ninety degrees, the magnitude of the cross-product equals $|A| \, |B| \sin \theta$, producing a vector perpendicular to both inputs. The length of this vector provides a quantitative measure of how "non-parallel" the two vectors are, while its orientation defines the unique perpendicular direction. This property allows precise construction of planes at arbitrary orientations relative to multiple vectors in space.

By leveraging the cross product in Dynamo, it is possible to compute normal vectors for each plane along a tunnel alignment. Specifically, the tangent vector of the tunnel curve serves as one input, and a secondary reference vector—typically the global vertical or another directional vector—is used to calculate a vector perpendicular to both. This perpendicular vector then defines the orientation of a plane that is locally normal to the tunnel axis, enabling the creation of cross-sectional geometries that satisfy the theoretical requirements of soil deformation models.

The theoretical framework of vector mathematics was subsequently applied in practice within the case study to generate a parametric system of cross-sectional points perpendicular to the tunnel alignment and projected onto the terrain surface. To initiate the process, two code blocks were created with numerical values of 1 and -1, which were individually connected to two instances of the *List.DropItems* node. The purpose of this operation was to impose a progressive direction along the discretized tunnel alignment, ensuring that all subsequent vectors respect the intended tunnel orientation and, by extension, its projection on the terrain surface.

The outputs of the *List.DropItems* nodes were then fed into the *Vector.ByTwoPoints* node, producing directional vectors that connect each point along the discretized tunnel alignment to its successive neighbor. These vectors represent the local tangent of the tunnel axis at each discrete point and serve as the primary input for defining planes perpendicular to the alignment.

To construct the geometry of the settlement basin on both sides of the tunnel cross-section, two instances of *the Vector.Cross* node were employed. The cross product requires two vectors: the first is the tangent vector along the tunnel, derived from the *Vector.ByTwoPoints* node, while the second is a reference vector, defined using the *Vector.ByCoordinates* node. In this case study, the reference vector was set with coordinates X = 0, Y = 0, and Z = 1, representing a vertical direction in global coordinates. The cross product thus produces two vectors perpendicular to the tunnel tangent at each discretized point.

To standardize the resulting vectors, the *Vector.Normalize* node was applied, producing unit vectors that are orthogonal to the tunnel axis but initially oriented in the same direction. This normalization step is critical, as it ensures that vector scaling and subsequent spatial manipulations are consistent across the entire alignment.

The next stage introduces parametric control over the analysis domain. Using the *Vector.Scale* node, each normalized vector is multiplied by a user-defined scalar value, supplied through a Number Slider node. This allows the width of the analysis area, corresponding to the lateral extent of potential soil deformation, to be directly controlled by the user. The scaled vectors define the positions of points at the boundaries of the analysis zone.

To generate the physical points in the Dynamo workspace, the *Geometry.Translate* node was employed. Two instances of this node were used for each discretized point: one translates along the positively oriented scaled vector, and the other along the negatively oriented vector. In this way, two points symmetric to the tunnel alignment are created for each discretized location along the projected axis, respecting both the perpendicular orientation and the user-defined width of the analysis domain.

Finally, the points generated on either side of the tunnel alignment were connected using the *Line.ByStartPointEndPoint* node, producing lines representing local cross-sectional boundaries of the potential deformation zone. To enable user-controlled discretization of these lines—thereby defining the resolution of the deformation analysis—the *Curve.PointAtEqualChordLength* node was applied. This node allows points along each line to be distributed evenly according to a user-defined chord length, providing parametric control over the precision of the analytical grid for soil deformation computations.

Through this methodology, a fully parametric and dynamically responsive set of cross-sectional points and lines was created along the projected tunnel alignment. The resulting geometry is consistent with the theoretical requirement of perpendicular cross-sections, while offering the flexibility to adjust both the lateral extent and the discretization density of the analysis area. This ensures that subsequent calculations of settlement, lateral displacement, or stress distribution can be conducted with both geometrical fidelity and parametric control.

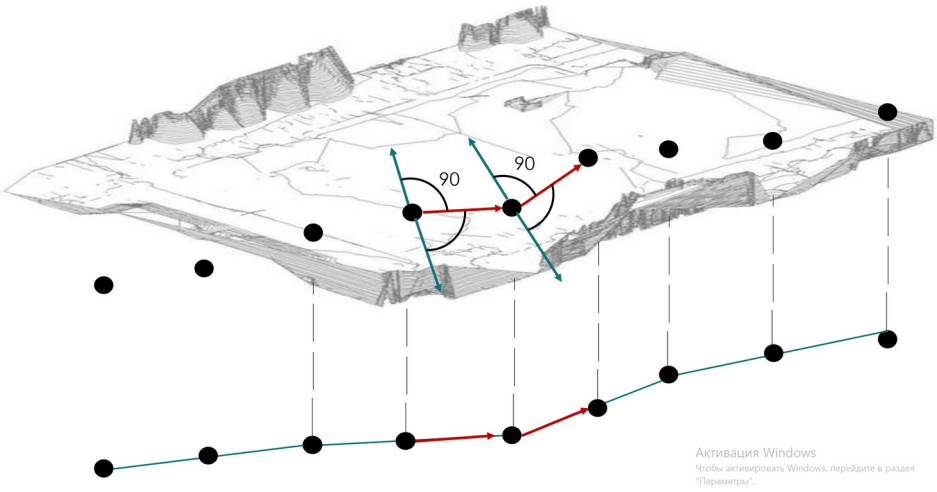

Figure 4.20. Sectional Vectors visualization [Symbolic Representation]

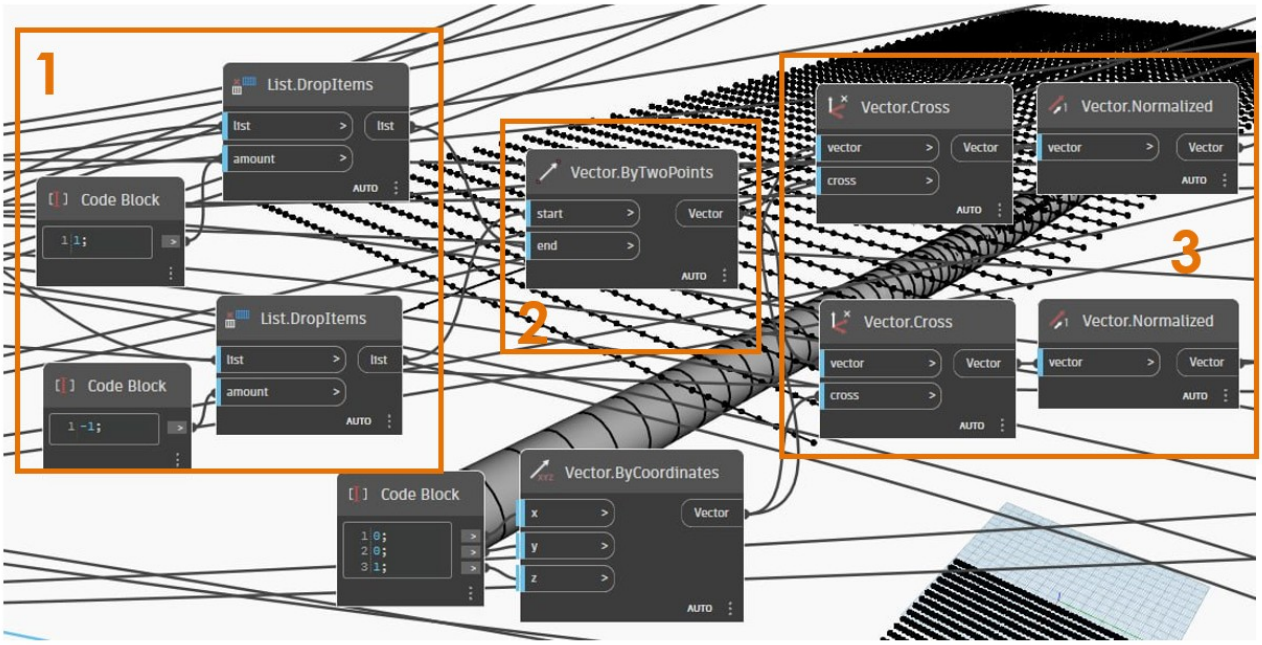

Figure 4.21. Visual Dynamo workflow

1. As an initial step, the discretized points along the tunnel alignment must be organized into an ordered list to provide the program with a clear definition of the tunnel's progression direction. The values assigned in the code blocks (−1 and 1) serve as directional indicators, ensuring that the computational workflow correctly interprets the sequence of points and establishes a consistent orientation for subsequent vector and cross-sectional operations.

2. The directional vector representing the local orientation of the tunnel is constructed between two consecutive discretized points along the alignment, such that it follows the intended progression of the tunnel. This ensures that each vector accurately reflects the tangent of the tunnel axis at that segment and provides a consistent basis for defining perpendicular planes and associated geometric operations.

3. The cross product of each vector along the tunnel alignment and its corresponding reference vector on the surface is normalized to a unit magnitude. By constraining the resulting vectors in this manner, they are ensured to be parallel within the X–Z plane while remaining properly oriented in the X–Y plane, thereby establishing a consistent and geometrically controlled basis for the generation of perpendicular cross-sectional directions along the alignment.

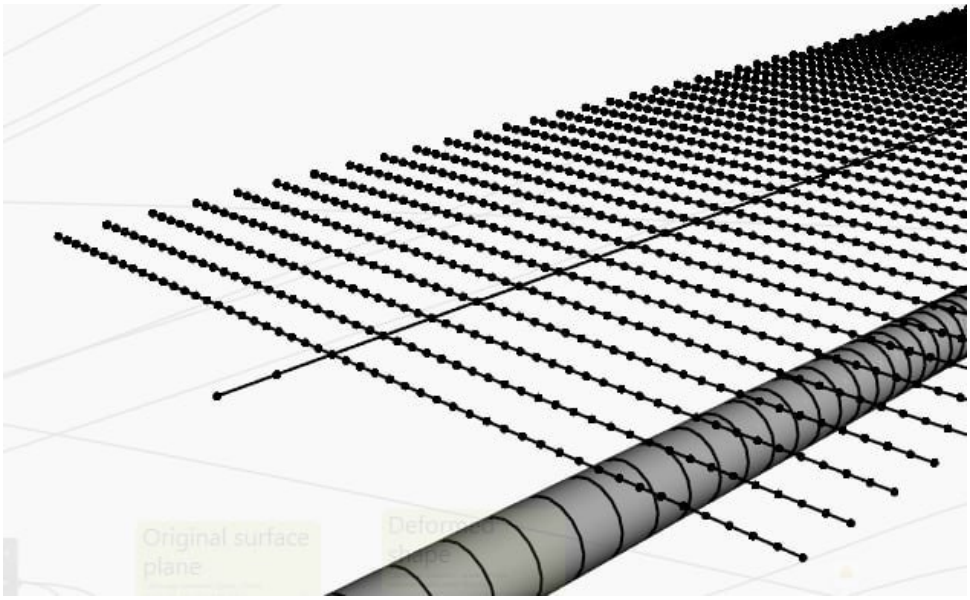

Figure 4.22. Resulting model in Autodesk Dynamo

The implementation of the procedures described results in the generation of a tunnel alignment curve accurately projected onto the terrain surface. This reconstructed line represents the locus of maximum expected settlement within subsequent deformation analyses, as classical soil mechanics models identify the vertical plane passing through the tunnel axis as the location of peak ground displacement. By ensuring that the alignment is geometrically consistent with the actual topography, the analytical framework preserves the physical relationship between excavation geometry and surface response.

The discretization of this projected alignment is defined to correspond directly to the segmentation logic of the tunnel model itself. In the presented case study, the number and position of discretization points coincide with the locations of the tunnel volume-generating sections (or segmental plates). This deliberate correspondence establishes a one-to-one geometric relationship between subsurface tunnel elements and their vertically aligned surface counterparts. Consequently, when a point on the terrain surface is positioned directly above a discretized point of the tunnel central axis, the local tunnel depth can be computed as the difference between their respective vertical coordinates (Δz). This depth parameter is of primary importance in settlement modeling, as the magnitude and spatial distribution of ground deformation are strongly dependent on the cover thickness above the tunnel crown.

The lateral extent of the analytical domain is likewise controlled parametrically. The perpendicular cross-sectional vectors generated through cross-product operations are normalized and subsequently scaled using the *Vector.Scale* node, with the scaling magnitude defined by a user-controlled Number Slider. The scaled vectors are then applied through the *Geometry.Translate* operation to produce symmetric points on both the positive and negative sides of the tunnel axis. These points define the transverse boundaries of the settlement analysis region. By adjusting the scaling factor, the user directly controls the width of the deformation basin considered in the computational model, enabling sensitivity analysis and adaptation to varying geotechnical conditions.

As a result, the complete terrain modeling and discretization workflow establishes an integrated

parametric system within Dynamo, beginning with terrain creation in Autodesk Revit, followed by geometric extraction, reconstruction into a dynamic surface, projection of the tunnel alignment onto the terrain, generation of perpendicular cross-sectional vectors through vector mathematics, and controlled discretization of both longitudinal and transverse analysis domains. The resulting model ensures geometric coherence between tunnel and terrain, preserves consistency with theoretical soil deformation assumptions, and provides user-controlled adaptability in both longitudinal resolution and transverse analytical width. This integrated parametric framework forms the foundation for reliable and analytically rigorous simulation of tunnel-induced ground settlements.

Chapter V: Case study description

The case study presented in this chapter plays a fundamental role in the validation and practical application of the methodology proposed in this thesis. The outputs of the analysis are intended to be used by INFRATRASPORTI.TO S.R.L. as a tool for the classification of potential building damage induced by tunnel excavation. In critical conditions, the results may also support the definition of ground improvement and mitigation measures along the analyzed tunnel section.

The selected case study is located in Via Giuseppe Luigi Lagrange, in the vicinity of Porta Nuova railway station, within the historical city center of Turin. The investigated tunnel section has an approximate length of 200 m and crosses a densely urbanized area characterized by continuous building frontage on both sides of the street. The tunnel alignment is almost perfectly coincident with the road axis, resulting in a simple and regular geometric configuration, which is particularly suitable for method development and validation.

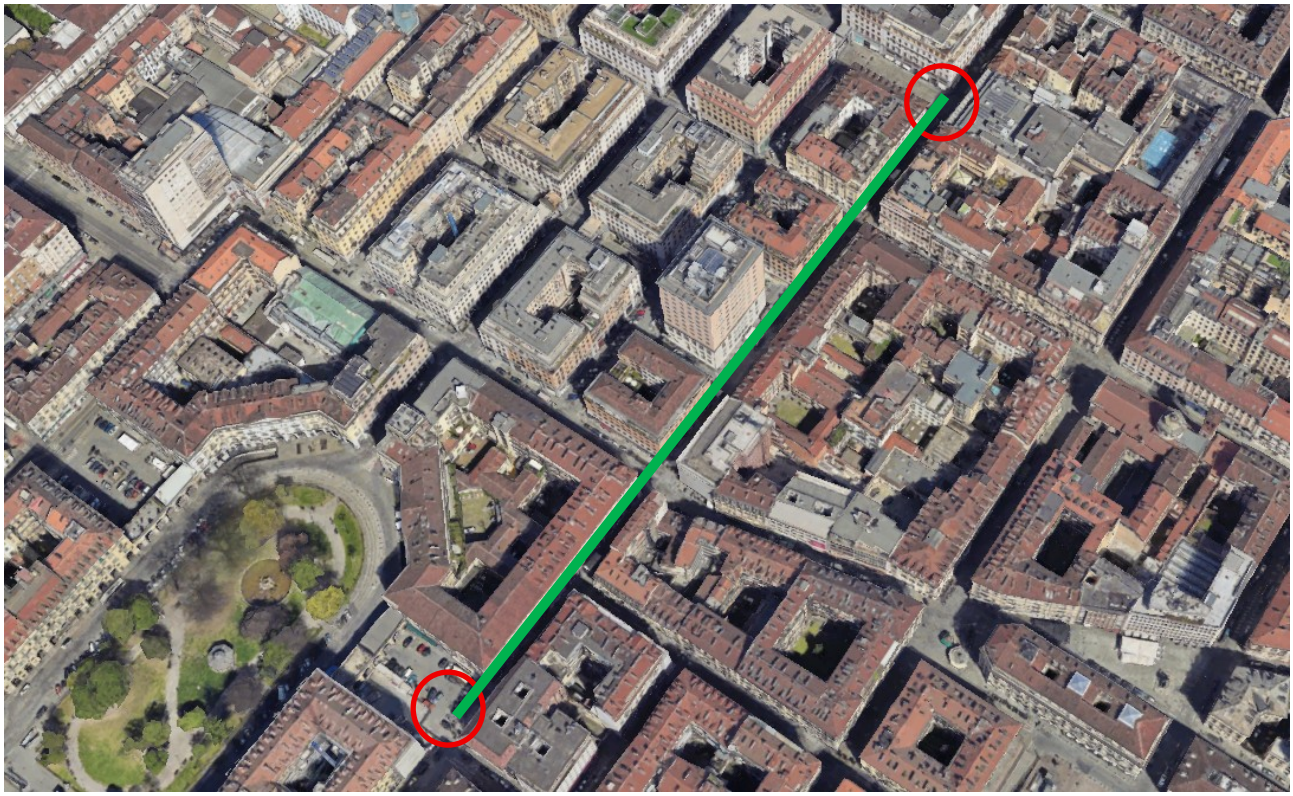

Figure 5.1. Analyzing section location [Google Earth]

The buildings along the analyzed section are predominantly historical constructions, dating back to the period between the 19th and early 20th centuries (1800–1900). They typically consist of commercial spaces at ground floor level and residential units on the upper floors, with an average building height of four stories. Due to the construction period and typology, the buildings are generally founded on shallow mat foundations and are characterized by a high level of structural vulnerability with respect to tunnelling-induced ground movements.

For these reasons, the selected urban section was identified as particularly representative and critical for assessing potential excavation-related damage and was therefore assigned for detailed analysis. The case study provides an appropriate framework to demonstrate the effectiveness of the proposed BIM-based methodology, which enables the reliable estimation of key damage indicators, such as maximum building settlement and angular distortion. These outputs are sufficient to classify the buildings according to the Italian damage classification criteria, confirming the applicability of the proposed method in real urban tunnelling projects.

5.1. Analyzing section geometrical details

The tunnel crossing the study area runs parallel to the pedestrian street of Via Lagrange. Along the segment considered in this analysis, the total width of the street is approximately 11 m. Assuming that the tunnel axis is perfectly aligned with the street axis, it is reasonable to consider that the buildings located along both sides of the street lie approximately at the periphery of the tunnel. This assumption is supported by the fact that the Earth Pressure Balance (EPB) Tunnel Boring Machine (TBM) employed for the construction of the second metro line in Turin has a diameter of 10 m, resulting in only a 1 m difference compared to the width of Via Lagrange.

In reality, building foundations are expected to be located closer to the tunnel axis than the façade lines. However, due to the unavailability of detailed foundation plans or georeferenced coordinates, the foundations are conservatively assumed to coincide with the façade perimeters. This approach is commonly adopted when a significant number of buildings must be assessed and detailed structural information is not accessible.

A total of 14 buildings were analyzed using the parameters required for classification according to Italian standards, namely: (I) the maximum settlement over the building footprint and (II) the maximum inclination induced by differential settlement along the structure.

Buildings characterized by complex geometries were simplified to quadrilateral shapes defined by four vertices. The selected vertices correspond to those closest to the tunnel axis. This simplification leads to an overestimation of the inclination, as the effective distance between points of maximum differential settlement is reduced. Nevertheless, such an approach is considered acceptable. Settlement distribution across the transverse section of a building is generally non-linear; therefore, representing the settlement profile by a linear interpolation between discrete points inherently neglects the formation of varying angular distortions along a curvilinear settlement trough. Consequently, adopting a reduced effective building width (in the case of complex geometries) to evaluate inclination provides a conservative and methodologically justified approximation.

Figure 5.2. Planar view of analyzing section with underlined buildings for damage assessment

The coordinates defining the beginning and the end of the analysis are arranged from the larger longitudinal coordinate of the tunnel axis to the smaller one. This orientation arises because the tunnel chainage system is defined in the direction opposite to the advance of the Tunnel Boring Machine (TBM).

Conversely, the finite element method (FEM) analyses of tunnel excavation carried out in Milan were developed assuming a progressive advancement consistent with the actual TBM movement. Accordingly, the regression models describing settlement basin value distribution are formulated with reference to the direction of tunnel excavation, which means along with the propagation of the boring process.

The origin of the coordinate system adopted for the present analysis is located at chainage 8+526.722 (measured along the tunnel axis), corresponding to the intersection between Via Lagrange and Via Rossi Conte.

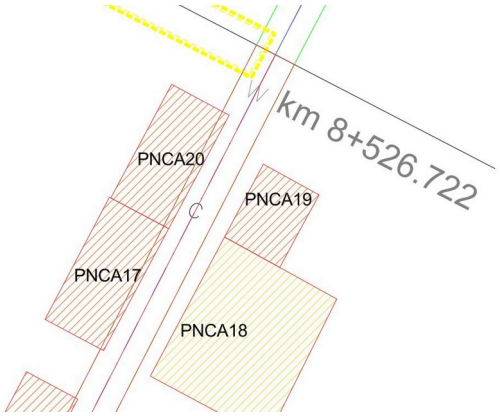

Figure 5.3. Analyzed segment beginning coordinate

The final longitudinal coordinate considered in the analysis corresponds to section 8+269.229, located at the intersection between Via Lagrange and Via Mazzini.

Accordingly, the total length of tunnel excavation influencing the buildings under investigation is 257.5 m. The excavation is performed using a Tunnel Boring Machine (TBM) with a diameter of 10 m, and the tunnel alignment is assumed to be coincident with the axis of the road.

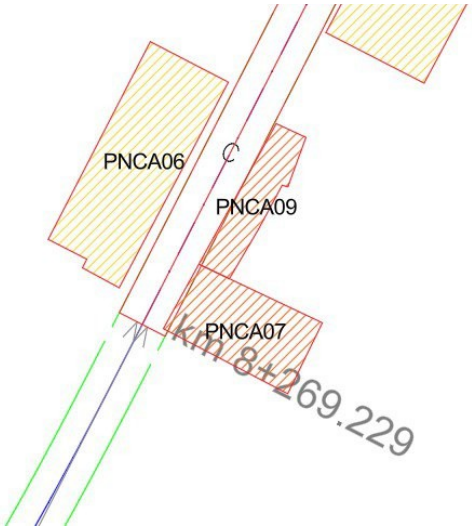

Figure 5.4. Analyzed segment end coordinate

The analyzed segment is situated between the projected stations Carlo Alberto station and Porta Nuova station, where the new alignment will intersect with the existing infrastructure of Turin Metro Line 1. This portion of the route is therefore of particular technical relevance, as it combines deep bored tunneling with proximity to major transportation facilities and previously constructed underground works.

Regarding the vertical alignment, it is essential to highlight the general design strategy adopted to mitigate potential impacts on surface and subsurface infrastructures. In the interstation section, the tunnel is positioned at the maximum feasible depth, subject to the allowable longitudinal gradient of the alignment and the prevailing geotechnical conditions. This approach is based on well-established geotechnical principles: deeper tunnels generally induce smaller surface settlements and reduced angular distortions, thereby limiting structural damage to buildings and utilities. Since shallow tunneling is typically associated with greater soil deformation and higher damage potential, increasing depth—within technical and operational constraints—represents an effective mitigation measure.

As the alignment approaches the stations, which are constructed using full top-down excavation methods, the tunnel profile gradually rises toward the ground surface. This design decision is primarily motivated by construction efficiency, as reducing the depth of the bored tunnel near the station boxes decreases the extent and complexity of station excavation works. Although a shallower tunnel alignment in the vicinity of the stations may locally amplify ground movements induced by the TBM excavation, it must be emphasized that the deformation associated with open-cut (top-down) excavation is significantly greater than that produced by mechanized tunneling under comparable soil conditions. Consequently, minimizing the depth and extent of open excavation is prioritized, even if this results in slightly increased tunnel-induced settlements near the stations.

Within the case-study segment, the vertical alignment includes the lowest point of the tunnel between Carlo Alberto and Porta Nuova stations, corresponding to an elevation of 200.7 m above sea level. This minimum elevation is reached at a longitudinal distance of 100.2 m from chainage 8+526.722, which defines the origin of the adopted coordinate system. From this deepest point, the alignment ascends progressively toward both stations. The highest elevation within the analyzed segment occurs at its terminal section, 8+269.229, where the tunnel axis reaches 206.9 m above sea level. Therefore, the total variation in tunnel axis elevation along the considered segment amounts to 6.2 m.

It should be noted that all reported elevations refer to the central axis of the tunnel. For an accurate assessment of the geometric distance between the tunnel and the ground surface, the radius of the TBM must be added to the axis elevation to determine the position of the tunnel crown. Furthermore, since the terrain elevation is not constant relative to mean sea level, the actual tunnel depth varies continuously along the alignment. A precise evaluation of tunnel depth at any given location requires comparison between the tunnel axis coordinates (x, y, z) and the corresponding ground surface coordinates (x, y, z). The vertical difference between these two sets of coordinates defines the depth of the tunnel axis, while inclusion of the tunnel radius enables calculation of the overburden thickness above the excavation.

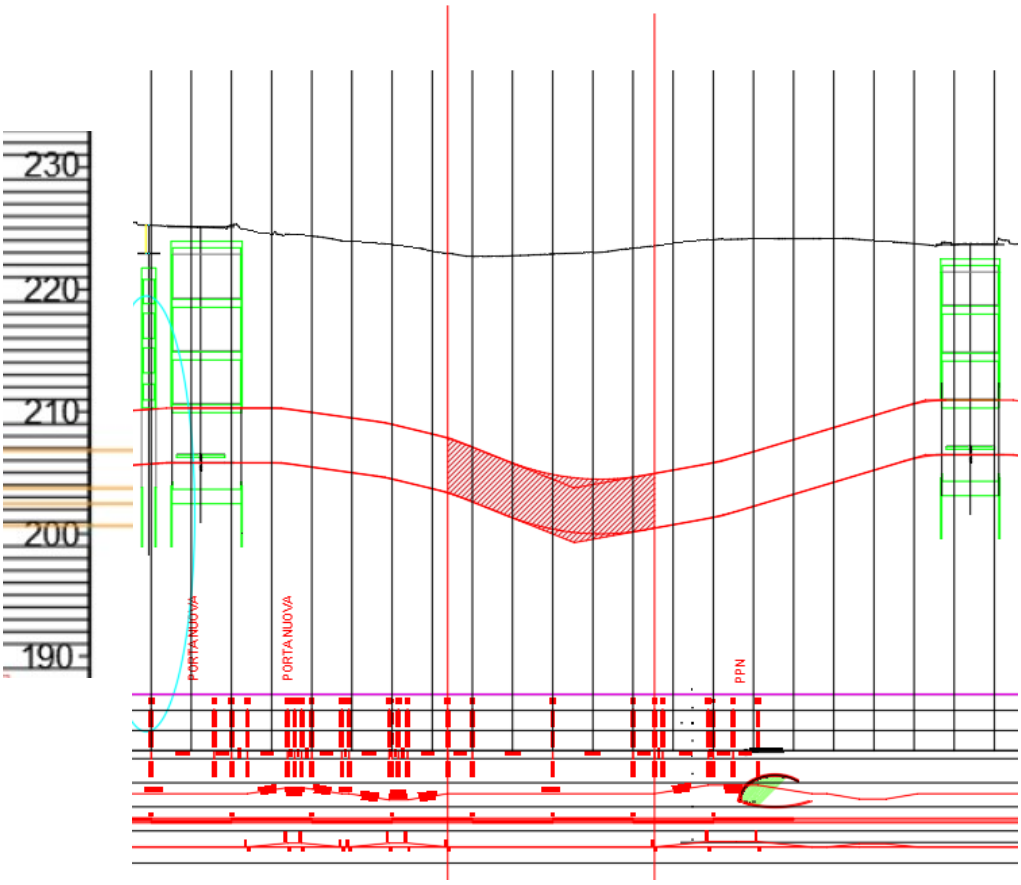

Figure 5.4. Analyzed segment vertical profile

5.2. Geological section

Following the description of the geometric characteristics of the alignment, the analysis now proceeds to the geological section of the investigated segment. The characterization of geological and geotechnical conditions represents a fundamental component of tunnel design and impact assessment, as soil stratigraphy and mechanical properties govern ground response to excavation, settlement development, and the interaction between the tunnel and surface structures. [INFRATRASPORTI.TO S.R.L 02_MTL2T1A0DGEOGENT003.2-0-3]

A detailed understanding of the geological profile is particularly important in urban tunneling projects, where spatial variability of soil layers, groundwater conditions, and the presence of anthropogenic deposits may significantly influence both construction performance and induced deformations. The distribution, thickness, and mechanical behavior of individual strata directly affect the stress redistribution around the excavation, the shape of the settlement trough, and the magnitude of surface and structural displacements.

Several methods are commonly employed for geological and geotechnical characterization in tunnel engineering. The most widely adopted approaches include in situ investigations—such as borehole drilling, Standard Penetration Tests (SPT), Cone Penetration Tests (CPT), and pressuremeter tests—

together with laboratory testing of collected samples to determine strength, stiffness, and compressibility parameters. In addition, geophysical surveys and geological mapping are frequently used to complement direct investigations and to interpolate conditions between boreholes. The integration of these methods enables the development of a reliable ground model, which forms the basis for numerical simulations and engineering assessments.

In the following sections, the geological conditions of the analyzed segment will be presented and discussed in detail. The adopted investigation methods and the resulting stratigraphic and geotechnical parameters will be described sequentially, providing the necessary framework for subsequent analyses of tunnel-induced ground movements and their effects on existing buildings.

GEOLOGICAL AND LITHOSTRATIGRAPHIC LEGEND

Soils of anthropogenic origin consisting of pebbles, gravels and sands, poorly thickened, non-cohesive, in which fragments of anthropogenic origin (bricks) are present (UID). Anthropogenic deposits (Actual). Unit mapped only in the sectors with the most significant thickness.

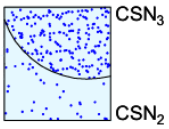

Sandy gravels, sands and silty sands, little to no alteration (CSN3) to weakly altered (CSN2). Fluvial deposits (Holocene - Present).

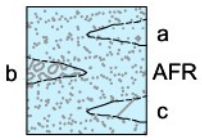

Fine to coarse heterometric gravels with the presence of polygenic clasts centimetric (locally decametric - metric) in a sandy-loam matrix and centimetric intercalations of fine sands and pebble levels; degree of cementation zero to medium (AFR). Fluvioglacial deposits (Pleistocene). Main sandy - silty levels. Main pebble levels. Main horizons with widespread presence of levels with weak to high degree of cementation.

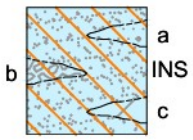

Fine to coarse heterometric gravels with the presence of polygenic clasts centimetric (locally decametric - metric) in a matrix sandy-loamy-clayey and centimetric intercalations of fine sands and pebbly levels, with diffuse alteration (reddish coloring) (INS). Deposits increate sedis attributable to the base of fluvioglacial deposits of the AFR unit (Pleistocene). Main sandy - silty levels (a). Main

pebble levels. Main horizons with widespread presence of levels with a weak to high degree of cementation.

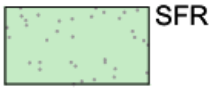

Yellowish-brown to grey, fine to coarse sands and fine, thickened gravels, generally altered in the upper part (SFR). Fluvial to marine-marginal deposits attributable to the SFR unit (Ferrere sands, Villafranchian Auct., Pliocene).

Grey and grey-blue silty clays with centimetric levels sandy - silty and gravelly - silty (FAA). Marine deposits with association with calcareous nannofossils referable to biozone MNN16A attributable to the FAA unit (Blue Clays or Lugagnano Clays, Lower Pliocene - Zanclean).

Grey silty clays, very compact and locally lithified (SAF). Marine deposits with association with calcareous nannofossils referable to biozone MNN11A attributable to the SAF unit (fossil St. Agatha Marls, Upper Miocene - Tortonian).

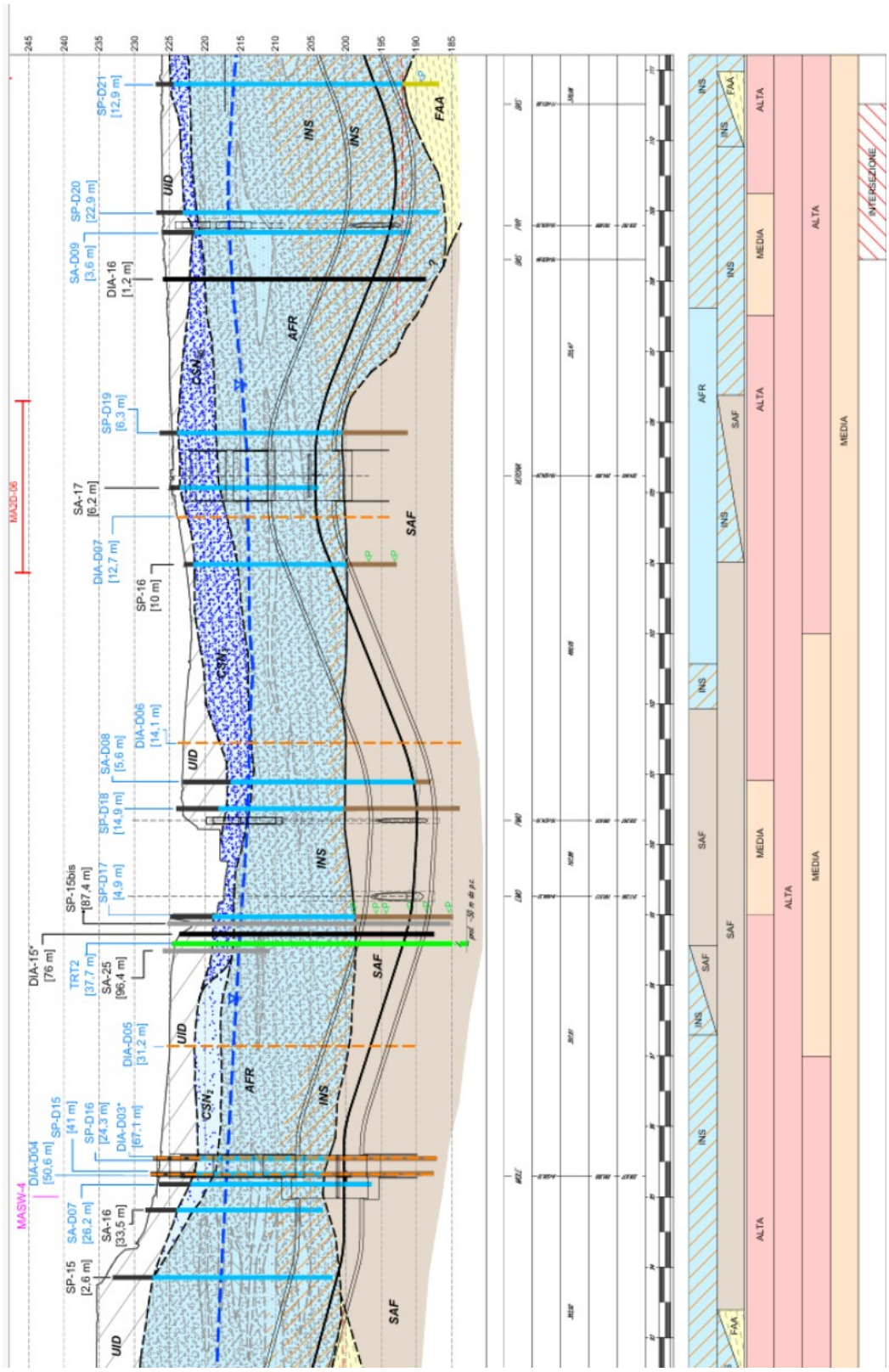

Figure 5.5. Geological section of analyzed segment

Within the analyzed segment between chainages 8+526.722 and 8+269.229, the geological profile comprises several distinct soil units identified from the available stratigraphic data.

The first unit consists of fine- to coarse-grained heterometric gravels with the presence of polygenic clasts of centimetric size, locally reaching decametric to metric dimensions, embedded in a sandy–loam matrix. Centimetric intercalations of fine sands and pebble levels are present, with a degree of cementation ranging from zero to medium. This formation is classified as AFR and corresponds to fluvioglacial deposits of Pleistocene age. Within this unit, the main components include sandy–silty levels, pebble levels, and horizons characterized by a widespread presence of layers exhibiting weak to high degrees of cementation.

A second unit identified along the segment is composed of fine- to coarse-grained heterometric gravels with polygenic clasts (centimetric, locally decametric to metric) within a sandy–loamy–clayey matrix, including centimetric intercalations of fine sands and pebbly levels, and showing diffuse alteration indicated by reddish coloration. This formation is classified as INS and represents in situ deposits attributable to the basal portion of the fluvioglacial AFR unit (Pleistocene). The principal constituents of this unit include sandy–silty levels (a), pebble levels, and horizons with widespread weak to high degrees of cementation.

At the deepest points of the analyzed segment grey silty clays, described as very compact and locally lithified, are encountered. These materials belong to the SAF unit and are identified as marine deposits containing calcareous nannofossils referable to biozone MNN11A, attributable to the fossil St. Agatha Marls (Upper Miocene – Tortonian).

From a tunneling perspective, the behavior of an Earth Pressure Balance (EPB) Tunnel Boring Machine (TBM) in such soils depends strongly on grain-size distribution, matrix composition, and degree of cementation. In heterogeneous fluvioglacial gravels (AFR and INS units), the presence of coarse clasts and variable cementation can lead to fluctuating excavation conditions, including changes in cutter wear, torque demand, and face stability. The sandy–silty matrix generally facilitates conditioning and pressure control in EPB operation; however, the occurrence of large clasts and cemented horizons may locally increase mechanical resistance and reduce excitability.

High levels of cementation are associated with increased apparent cohesion and stiffness of the soil mass. This enhanced cohesion improves short-term face stability but simultaneously results in greater cutting resistance and higher mechanical loads on the TBM cutterhead and tools. In strongly cemented or partially lithified zones, excavation conditions may approach those encountered in weak rock, requiring adjustments in operational parameters.

In the deepest sections, the compact and locally lithified grey silty clays of the SAF unit typically exhibit low permeability and significant stiffness. In EPB tunneling, such cohesive soils generally provide favorable face support conditions due to their inherent stability; however, their compact nature may increase cutting forces and energy consumption. Overall, the heterogeneity of the formations encountered necessitates careful control of TBM operational parameters to maintain face stability and minimize ground disturbances.

5.3 Geotechnical section

Following the description of the geological framework, the analysis proceeds to the geotechnical characterization of the investigated segment. Although closely related, the geological and geotechnical sections serve distinct purposes within tunnel engineering studies.

The geological section describes the origin, stratigraphy, depositional environment, and lithological composition of the soil and rock formations. It focuses on the spatial distribution of units, their genesis (e.g., fluvioglacial or marine), and their qualitative characteristics. In contrast, the geotechnical section translates this geological information into engineering terms by defining the mechanical and hydraulic properties of the identified units. While geology answers the question of what materials are present and how they were formed, geotechnics addresses how these materials will behave under loading and excavation. [INFRATRASPORTI.TO S.R.L 02_MTL2T1A0DGEOGENT003.2-0-3]

This distinction is particularly significant in tunneling projects. The mechanical properties of soils—such as stiffness, strength parameters (cohesion and friction angle), compressibility, and permeability—directly govern the ground response to excavation. These parameters determine the magnitude and distribution of stresses around the tunnel, the development of the settlement trough, and the resulting deformations at the ground surface. Consequently, it is the geotechnical characterization, rather than the purely geological description, that enables prediction of settlements, evaluation of building inclinations, and assessment of potential structural damage.

In other words, the deformations induced by tunnel excavation are controlled by the mechanical behavior of the encountered soils. Even formations of similar geological origin may exhibit significantly different deformation responses depending on their degree of cementation, density, consolidation state, and stiffness.

In the following subsections, the identified geological formations will be reorganized into corresponding geotechnical units. Each unit will be described in terms of its relevant engineering parameters, providing the basis for subsequent numerical modeling and assessment of tunnel-induced ground movements.

UNITA' 1

Topsoil represents the uppermost layer of the ground profile, generally extending from the surface to a depth of approximately 1–2 meters, depending on local conditions. It is formed through long-term weathering processes, biological activity, and, in urban environments, may include reworked or anthropogenic materials. Topsoil is characterized by a heterogeneous composition, often containing organic matter and debris, which makes it unsuitable as a bearing stratum for structural foundations.

From a geotechnical perspective, topsoil typically exhibits low density, loose structure, and high compressibility. Its shear strength is generally low, with limited cohesion and/or friction angle, and its stiffness (Young's modulus) is considerably lower than that of deeper soils. Permeability varies depending on grain size, being higher in sandy topsoils and lower in silty or clayey variants. The combination of high compressibility, low strength, and heterogeneity makes topsoil prone to settlements under applied loads and sensitive to moisture variations.

UNITA' 2

Loose to lightly cemented gravel and sand refers to a coarse-grained soil in which individual particles are weakly bonded or uncemented, with a degree of cementation typically ranging from 0 to 25%. Such soils are common in fluvial, glacio-fluvial, and alluvial deposits and often occur in heterogeneous sequences with varying particle sizes.

From a geotechnical perspective, these soils are characterized by high permeability and generally low to moderate cohesion, with shear strength primarily controlled by internal friction between grains. The degree of cementation, even if low, can locally increase apparent cohesion and stiffness, improving short-term stability. The density of the material varies from loose to medium-dense, which influences compressibility and settlement behavior. Loose, uncemented layers tend to exhibit higher compressibility and larger deformations under applied loads, while lightly cemented zones display reduced compressibility and slightly higher stiffness.

UNITA' 2B

Thickened silty sands and silty–sandy gravels are coarse-grained soils in which sand and gravel fractions are mixed with a significant proportion of fines (silt), with a degree of cementation generally ranging from 0 to 25%. These soils are commonly associated with fluvial, glacio-fluvial, or alluvial depositional environments, where variable energy conditions lead to heterogeneous layering and occasional weak cementation between grains.

From a geotechnical standpoint, the mechanical behavior of these soils is influenced both by the granular skeleton and the fine content. The presence of silt increases compressibility compared to clean sands and gravels, while lightly cemented zones exhibit enhanced apparent cohesion and stiffness. Shear strength is primarily frictional, controlled by the relative density and particle interlock, but low degrees of cementation provide additional cohesion that can improve short-term stability. Permeability remains relatively high, although slightly reduced by the silt content, and compressibility varies with density and cementation, with looser or uncemented layers showing greater settlement potential.

UNITA' 3

Gravel and sand with weak to medium bonding refers to coarse-grained soils in which individual particles are partially cemented, with a bonding or cementation degree typically between 25% and 50%. These soils are commonly found in fluvial, glacio-fluvial, and colluvial deposits, where natural processes such as calcite precipitation, iron oxide accumulation, or compaction have led to partial interparticle bonding. From a geotechnical perspective, the presence of weak to medium cementation significantly influences the mechanical behavior of these soils. Shear strength is enhanced due to the combined effect of particle interlock and apparent cohesion provided by cementation, while frictional resistance between grains continues to play a primary role. Stiffness and Young's modulus are higher than in loose or uncemented gravel and sand, resulting in reduced compressibility and smaller settlements under applied loads. Permeability may be moderately reduced relative to uncemented layers, depending on the extent and continuity of cemented zones.

UNITA' 4

Medium to highly cemented gravel and sand refers to coarse-grained soils in which the particles are strongly bonded, with a degree of cementation ranging between 50% and 75%. Such soils are typically the result of natural diagenetic processes, including calcite, silica, or iron oxide precipitation, and are often encountered in fluvial, glacio-fluvial, or colluvial deposits where compaction and chemical bonding have reinforced the granular skeleton.

From a geotechnical perspective, medium to highly cemented gravels and sands exhibit significantly enhanced mechanical properties compared to weakly cemented or uncemented soils. Shear strength is markedly higher due to the combined effect of particle interlock and substantial apparent cohesion provided by cementation. Stiffness and Young's modules are elevated, resulting in reduced compressibility and minimal settlements under applied loads. Permeability is generally lower than in uncemented or lightly cemented soils, particularly, where cementation forms continuous bonds between particles.

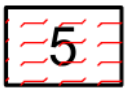

UNITA' 5

Clayey–sandy–gravelly silt (Blue Clays) represents a fine- to medium-grained cohesive soil, typically characterized by a silty matrix with varying proportions of clay, sand, and gravel. These soils often exhibit a bluish coloration due to the presence of specific clay minerals and low oxidation conditions and are commonly associated with marine or lacustrine depositional environments.

From a geotechnical perspective, blue clays display high plasticity and significant cohesion, which imparts considerable shear strength under low to moderate confining pressures. The combination of clay and silt content results in low permeability, reduced drainage capacity, and relatively low deformability in short-term conditions, while long-term consolidation may lead to notable settlements. The presence of sand and gravel fractions can locally increase stiffness and reduce compressibility, although the overall behavior remains dominated by the cohesive matrix. Young's modulus is moderate to low, depending on moisture content and natural over-consolidation, while Poisson's ratio typically ranges between 0.3 and 0.45.

UNITA' 6

Slightly clayey sandy silt (Villafranchian deposits) represents a fine- to medium-grained soil composed primarily of silt and sand with a minor clay fraction. These deposits are of Villafranchian age (Late Pliocene to Early Pleistocene) and are typically associated with fluvial and alluvial depositional environments, where variable energy conditions have produced well-mixed, slightly cohesive sediments. From a geotechnical perspective, slightly clayey sandy silts exhibit low to moderate cohesion and primarily frictional behavior, with shear strength controlled by particle interlock and the small clay content. The stiffness of these soils is moderate, with Young's modulus higher than that of pure silts or clays but lower than coarse-grained gravels. Compressibility is moderate, and settlements under applied loads can be significant, particularly in loose or lightly compacted zones. Permeability is relatively high compared to clayey soils, facilitating drainage, but may be locally reduced in areas with higher silt content.

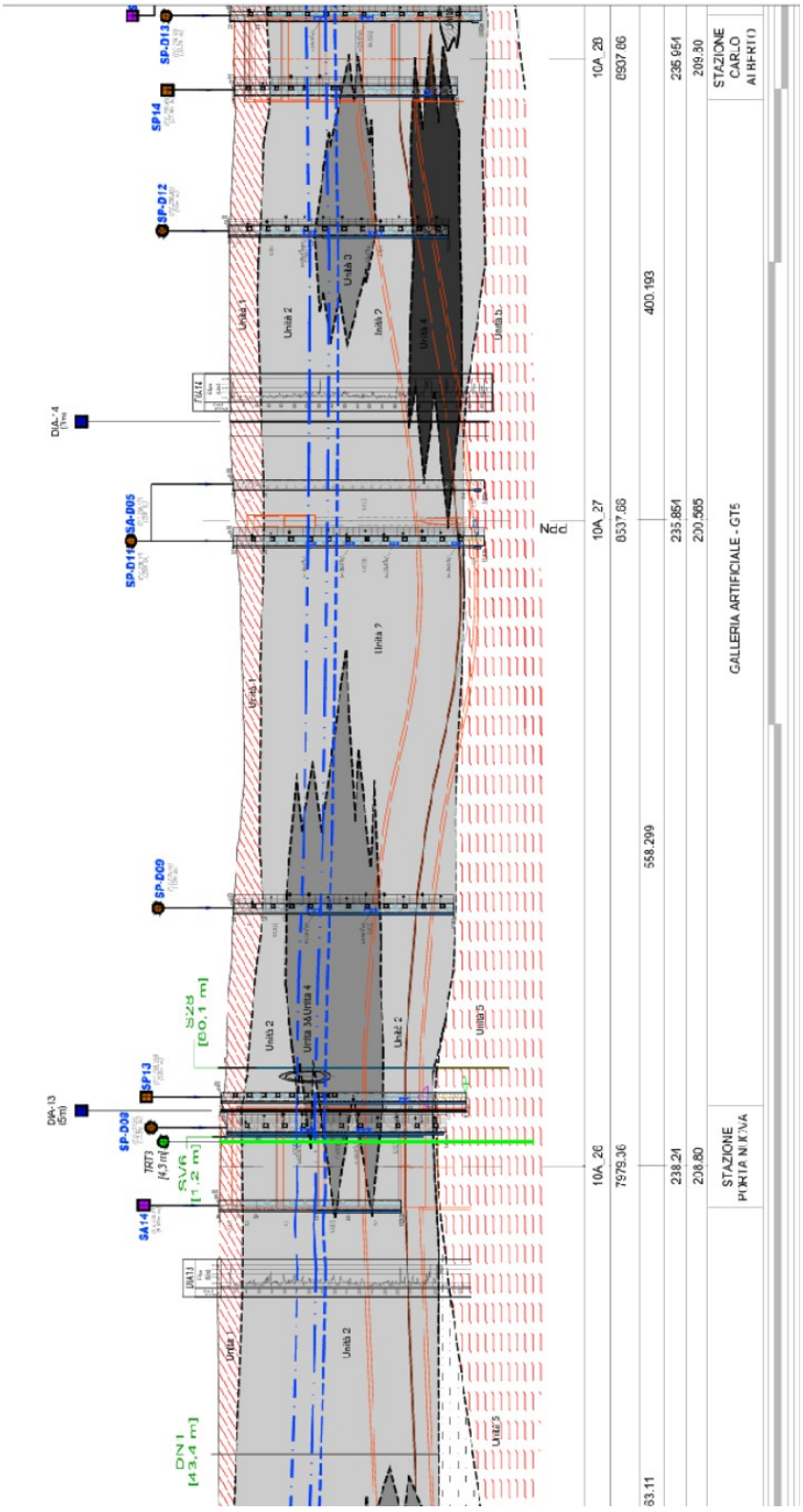

Figure 5.6. Geotechnical section of analyzed segment [INFRATRASPORTI.TO S.R.L 02_MTL2T1A0DGEOGENT003.2-0-3]

Unità	Geologia	Peso di volume (γ)	Coesione c′ (kPa)	Angolo resistenza φ′	Modulo (MPa)	Poisson (–)	Coeff. permeabilità (m/s)
1	UID	18÷19	0	29÷31	12÷16	0.30	$2{\cdot}10^{-5}$ a $8{\cdot}10^{-6}$
2	AFR-INS	18÷19	10÷15	36÷38	150÷170	0.30	$2{\cdot}10^{-5}$ a $8{\cdot}10^{-6}$
3	AFR-INS	19÷20	30÷50	38÷40	170÷200	0.30	$8{\cdot}10^{-6}$ a $5{\cdot}10^{-6}$
4	AFR-INS	19÷20	50÷100	38÷40	200÷260	0.30	$8{\cdot}10^{-6}$ a $5{\cdot}10^{-6}$
6	SFR	18÷20	15÷25	30÷32	90÷100	0.35	$5{\cdot}10^{-6}$
5	FAA	19÷21	35÷40	22-26	50÷80	0.35	$2{\div}6{\cdot}10^{-9}$
7	SAF	20÷21	25÷50	26÷28	100÷200	0.35	$2{\div}6{\cdot}10^{-9}$

Table 5.1. Mechanical properties of analyzed segment

From a geotechnical perspective, the soil section between chainages 8+526.722 and 8+269.229 can be divided into distinct units. Unit 1 corresponds to the topsoil, forming the uppermost layer. Unit 2, representing loose to lightly cemented gravel and sand, constitutes the major part of the profile. Unit 5 comprises clayey–sandy–gravelly silt, which occurs at the lowest points of the section.

The tunnel alignment primarily excavates through Unit 2 (loose to lightly cemented gravel and sand), with the lower portion of the TBM passing into Unit 5 (clayey–sandy–gravelly silt). In this context, the behavior of an Earth Pressure Balance (EPB) TBM is strongly influenced by the mechanical properties of these soils. In the coarse, granular Unit 2, the TBM must manage face stability in a medium- to high-permeability material with limited cohesion. Although lightly cemented zones provide some apparent cohesion and increased stiffness, the heterogeneous composition of gravels and sands may lead to fluctuations in cutting resistance, torque, and soil flow into the machine chamber. The cohesive and fine-grained nature of Unit 5 at the lower part of the TBM improves face stability, facilitates soil conditioning, and reduces the risk of excessive particle loss, while the low permeability of the clayey–sandy–gravelly silt requires careful control of excavation pressures to avoid over-pressurization and soil heave.

Surface settlements induced by the tunnel are predominantly controlled by Unit 1 (topsoil) and Unit 5 (clayey–sandy–gravelly silt), as these layers constitute the primary overburden above the tunnel. The topsoil, with its low stiffness and high compressibility, amplifies surface displacements, while the deeper clayey–sandy–gravelly silt governs the transmission of deformations from the tunnel to the surface due to its cohesive nature and relatively low permeability. Unit 2, forming the main part of the tunnel envelope, influences TBM performance and local soil-structure interaction but contributes less directly to surface settlement because it is largely situated around the mid-height of the excavation.

5.4. Justification of regression model usage for Turin soil conditions

The Finite Element Analysis (FEA) presented in Subchapter 2.4, Settlement Analytical Theory and FEM Project Background, was originally developed within the framework of the 2010 reference doctoral thesis concerning settlement assessment and overall settlement behavior during the excavation works of the metro line in Milan.

The present chapter builds upon that analytical foundation and is devoted to a rigorous geotechnical engineering evaluation aimed at demonstrating that the regression models derived from the FEM analyses are technically reliable and methodologically consistent for subsequent implementation within a BIM-based framework. Specifically, it seeks to substantiate the suitability of these FEM outputs as validated input parameters for a Building Information Modeling (BIM) methodology applied to soil dynamics and structural damage assessment in Turin.

Through this approach, the chapter establishes the theoretical and practical continuity between advanced numerical geotechnical modeling and integrated digital processes for infrastructure impact assessment.

5.4.1 Geometrical characteristics differences

The alignment of the tunnel axis in the FEM model does not coincide with the geometry of the case study segment in either horizontal or vertical alignment. A similar discrepancy can also be observed in the terrain configuration. Nevertheless, the outputs derived from the regression models are based on the geometric parameters of the tunnel, including the depth distribution and the TBM diameter. These two parameters collectively define the tunnel overburden, which serves as a principal input variable in the analytical functions.

The FEM analyses were conducted by considering the ratio between the tunnel overburden and the tunnel diameter as the governing parameter:

Model A: Overburden H = 1.23D

Model B: Overburden H = 2D

Model C: Overburden H = 3D

Model D: Overburden H = 4D

Accordingly, the regression models are applicable to any depth distribution, since the geometric characteristics of the tunnel are incorporated as variable input parameters within the formulation. In this context, geometry particularly the depth and diameter—enters the model as independent variables rather than fixed quantities.

More importantly, the validity and transferability of the models primarily depend on the coefficients associated with these variables. These coefficients are derived based on the governing soil parameters and therefore reflect the mechanical behavior of the ground. Consequently, the application of the regression models to other cases is justified provided that the soil conditions—and thus the derived coefficients—are sufficiently similar.

5.4.2 Soil properties similarities

Based on the analysis of the studied section, which was subdivided into equal segments to evaluate the proportional distribution of soil units, it was determined that the principal transverse area of the section is predominantly composed of Unit 2 soils. Specifically, Unit 2 soils constitute approximately 73% of the total geotechnical cross-section relative to the other identified soil units.

[INFRATRASPORTI.TO S.R.L 02_MTL2T1A0DGEOGENT003.2-0-3]

Furthermore, with particular reference to the soils directly encountered by the TBM cutterhead, the proportion of Unit 2 soils increases to 82%. This indicates that Unit 2 soils represent the dominant geotechnical formation both within the overall section and, more significantly, within the excavation face.

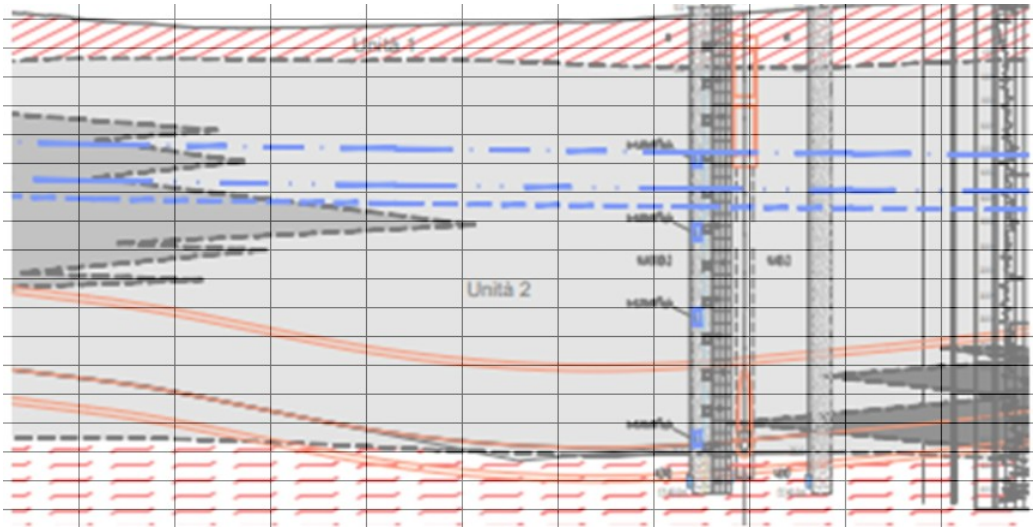

Figure 5.7. Analysis of soil areas ratios

The whole soil mass for FEM analysis is done according to homogeneous soil parameters, so there is no any soil differentiation in the tunnel section as in the case of case study or any real soil condition studies in general, but according to the fact that soil in FEM is designed as one soil type, it can be compared with only one soil type from case study segment, and most strategic decision according to soil types distribution would be taking the mechanical parameters of Unit 2 as the comparable ones:

- Cohesion (kPa) : 10
- Angle of shear resistance (°) : 36
- Angle of dilatancy (°) : 10
- Specific Weight (kN/m3) : 18
- Young's modulus (MPa) : 150
- The Poisson ratio: 0.3

Soil properties of the soil that were inserted as a mechanical input to the FEM analysis are the following ones:

- Cohesion (kPa) : 0.1
- Angle of shear resistance (°) : 35
- Angle of dilatancy (°) : 10
- Specific Weight (kN/m3) : 18
- Young's modulus (MPa) : 75
- The Poisson ratio : 0.3

	Soil used for FEM analysis	Unit 2 soil [Turin]
Cohesion (kPa)	0.1	10
Angle of shear resistance (°)	35	36
Angle of dilatancy (°)	10	10
Specific Weight (kN/m3)	18	18
Young's modulus (MPa)	75	150
The Poisson ratio	0.3	0.3

Table 5.2. Mechanical properties comparison of soil properties in FEM with soil properties of case study

For two soils to be considered comparable in the context of tunnel-induced settlements, their key geotechnical parameters should be similar. These include unit weight, strength parameters (such as internal friction angle), and, where relevant, stiffness properties.

In the present case, the soils under comparison exhibit identical unit weights (γ = 18 kN/m³). As a result, the vertical stress, defined as $\sigma_v = \gamma \cdot z$, is the same at any given depth for both soils. Since vertical stress is the primary component governing overburden loading, this represents an important condition of equivalence.

The first difference between the two soils lies in the internal friction angle, equal to 36° for the case study soil and 35° for the FEM model. This parameter affects the lateral earth pressure coefficient, defined as $K = 1 - \sin(\varphi)$. However, the numerical difference between sin(35°) and sin(36°) is very small, leading to only minor variations in horizontal stress ($\sigma_h = K \cdot \sigma_v$).

Therefore, both vertical and horizontal stress conditions can be considered effectively equivalent. This supports the assumption that the FEM-based simulation results are applicable to the analyzed soil conditions, particularly in terms of stress distribution governing ground deformation.

In practical terms, this implies that the horizontal pressure applied to the cutterhead of the TBM under Earth Pressure Balance (EPB) conditions remains effectively the same for both soils, provided tunnel depth is treated as a variable within the regression formulation.

Therefore, the FEM-based regression models developed for soil with a friction angle of 35° can be considered applicable to soil with a friction angle of 36°, particularly when geometric parameters—such as tunnel alignment and TBM diameter—are incorporated as variables. This conclusion is further supported by the fact that the FEM analyses were performed for four different tunnel overburden-to-diameter ratios, ensuring that the parametric study captures variations in stress distribution due to geometric scaling.

A significant difference between the soils under consideration arises in relation to cohesion, which represents one of the key parameters governing soil stability.

For the soil adopted in the FEM simulations and in the derivation of the corresponding regression models, the cohesion value was taken as $c = 0.1$ kPa, effectively representing a cohesionless material. This assumption is consistent with the geotechnical conditions typical of Milan, where the subsoil in many urban areas can be described as sandy gravel with negligible apparent cohesion. In such soils, mechanical stability is primarily ensured by interparticle friction, while cohesive bonding plays an insignificant role.

In contrast, the soil encountered in the case study segment (Unit 2) is considerably more cemented, with reported cohesion values ranging from 10 to 15 kPa. This represents an increase of approximately two orders of magnitude compared to the value adopted in the FEM input parameters. Undoubtedly, if the FEM model were recalibrated with cohesion values 100 times greater, different coefficients would be obtained in the resulting mathematical relationships, reflecting the enhanced shear strength and reduced deformability of the material.

At this stage, it is important to emphasize that cohesion is primarily associated with the shear strength and failure criterion of soil, as defined by the Mohr–Coulomb model. Cohesion contributes directly to the ultimate shear resistance and thus becomes particularly relevant when the stress state approaches failure conditions. However, within the scope of the present analysis, all calculated deformations (strains) remain within the non-failure strain domain. Provided that the TBM face pressure is properly calculated and correctly applied, the stress path does not approach the failure envelope. Therefore, the influence of cohesion on soil response is significantly reduced under these serviceability-level conditions, and its effect can reasonably be neglected for the purposes of deformation prediction.

From a mechanical standpoint, cohesion enhances soil stability under identical stress conditions and generally leads to smaller strains. A soil with higher cohesion will exhibit reduced deformability, which in turn results in smaller settlements both at the surface and within the subsurface layers. Consequently, incorporating realistic cohesion values for Unit 2 soil would likely decrease the predicted deformations.

From an engineering perspective, neglecting cohesion in the regression model places the analysis on the conservative (safe) side. Since the FEM-based formulations were derived assuming essentially cohesionless conditions, the predicted settlements are expected to be greater than those that would occur in reality for a more cemented soil such as Unit 2. In other words, the model intentionally overestimates deformations rather than underestimates them, which is preferable in urban tunneling design where serviceability limit states are critical.

Furthermore, the uppermost one to two meters of the soil profile consist of topsoil layers characterized by negligible or zero cohesion. This implies that any strain originating in the deeper Unit 2 soil will not be mitigated or reduced near the surface by cohesive resistance within the overlying Unit 1 layer. Therefore, even if Unit 2 exhibits significant cohesion at depth, its beneficial influence on limiting surface settlements is not effectively transmitted through the cohesionless upper layers.

For these reasons, the decision to neglect cohesion in the FEM-based regression models is justified both from a conservative engineering standpoint and in light of the stratigraphic characteristics of the soil profile and the elastic stress regime considered in the analysis.

Another parameter that exhibits a pronounced difference between the two soils is the Young’s

modulus (*E*). In the FEM model, the adopted value of Young's modulus was 75 MPa, whereas in the case study segment (Unit 2) the reported value is approximately 150 MPa, indicating a twofold increase in soil stiffness.

At first glance, such a discrepancy could be expected to significantly influence the predicted settlement response, since Young's modulus governs the elastic - plastic deformability of the soil. A higher modulus generally implies smaller strains under the same stress increment, and therefore reduced settlements. However, in the present study this issue was directly addressed within the FEM framework.

Specifically, the numerical analyses were performed parametrically by assuming multiple values of Young's modules, namely 20, 30, 75, and 150 MPa. This range was intentionally selected to represent soft to relatively stiff granular soils and to evaluate the sensitivity of settlement distribution to variations in stiffness. The results of these simulations indicate that the differences in predicted settlement profiles are negligible within the investigated range of modulus values. Although minor variations in absolute displacement values can be observed, the overall shape of the settlement trough and the governing relationships remain practically unchanged.

This outcome suggests that, under the considered stress regime—where deformations remain within the elastic domain and TBM face pressure is appropriately controlled—the settlement response is not highly sensitive to variations in Young's modulus within the examined interval. Consequently, the regression models developed based on FEM analyses with a representative modulus value (e.g., 75 MPa) can be reliably applied to soils with different stiffness values, including those with Young's modulus equal to 150 MPa.

Therefore, despite the apparent numerical difference in stiffness between the FEM input soil and the Unit 2 soil from the case study, the applicability of the derived regression models for settlement prediction remains justified.

Chapter VI: Buildings degree of damage estimation in BIM Dynamic Model

6.1. FEM Regression models application

The subsequent chapter focuses on the application of regression models derived from Finite Element Method (FEM) analysis to the parametric tunnel–terrain system previously established. The comprehensive FEM procedure, including model configuration, boundary conditions, material constitutive laws, calibration strategy, and interpretation of numerical outputs, is described in detail in Subchapter 2.4, *"FEM Analysis: Predictive Models Establishment"*. That section presents the methodological framework through which predictive relationships for tunnel-induced settlements were formulated and validated.

The regression models implemented in the present study originate from FEM simulations conducted using soil parameters representative of the Milan geological context. A key geotechnical characteristic of Milan soils, particularly in the analyzed segments, is their relatively low degree of cementation. This condition leads to negligible or near-zero effective cohesion, with settlement behavior largely governed by frictional resistance and stress-dependent stiffness. In contrast, the soils encountered in the Turin case study are characterized by a higher degree of cementation, resulting in significant apparent cohesion and enhanced structural bonding within the soil matrix.

At first consideration, this difference in cohesion could suggest limited transferability of predictive models derived under Milan soil conditions to the Turin geological setting. However, this issue is rigorously examined in Subchapter 5.4, *"*Justification of regression model usage for Turin soil conditions*"*. That section provides a detailed comparison of key soil parameters, including unit weight, friction angle, stiffness modulus, and stress–strain response characteristics.

The comparative analysis demonstrates that several fundamental mechanical properties remain sufficiently similar between the two soil contexts to justify the application of the derived predictive relationships. Moreover, for parameters that differ—particularly cohesion—the divergence operates conservatively with respect to settlement prediction. From both empirical and theoretical perspectives, increased soil cohesion contributes to greater ground stability and reduced deformation magnitudes under comparable loading conditions. Consequently, applying models derived from low-cohesion (Milan-type) soils to higher-cohesion (Turin-type) soils does not introduce non-conservative bias; rather, it positions the analysis on the safe side by potentially overestimating settlement magnitudes.

From a methodological standpoint, the integration of FEM-derived predictive functions into the parametric Dynamo framework enables the transformation of numerical simulation results into analytically accessible settlement models. These models are subsequently applied along the discretized tunnel alignment and across the parametrically defined transverse sections of the terrain. By embedding FEM-calibrated formulative expressions within the computational workflow, the system bridges high-fidelity numerical simulation and dynamic parametric modeling, ensuring both theoretical rigor and practical adaptability.

Thus, the present chapter establishes the theoretical legitimacy and engineering reliability of applying

FEM-derived settlement regression models—originally calibrated for Milan soil conditions—to the Turin case study. The justification is grounded in comparative geotechnical analysis and supported by conservative assumptions, ensuring that the implemented deformation predictions remain analytically sound and structurally safe within the defined modeling framework.

The fundamental mathematical basis for the settlement analysis applied in this research is the classical expression proposed by Ralph B. Peck (1969), which describes the transverse settlement trough induced by tunnel excavation as a Gaussian distribution: Formula [1]

where $S(y)$represents the vertical settlement at a horizontal distance $y$from the tunnel centerline, S_{max}denotes the maximum settlement occurring directly above the tunnel axis, and $i$is the horizontal distance from the centerline to the point of inflection of the settlement curve, commonly referred to as the trough width parameter or tangent inclination parameter.

The formulation assumes that the settlement basin follows a Gaussian (normal) distribution, characterized by a smooth concave profile near the central axis and progressively convex curvature toward the flanks of the trough. Furthermore, the transverse settlement profile is assumed to be perfectly symmetric with respect to the vertical plane passing through the tunnel axis. Despite its conceptual simplicity, this representation remains one of the most influential and widely applied theoretical models in tunneling engineering for estimating ground movements induced by underground excavation.

According to Attewell and Farmer (1974), Burland et Al. (1977), Burland, O'Reilly and New (1982), Mair, Taylor and Burland (1996), the above hypothesis (the Gaussian shape of the subsidence line) is duly confirmed by field measurements.

Further refinement of the approach was introduced by C. P. O'Reilly and B. M. New (1982), who developed theoretical expressions for determining the parameters i, S_{max}, and the associated volume change, based on the concept of percentage volume loss. This classical theoretical–empirical methodology links observed or assumed excavation-induced volume loss to the geometry of the settlement basin, thereby providing a practical engineering framework for predicting surface deformations.

In the present case study, while the Gaussian formulation of Peck (1969) is retained as the governing structural form of the settlement trough, the key parameters $S_{max}$and i are not determined solely through traditional empirical correlations. Instead, they are substituted with corresponding predictive expressions derived from calibrated FEM simulations, as established in the preceding chapters. This substitution allows the analytical model to preserve the well-validated Gaussian geometry while integrating site-specific mechanical behavior captured through numerical analysis. Consequently, the resulting settlement predictions are less generalized and better aligned with the actual geotechnical conditions of the investigated site, reducing potential overestimation and enhancing the realism and reliability of the deformation assessment.

Final regression models:

- $w_{max,0} = 0.71 * (H/D) - 15.141$
  Maximum settlement

- $w_{max} = -39.689*(Z/H)^3 + 32.025*(Z/H)^2 – 10.96*(Z/H) + w_{max,0}$
  Maximum settlement in inner soil layers

- $i_{y,0} = 4.176*(H/D) + 0.719$
  Settlement basin tangent inclination on the surface

- $i_y = -9.307*(Z/H) + i_{y,0}$
  Settlement basin tangent inclination in inner soil layers

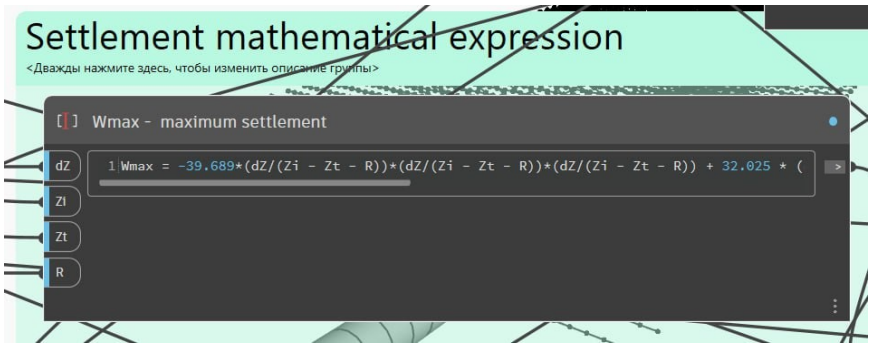

Figure 6.1. Code block with maximum settlement derivation

The first implemented predictive expression, denoted as $w_{max,0}$, governs the estimation of the maximum vertical settlement occurring along the projection of the tunnel axis onto the terrain surface. In accordance with the Gaussian settlement formulation adopted as the theoretical basis of this research (after Ralph B. Peck, 1969), this parameter represents the peak value of the subsidence trough and constitutes the principal input for subsequent evaluation of transverse settlement distribution.

The regression model for $w_{max,0}$incorporates two primary variables:

1. The radius of the TBM cutterhead, defined as a user-controlled parametric input within the Dynamo environment. This parameter directly influences the excavation diameter and, consequently, the potential volume loss and induced ground response.

2. The overburden depth of the tunnel is determined automatically by the computational workflow. The overburden is calculated as the vertical difference between corresponding discretized points along the tunnel axis and the projected alignment points located on the terrain surface.

A critical aspect of the model lies in the consistent discretization of both geometries. Because the tunnel axis and its surface projection are generated from the same discretization parameter, their point densities and positional correspondence are identical. This ensures a one-to-one relationship between subsurface and surface points, enabling accurate computation of the vertical distance between them.

To obtain the effective overburden depth above the tunnel crown, the radius of the TBM cutterhead is subtracted from the vertical coordinate difference. This adjustment is essential, as the initial vertical difference represents the depth to the tunnel axis rather than to the tunnel crown. By subtracting the excavation radius, the model correctly determines the soil cover thickness above the uppermost boundary of the tunnel along its entire length.

Through this automated and parametrically controlled procedure, the overburden depth becomes a spatially variable quantity that accurately reflects terrain elevation changes and tunnel alignment geometry. The resulting values are then introduced into the regression expression defining $w_{\max,0}$, allowing maximum settlement to vary consistently along the tunnel alignment in response to both geometric and geotechnical conditions.

This formulation ensures that the estimation of maximum settlement is not treated as a constant value but as a dynamically computed parameter, fully integrated within the parametric tunnel–terrain system and responsive to user-defined excavation geometry as well as topographic variation.

In addition to the evaluation of maximum settlement at the ground surface, the developed analytical framework extends the calculation to subsurface soil layers located at a predefined depth below the terrain. The maximum settlement within these inner layers, denoted as $w_{\max}$, is formulated as a function of three principal variables:

1. The previously computed maximum surface settlement $w_{\max,0}$;

2. The depth of analysis below the terrain surface, defined as a user-controlled input parameter;

3. The spatially variable tunnel overburden, automatically derived along the tunnel alignment.

The maximum surface settlement $w_{\max,0}$ serves as the reference magnitude, corresponding to the peak of the Gaussian settlement basin at ground level, in accordance with the formulation introduced by Ralph B. Peck (1969). To extend the model into the subsurface, the vertical position of the considered soil layer is incorporated into the mathematical expression.

The depth of analysis is introduced parametrically, allowing the user to specify the vertical distance below the terrain at which settlement is to be evaluated. Simultaneously, the program automatically accounts for the local overburden above the tunnel crown, which varies along with the alignment due to terrain elevation changes. Because both the tunnel axis and its surface projection share identical discretization density, each longitudinal position along the tunnel has a corresponding overburden value and a corresponding analysis depth.

The resulting formulation produces the distribution of maximum settlement values along the projection of the tunnel path but evaluated at a fixed depth beneath the terrain rather than at the surface. In practical terms, this enables the assessment of soil deformation not only at ground level but also at any intermediate stratum of interest, such as foundation levels of existing structures or critical underground utilities.

By incorporating both user-defined analysis depth and automatically computed overburden, the model ensures that subsurface maximum settlement is spatially variable and consistent with both geometric and geotechnical conditions. This extension significantly enhances the analytical capacity of the parametric system, transforming it from a surface-based evaluation tool into a three-dimensional predictive framework for soil deformation assessment.

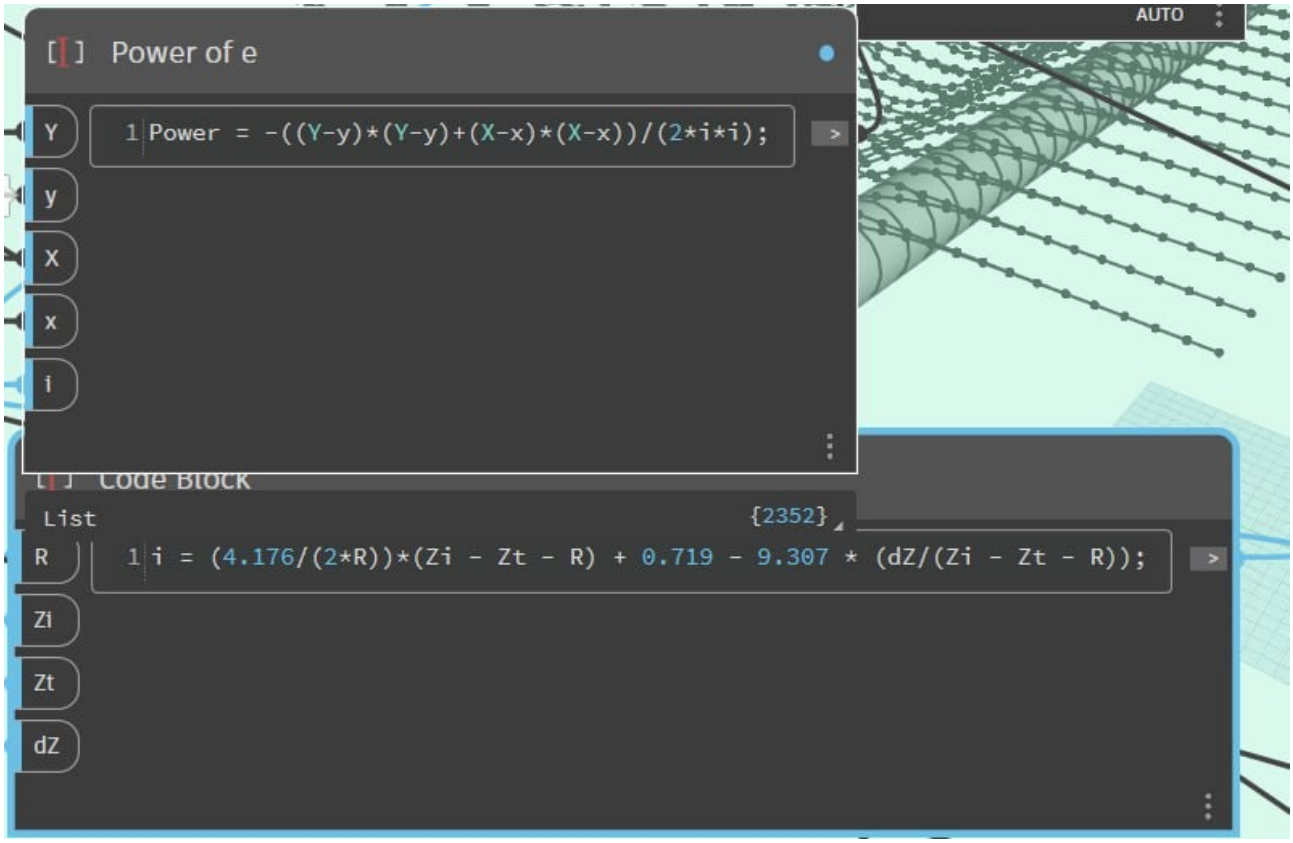

Figure 6.2. Code block with "I" parameter regression model

An analogous computational logic is applied to the determination of the tangent inclination parameter *i*, which defines the horizontal distance from the tunnel centerline to the inflection point of the Gaussian settlement trough. Within the framework originally proposed by Ralph B. Peck (1969), the parameter *i*governs the width and spatial dispersion of the settlement basin and therefore represents a fundamental variable in deformation prediction.

For the evaluation of i at the terrain surface, the required inputs are derived directly from the parametric tunnel–terrain model. These include:

- The Z-coordinates of discretized points along the tunnel axis;
- The Z-coordinates of the corresponding projected points on the terrain surface, organized in clustered form to preserve positional consistency;
- The radius of the TBM cutterhead, defined as a user-controlled parameter.

The overburden thickness above the tunnel crown is computed by subtracting the tunnel radius from

the vertical difference between corresponding surface and axis points. This procedure ensures that the parameter $i$is calculated based on the effective soil cover rather than the depth to the tunnel axis. Because the discretization density of both geometries is identical, each longitudinal position along the tunnel alignment possesses a unique and precisely defined overburden value.

For deeper soil layers, the regression model incorporates an additional parameter: the analysis level dZ, defined by the user as the depth below the terrain at which the settlement trough characteristics are to be evaluated. In this case, the effective vertical distance between the tunnel crown and the considered soil layer is determined by combining the computed overburden with the specified analysis depth. The output of the surface-based inclination parameter $i_0$then serves as the reference condition, which is subsequently adjusted according to the modified geometric relationship at depth.

As a result, the tangent inclination parameter becomes a spatially variable function along the tunnel alignment and across different soil layers. This parametric formulation ensures that the width of the settlement basin adapts consistently to changes in terrain elevation, tunnel geometry, and analysis depth. Consequently, both surface and subsurface deformation analyses remain geometrically coherent and mechanically representative within the integrated computational model.

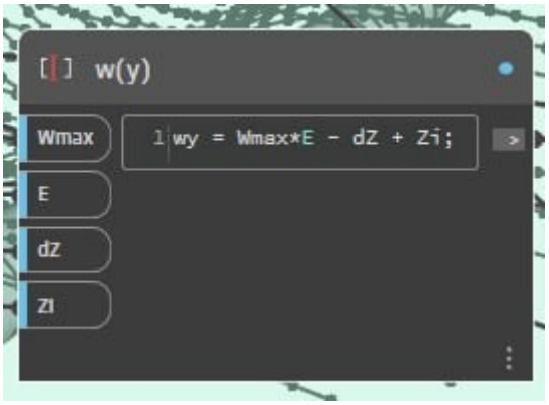

Figure 7.3. Code block with settlement distribution expression

After the derivation of spatially variable expressions for w_{max} and i, these parameters are introduced into the Gaussian settlement formulation proposed by Ralph B. Peck (1969).

Within this formulation, the only independent variable is the horizontal distance from the tunnel axis. While the analytical expression itself is mathematically straightforward, the definition and computation of the distance parameter in a three-dimensional parametric model presents a nontrivial geometric challenge.

In the developed computational workflow, the discretization governing the establishment of the settlement basin is not defined with respect to the global coordinate system. Instead, it is constructed locally, following directions strictly perpendicular to the projected tunnel alignment on the terrain surface. Consequently, the evaluation of the distance variable cannot rely solely on global X or Y offsets; it must be determined relative to each individual point along the tunnel axis projection and measured along its corresponding perpendicular cross-section.

The procedure for estimating the distance parameter is therefore defined as follows. First, the coordinates of discretized points lying on the tunnel alignment projection at the terrain surface are clustered, and their X and Y components are extracted. For each of these central alignment points, two perpendicular lines extend in opposite directions, generated through previously defined vector operations. Each perpendicular line is discretized into n segments, producing a set of points with coordinates $X_n$and $Y_n$on both sides of the axis.

For a given alignment point with coordinates (X, Y), the distance to any discretized point on the corresponding perpendicular section is computed using the Euclidean distance formula in the horizontal plane:

$$d = \sqrt{(X_n - X)^2 + (Y_n - Y)^2}$$

Because the Gaussian formulation includes the squared distance term y^2, the use of squared coordinate differences inherently eliminates any sign dependency, ensuring that distances on both sides of the tunnel axis contribute symmetrically to the settlement trough. This approach is consistent with the fundamental assumption of transverse symmetry embedded in the original Gaussian hypothesis.

From a strictly theoretical standpoint, the vertical coordinate difference should also be incorporated into the full three-dimensional distance calculation. However, in the present case study, this component is intentionally neglected. The investigated urban area exhibits minimal natural topographic variation, and local elevation changes are predominantly artificial, introduced for surface drainage purposes. Given the relatively small magnitude of these variations compared to tunnel depth and basin width, their influence on transverse settlement geometry is considered negligible. Therefore, the horizontal (planimetric) Euclidean distance provides a sufficiently accurate representation for the purposes of deformation modeling.

By defining the distance parameter locally—relative to each projected tunnel alignment point and along strictly perpendicular directions—the implemented procedure ensures geometric consistency with theoretical soil deformation models. The Gaussian settlement basin is thus generated in a manner that is both mathematically rigorous and fully compatible with the parametric, three-dimensional tunnel–terrain system established in the preceding chapters.

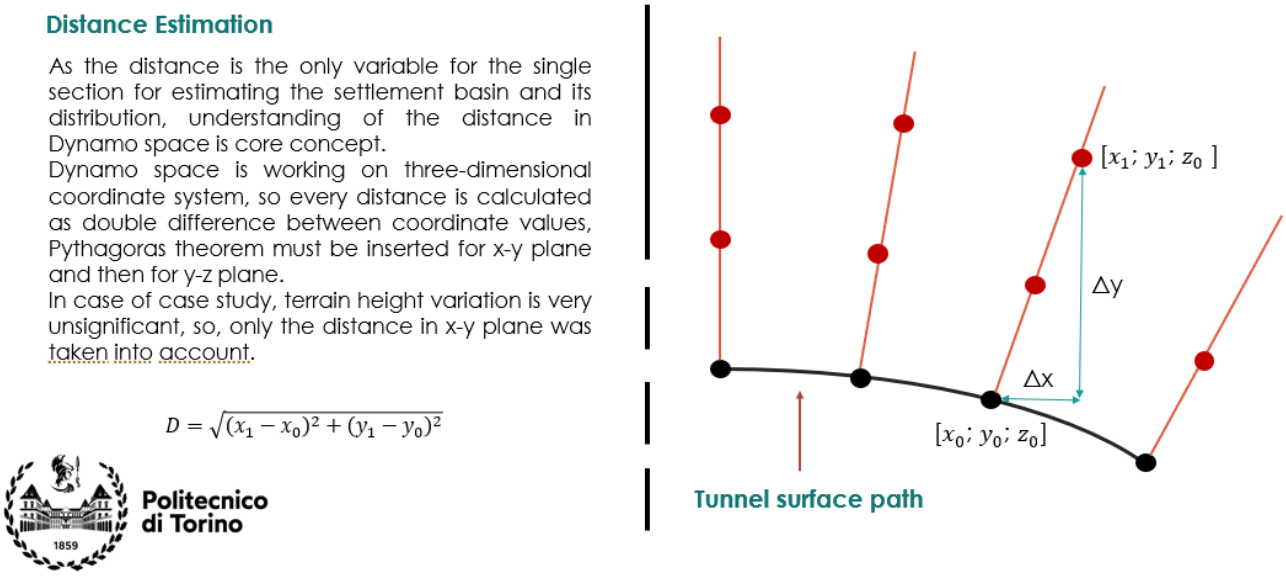

Figure 6.4. Visual recap of distance distribution

After extracting the discretized points generated along the transverse lines, their Cartesian coordinates are separated using the Dynamo nodes Point.X, Point.Y, and Point.Z. This enables independent manipulation of spatial components required for settlement simulation.

The X and Y coordinates of the discretized terrain points remain unchanged, as horizontal displacement is not considered within the scope of the present model. The vertical coordinate (Z), however, is modified to simulate soil settlement induced by tunnel excavation.

The first step in the deformation procedure consists of identifying the points located directly above the tunnel axis projection on the terrain surface. These points represent the locations where maximum vertical settlement occurs.

The maximum surface settlement $w_{max,0}$is calculated using the regression-based regression model derived from FEM simulations:

$$w_{max,0} = 0.71 \cdot \left(\frac{H}{D}\right) - 15.141$$

where:

- $H$is the overburden depth, defined as the vertical distance between the tunnel axis and the corresponding point on the terrain surface,
- $D$is the tunnel diameter (derived from the TBM radius input).

The overburden value $H$is automatically determined within the Dynamo environment by computing the difference between the Z-coordinate of the tunnel axis discretization point and the Z-coordinate of its corresponding projected point on the terrain surface. Since the tunnel axis geometry and its surface projection are already parametrically linked, this calculation is performed for each discretization point along the tunnel alignment.

The tunnel diameter $D$is defined through user input of the TBM radius, ensuring full parametric adaptability of the model.

Once the maximum settlement value $w_{max,0}$ is computed for each point located on the tunnel projection path, the new vertical coordinate is obtained by subtracting the calculated settlement from the original terrain elevation:

$$Z_{new} = Z_{original} - w_{max,0}$$

This operation produces the physical location of the points corresponding to maximum settlement along the tunnel alignment. The subtraction reflects downward vertical displacement, consistent with the assumed sign convention.

The updated Z-coordinates are then recombined with the unchanged X and Y coordinates to generate new points representing the deformed soil surface directly above the tunnel axis.

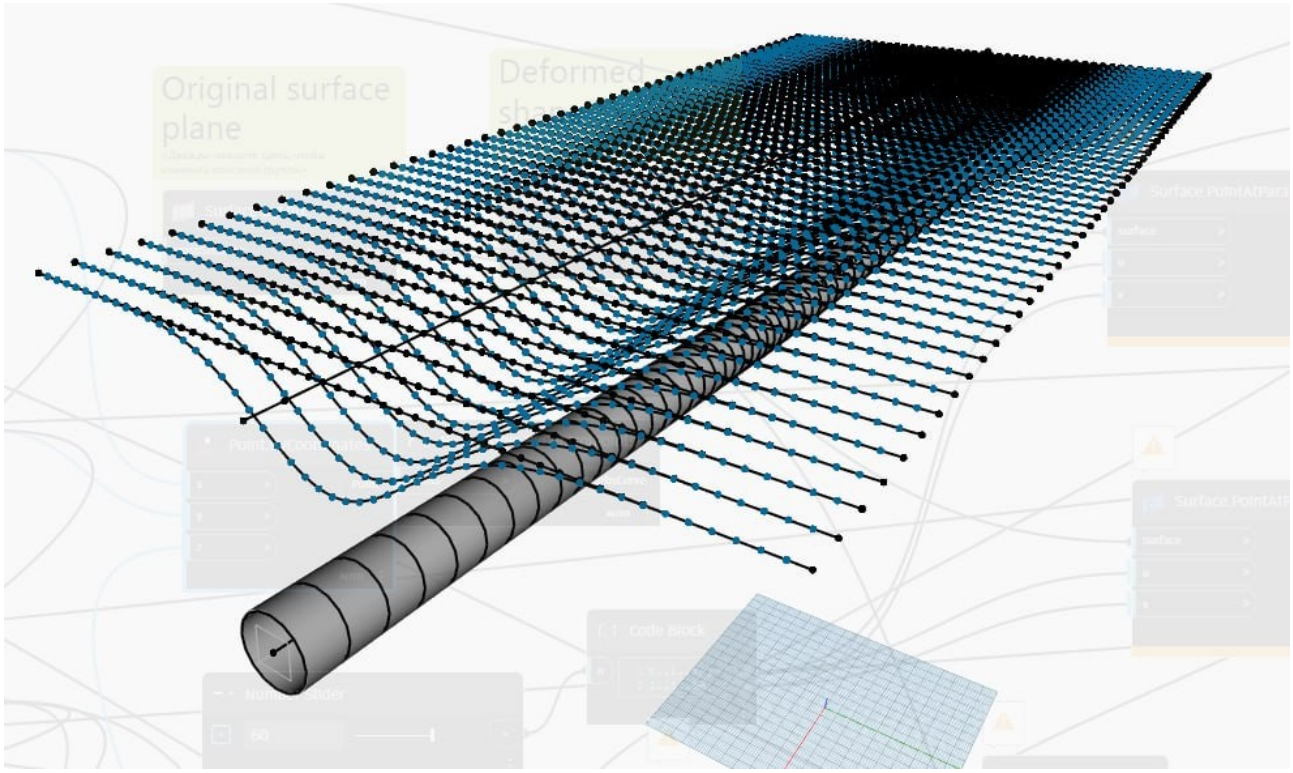

Figure 6.5. Settlement distribution Dynamo space visualization [1]

Following the calculation of maximum surface settlement along the tunnel alignment projection, the next stage of the procedure involves defining the spatial distribution of settlement across each transverse section. This distribution is governed by the settlement trough width parameter, commonly denoted as i, which controls the lateral extent and curvature of the settlement basin.

The value of the trough width parameter is determined by using a regression-based regression model derived from previously conducted FEM simulations. Similar to the maximum settlement formulation, this model depends exclusively on geometric tunnel characteristics, namely the overburden depth and tunnel diameter.

It is important to emphasize that the trough width parameter is not directly assigned to terrain points. Instead, it represents a governing coefficient within the Gaussian-type settlement distribution model, originally proposed by Peck (1969), which describes the transverse shape of the settlement basin. Within this framework, the magnitude of settlement at any given location depends on three components: the maximum settlement value, the trough width parameter, and the horizontal distance from the tunnel axis.

Since the maximum settlement and trough width parameters are already defined through parametric expressions, the remaining variable required for settlement evaluation is the horizontal distance between the tunnel alignment and each discretized terrain point.

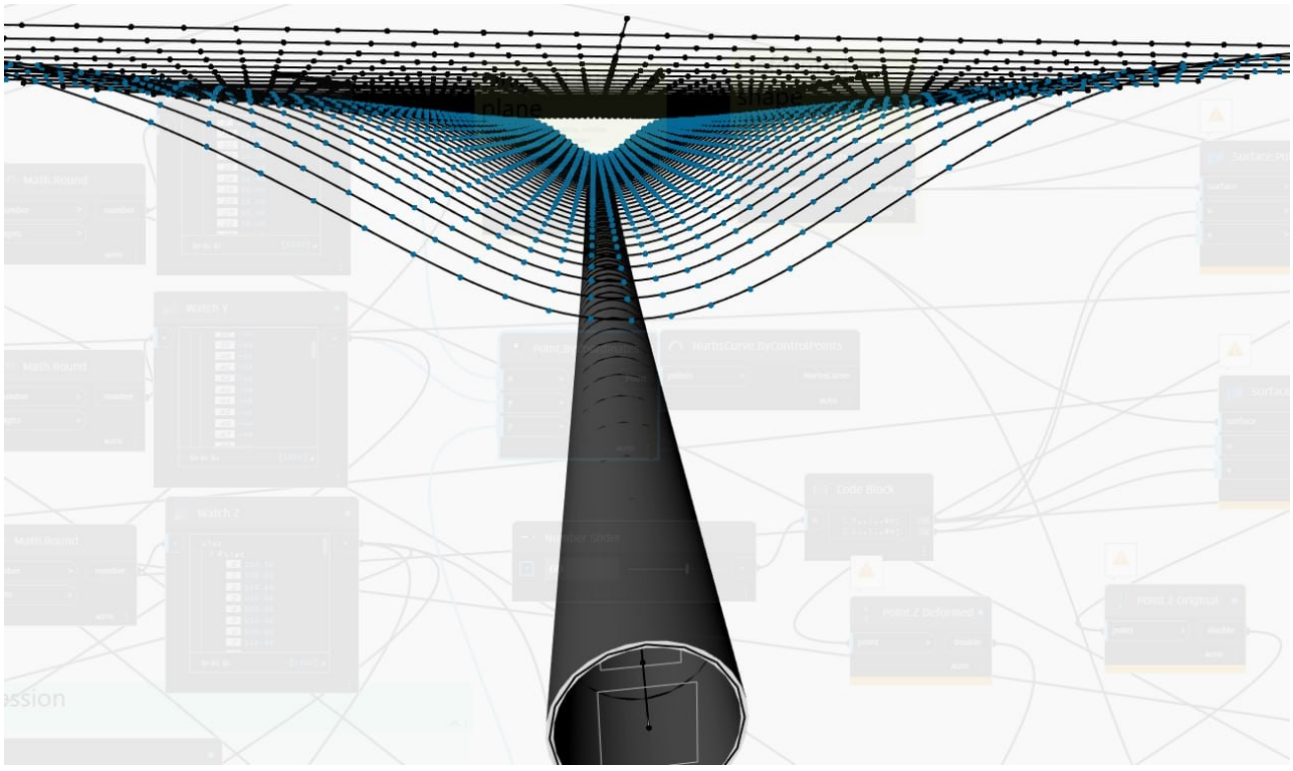

Figure 6.6. Settlement distribution Dynamo space visualization [2]

Once the horizontal distance parameter has been determined, the Gaussian settlement distribution is evaluated for every discretized terrain point. The previously calculated maximum settlement and trough width parameter are inserted into the settlement function, and the horizontal distance value corresponding to each point is used to compute its vertical displacement.

The model ensures that settlement magnitude decreases progressively as the horizontal distance from the tunnel axis increases. Consequently, points located directly above the alignment experience maximum displacement, while points further away exhibit reduced settlement, forming the characteristic symmetrical settlement trough.

For each terrain point, the calculated settlement value is used to modify its vertical coordinate. The original X and Y coordinates are preserved to maintain planimetric consistency, while the Z coordinate is reduced by the computed settlement magnitude. This operation effectively generates a new set of spatial points representing the deformed soil surface.

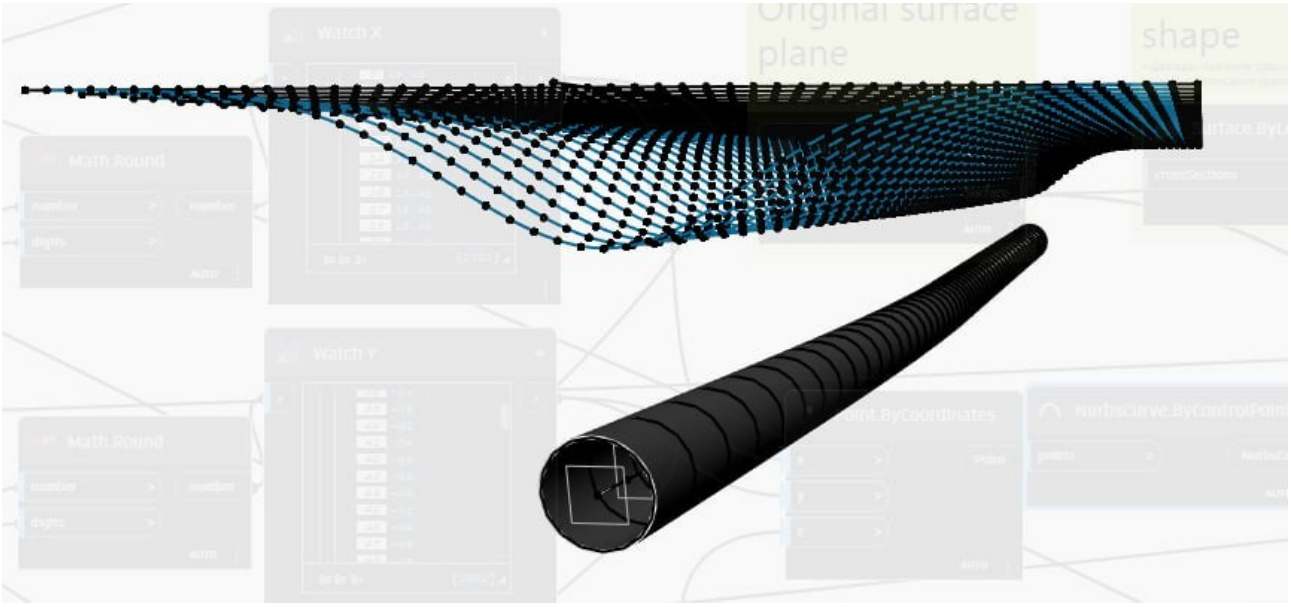

Figure 6.7. Settlement distribution Dynamo space visualization [3]

After computing and assigning settlement values to all discretized terrain points along every transverse section, new points are created as copies of the original terrain geometry, incorporating the updated vertical coordinates. The collection of these modified points defines the geometry of the settlement basin.

Because the procedure is executed sequentially for each discretized alignment point along the tunnel path, the transverse settlement sections are continuously distributed along the entire tunnel alignment. The aggregation of these sections produces a coherent three-dimensional settlement surface representing the predicted ground deformation caused by tunnel excavation.

The entire workflow remains fully parametric. Any modification of tunnel depth, diameter, or alignment geometry automatically updates the overburden calculation, trough width parameter, maximum settlement value, and final terrain deformation. This parametric dependency ensures consistency between tunnel design variables and predicted ground response, enabling integration of settlement analysis within the BIM-based modelling environment and supporting further evaluation of potential structural impacts on surface buildings.

6.2. Deformed terrain modelling. Danger zones classification

Following the computation of settlement values at discretized analysis points, a continuous deformed terrain surface is generated within the BIM environment. The procedure follows the same geometric logic that was previously applied for the reconstruction of the original terrain model, thereby ensuring methodological consistency.

The settlement basin is defined by a structured grid of points arranged along transverse sections perpendicular to the tunnel alignment. For each transverse section, settlement points are connected using the *NurbsCurve.ByControlPoints* node with a curve degree equal to 1. A first-degree NURBS curve corresponds to linear interpolation between adjacent control points. Although the interpolation is linear, the relatively high density of discretization points results in a smooth geometric representation of the Gaussian settlement profile along each section. This approach preserves numerical accuracy of the computed settlement values while maintaining geometric robustness and computational efficiency.

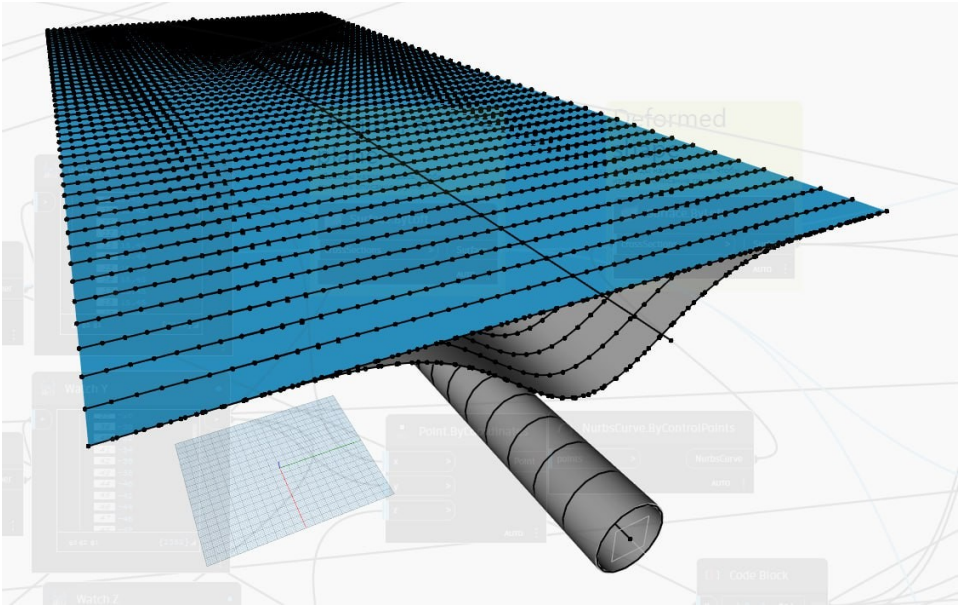

Figure 6.8. Original terrain with line discretization

Once all transverse settlement curves are generated, they are ordered sequentially along the longitudinal direction of the tunnel alignment. The deformed terrain surface is then constructed using the *Surface.ByLoft* node, which lofts between adjacent settlement curves to produce a continuous three-dimensional surface. The lofting procedure is identical to that used in the reconstruction of the original terrain surface, where imported elevation lines were connected to form the initial topographic

model. By applying the same modelling principle to both original and deformed states, geometric consistency between the two surfaces is ensured.

A specific consideration in the modelling process concerns unit consistency and visualization scale. Input parameters used in the regression-based settlement model, such as tunnel depth and diameter, are expressed in meters, while the computed settlement values are obtained in millimeters. These settlement values are directly subtracted from the Z-coordinates of the original terrain surface, which are defined in meters, without unit conversion. Consequently, the resulting deformations are effectively exaggerated by a factor of 1000 in the vertical direction.

This vertical exaggeration is introduced intentionally for visualization purposes. In real scale, surface settlements induced by tunnelling are typically on the order of several millimeters to a few centimeters, whereas terrain elevations in urban environments are measured in meters. Without exaggeration, the settlement trough would be visually imperceptible within the BIM model. Therefore, the generated deformed surface represents a geometrically amplified visualization of the settlement basin, enabling clear interpretation of deformation patterns. It is emphasized that all analytical evaluations and subsequent damage assessments are performed using the actual (non-exaggerated) settlement values derived from the regression models.

Through this procedure, a parametric three-dimensional representation of tunnel-induced terrain deformation is established within the BIM environment, forming the basis for subsequent analysis of building settlements and structural damage classification.

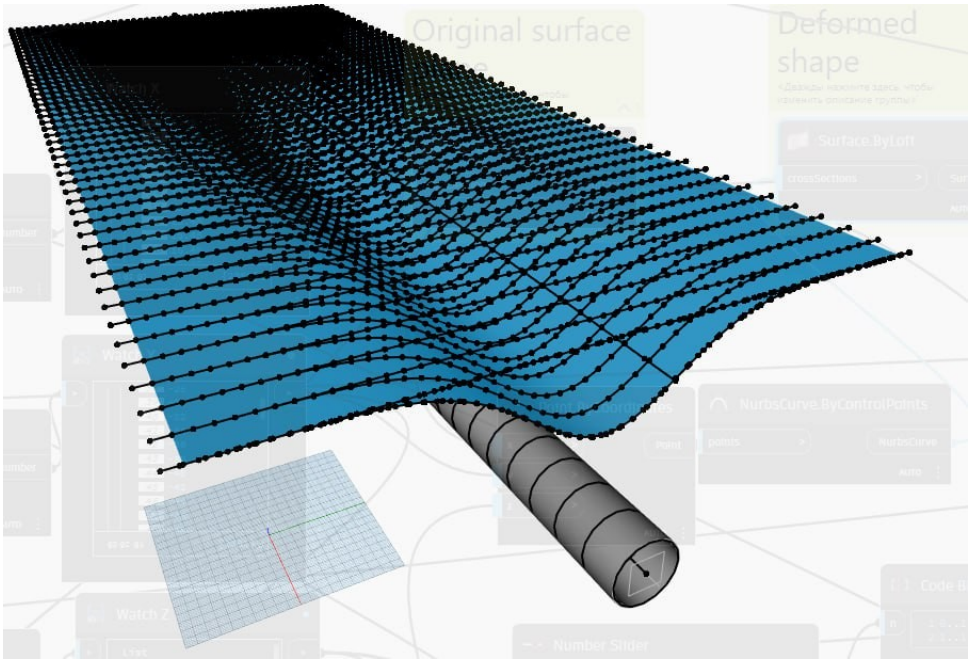

Figure 6.9. Deformed surface following regression models [View 1]

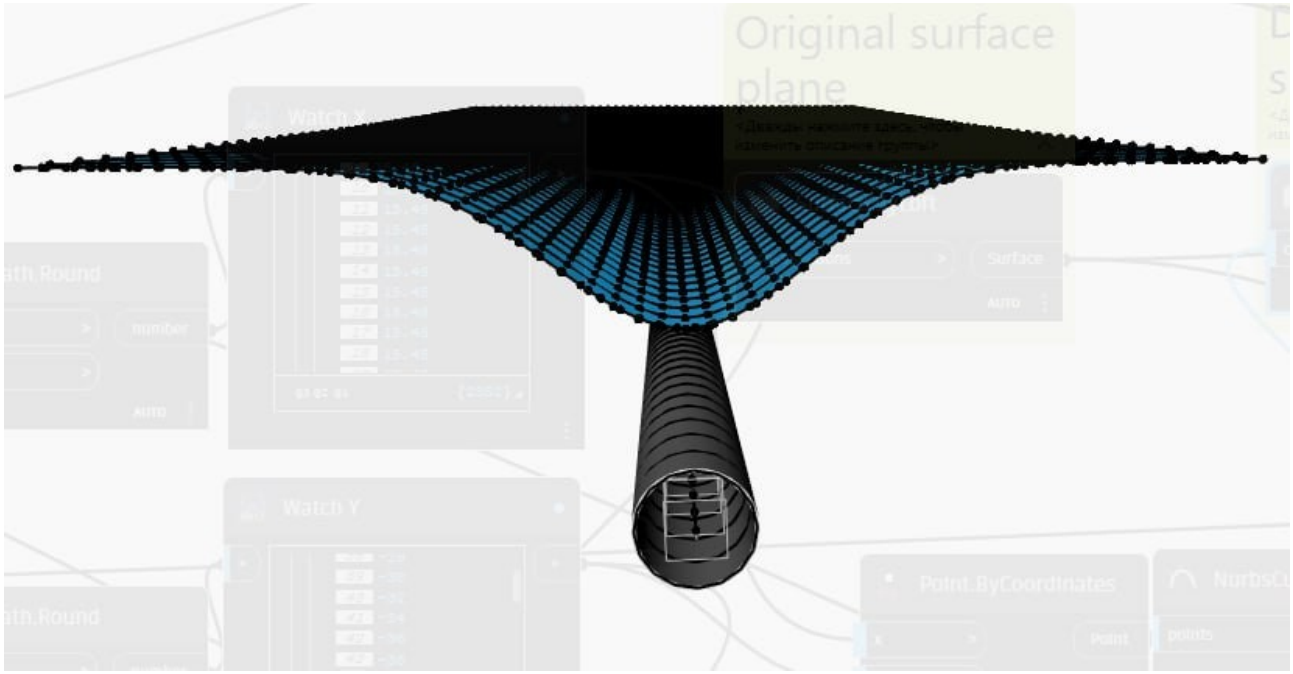

Figure 6.10. Deformed surface following regression models [View 2]

An essential stage of the settlement-induced damage assessment methodology is the visualization of risk zones in plan view. This stage consists of generating a color-coded representation of vertical settlement magnitudes directly on the terrain surface, allowing rapid identification of buildings located within zones of different deformation intensity. The resulting planimetric map provides an intuitive interpretation of tunnel-induced ground movements and supports preliminary structural risk assessment.

In contrast to the structured transverse discretization used for modelling the settlement basin along the tunnel alignment, the visualization procedure requires a homogeneous grid applied to the entire terrain surface. This ensures uniform spatial resolution and consistent classification of settlement values across the study area.

To generate this grid, the terrain surface is discretized using its local parametric coordinate system defined by parameters *u* and *v*, corresponding to the length and width directions of the surface. A two-directional discretization is achieved by applying a cross-product operation between the *u* and *v* divisions. Without the cross-product, default discretization would generate points only along the parametric diagonal. The cross-product distributes points across the entire domain, and each intersection becomes a grid point mapped into the global coordinate system.

The node *Surface.PointAtParameter* is used to extract the spatial coordinates (X, Y, Z) of each grid point. Since the coordinates are accessible independently, clustering and classification can be performed according to a single parameter. In this study, the classification criterion is vertical displacement along the Z-axis.

The settlement magnitude is computed as the difference between the elevation of the original terrain surface and the elevation of the corresponding point on the deformed surface. An optional underground reference level may be introduced if subsurface settlement visualization is required. The settlement value is defined as:

$$z_{val} = -(Z_i - d_z - z)$$

where:

- Z_i is the Z-coordinate of the original terrain surface,
- z is the Z-coordinate of the deformed surface at the same planimetric position,
- d_z is an optional underground reference depth defined by the user,
- z_{val} represents vertical settlement in millimeters.

The classification of settlement values into risk zones is implemented using a Dynamo code block with conditional operators. The code assigns a specific ARGB color to each point depending on the magnitude of settlement:

Figure 6.11. Code block for settlement distribution

The threshold values (in millimeters) define settlement intensity classes:

- < −25 mm – very high settlement (dark red)
- −25 to −20 mm – high settlement (red)
- −20 to −15 mm – moderately high settlement (orange)
- −15 to −10 mm – medium settlement (yellow)
- −10 to −5 mm – low settlement (green)
- −5 mm – negligible settlement (blue)

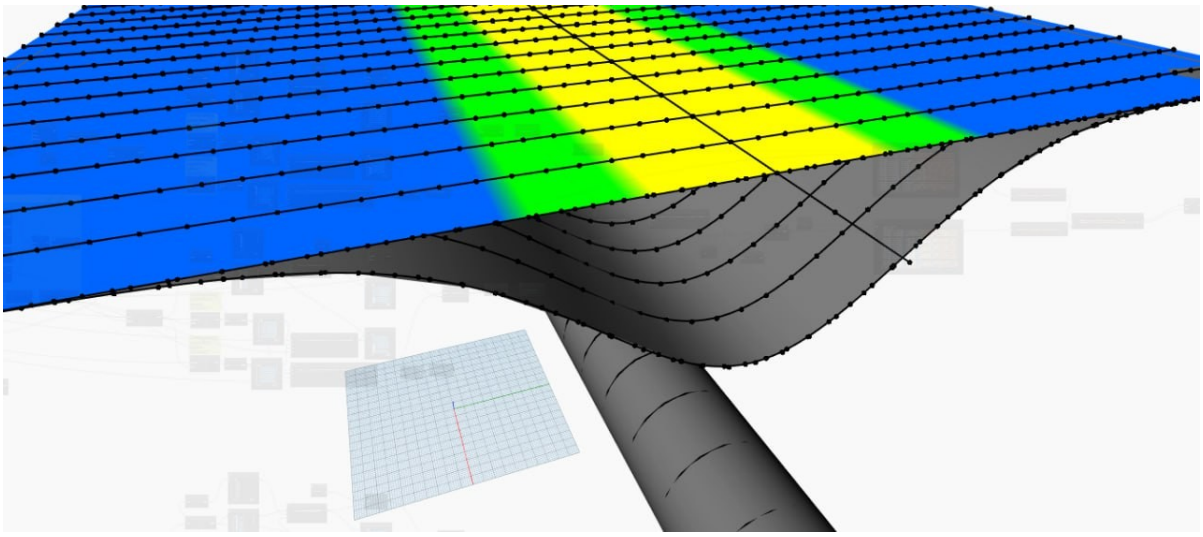

Figure 6.12. Resulting model with original terrain, deformed terrain and color distribution

Although both original and deformed terrain surfaces are required as inputs for the computation, the resulting color distribution is applied to the original (undeformed) terrain surface. This ensures that settlement risk zones are clearly visualized in plan view without geometric distortion caused by vertical exaggeration of the deformed surface.

The final output is a continuous, color-coded settlement map aligned with the tunnel trajectory. Buildings inserted into the BIM model can be directly assessed according to the zone in which they are located. Structures within red or dark red areas are preliminarily classified as high-risk, yellow zones indicate medium risk, while green or uncolored zones represent low-risk conditions.

This automated and parametric procedure enables reproducible and objective identification of buildings exposed to varying levels of tunnel-induced ground deformation. It serves as a transitional analytical layer between numerical settlement modelling and detailed structural damage classification within the BIM-based risk assessment framework.

6.3. Comparison of Dynamo abilities with Microsoft Excel computations

Although the regression models used for estimating maximum settlement and the settlement trough width parameter can be implemented in conventional spreadsheet software such as Microsoft Excel, the use of Autodesk Dynamo provides significant methodological and analytical advantages, particularly in projects involving complex three-dimensional geometric interaction between tunnels and buildings. While spreadsheet-based tools are capable of evaluating analytical expressions once geometric input parameters are defined, they rely heavily on manual identification and measurement of these parameters. In tunnel–structure interaction problems, such manual procedures introduce subjectivity, limit scalability, and may overlook critical geometric configurations.

In traditional engineering practice, assessment of tunnel-induced settlements at buildings is commonly performed using one or several representative cross-sections selected by the design engineer. The choice of such sections is typically based on engineering judgement and experience. For each selected section, geometric parameters including horizontal offset between the tunnel axis

and the building, as well as tunnel depth relative to the structure, are manually measured from plan drawings and longitudinal profiles. These measured values are then inserted into analytical or empirical formulations, such as the Gaussian settlement distribution proposed by Peck (1969), within a spreadsheet environment. Although this approach is straightforward for simple geometries and a limited number of structures, it becomes increasingly inefficient and potentially inaccurate when dealing with complex tunnel alignments and multiple buildings.

The geometric interaction between a tunnel and a building is inherently spatial and continuously variable. As the tunnel advances beneath or adjacent to a structure, the depth of the tunnel relative to the building changes along the longitudinal alignment. Simultaneously, the horizontal distance between the tunnel axis and different points along the building footprint also varies. Furthermore, the spatial orientation and position of buildings relative to the tunnel may be irregular and arbitrary. Importantly, the location at which the tunnel is closest to a building in plan view does not necessarily correspond to the most critical location in terms of induced settlement, since the tunnel depth must also be considered in determining the maximum settlement magnitude and the width of the settlement trough. Consequently, the selection of a single representative section may fail to capture the most unfavorable geometric configuration governing structural response.

Within the parametric environment of Dynamo, building geometry can be discretized systematically, allowing the evaluation of settlement response at multiple locations simultaneously. The edges of building footprints are discretized into a number of points defined according to the desired analytical resolution. Instead of evaluating only one manually selected section, settlement analysis is performed at all discretized points along the building perimeter. For each of these points, the required geometric parameters are computed automatically, and the regression-based settlement model is evaluated. The resulting settlement values are stored as a list corresponding to all potential interaction sections along the building. By applying list-processing operations such as maximum or minimum value extraction, depending on the adopted settlement sign convention, the most critical settlement value can be identified automatically. This procedure eliminates subjective section selection and ensures that the governing geometric configuration is determined objectively.

A key element enabling this automated spatial evaluation is the *Geometry.Closest* node available in Dynamo. This tool computes the shortest distance between a reference point and a target geometry, which may be represented by a point, curve, surface, or solid. Conceptually, the algorithm determines the minimal Euclidean distance between geometric entities by identifying the point of tangency at which the connecting segment is perpendicular to the target geometry. When applied between discretized building edge points and the projected tunnel alignment curve on the ground surface, the node identifies the corresponding closest points on the tunnel alignment. The resulting shortest distance provides the horizontal offset required as input for the Gaussian settlement formulation.

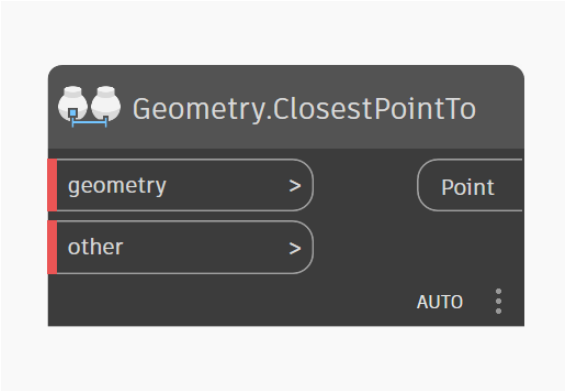

Figure 6.13. GeometryClosestPointTo node

The same procedure can be extended to determine tunnel depth. By applying the *Geometry.Closest* node between alignment points projected on the ground surface and the original underground tunnel axis, the corresponding points on the axis are identified even if they do not coincide with previously discretized axis nodes. The vertical distance between these corresponding points yields the local tunnel depth. This depth value serves as an input parameter for regression models used to determine the maximum settlement and the settlement trough width parameter. In this manner, both essential geometric variables required for settlement estimation—horizontal distance and tunnel depth—are obtained automatically and consistently for each discretized building point.

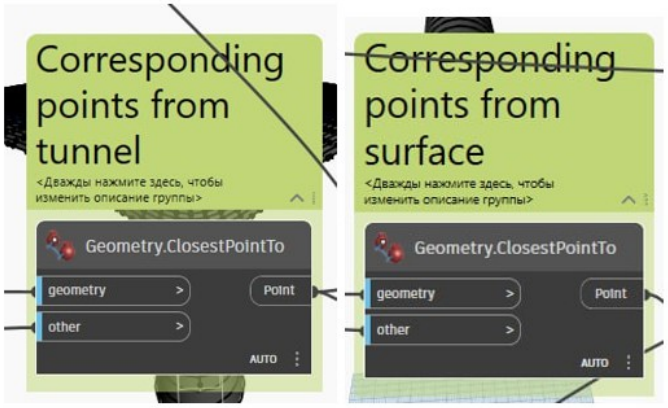

Figure 6.14. GeometryClosestPointTo node application

In contrast, within a spreadsheet-based workflow, distances must be manually measured from plan drawings and depths from longitudinal profiles for each considered section. Each section must be evaluated individually, and the engineer must decide in advance which configuration is representative or critical. This procedure is not only time-consuming but also prone to measurement inaccuracies and subjective judgement. Moreover, it becomes impractical when analyzing multiple buildings within a single project, especially when tunnel geometry is non-uniform or curved.

The Dynamo-based methodology enables simultaneous analysis of numerous buildings and multiple potential critical sections for each building within a unified parametric framework. All geometric relationships are derived directly from the three-dimensional BIM model, ensuring consistency between design geometry and analytical evaluation. The approach transforms the assessment from a

section-based deterministic procedure into a continuous parametric spatial analysis. As a result, the reliability, reproducibility, and scalability of tunnel-induced building settlement assessment are significantly enhanced, while reducing human error and increasing computational efficiency.

6.4. Developed procedure for buildings damage analysis

The first step in extending the settlement analysis from greenfield conditions to soil–structure interaction consists of incorporating building geometry into the computational environment. In the present study, building models are transferred from the Autodesk Revit environment into Autodesk Dynamo using the *SelectModel.Elements* node. Through this procedure, each building is imported as a solid body, preserving its three-dimensional geometric characteristics.

A fundamental requirement for consistent spatial analysis is the use of a unified coordinate system. The coordinate system adopted for tunnel alignment and terrain modelling in Dynamo must coincide with that used for building modelling in Revit. This ensures correct reconstruction of the urban environment and prevents spatial misalignment between terrain, tunnel, and structures. Once imported, the building solids are positioned directly on the parametric terrain surface, which has previously been discretized using two grid systems: a transverse discretization centered on the tunnel alignment for settlement basin modelling and a homogeneous surface discretization used for settlement visualization and classification.

To identify the portion of terrain affected by each building, the *Geometry.Closest* node is applied using two inputs: (1) the points of homogeneous terrain discretization and (2) the solid geometry of the building. This operation determines, for each terrain grid point, the closest point on the building solid. Points whose closest location lies on or within the building boundary are thereby identified as belonging to the building footprint. The output *Geometry.ClosestPointTo* provides the subset of terrain discretization points that are located within the building's projected area.

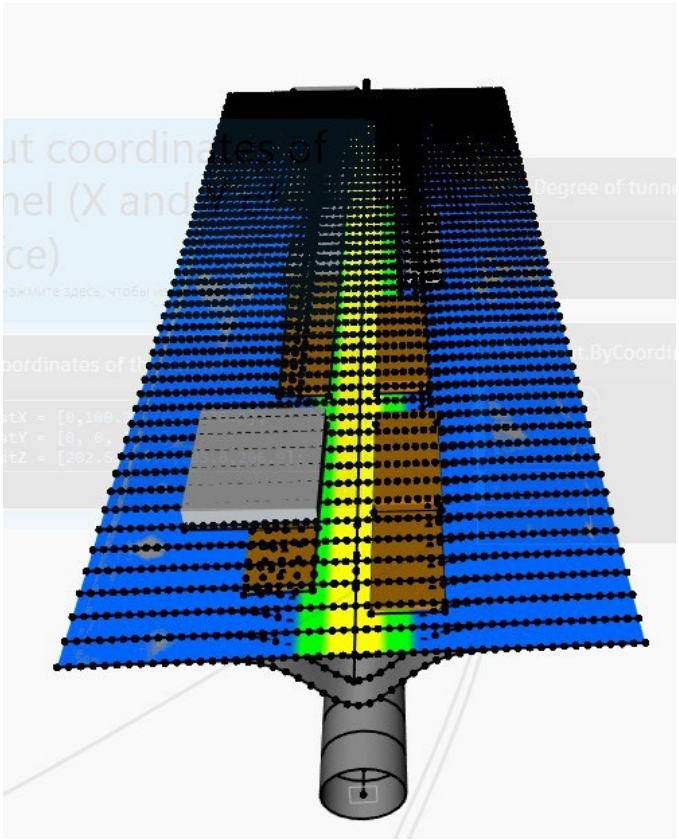

Figure 6.15. BIM model of tunnel, terrain and buildings with simulation of settlement

Once the relevant grid points corresponding to the building footprint are identified, the geometric relationship between these points and the tunnel is established. The *Geometry.Closest* node is applied again, this time between the selected terrain points and the projected tunnel alignment curve on the ground surface. This yields the corresponding closest points along the tunnel path in plan view and allows automatic determination of the horizontal distance required as input for the settlement calculation.

To determine the local tunnel depth at each considered location, the same procedure is repeated between the identified surface alignment points and the original tunnel axis located underground. Even if the corresponding underground points are not part of the initial discretization of the tunnel axis, the *Geometry.Closest* operation ensures that the correct geometrically corresponding points are identified. The vertical distance between these paired points represents the local tunnel depth beneath the building.

The local tunnel depth, together with the tunnel radius and the depth of the building foundation, constitutes the geometric input for the regression models used to estimate the maximum settlement and the settlement trough width parameter (i). These parameters are subsequently introduced into Peck's (1969) Gaussian settlement formulation, in which the independent variable is the horizontal distance between each building-related terrain point and its corresponding point on the tunnel alignment in plan view.

Through this procedure, a settlement value is computed for every discretized terrain point located within the building footprint. The total number of evaluated points depends on the density of the homogeneous terrain grid. The resulting set of settlement values represents the spatial distribution of tunnel-induced ground movement beneath the structure. From this dataset, the governing settlement

value is identified using the *List.Maximum* node, thereby determining the maximum settlement experienced within the building's footprint.

This parametric and fully automated workflow enables objective identification of the most critical settlement location for each building, eliminating the need for manually selected representative sections and ensuring that the maximum settlement is determined based on the complete three-dimensional geometric interaction between tunnel and structure.

6.5. Simplified edge-based approach for building settlement and inclination assessment

Although the previously described method based on homogeneous terrain discretization provides a detailed and spatially continuous evaluation of settlements beneath building footprints, it may become computationally demanding due to the large number of discretization points involved. In projects comprising multiple buildings and high-resolution terrain grids, the operational load on the computer system increases significantly, affecting performance and calculation time.

For the specific case study considered in this research, geometric configuration allows for a justified simplification. The tunnel alignment runs directly beneath a roadway, and the surrounding buildings are predominantly oriented parallel to the tunnel axis. Under such geometric conditions, it can be reasonably assumed that the maximum settlement within a building will occur along the edge closest to the tunnel alignment. Consequently, instead of analyzing the entire building footprint, a reduced model focusing on the front and rear edges of the structure can be adopted without significant loss of accuracy.

6.5.1 Geometric Definition of Buildings

In the simplified approach, each building is represented by four vertex points defining its rectangular footprint. The coordinates of these vertices are extracted from CAD documentation (e.g., from AutoCAD or tabulated data in Microsoft Excel) and inserted into Autodesk Dynamo using the *Point.ByCoordinates* node. The points are connected by *Line.ByStartPointEndPoint* to form the boundary edges of the building footprint. These boundary lines are subsequently connected using *Surface.ByLoft* to generate a planar surface representing the building in the analytical model. For visualization purposes, this surface may be assigned a color corresponding to a user-defined vulnerability index, allowing immediate graphical differentiation of structural susceptibility.

Identification and Discretization of Critical Edges

To evaluate settlement distribution, the two edges of primary interest are identified:

- the edge closest to the tunnel alignment (front edge),
- the edge farthest from the tunnel alignment (rear edge).

These edges are discretized using the Curve.PointAtEqualChordLength node, which generates evenly spaced points along each selected edge. The discretization density is selected according to the required analytical precision.

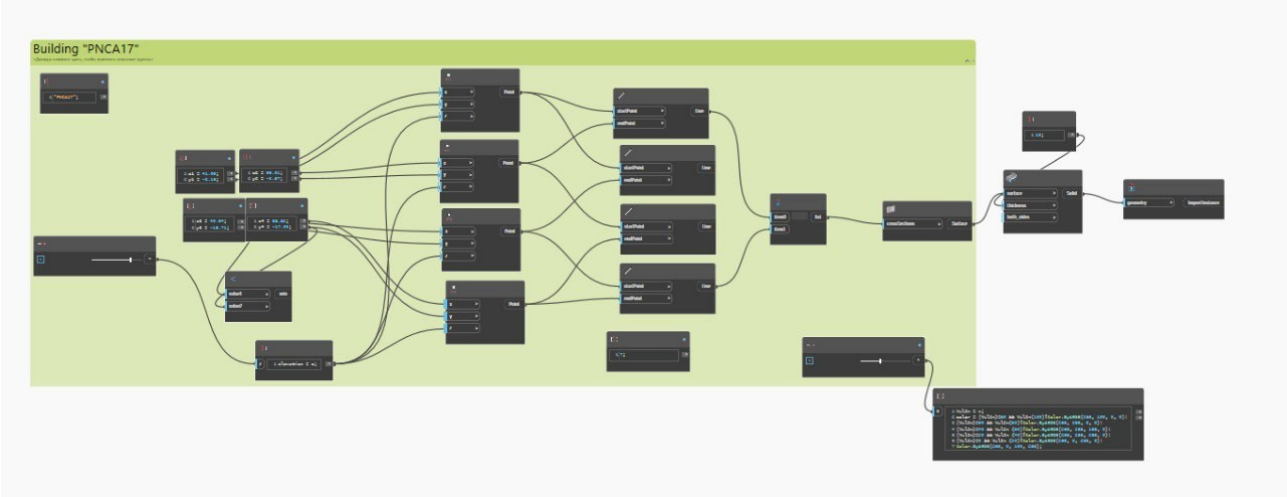

Figure 6.16. Buildings plane Geometry Reconstruction

6.5.2 Determination of Geometric Parameters

For each discretized point on the selected building edges, the horizontal distance to the tunnel alignment is determined using the *Geometry.Closest* node applied between the building edge points and the projected tunnel alignment curve on the ground surface. This operation yields the corresponding closest points along the tunnel path and provides the planimetric distance required for settlement calculation.

To determine the local tunnel depth, the *Geometry.Closest* node is applied again between the identified alignment points on the surface and the actual tunnel axis located underground. The vertical distance between these two corresponding points defines the tunnel depth at that specific longitudinal position.

6.5.3 Settlement Calculation

The computed geometric parameters are then used as inputs for regression models derived from prior finite element analyses. These regression models express:

- the maximum surface settlement S_{max},
- the settlement trough width parameter i,

as functions of tunnel depth, tunnel radius, and foundation depth.

Referring to formula [1]

This procedure yields a set of settlement values corresponding to all discretized points along the selected building edges. Using the *List.Maximum* node, the maximum settlement value is extracted and adopted as the governing settlement parameter for the building.

6.5.4 Evaluation of Building Inclination (Angular Distortion)

To evaluate potential structural damage due to differential settlement, angular distortion is calculated between corresponding points on the front and rear edges of the building. For each discretized point on the front edge, the settlement at the geometrically corresponding point on the rear edge is determined using the same procedure described above: identification of the closest tunnel alignment point, determination of local tunnel depth, evaluation of regression models, and application of Peck's formula. (1969)

The angular distortion $\beta$is computed as:

$$\beta = \frac{\Delta S}{L}$$

where:

- $\Delta S$is the difference between settlements at corresponding front and rear edge points,
- $L$is the horizontal distance between those two points.

The distance $L$is calculated using the Euclidean planimetric distance formula:

$$L = \sqrt{\left(X_n - X\right)^2 + \left(Y_n - Y\right)^2}$$

where $\left(X, Y\right)$and $\left(X_n, Y_n\right)$represent the coordinates of corresponding points on the front and rear edges, respectively.

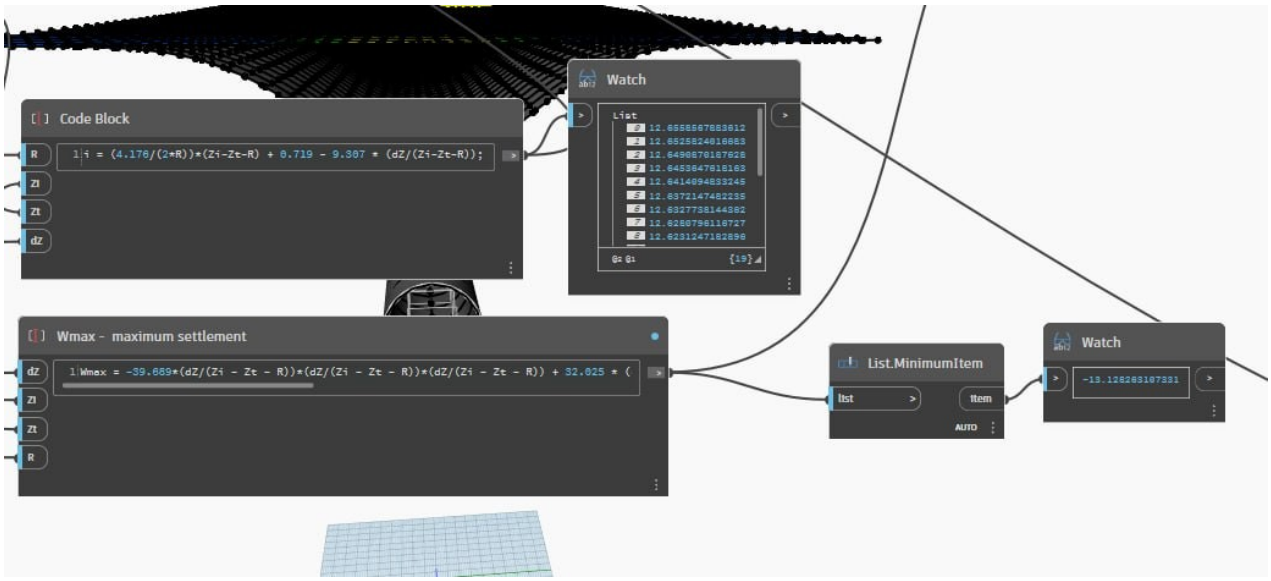

Figure 6.17. Biggest parameter among set of parameters identification

This procedure produces a set of angular distortion values along the building length. The maximum value is extracted using the *List.Maximum* node and adopted as the critical inclination parameter governing structural damage assessment.

6.5.5 Damage Classification According to the Turin Metro Line 2 Methodology

A major advantage of the simplified edge-based settlement assessment is its scalability. Because the procedure significantly reduces computational demand, a large number of buildings can be analysed simultaneously within the same parametric environment. This enables district-scale vulnerability assessment rather than isolated building-by-building evaluation.

For damage classification, the methodology adopted for the Turin Metro Line 2 project is implemented. The classification is performed separately for two governing parameters:

1. Maximum vertical settlement S_{max}
2. Maximum angular distortion β

The separation is necessary because the same building may fall into different damage categories depending on whether settlement magnitude or differential deformation governs structural response.

The classification system combines:

- A Vulnerability Index (V) assigned to each building,
- Computed deformation parameters,
- Threshold matrices defining damage grades.

The Vulnerability Index is provided as user input and typically ranges from 0 to 100, subdivided into the following vulnerability classes:

- 0–20: Irrelevant
- 20–40: Low
- 40–60: Medium
- 60–80: High
- 80–100: Very High

---

1. Classification Based on Maximum Settlement

For settlement-based damage classification, the following parameters are defined:

- Smax – computed maximum settlement (mm)
- VulIN – Vulnerability Index (V)

The logic is implemented in a Dynamo Code Block using conditional operators.

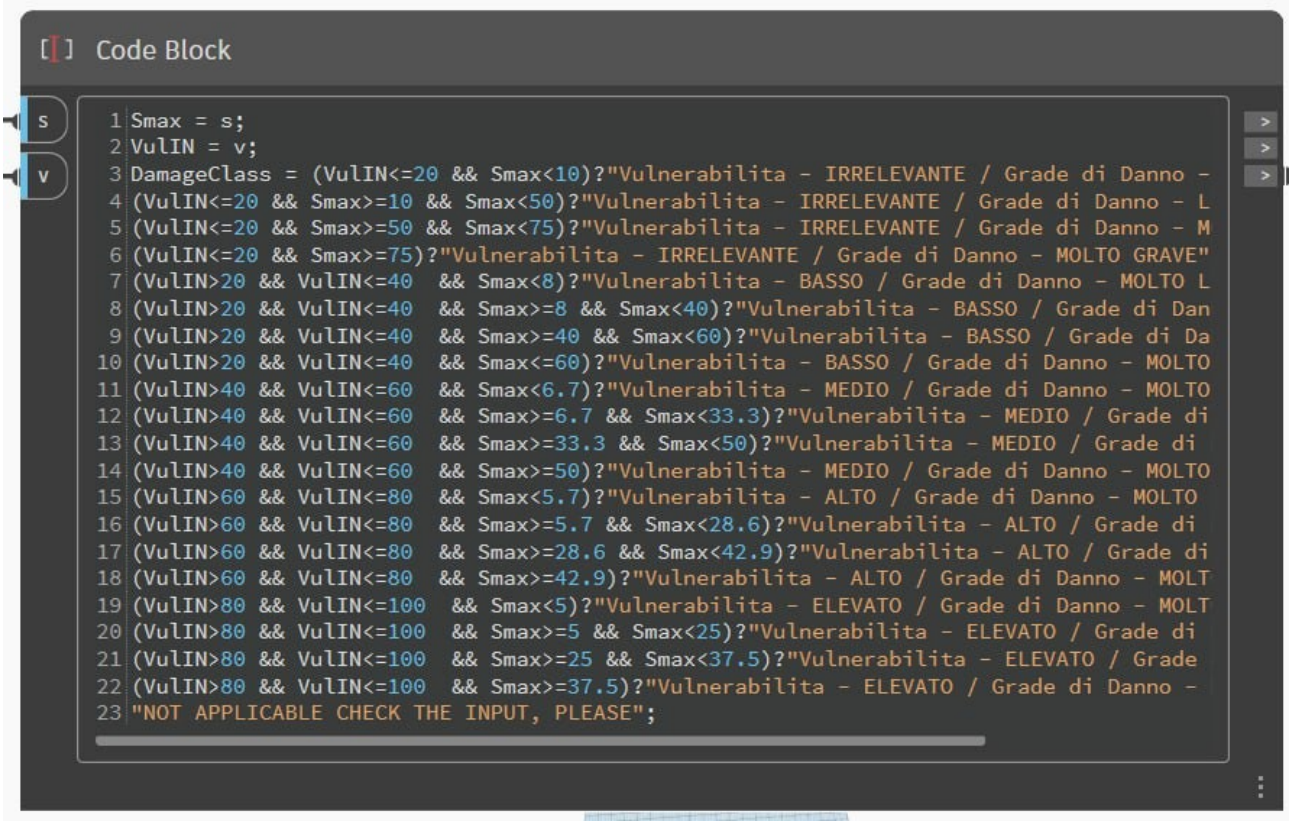

Figure 6.18. Code for damage classification according to Maximum settlement

This classification matrix reflects the principle that buildings with higher vulnerability require lower settlement thresholds to reach the same damage grade.

2. Classification Based on Maximum Angular Distortion

The following parameters are defined:

- AngINC – maximum angular distortion
- VulIN – Vulnerability Index

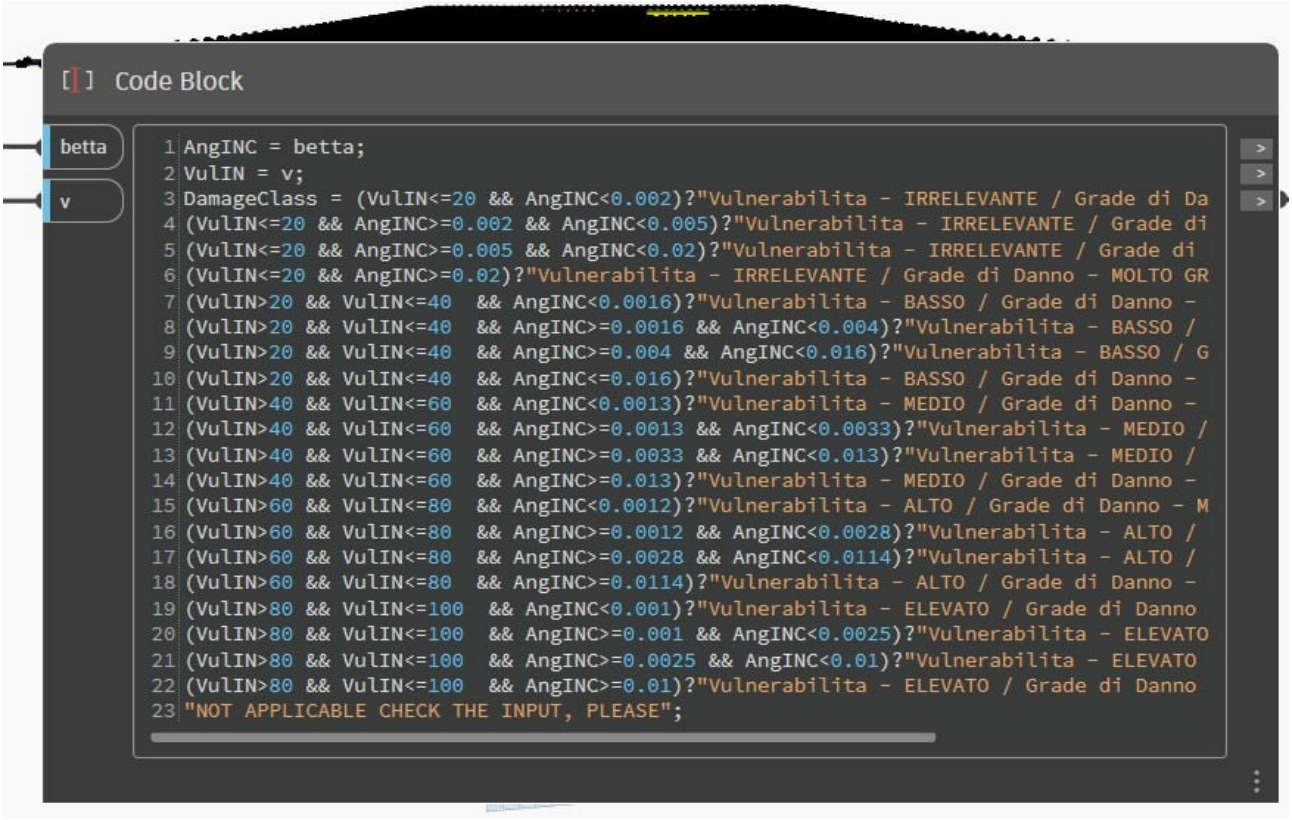

Figure 6.19. Code for damage classification according to Maximum distortion angle

Methodological Significance:

This classification system enables automated and consistent structural risk evaluation for a large number of buildings. Because settlement and angular distortion are assessed independently, the methodology reflects the fact that different deformation mechanisms may govern structural damage.

The implementation within Dynamo ensures:

- Full automation
- Elimination of subjective judgement
- Immediate updating when tunnel geometry changes
- Simultaneous large-scale urban analysis

The approach therefore represents a fully integrated BIM-based risk classification system aligned with the methodology adopted in the Turin Metro Line 2 project, adapted into a parametric computational framework suitable for large-scale infrastructure assessments.

6.6. Interoperability of results – geometrical and numerical output

A dedicated subchapter addresses the interoperability of results generated from the simulation environment, focusing on the transfer and further use of both geometrical and numerical outputs produced within Autodesk Dynamo. The objective is to demonstrate how the data obtained from the parametric simulation workflow can be efficiently integrated into commonly used engineering and design platforms, ensuring that the results of the computational analysis can be interpreted, documented, and applied within standard professional practice.

The subchapter is structured into two main parts, each corresponding to a different type of output produced by the simulation model:

The first part addresses the interoperability of geometrical outputs. The geometry generated in the simulation environment—including tunnel geometry, settlement surfaces, and related spatial elements—is transferred from Autodesk Dynamo into Autodesk Revit. Within the Revit environment, the imported geometry can be visualized and organized through standard Revit view representations, such as plan views (planimetry), elevations, and cross-sections. These views enable a clear graphical interpretation of the simulation results and allow the generated geometries to be incorporated directly into BIM documentation workflows. Furthermore, the Revit model can be exported to widely used CAD platforms, such as Autodesk Civil 3D and AutoCAD, where the geometrical outputs can be further processed, annotated, and integrated into conventional engineering drawings and project documentation.

The second part of the chapter focuses on the interoperability of numerical results. In addition to the geometric representation of the simulation outputs, the computational model developed in Autodesk Dynamo produces a series of numerical values related to settlement, inclination, and other parameters associated with the analyzed buildings and ground deformation patterns. These numerical datasets can be directly exported to Microsoft Excel, where they can be organized into structured tables for further analysis, statistical processing, and reporting. The use of spreadsheet-based tools enables efficient management of large datasets and facilitates the preparation of summary tables, charts, and comparative analyses required for engineering evaluation.
By separating the workflow into geometrical and numerical interoperability pathways, the chapter illustrates how the results obtained from the simulation environment can be seamlessly integrated into both BIM-based design workflows and conventional analytical tools, ensuring that the generated data remains accessible, interpretable, and applicable within broader engineering practice.

6.6.1 Interoperability of geometrical results

The first part of the interoperability workflow concerns the transfer of geometrical outputs generated in the simulation environment to BIM and CAD platforms. Within Autodesk Dynamo, the computational process produces several key geometric elements, including the parametric tunnel model, the original terrain surface, and most importantly the deformed terrain surface representing the predicted settlement basin. The geometrical output produced directly in the Dynamo environment is illustrated in Figure 6.20. In order to clearly visualize the deformation pattern, the generated deformation geometry is typically displayed using an amplified scale factor of 1000, which allows relatively small settlement values to become visually interpretable within the modelling environment

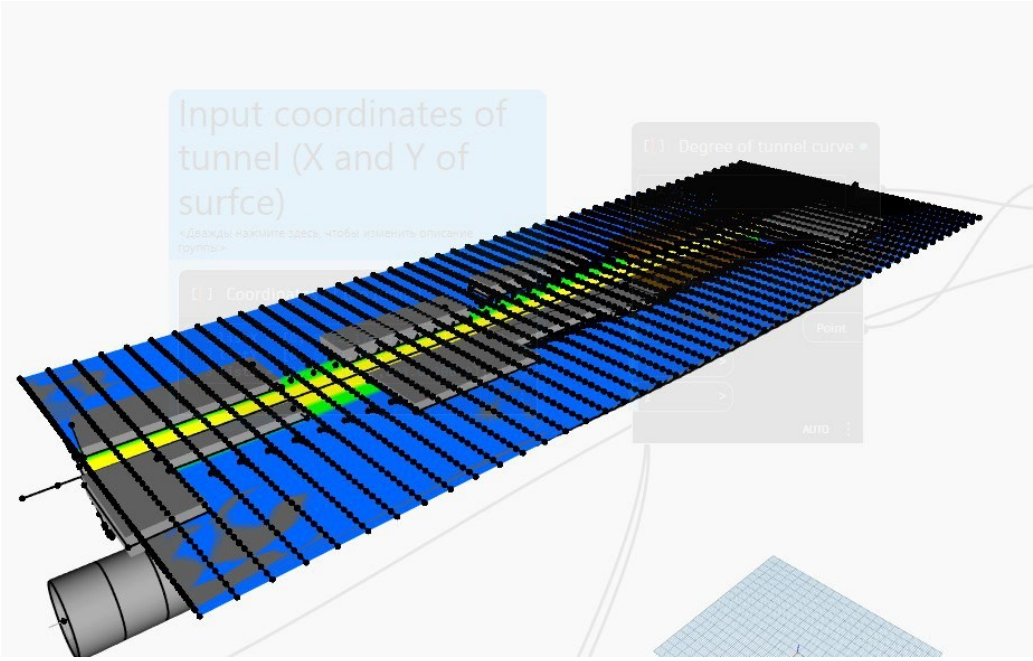

Figure 6.20. Simulation done in Autodesk Dynamo

The transfer of the generated geometry from Dynamo to Autodesk Revit is performed using the ImportInstance.ByGeometry node. This node is connected directly to the final geometric outputs of the model and allows the tunnel geometry, terrain surface, and deformation surfaces to be transferred automatically into the Revit environment while preserving their original coordinate system and spatial position. The resulting three-dimensional geometry imported into the Revit environment is presented in Figure 6.21.

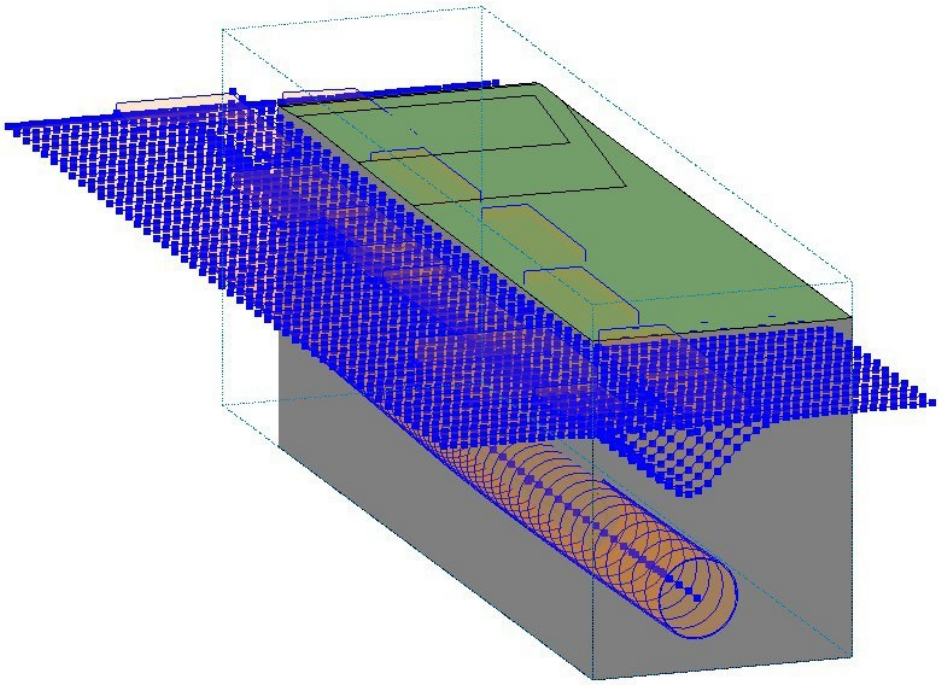

Figure 6.21. Tunnel geometry and deformed terrain transferred to Autodesk Revit [3D]

Although the initial tunnel alignment is typically imported from Revit into Dynamo for analysis, the parametric structure of the model allows the tunnel design to be modified directly within Dynamo if the obtained settlement results are not satisfactory. For instance, adjustments can be made to parameters such as the tunnel radius or the critical coordinates defining the horizontal and vertical alignment. When the updated tunnel geometry is transferred back into the Revit workspace, the previously existing tunnel element is not automatically removed. As a result, both the original and modified tunnel geometries remain visible, providing a direct opportunity to visually compare alternative design configurations and evaluate their influence on the resulting settlement patterns.

In addition to the tunnel geometry, the deformed terrain surface is transferred as a geometric plane representing the settlement profile. Depending on the analysis requirements, this surface can be positioned either at the terrain level or below the ground surface in cases where subsurface deformation analysis is required.

Once the geometry is available in the Revit environment, the results can be examined using standard visualization and documentation tools. Within the View section of the Revit interface, planimetric views can be generated at selected elevation levels in order to observe the spatial distribution of settlements across the terrain surface. An example of such a planimetric visualization is presented in Figure 6.22, where the settlement distribution can be interpreted in a two-dimensional plan representation.

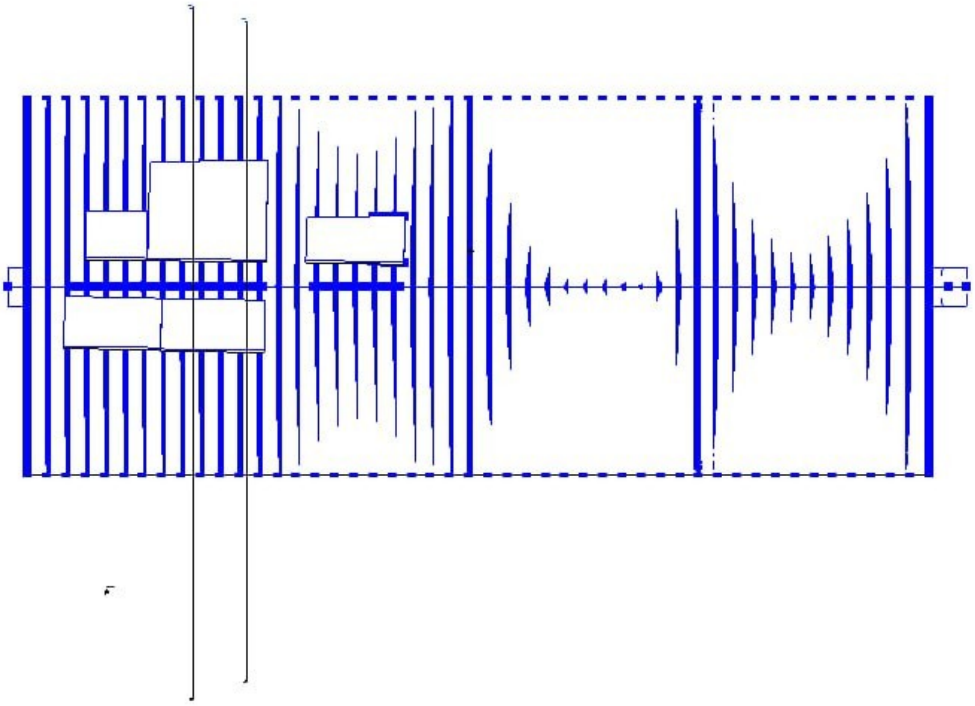

Figure 6.22. Planimetric view of parametric model transferred to Revit

Furthermore, by using the Section tool, it is possible to create perpendicular or diagonal cross-sections through the terrain model. These sections allow the deformation profile to be analyzed in detail and enable direct measurement of settlement values at any location, including specific points along building foundations or across the terrain surface. A representative cross-sectional visualization of the settlement trough obtained in this manner is shown in Figure 6.23.

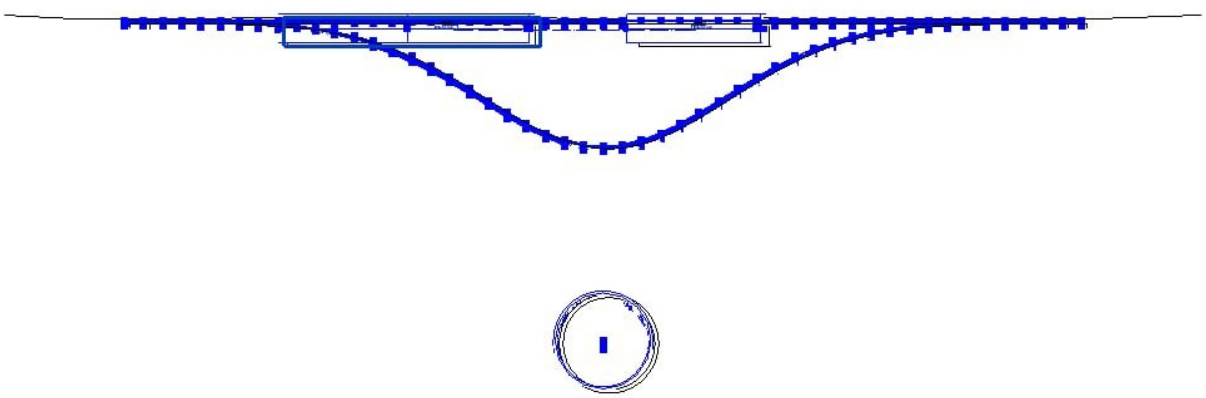

Figure 6.23. Transversal section of settlement distribution done in Revit

The generated planimetric views and cross-sections can be further exported for use in conventional CAD environments. Through the Export → CAD → DWG functionality in Autodesk Revit, the created views can be transferred directly to AutoCAD or other compatible platforms such as Autodesk Civil 3D. This export process converts the BIM-based visualization into a fully compatible CAD drawing format, enabling further processing, annotation, and integration into engineering documentation.

Such interoperability is particularly useful for geotechnical and ground improvement design. The exported drawings allow engineers to identify zones where settlement and inclination values may lead to potentially critical conditions for buildings or infrastructure, as well as areas characterized by unstable soil structure. Based on this information, appropriate mitigation measures—such as soil stabilization, reinforcement strategies, or foundation modifications—can be designed and incorporated into the overall engineering project workflow.

6.6.2 Interoperability of numerical results

The second part of the interoperability workflow concerns the transfer of numerical results generated in the simulation environment to spreadsheet-based analysis tools. Within Autodesk Dynamo, numerical data obtained from the computational model can be exported directly to Microsoft Excel using a node specifically designed for this purpose, namely *Data.ExportToExcel*.

The *Data.ExportToExcel* node allows structured numerical datasets generated in Dynamo to be written directly into an Excel spreadsheet. In order to execute this operation, the node requires several input parameters: File Path, Sheet Name, Start Row, Start Column, and Data.

The File Path input specifies the location of the Excel file that will receive the exported data. This is typically defined using the File Path node, which links the Dynamo script to the target Excel file. It is recommended that the Excel file be opened simultaneously during the export process, as this allows the user to immediately observe and verify the changes occurring in the spreadsheet.

The Sheet Name parameter defines the worksheet in which the data will be written. This input can be provided using a Code Block node containing the name of the desired worksheet. Similarly, the Start Row and Start Column parameters define the exact position within the worksheet where the data export begins. These values can also be assigned through a Code Block using numerical inputs. Alternatively, Number Slider nodes can be used to control these parameters, provided that the slider values are restricted to integer numbers.

The most complex part of the workflow concerns the preparation of the Data input, which must be organized in a structured list format compatible with Excel. The first step involves defining the column headers. These are written in a Code Block as string values. In the present case study, the column titles are:
“Building code”, “Vulnerability index”, “Maximum settlement”, “Maximum distortion angle”, “Classification by Maximum settlement”, and “Classification by Maximum distortion angle”.

These strings are then connected to a *List.Create* node, where they are arranged in the exact order in which the columns should appear in the Excel spreadsheet. After defining the column headers, a second *List.Create* node is used to organize the numerical results corresponding to each column. It is essential that the data in this list follow the same order as the column names, ensuring that each dataset is correctly aligned with its corresponding header in the spreadsheet.

Finally, both lists - the column header list and the list containing the numerical values—are connected to the Data input of the *Data.ExportToExcel* node. Once executed, this configuration automatically generates a structured table within the Excel worksheet containing all numerical outputs of the simulation. The complete workflow for exporting numerical data from Dynamo to Excel is summarized in Figure 6.24.

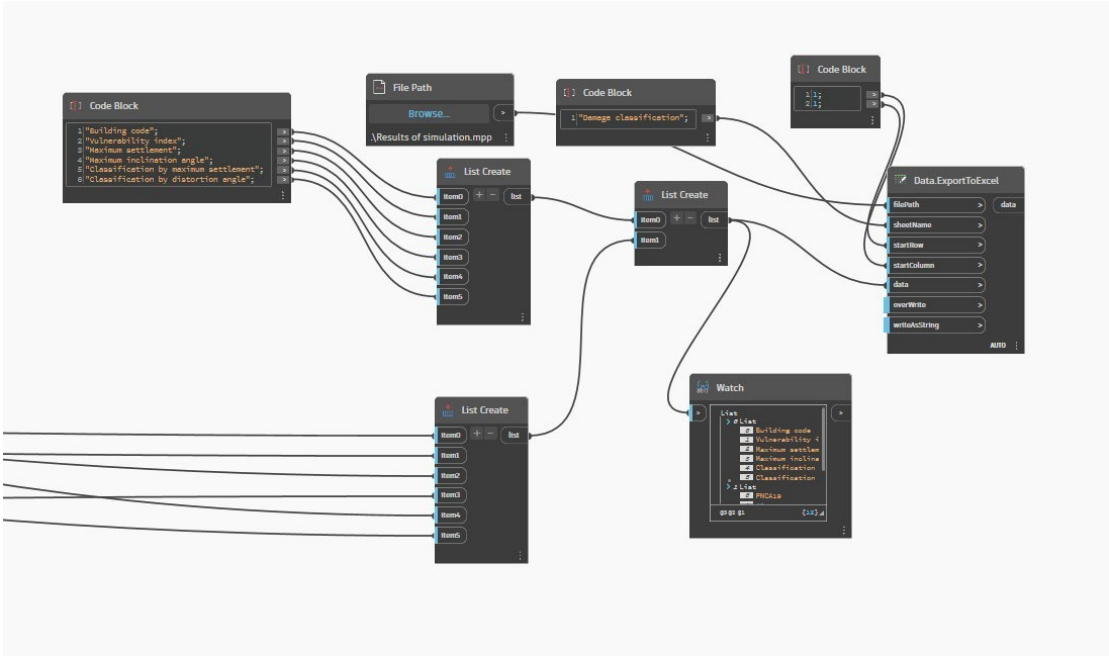

Figure 6.24. Workflow for Data Transfer

As previously described, the export of numerical data from Autodesk Dynamo to Microsoft Excel is performed immediately after the execution of the computational script, allowing the user to observe the updated values in real time. This immediate update provides an efficient way to verify simulation outputs and monitor changes in the calculated parameters without the need for manual data transfer.

Another important aspect of this workflow is that the Excel table does not automatically overwrite the entire worksheet during each execution of the Dynamo script. Instead, the update begins from the specified start row and start column, meaning that only the cells located after the defined starting position are modified. All cells located before the selected starting cell remain unchanged, preserving any previously written information. This feature allows the user to maintain additional notes, headers, or supplementary calculations in the upper part of the spreadsheet without affecting the automated data export.

Furthermore, this functionality makes it possible to construct the spreadsheet table progressively. By modifying the start row and start column parameters, new datasets can be appended to the existing table, enabling a step-by-step accumulation of simulation results within the same Excel file. Such an approach can be particularly useful when analyzing multiple scenarios or when storing results from different simulation runs within a single document.

The numerical data transferred to the Excel spreadsheet are illustrated in Table 6.1. As shown in the table, the exported table contains the calculated parameters and classification results generated by the simulation model. It should be noted that some advanced formatting options available in Excel—such as text styles, cell dimensions, cell colors, and text colors—cannot be directly controlled through the Dynamo export process. Consequently, additional formatting adjustments may be required within the Excel file itself after the data transfer has been completed.

Nevertheless, the essential aspect of this workflow is that the computed results and the corresponding damage classification are automatically transferred from the simulation environment into the Excel spreadsheet, ensuring an efficient and reliable method for documenting and further processing the numerical outputs of the analysis.

Building code	Vulnerability index	Maximum settlement	Maximum inclination angle	Classification by maximum settlement	Classification by distortion angle
PNCA19	40	11	0.0007	Vulnerabilita - BASSO / Grade di Danno - LIEVE	Vulnerabilita - BASSO / Grade di Danno - MOLTO LIEVE
Building code	Vulnerability index	Maximum settlement	Maximum inclination angle	Classification by maximum settlement	Classification by distortion angle
PNCA18	37	11	0.0009	Vulnerabilita - BASSO / Grade di Danno - LIEVE	Vulnerabilita - BASSO / Grade di Danno - MOLTO LIEVE
Building code	Vulnerability index	Maximum settlement	Maximum inclination angle	Classification by maximum settlement	Classification by distortion angle
PNCA20	57	14	0.0006	Vulnerabilita - MEDIO / Grade di Danno - LIEVE	Vulnerabilita - MEDIO / Grade di Danno - MOLTO LIEVE
Building code	Vulnerability index	Maximum settlement	Maximum inclination angle	Classification by maximum settlement	Classification by distortion angle
PNCA17	40	14	0.0007	Vulnerabilita - BASSO / Grade di Danno - LIEVE	Vulnerabilita - BASSO / Grade di Danno - MOLTO LIEVE
Building code	Vulnerability index	Maximum settlement	Maximum inclination angle	Classification by maximum settlement	Classification by distortion angle
PNCA15	55	12	0.0007	Vulnerabilita - MEDIO / Grade di Danno - LIEVE	Vulnerabilita - MEDIO / Grade di Danno - MOLTO LIEVE
Building code	Vulnerability index	Maximum settlement	Maximum inclination angle	Classification by maximum settlement	Classification by distortion angle
PNCA13	36	12	0.0007	Vulnerabilita - BASSO / Grade di Danno - LIEVE	Vulnerabilita - BASSO / Grade di Danno - MOLTO LIEVE
Building code	Vulnerability index	Maximum settlement	Maximum inclination angle	Classification by maximum settlement	Classification by distortion angle
PNCA12	48	13	0.0008	Vulnerabilita - MEDIO / Grade di Danno - LIEVE	Vulnerabilita - MEDIO / Grade di Danno - MOLTO LIEVE
Building code	Vulnerability index	Maximum settlement	Maximum inclination angle	Classification by maximum settlement	Classification by distortion angle
PNCA10	37	13	0.0008	Vulnerabilita - BASSO / Grade di Danno - LIEVE	Vulnerabilita - BASSO / Grade di Danno - MOLTO LIEVE
Building code	Vulnerability index	Maximum settlement	Maximum inclination angle	Classification by maximum settlement	Classification by distortion angle
PNCA09	45	13	0.0009	Vulnerabilita - MEDIO / Grade di Danno - LIEVE	Vulnerabilita - MEDIO / Grade di Danno - MOLTO LIEVE
Building code	Vulnerability index	Maximum settlement	Maximum inclination angle	Classification by maximum settlement	Classification by distortion angle
PNCA07	45	14	0.0009	Vulnerabilita - MEDIO / Grade di Danno - LIEVE	Vulnerabilita - MEDIO / Grade di Danno - MOLTO LIEVE
Building code	Vulnerability index	Maximum settlement	Maximum inclination angle	Classification by maximum settlement	Classification by distortion angle
PNCA06	38	12	0.0009	Vulnerabilita - BASSO / Grade di Danno - LIEVE	Vulnerabilita - BASSO / Grade di Danno - MOLTO LIEVE
Building code	Vulnerability index	Maximum settlement	Maximum inclination angle	Classification by maximum settlement	Classification by distortion angle
PNCA16	56	14	0.0007	Vulnerabilita - MEDIO / Grade di Danno - LIEVE	Vulnerabilita - MEDIO / Grade di Danno - MOLTO LIEVE
Building code	Vulnerability index	Maximum settlement	Maximum inclination angle	Classification by maximum settlement	Classification by distortion angle
PNCA14	52	8	0.0008	Vulnerabilita - MEDIO / Grade di Danno - LIEVE	Vulnerabilita - MEDIO / Grade di Danno - MOLTO LIEVE
Building code	Vulnerability index	Maximum settlement	Maximum inclination angle	Classification by maximum settlement	Classification by distortion angle
PNCA11	31	13	0.0009	Vulnerabilita - BASSO / Grade di Danno - LIEVE	Vulnerabilita - BASSO / Grade di Danno - MOLTO LIEVE

Table 6.1. Direct Dynamo computational output in Excel

The presented interoperability workflow demonstrates how both geometrical and numerical outputs generated within Autodesk Dynamo can be efficiently transferred to other widely used engineering software environments. This capability ensures that the results of the computational model are not limited to the simulation environment itself but can be integrated into standard BIM, CAD, and data-processing workflows commonly applied in engineering practice.

The transfer of geometrical outputs enables the visualization and interpretation of simulation results within Autodesk Revit, where tunnel geometry, terrain surfaces, and deformation models can be examined through planimetric views, elevations, and cross-sections. These views provide a clear graphical representation of predicted ground deformation and allow direct measurement of settlement values at any selected location. Through the export of these views to CAD formats compatible with AutoCAD and Autodesk Civil 3D, the generated geometrical information can be further incorporated into conventional engineering drawings and project documentation. Such integration facilitates practical engineering tasks such as settlement assessment, design comparison, and the planning of potential ground improvement measures.

At the same time, the interoperability workflow also enables the direct transfer of numerical outputs to Microsoft Excel, allowing the calculated parameters to be automatically organized in structured tables. This process ensures efficient management of large datasets while enabling further analysis, comparison of results, and preparation of engineering reports. Although some visual formatting adjustments may still be required within Excel, the essential computational outputs—including settlement values, inclination parameters, and damage classifications—are transferred automatically, significantly reducing the possibility of manual errors during data processing.

The combined use of these interoperability pathways demonstrates that the developed parametric workflow provides not only efficient simulation capabilities but also effective integration with widely used engineering tools. As a result, the generated results can be easily interpreted, documented, and applied within practical design and analysis processes, supporting a streamlined workflow from parametric modelling and simulation to engineering evaluation and project documentation.

6.7. Comparison of results with the methodology adopted by INFRATRASPORTI.TO S.R.L.

The final stage of the case study focuses on the assessment of tunneling-induced ground deformation and its potential impact on existing buildings located along a selected segment of Via Lagrange in Turin. The analyzed section corresponds to the planned excavation of the second metro line tunnel, specifically the segment between chainages 8+526.722 and 8+269.229. Within this area, a total of 14 buildings potentially affected by the tunnel excavation were investigated in order to determine the expected levels of settlement and structural inclination. Location of the buildings according to their codes is possible to see on Figure 6.25.

For each building, the analysis produced values of maximum settlement and maximum inclination angle, which represent key indicators commonly used for evaluating the potential risk of structural damage caused by differential ground movements. According to the damage classification system adopted by INFRATRASPORTI.TO S.R.L., the calculated inclination values for all analyzed structures fall within the categories “Lieve” (slight) and “Molto lieve” (very slight), indicating a relatively low level of expected structural impact resulting from the tunneling activity.

Figure 6.25. Planar view of analyzing section with underlined buildings for damage assessment

The results of the performed analysis are summarized in Table 6.2. which presents the calculated parameters and corresponding damage classifications for each investigated building. The first column

contains the identification codes assigned to the buildings within the study area. The second column provides the vulnerability index associated with each structure. The third column presents the calculated maximum settlement values, while the fourth column reports the corresponding maximum inclination angles derived from the settlement distribution beneath each building. The fifth column indicates the damage classification based on the maximum settlement values, and the sixth column provides the damage classification based on the maximum distortion or inclination angle.

	Building code	Vulnerability index		Maximum settlement [mm]	Maximum inclination grade [-]	Classification by maximum settlement	Classification by distortion grade
1	PNCA06	38	BASSO	12	0.0009	LIEVE	MOLTO LIEVE
2	PNCA07	45	MEDIO	14	0.0009	LIEVE	MOLTO LIEVE
3	PNCA09	45	MEDIO	13	0.0009	LIEVE	MOLTO LIEVE
4	PNCA10	37	BASSO	13	0.0008	LIEVE	MOLTO LIEVE
5	PNCA11	31	BASSO	13	0.0009	LIEVE	MOLTO LIEVE
6	PNCA12	48	MEDIO	13	0.0008	LIEVE	MOLTO LIEVE
7	PNCA13	36	BASSO	12	0.0007	LIEVE	MOLTO LIEVE
8	PNCA14	52	MEDIO	8	0.0008	LIEVE	MOLTO LIEVE
9	PNCA15	55	MEDIO	12	0.0007	LIEVE	MOLTO LIEVE
10	PNCA16	56	MEDIO	14	0.0007	LIEVE	MOLTO LIEVE
11	PNCA17	40	BASSO	14	0.0007	LIEVE	MOLTO LIEVE
12	PNCA18	37	BASSO	11	0.0009	LIEVE	MOLTO LIEVE
13	PNCA19	40	BASSO	11	0.0007	LIEVE	MOLTO LIEVE
14	PNCA20	57	MEDIO	14	0.0006	LIEVE	MOLTO LIEVE

Table 6.2. Results of maximum settlement and distortion angle inclination derived by developed method

The assessment required the definition of several was geometrically represented by the coordinates of its boundary vertices, with the basic representation consisting of a quadrilateral defined by four points corresponding to the building footprint. In cases where the building geometry was more complex or composed of multiple connected blocks, the block located closest to the tunnel axis was selected for analysis, as it is expected to experience the most significant ground deformation. Additional input parameters included the structural vulnerability index of the building as well as the depth of its foundation system. Within the considered case study, the analyzed foundations were located at depths of 4 m, 7 m, and 10 m below the ground surface, reflecting the typical range of foundation depths encountered in the investigated urban environment.

An important aspect of the analysis is that the building inclination was evaluated while accounting for spatial variations in the settlement basin geometry. Rather than assuming a uniform settlement beneath the entire building footprint, the method considers the three-dimensional distribution of ground deformation across the foundation area. This was achieved using advanced modelling capabilities available within the Autodesk Dynamo environment.

Specifically, the foundation area of each building was discretized into a regular computational grid, allowing the settlement to be estimated at multiple points across the structure. In the present case study, a 5 × 5 grid was applied to each building footprint, resulting in a set of discretized nodes where settlement values were calculated based on the predicted settlement surface. This approach enables the reconstruction of a three-dimensional settlement field beneath the building, from which the true maximum settlement values and differential movements along the foundation plane can be determined. Consequently, the resulting inclination angles are calculated with greater accuracy, as they reflect the actual variation of settlements within the building footprint rather than relying on simplified assumptions.

In order to verify the reliability of the obtained results, they were compared with the analyses performed by INFRATRASPORTI.TO S.R.L. during the risk assessment stage of the project. The BIM-based parametric modelling method applied in the present study relies on regression relationships derived from simulations conducted using the Finite Element Method (FEM). Consequently, the calculated values of settlement and building inclination are expected to approximate the results that would be obtained through detailed FEM simulations.

However, for the specific segment of Via Lagrange in Turin considered in this case study, no buildings were subjected to FEM analysis by the company. According to the adopted risk assessment procedure, detailed FEM simulations are carried out only when the preliminary evaluation indicates that the potential damage category for a building reaches at least the "Moderato" (moderate) level. This preliminary evaluation is typically based on simplified empirical or semi-empirical methods. Since none of the buildings within the analyzed segment exceeded this threshold, a detailed FEM analysis was not performed for any of them.

As a result, the available reference data for comparison consist only of the conservative estimates obtained using empirical and semi-empirical methods. These include approaches proposed by Ralph B. Peck, (1969) Michael P. O'Reilly, and Barry M. New (1982), which are commonly used for preliminary assessment of tunneling-induced settlements and associated structural damage. The results derived from these methods, which generally provide exaggerated or conservative estimates of settlement effects, are summarized in Table 6.3 and serve as a reference for evaluating the outcomes obtained through the parametric modelling approach.

	Building code	Vulnerability index		Maximum settlement [mm]	Maximum inclination grade [-]
1	PNCA06	38	BASSO	27	0.002
2	PNCA07	45	MEDIO	29	0.002
3	PNCA09	45	MEDIO	28	0.002
4	PNCA10	37	BASSO	27	0.002
5	PNCA11	31	BASSO	30	0.002
6	PNCA12	48	MEDIO	27	0.002
7	PNCA13	36	BASSO	23	0.001
8	PNCA14	52	MEDIO	14	0.002
9	PNCA15	55	MEDIO	23	0.001
10	PNCA16	56	MEDIO	29	0.002
11	PNCA17	40	BASSO	28	0.002
12	PNCA18	37	BASSO	24	0.002
13	PNCA19	40	BASSO	21	0.001
14	PNCA20	57	MEDIO	25	0.002

Table 6.3. Results of maximum settlement and distortion angle inclination derived by INFRATRASPORTI.TO S.R.L. [Empirical method]

Due to the absence of results obtained through detailed FEM analysis for buildings located directly within the investigated segment, an alternative verification procedure was adopted. The selected approach is based on the comparison of empirical and numerical results for a group of buildings located in the surrounding area of the project corridor, where both methods had previously been applied. The considered buildings include PAPN 03, PAPN 18, PNCA41, PNCA 43, RM02, and CAMO15, all situated within an approximate ±1 km distance from the analyzed segment of Via

Lagrange in Turin.

The selection of these buildings is justified by the fact that they are located within the same urban and geological context, meaning that the soil conditions and geotechnical characteristics do not vary significantly from those present in the case study segment. For these structures, both empirical methods and detailed analyses based on the Finite Element Method were carried out by INFRATRASPORTI.TO S.R.L. during the project's risk assessment phase.

By comparing the results obtained from these two approaches, it becomes possible to estimate the degree of overestimation typically produced by empirical methods when compared to the more accurate FEM simulations. In particular, the percentage difference between the empirical predictions and the corresponding FEM results can be calculated for both maximum settlement and maximum inclination angle. This percentage difference represents the exaggeration factor commonly associated with simplified empirical approaches used during preliminary risk assessments.

Once the exaggeration percentages are determined for the selected reference buildings, the same procedure can be applied to the buildings located within the case study segment. By comparing the predicted results obtained through the developed BIM-based parametric modelling method with the expected range derived from the empirical-to-FEM relationship, it becomes possible to evaluate whether the proposed methodology produces realistic and consistent predictions relative to established numerical analyses.

The results of maximum settlement and inclination angle obtained for the selected reference buildings using both empirical methods and FEM simulations are summarized in Table 6.4, which provides the basis for estimating the empirical exaggeration factors and performing the subsequent verification of the BIM-based modelling approach.

				Emperical Method Peck, O'really & New		FEM simulation	
	Building code	**Vulnerability index**		**Maximum settlement [mm]**	**Maximum inclination grade [-]**	**Maximum settlement [mm]**	**Maximum inclination grade [-]**
1	**PAPN03**	37	BASSO	29	0.004	19	0.002
2	**PAPN18**	37	BASSO	32	0.002	15	0.001
3	**PNCA41**	73	ALTO	37	0.003	19	0.001
4	**PNCA43**	76	ALTO	65	0.008	32	0.003
5	**RM02**	53	MEDIO	45	0.004	23	0.002
6	**CAMO15**	76	ALTO	38	0.003	16	0.001

Table 6.4. Results of maximum settlement and distortion angle inclination derived by INFRATRASPORTI.TO S.R.L. [Empirical method & FEM simulation]

The overestimation of both maximum settlement and inclination angle obtained through the empirical assessment procedures adopted by INFRATRASPORTI.TO S.R.L. was quantified by comparing the empirical results with those derived from detailed Finite Element Method (FEM) simulations. The percentage of overestimation was calculated using the standard relationship:

$$\text{Overestimation } \backslash(\%\backslash) = \frac{\text{Empirical value} - \text{FEM value}}{\text{FEM value}} \times 100$$

where the empirical value corresponds to the maximum settlement (S_{emp}) or inclination angle (β_{emp}) estimated using simplified methods, and the FEM value corresponds to the result obtained from

numerical simulations (S_{FEM} or β_{FEM}).

For maximum settlement **(Smax)**, the computed overestimation percentages for the reference buildings are as follows:

Emperical	FEM	
Max. settlement [mm]	**Max. settlement [mm]**	Overestimation percent [%]
29	19	52.6
32	15	113.3
37	19	94.7
65	32	103.1
45	23	95.7
38	16	137.5

Table 6.5. Overestimation percent computation for max. settlement according to results computed by INFRATRASPORTI.TO S.R.L. [Empirical method & FEM simulation]

The results indicate that the empirical methods consistently produce higher settlement estimates than FEM simulations, with an average overestimation of approximately **99.5%**, meaning that, on average, the empirical predictions are roughly twice as large as the FEM-based results for these buildings.

For maximum inclination angle **(βmax)**, the overestimation percentages are as follows:

Emperical	FEM	
Max. inclination grade [-]	**Max. inclination grade [-]**	Overestimation percent [%]
0.004	0.002	100.0
0.002	0.001	100.0
0.003	0.001	200.0
0.008	0.003	166.7
0.004	0.002	100.0
0.003	0.001	200.0

Table 6.6. Overestimation percent computation for max. inclination grade according to results computed by INFRATRASPORTI.TO S.R.L. [Empirical method & FEM simulation]

These results demonstrate that empirical procedures also significantly overestimate building inclination, with exaggerations ranging from 100% to 200% and an average overestimation of approximately **144%**. This confirms the conservative nature of empirical methods, which are intentionally designed to provide upper-bound estimates of ground deformation and structural response during preliminary tunneling risk assessments.

By quantifying these exaggeration percentages, it becomes possible to adjust and interpret predictions obtained through the BIM-based parametric modelling method, ensuring that the results for buildings within the case study segment are consistent with the expected relationship between empirical and FEM-based analyses. This approach provides a practical framework for verifying the reliability of the

parametric model in the absence of direct FEM data for the analyzed segment.

The verification of the BIM-based parametric model was conducted by comparing its results with the empirical estimates provided by INFRATRASPORTI.TO S.R.L. for each building within the case study segment. The comparison focused on the maximum settlement (Smax) and maximum inclination (βmax), with the percentage of overestimation calculated as:

$$\text{Overestimation } \backslash(\%\backslash) = \frac{\text{Empirical value} - \text{BIM value}}{\text{BIM value}} \times 100$$

The results for each building are summarized as follows (values of Smax and βmax are reported in Tables 6.2 and 6.3):

BIM	Emperical	
Maximum settlement [mm]	**Maximum settlement [mm]**	Overestimation percent [%]
12	27	125.0
14	29	107.1
13	28	115.4
13	27	107.7
13	30	130.8
13	27	107.7
12	23	91.7
8	14	75.0
12	23	91.7
14	29	107.1
14	28	100.0
11	24	118.2
11	21	90.9
14	25	78.6

Table 6.7. Overestimation percent computation for max. settlement according to results computed by BIM analysis [Empirical method & BIM parametric simulation]

BIM	Emperical	
Maximum inclination grade [-]	**Maximum inclination grade [-]**	Overestimation percent [%]
0.0009	0.002	122.2
0.0009	0.002	122.2
0.0009	0.002	122.2
0.0008	0.002	150.0
0.0009	0.002	122.2
0.0008	0.002	150.0
0.0007	0.001	42.9
0.0008	0.002	150.0
0.0007	0.001	42.9
0.0007	0.002	185.7
0.0007	0.002	185.7
0.0009	0.002	165.2
0.0007	0.001	42.9
0.0006	0.002	233.3

Table 6.8. Overestimation percent computation for max. inclination grade according to results computed by BIM analysis [Empirical method & BIM parametric simulation]

The average overestimation across all 14 buildings is calculated as follows:

- Average settlement overestimation: **104.2%**
- Average inclination overestimation: **133.8%**

These results demonstrate that the empirical methods consistently predict higher settlements and larger inclination angles than the BIM-based parametric model. Settlement overestimation ranges from 75% to 130%, while inclination overestimation ranges from 42.9% to 233.3%, confirming the conservative nature of empirical approaches.

The quantified overestimation percentages provide a reference for interpreting empirical results in relation to the BIM-based method, verifying that the BIM-Dynamo model produces physically consistent and reliable predictions, and supporting its applicability for accurate assessment of building response along the analyzed tunnel segment.

6.8. Comparative Evaluation of Empirical and FEM Results and Validation of the BIM–FEM Regression Method

A comparative analysis of the overestimation percentages provides insight into the performance of the developed BIM-based parametric modelling method relative to traditional approaches. For the reference buildings analyzed near the case study segment, empirical methods were found to overestimate maximum settlement (Smax) by an average of approximately **99.5%** and maximum inclination angle (βmax) by **144%** when compared to FEM results. These figures reflect the known conservative nature of empirical methods, which are intended to provide safe upper-bound estimates in preliminary tunneling risk assessments.

When the same empirical results are compared with the BIM-Dynamo predictions for the buildings within the actual case study segment, settlement overestimation averages **104.2%,** while inclination overestimation averages **133.8%.** These ranges are closely aligned with the FEM-based overestimation, indicating that the BIM-based method produces results that are consistent with numerical expectations while avoiding the systematic exaggeration inherent in empirical procedures.

Graph 6.1 presents a comparison of the overestimation of maximum settlement obtained using the Empirical–FEM and Empirical–BIM approaches. The results are arranged in ascending order to facilitate a direct comparison of their distribution. It can be observed that both methods exhibit a very similar trend, with the overestimation values closely aligned across the entire range.

The near coincidence of the two distributions indicates that the BIM-based approach provides results that are consistent with those obtained from the FEM-based method. This suggests that the BIM method can be considered a reliable alternative for estimating maximum settlement.

A similar observation can be made for inclination grade overestimation in Graph 6.2, where the distributions of results from both approaches also show strong agreement, further supporting the validity of the BIM-based method.

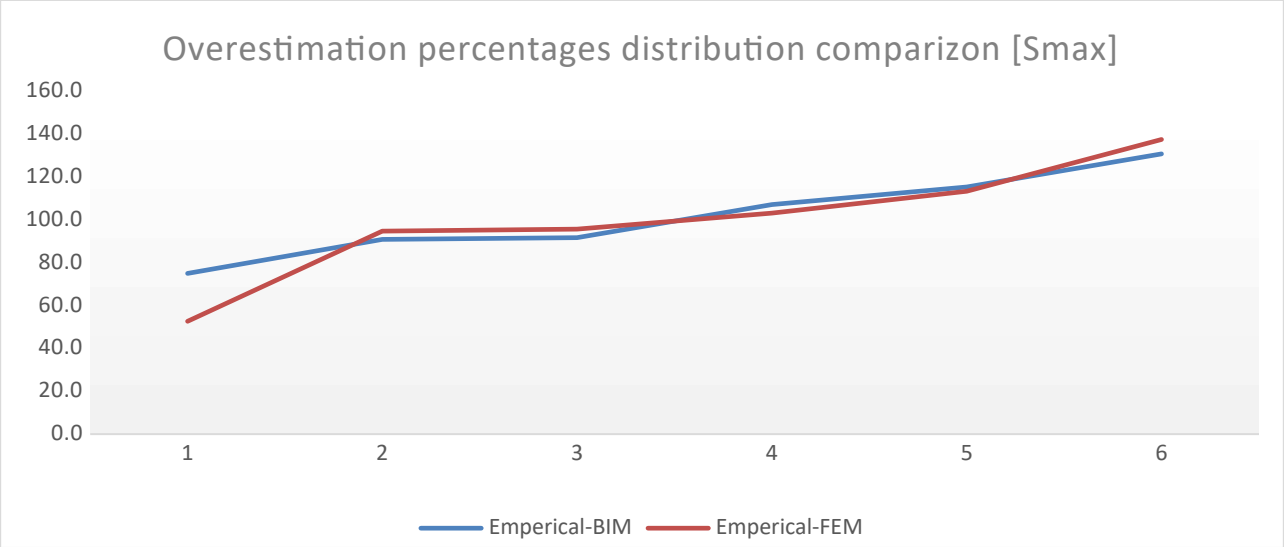

Graph 6.1. Overestimation percent distribution Smax Empirical – FEM & Empirical - BIM

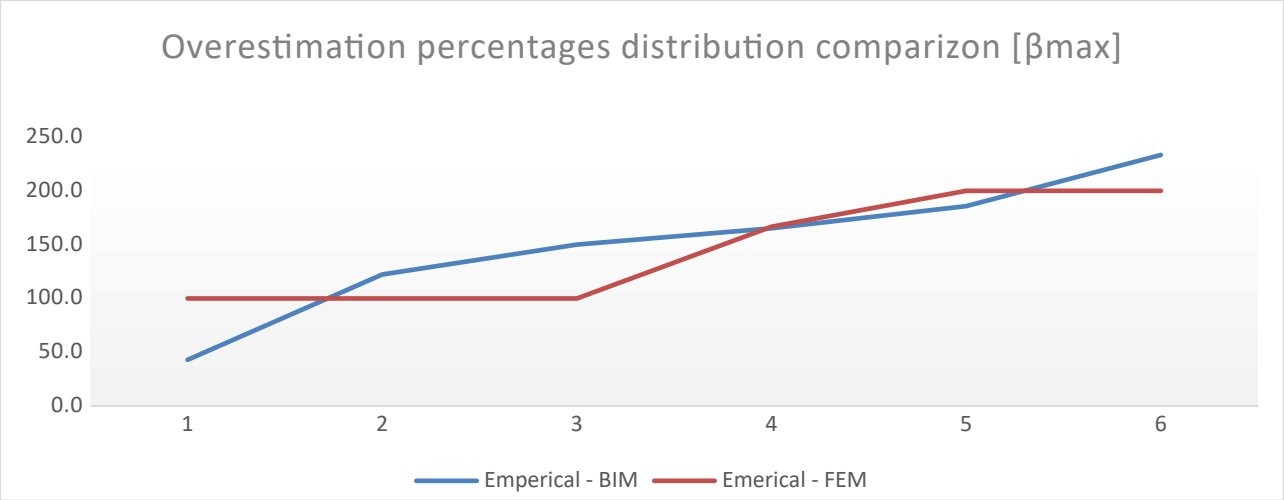

Graph 6.2. Overestimation percent distribution βmax Empirical – FEM & Empirical - BIM

This comparison demonstrates several key points:

1. The BIM-based method accurately captures the deformation behavior of buildings in response to tunneling-induced settlements, providing predictions that are physically realistic and comparable to FEM results.
2. Unlike purely empirical methods, which tend to systematically overestimate both settlement and inclination, the BIM model allows for direct computation of building response based on parametric inputs, incorporating foundation depth, geometry, and spatial discretization.
3. The method integrates the flexibility of parametric modelling in Dynamo with regression models derived from FEM analyses, combining the efficiency of empirical approaches with the precision of numerical simulation.
4. Given that the overestimation percentages relative to empirical methods are consistent with those derived from FEM comparisons, the BIM-based approach offers a reliable, safe, and computationally efficient tool for evaluating building deformation along complex tunnel alignments.

Therefore, the developed BIM-Dynamo methodology provides a robust and justifiable alternative to traditional empirical analyses, capable of producing accurate settlement and inclination predictions, while preserving the conservative safety margin required for tunneling risk assessment. Its applicability to arbitrary tunnel geometries and building layouts ensures that it can be adopted for practical engineering design and monitoring purposes in urban tunneling projects.

6.9. Model Validation Through Parametric Input Variations

This chapter is dedicated to the verification of the parametric behavior of the developed computational model for the analysis of tunnel-induced ground settlements. After the methodology and its application within the case study were presented in the previous sections, it was necessary to evaluate whether the implemented workflow correctly responds to variations in the main geometric input parameters. The objective of this chapter is therefore to demonstrate that the proposed framework dynamically adapts to different tunnel configurations and that the generated settlement basin consistently reflects these changes.

To assess the responsiveness and robustness of the model, a series of controlled modifications of the input parameters were performed. The first set of tests involved changing the underground level of the tunnel in order to evaluate how variations in tunnel depth influence the resulting settlement basin. Since tunnel depth is one of the key variables governing the amplitude of surface settlements, this step allowed verification that the model produces deformation patterns that correspond to the expected behavior.

Subsequently, the tunnel radius was varied to examine how the settlement basin responds to changes in tunnel size. This test aimed to confirm that the implemented regression-based formulation correctly adjusts the width and magnitude of the predicted settlement profile when the geometric characteristics of the tunnel are modified.

Finally, variations of both the horizontal and vertical tunnel alignment were introduced. These tests were conducted to verify that the settlement basin strictly follows the spatial configuration of the tunnel and that any modification of the alignment automatically updates the generated deformation surface as well as the associated numerical outputs. Particular attention was given to confirming that the system correctly recognizes the relative position of buildings with respect to the tunnel projection after alignment changes.

Through these parametric tests, the chapter demonstrates that the developed model maintains consistency and reliability under different geometric conditions, confirming its applicability as a flexible tool for the assessment of tunnel-induced settlements and their potential impact on surrounding structures.

6.8.1 Variation of level of underground

In order to verify the parametric response of the model with respect to the level at which the settlement analysis is performed, a series of simulations were carried out by varying the vertical offset parameter dZ. The objective of this test was to confirm that the deformation surface generated by the model behaves consistently with established geotechnical principles when the level of observation moves below the terrain surface.

The reference configuration was defined with $dZ = 0$, corresponding to settlement evaluation directly at the terrain surface. In this configuration, all coefficients in the regression equations that are multiplied by the parameter dZ are annulled, meaning that the regression model operates without the influence of the underground level variation. This case therefore serves as the baseline scenario against which the other simulations are compared.

Following the baseline case, two additional simulations were performed by assigning values of $dZ = 5\,\text{m}$ and $dZ = 10\,\text{m}$. These inputs represent settlement analysis conducted at underground levels located 5 m and 10 m below the terrain surface.

From a modelling perspective, the first expected outcome of this variation is purely geometric: the generated deformation surface should be translated vertically downward by the corresponding value

of the input parameter. In other words, the deformed plane should physically appear 5 m and 10 m below the terrain surface for the respective cases, confirming that the parametric control of the analysis level is correctly implemented.

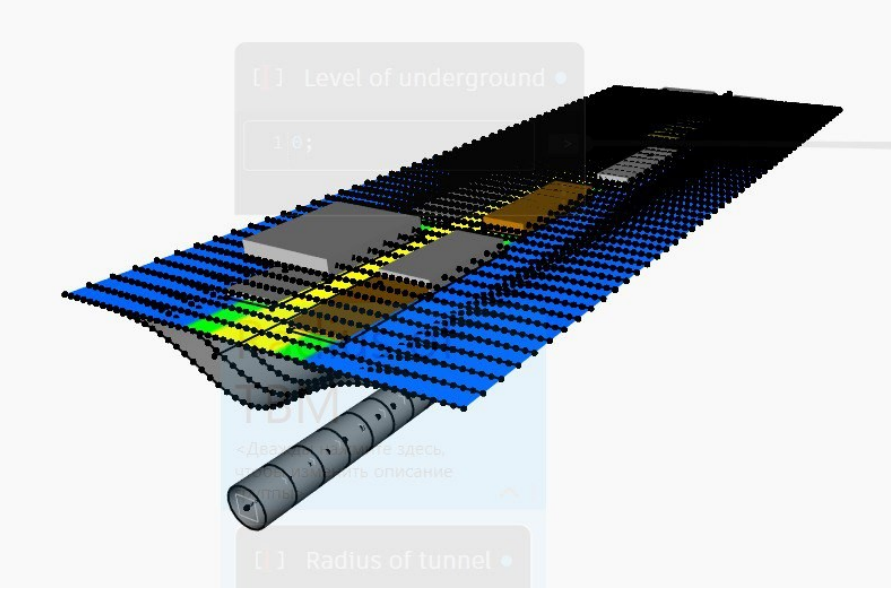

Figure 6.26. Geometrical output with dZ = 0, surface level

Beyond this geometric behavior, the variation also allows verification of the geotechnical consistency of the predicted settlement distribution. The regression models used in the workflow are derived from numerical analyses that follow the conceptual framework of the Peck's Theory (1969) for tunnel-induced ground settlements. Within this framework, the settlement trough is governed by the assumption that the volume loss associated with tunnel excavation remains constant over the influenced area. This principle establishes a relationship between the maximum settlement value and the width of the settlement basin.

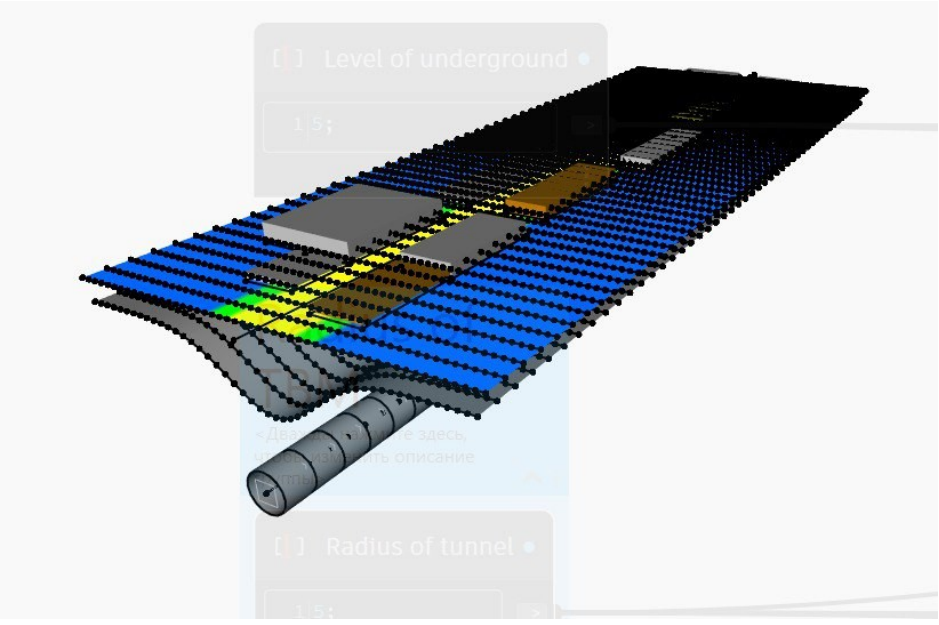

Figure 6.27. Geometrical output with dZ = 5, 5 meters under the ground

When this concept is extended to different elevations within the soil mass, both the maximum settlement and the trough width parameter become functions of depth. For a given depth level above the tunnel axis, the settlement distribution may be expressed as:

$$S(x,z)=S_{max}(z)\ e^{\frac{-x^2}{2i(z)^2}} \quad [7]$$

Here, $z$represents the vertical distance from the tunnel axis to the considered horizontal plane within the ground. The terms $S_{max}(z)$and $i(z)$therefore describe the maximum settlement and trough width at that particular depth. Importantly, empirical observations show that the trough width parameter $i$is approximately proportional to the vertical distance from the tunnel axis:

$$i=K*z \quad [8]$$

In this relation, $K$is an empirical coefficient that depends primarily on soil type and stiffness. For example, in sands the value of $K$is typically around 0.25–0.45, while in clays it is commonly around 0.4–0.6. The variable $z$is the distance from the tunnel axis to the considered level in the ground.

This equation clearly indicates that the trough width increases with increasing distance from the tunnel axis. Consequently, settlement basins evaluated at deeper subsurface levels—closer to the tunnel—have smaller values of z, which results in smaller values of i. A smaller value of i mathematically produces a narrower settlement basin, because the exponential term in the Gaussian equation decays more rapidly with horizontal distance. In other words, settlement decreases more quickly away from the tunnel centerline when the trough width parameter is small.

In addition to the change in trough width, the maximum settlement also varies with depth. The maximum settlement is largest near the tunnel and decreases progressively toward the ground surface. This phenomenon can be understood through the principle of volume conservation of the settlement trough. The total volume of the settlement trough per unit length of tunnel is commonly expressed as:

$$V_s=\sqrt{2\pi}\ S_{max}\ i \quad [9]$$

In this equation, $V_s$represents the volume of ground settlement per unit length of the tunnel, which is directly related to the volume of ground loss caused by excavation. The parameters $S_{max}$and $i$again represent the maximum settlement and the trough width parameter. For a given excavation stage and a given amount of ground loss, the settlement volume $V_s$remains approximately constant at different horizontal planes above the tunnel.

Because the settlement volume remains approximately constant, the relationship between $S_{max}$and i becomes inversely proportional. When the trough width $i$is small —such as at subsurface levels close to the tunnel—the maximum settlement must be relatively large to maintain the same total volume of deformation. Conversely, at the ground surface the trough width becomes larger due to the increasing value of z, and therefore the maximum settlement must decrease to maintain the same settlement volume.

This mathematical relationship reflects the physical process of displacement redistribution within the

soil mass. When the tunnel is excavated, the initial ground deformation occurs around the tunnel boundary, particularly near the crown. At this stage, the vertical displacement is highly concentrated, and the surrounding soil experiences localized stress release and plastic deformation. As a result, the settlement trough immediately above the tunnel is deep and narrow, with large vertical movements occurring directly above the excavation.

As the displacement propagates upward through the soil layers, the soil mass redistributes the deformation through mechanisms such as soil arching and shear transfer between particles. These mechanisms cause the displacement field to spread laterally. Each successive soil layer above the tunnel transmits the movement not only vertically but also horizontally, causing the settlement to affect a wider region. This progressive lateral spreading results in a wider settlement trough at higher elevations.

At the same time, because the deformation is distributed across a larger horizontal area, the magnitude of vertical settlement at any single point decreases. Therefore, the maximum settlement measured at the ground surface becomes smaller than the settlement measured at levels closer to the tunnel.

Numerical analyses using finite element methods (FEM) confirm this behavior. In FEM simulations of tunnel excavation, displacement contours typically show a bulb-shaped deformation zone originating at the tunnel crown. Close to the tunnel, displacement vectors are largely vertical and concentrated. As the distance from the tunnel increases, these displacement vectors gradually diverge outward, indicating that the deformation is spreading horizontally as it moves toward the surface. This produces settlement profiles that are steep and narrow near the tunnel but progressively wider and flatter at higher levels.

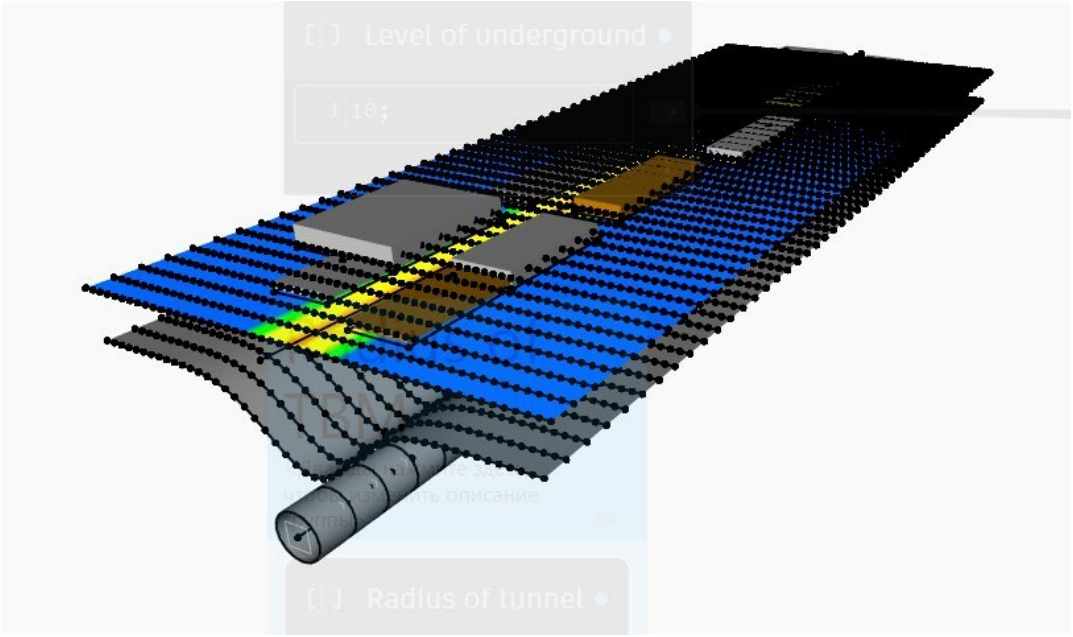

Figure 6.28. Geometrical output with dZ = 10, 10 meters under the ground

The results obtained from the simulations confirm this expected behavior. As illustrated in Figures 6.26, 6.27, and 6.28, the deeper the level of analysis, the narrower the settlement basin becomes. This effect can be clearly observed through the color distribution representing settlement magnitudes. The zones corresponding to intermediate settlement values, represented by green and yellow colors,

progressively decrease in width as the value of dZ increases. As a result, the spatial extent of the influence area becomes smaller, and some buildings previously located within the affected zone move outside the settlement basin.

At the same time, the maximum settlement values increase with depth. This behavior is particularly visible in Figure 6.28 corresponding to the case $dZ = 10\,\text{m}$, where the appearance of orange color directly above the tunnel alignment indicates settlement values exceeding 20 mm. This confirms that the reduction of the basin width is accompanied by an increase in the maximum settlement magnitude, consistent with theoretical expectations.

The obtained results demonstrate that the developed model correctly reproduces the expected physical behavior of settlement distribution when the level of analysis changes. Both the geometric response of the deformation surface and the variation of settlement parameters follow the anticipated geotechnical trends. Therefore, the parametric functionality of the model with respect to the underground level variation can be considered verified and the model behavior approved for this parameter.

6.8.2 Variation of the radius of the tunnel

One of the initial parameters considered in the developed parametric model is the radius of the tunnel. This parameter represents a geometric characteristic of the tunnel cross-section and is typically determined during the design stage. Unlike many geological or geotechnical parameters, which are governed by natural ground conditions, the tunnel radius is a design-controlled variable and can therefore be modified if risk analysis, safety verification, or other design assessments indicate that the predicted ground response is not satisfactory.

Within the framework of the present study, the radius of the tunnel is incorporated as one of the independent variables in the regression relationships derived from finite element method (FEM) simulations. These regression models are subsequently implemented into the line discretization of the terrain, which allows the prediction of ground settlements along the analyzed profile.

Because the tunnel radius is explicitly included as a variable in the regression formulations, any variation in its value directly influences the calculated settlement response. As a result, changes in tunnel radius are expected to affect not only the numerical magnitude of settlements but also the geometrical characteristics of the settlement basin, including its width and shape. Consequently, the analysis of radius variation represents an important component of parametric investigation, as it enables the evaluation of how modifications in tunnel geometry influence the predicted ground deformation behavior.

From a theoretical standpoint, empirical observations summarized by Ralph B. Peck (1969) and later confirmed by numerical modelling indicate that the radius of the tunnel directly influences the magnitude and concentration of ground deformation caused by excavation. When a larger tunnel radius is introduced in the model, the excavation affects a larger cross-section of the soil mass. Even if the same relative ground loss conditions are assumed, the absolute volume of disturbed soil becomes greater because the excavated area increases. As a result, the amount of vertical ground movement that develops above the tunnel also increases. In practical terms, this means that the maximum settlement at the center of the settlement basin becomes larger when the tunnel radius increases.

However, the increase in tunnel radius does not necessarily lead to a proportional widening of the settlement basin. Instead, the deformation tends to become more concentrated above the tunnel axis. The larger excavation causes stronger stress redistribution around the tunnel and promotes soil arching above the crown. This arching mechanism transfers part of the loads to the surrounding ground and limits the horizontal propagation of displacements. Consequently, settlements decrease more rapidly with horizontal distance from the centerline.

Because of this behavior, the general form of the settlement trough remains similar, but its geometrical proportions change. For larger tunnel radius, the settlement basin typically becomes deeper and steeper, with higher settlement values near the centerline and a more pronounced curvature of the profile. In contrast, when a smaller tunnel radius is considered, the ground disturbance is less intense and the deformation spreads more gradually through the soil mass. The resulting settlement basin is therefore shallower and relatively wider, with a more gradual reduction of settlement away from the centerline.

In the context of the developed parametric model, this means that increasing the tunnel radius is expected to produce settlement curves characterized by higher maximum settlements and a more concentrated deformation zone, while reducing the radius should result in smaller maximum settlements and a more gently distributed settlement basin. The overall settlement profile retains its characteristic trough shape, but the depth and steepness of the basin vary depending on the selected tunnel radius.

In Figure 6.29, the results of the numerical simulation illustrating soil settlement are presented for the original case study, considering a tunnel with a radius of 5 m. For the given tunnel geometry, the resulting settlement distribution extends over a relatively wide area. This distribution is visually represented on the terrain surface using a color scale, where green indicates settlements ranging between 5 and 10 mm, while yellow corresponds to settlements between 10 and 15 mm.

The colored zones clearly demonstrate that the spatial extent of the settlement trough is considerably larger than the geometric dimensions of the tunnel itself. Such a pattern is typical for tunneling-induced ground movements, where the effects propagate through the surrounding soil mass and influence the ground surface over a significantly broader area than the excavation profile.

Within this influence zone, several buildings are situated such that their entire foundation footprints fall inside the area affected by ground settlement. This condition indicates a potential interaction between the tunneling process and the built environment, which may lead to structural responses depending on the magnitude and gradient of the induced deformations.

The simulated deformation of the ground surface exhibits a smooth, Gaussian-type settlement profile, which is characteristic of tunneling-induced subsidence. The resulting surface shape reveals clearly distinguishable convex and concave zones, reflecting the gradual transition from the maximum settlement near the tunnel axis to the unaffected ground at greater distances. This smooth distribution further confirms the typical behavior of settlement troughs generated by underground excavations in homogeneous soil conditions.

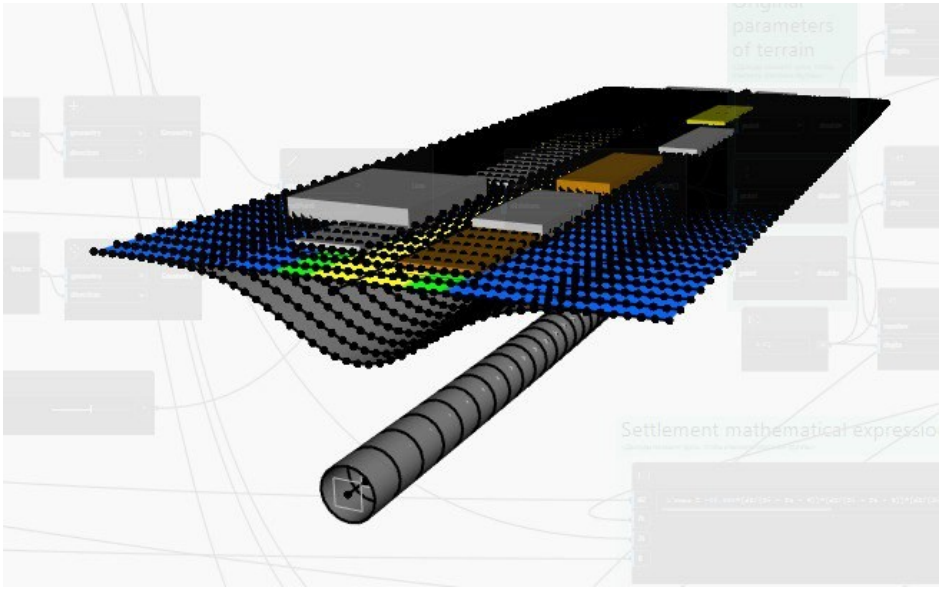

Figure 6.29. Settlement basin induced by tunnel with radius of 5 meters

In Figure 6.30, the input parameter representing the tunnel radius is increased to 8 m, allowing the effects of this modification to be examined within the simulation environment. The first aspect that should be emphasized is the immediate geometric response of the parametric model to the change in the input parameter. Once the tunnel radius is adjusted, the generated tunnel geometry automatically updates, producing a tunnel with a larger cross-sectional dimension. At the same time, the circular cross-sections remain perpendicular to the tunnel alignment, and the surface connecting these sections is automatically recalculated to maintain a continuous and geometrically consistent tunnel body. This behavior demonstrates the adaptability and robustness of the parametric modelling framework used in the study.

More importantly, the modification of the tunnel radius results in noticeable changes in the predicted ground settlement. As expected, the maximum settlement value directly above the tunnel axis increases compared to the simulation performed for the 5 m radius case. This increase can be observed not only through the visual interpretation of the deformation surface but is also confirmed by the corresponding numerical output values obtained from the simulation.

In accordance with Ralph B. Peck's theory (1969) of settlement, which assumes a constant volume loss during tunnelling, an increase in the maximum settlement at the center of the trough is accompanied by a reduction in the lateral extent of the influence area. Consequently, the settlement basin becomes narrower while the central settlement values increase. In the graphical representation of the deformation surface, the concave and convex zones within the settlement trough begin to appear more uniform and concentrated around the tunnel axis, reflecting the redistribution of ground deformation.

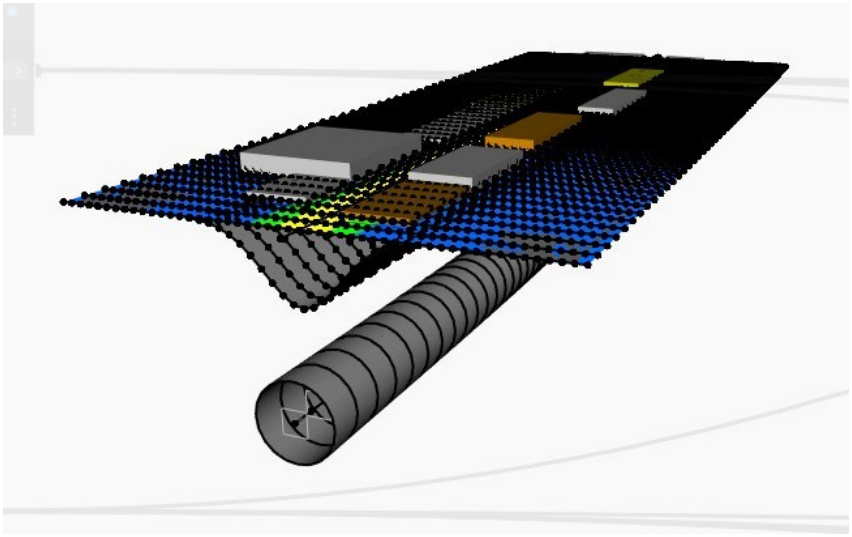

Figure 6.30. Settlement basin induced by tunnel with radius of 8 meters

As the next step, Figure 6.31 illustrates the results obtained when the tunnel radius is further increased to 15 m. In this scenario, the same general pattern observed in the previous simulations is repeated, but at a larger magnitude. The influence zone becomes significantly narrower, and as a result, some of the previously affected buildings are no longer located within the settlement impact area. However, the structures that remain within the influence zone experience higher settlement values, which consequently lead to larger inclination angles and potentially more critical structural responses.

Additionally, the geometry of the settlement basin undergoes a further transformation. The deformation profile begins to resemble a more triangular shape, indicating a stronger concentration of settlement near the tunnel axis. The previously distinguishable convex and concave regions of the deformation surface gradually converge, visually approaching a single transition line, which reflects the increasingly steep gradients of ground deformation associated with the larger tunnel radius.

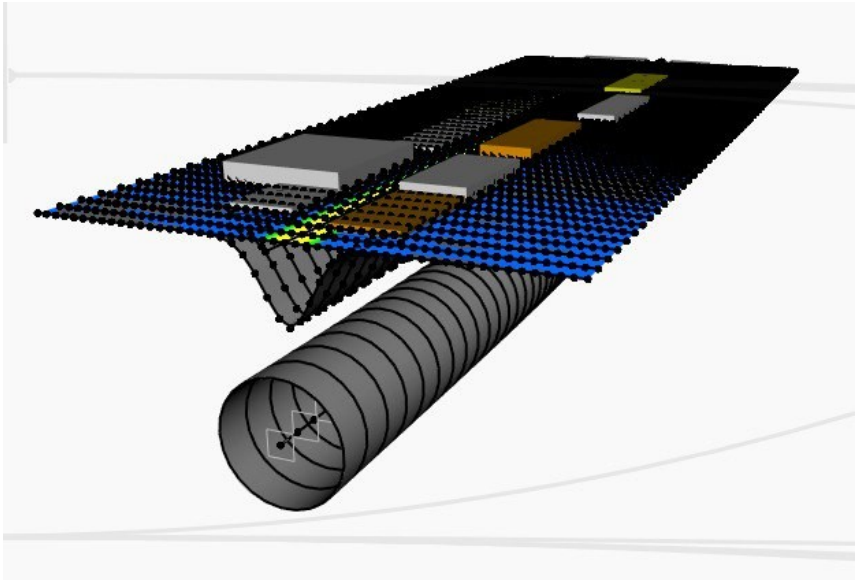

Figure 6.31. Settlement basin induced by tunnel with radius of 15 meters

Overall, the behavior of the parametric model developed in Autodesk Dynamo using regression models derived from Finite Element Method (FEM) simulations has been successfully verified with respect to variations in the tunnel geometry. The model demonstrates a consistent and reliable response when the tunnel radius is modified, automatically updating the corresponding geometric representation of the tunnel within the computational environment.

More importantly, the resulting ground settlement distributions produced by the parametric framework align well with theoretical expectations and previously established numerical analyses. The observed patterns of settlement development are fully consistent with the principles described in Ralph B. Peck (1969), which predicts the relationship between maximum settlement, volume loss, and the spatial extent of the settlement trough.

Furthermore, the numerical outputs associated with ground deformation and the resulting building damage indicators are automatically recalculated as the tunnel parameters change. This automated updating process confirms that the parametric workflow effectively integrates geometric modelling with predictive settlement assessment, allowing the model to dynamically reflect the structural and geotechnical implications of tunnel parameter variations. As a result, the developed system provides a reliable tool for rapidly evaluating the potential impact of tunnelling on surrounding ground conditions and adjacent structures.

6.8.3 Modification of horizontal and vertical alignment

The final stage of verification concerns modifications of the tunnel's horizontal and vertical alignment. The purpose of this stage is to demonstrate that the developed parametric method can be applied not only to the specific geometry of the case study but also to tunnels with more complex spatial configurations.

In the original case study, the tunnel—approximately 267 m in length—is represented by a straight alignment beneath Via Lagrange in Turin. Within the model code, the cross-sections generated along the tunnel path are defined so that they remain perpendicular to the tunnel's horizontal alignment. However, because the case study geometry consists of a straight line, the capability of this part of the code based on vector cross-product rotation was not fully demonstrated in the initial simulations.

When modifying the horizontal alignment, several key requirements must be satisfied in order to confirm the correctness of the model behavior. First, the maximum depth of the settlement basin must strictly follow the tunnel alignment, meaning that the point of maximum settlement should always be located directly above the tunnel axis. Second, all generated cross-sections must remain perpendicular to the local direction of the tunnel path. Finally, the settlement distribution along each section must remain smooth and continuous, ensuring that the distance variable used in the regression models is correctly evaluated and that no bias is introduced into the settlement calculations.

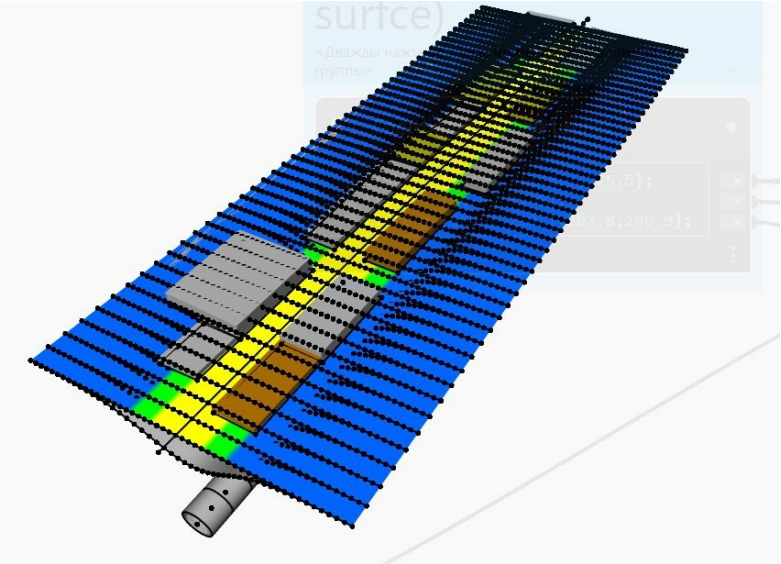

Figure 6.32. Original horizontal alignment

For experimental purposes, the first modification involved shifting the y-coordinate of the tunnel path at the midpoint of the alignment by 10 m to the left. After running the simulation, the resulting geometry showed that the tunnel path adopted a smooth quadratic curve, without generating sharp angles in either the horizontal or vertical alignment. The computed settlement trough followed the modified tunnel trajectory, all generated sections remained perpendicular to the alignment, and the settlement distribution across the sections remained smooth and uniform. These results confirm that the implemented geometric procedure performs correctly under moderate alignment modifications.

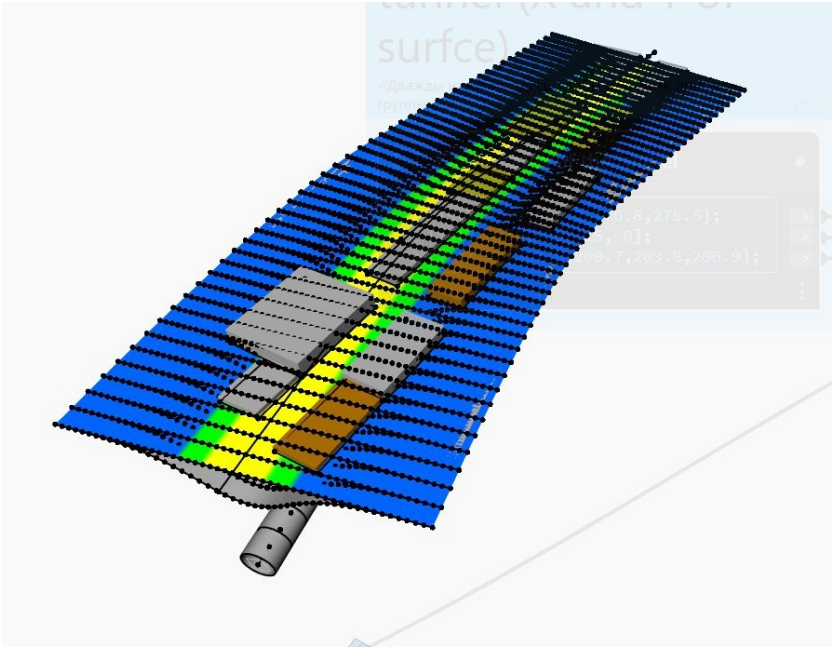

Figure 6.33. Circular horizontal alignment with 10 m in Y coordinates movement

A more demanding test was then introduced by applying a double horizontal deviation. In this configuration, the tunnel alignment was displaced by 20 m in opposite directions at approximately 33% and 66% of its total length, producing a double-curved trajectory. Even under this more complex geometric condition, the model demonstrated stable and accurate performance. The discretized sections remained perpendicular to the local tangent of the tunnel alignment at every point, while the settlement distribution continued to be calculated correctly based on the spatial distance between points along the tunnel axis and the corresponding section locations.

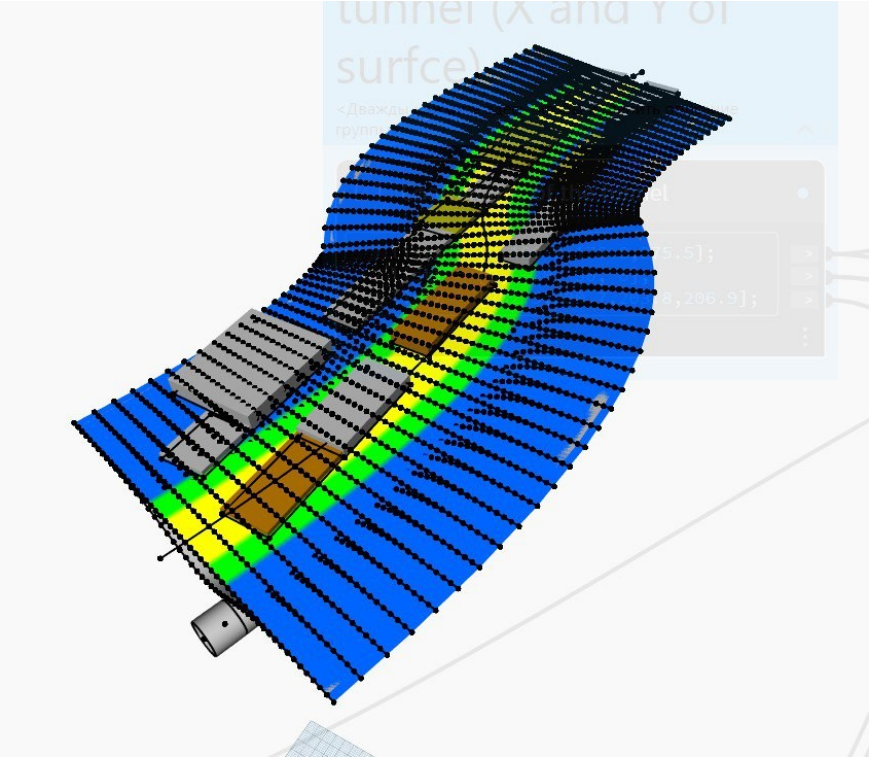

Figure 6.34. Double curved horizontal alignment Y [20;-20]

Verification was also performed for vertical alignment modifications. In this case, the expected changes do not primarily affect the horizontal position of the settlement trough but rather influence the magnitude of maximum settlement and the slope of the deformation profile. This behavior occurs because variations in the vertical alignment directly modify the tunnel depth relative to the ground surface, which is one of the key parameters within the regression models derived from Finite Element Method (FEM) simulations.

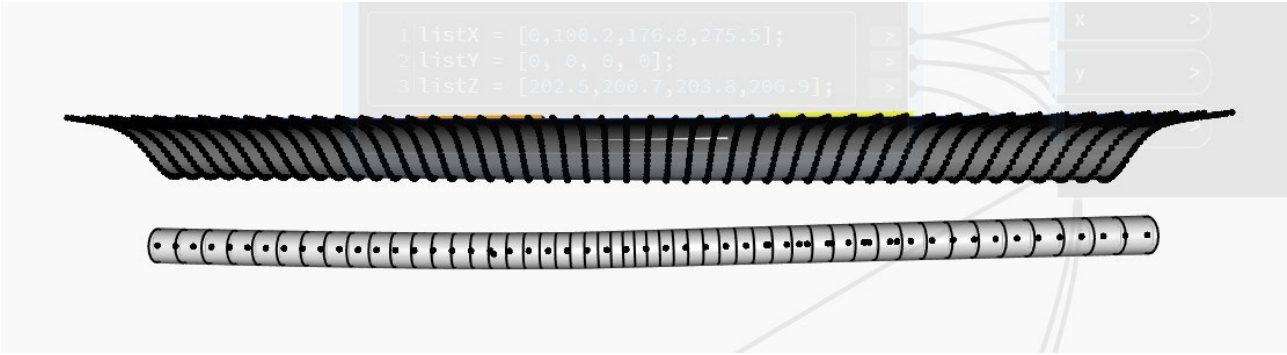

Figure 6.35. Original vertical alignment

Two deformation scenarios were analyzed. In the first scenario, the tunnel was positioned closer to the ground surface near the boundaries of the alignment and deeper in the central section. In the second scenario, the opposite configuration was applied, with the tunnel shallower in the central part and deeper toward the ends. The simulation results in both cases confirmed the expected geotechnical behavior: when the tunnel approaches the surface, maximum settlement increases and the settlement trough becomes steeper, leading to larger inclination angles. Conversely, as the tunnel depth increases, maximum settlement decreases while the lateral extent of the influence area becomes larger.

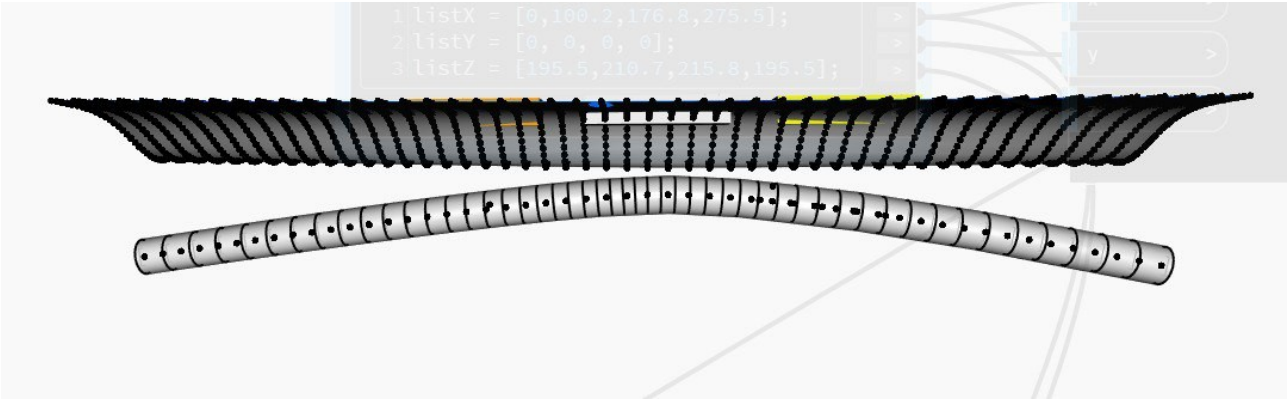

Figure 6.36. Vertical alignment modification 1

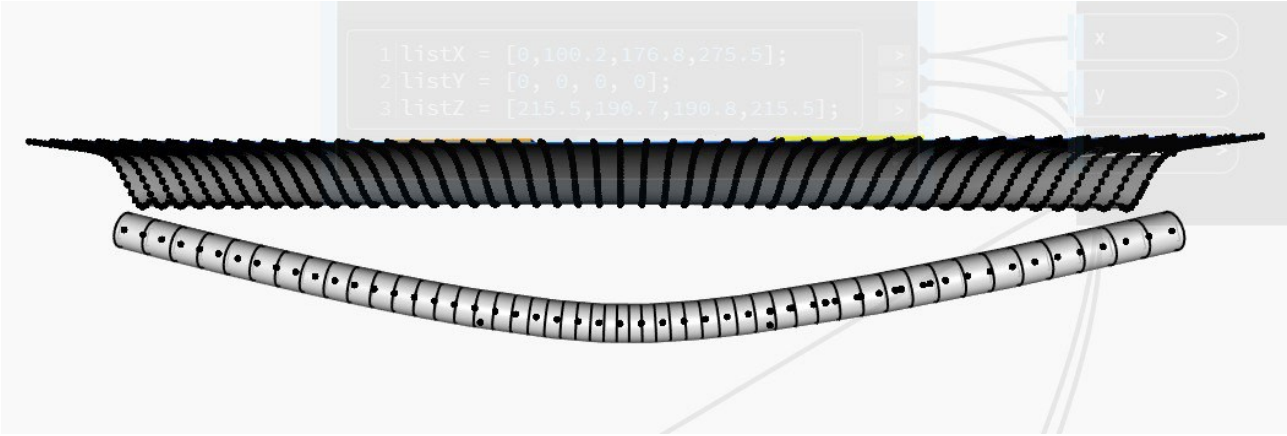

Figure 6.37. Vertical alignment modification 2

Based on the conducted tests, the parametric model has been successfully verified with respect to both horizontal and vertical alignment modifications. The performed simulations demonstrate that the implemented modelling framework responds consistently and reliably to changes in the spatial configuration of the tunnel geometry. In particular, the automated generation of tunnel geometry, section orientation, and settlement distribution remains stable even when the alignment deviates significantly from the original straight-line configuration used in the case study beneath Via Lagrange in Turin.

The verification results confirm that the geometric procedures embedded in the parametric workflow correctly handle complex alignment conditions. The cross-sectional planes generated along the tunnel path remain perpendicular to the local direction of the tunnel axis at every discretized point, ensuring

geometric consistency throughout the entire model. At the same time, the computational routines responsible for estimating settlement distribution continue to produce smooth and continuous deformation surfaces. This behavior indicates that the implemented distance-based variables and interpolation procedures are functioning correctly and are not affected by local curvature or alignment variations.

The developed parametric model was verified through a series of simulations in which the principal geometric parameters of the tunnel were systematically modified. The purpose of these tests was to evaluate the reliability, consistency, and adaptability of the modelling workflow when subjected to variations in tunnel geometry and alignment. The parametric framework was implemented in Autodesk Dynamo and is based on regression relationships derived from simulations performed using the Finite Element Method (FEM).

The first stage of verification focused on the analysis of vertical underground settlement behavior. In this step, the deformation plane was intentionally positioned below the terrain surface, enabling visualization of the deformation patterns developing within the internal soil layers rather than only at the ground surface. This approach allowed a clearer interpretation of how settlements propagate from the tunnel excavation through the soil mass toward the ground surface. The obtained deformation surfaces exhibited smooth and continuous settlement profiles, indicating that the model correctly captures the expected mechanisms of subsurface soil deformation. The observed settlement basin geometry corresponds well with the theoretical principles described in Ralph B. Peck's Settlement Theory (1969), which predicts a Gaussian-type distribution of settlements above underground excavations.

Further verification was carried out by modifying the tunnel radius, which represents one of the most influential geometric parameters affecting ground deformation. Increasing the radius resulted in predictable changes in the settlement basin, including higher maximum settlement values above the tunnel axis and corresponding adjustments in the extent of the influence zone. The parametric model responded immediately to these input changes by automatically updating the tunnel geometry as well as the associated numerical outputs related to ground deformation and building damage indicators. The consistency between visual deformation patterns and numerical output values confirms that the computational component of the model is properly integrated with the geometric representation.

Additional verification tests addressed modifications of the horizontal tunnel alignment. The original case study considered a straight tunnel alignment beneath Via Lagrange in Turin; therefore, additional experimental scenarios were introduced in order to evaluate the behavior of the model under curved alignment conditions. When deviations were applied to the tunnel path, the parametric algorithm successfully generated a continuous tunnel geometry while maintaining cross-sections that remain perpendicular to the local direction of the tunnel alignment. At the same time, the calculated settlement trough followed the modified tunnel trajectory, and the settlement distribution across generated sections remained smooth and physically consistent. These results demonstrate that the geometric procedures based on vector operations function correctly even for more complex spatial tunnel paths.

Verification was also performed for vertical alignment modifications, which influence the depth of the tunnel relative to the ground surface. Since tunnel depth represents a key parameter in the FEM-derived regression models, variations in vertical alignment directly affect the magnitude and spatial distribution of predicted settlements. When the tunnel approaches the surface, the simulations show an increase in maximum settlement values together with steeper deformation gradients. Conversely, greater tunnel depths lead to smaller maximum settlements while expanding the lateral extent of the

influence zone. These results correspond well with established geotechnical observations regarding the relationship between tunnel depth and ground deformation.

The conducted tests demonstrate that the parametric model maintains stable geometric generation and consistent settlement prediction under a wide range of geometric configurations. Tunnel geometry, settlement distribution, and related numerical outputs remain fully synchronized within the modelling framework, ensuring that modifications of key parameters are immediately reflected in both visual and numerical results. The developed methodology can therefore be applied to tunnels with diverse three-dimensional geometries, extending beyond the specific configuration used in the presented case study and providing a reliable tool for the rapid evaluation of tunneling-induced ground settlement and its potential effects on surrounding structures.

Chapter VII: Conclusion

The main objective of this thesis was to develop, programmatically implement, and introduce a new intuitive method for automated prediction of soil deformation caused by tunnel construction. The key task of the project was to transform popularly used analytical models and methods of analysis into a working digital tool in the 'Dynamo' and 'Revit' environment, providing analysis that are, at the first place, giving justified results that can give reliable expectations on future deformations caused by tunnel excavation, and by the second place, lower time consumption for execution, because it does not include manual modelling of elements and soil masses.

The method is based on the following data:

1. Finite element modeling (FEM) results describing the volumetric field of soil deformation around the tunnel.
2. Regression functions derived from them, linking the geometry of the tunnel (depth H, radius R) and the depth of the calculation point relative to the surface (Z) with the magnitude of the vertical displacement.

The practical result of the executed work was the development of a comprehensive parametric algorithm in Dynamo, which implements a clear step-by-step workflow that can be used for the future geotechnical analysis (for the soil types similar to ones where FEM analysis was executed):

STAGE 1: Creating a calculation model.

- The tunnel geometry can be defined flexibly: by entering the coordinates following the Revit model of tunnel in Dynamo using any coordinate system (as the calculations are based on the difference between coordinates of the objects in Dynamo user space) axis of tunnel is automatically constructed as "spline" line going through points following the quadratic function both in x - y and y - z planes, inserting the radius of tunnel already gives it a solid form;
  Alignment of the tunnel can be also directly transferred from the Revit workspace, if it respects the same coordinate system as terrain and urban environment that is going to be analyzed.

- The topography (ground level) is entered in a similar way: by coordinates, by importing the surface from Revit or from an external file.

STAGE 2: Calculation and 3D visualization of deformations.

- The running of program after all necessary inputs, the core of the algorithm automatically calculates the displacement field using the provided regression functions and constructs a 3D surface of soil deformation.

- To analyze the internal layers, one more input parameter is preprogrammed and must be inserted – the level of analysis respect to the ground surface (by default it is 0). Such an input gives an opportunity to analyze soil deformations also inside the ground.

STAGE 3: Analysis of the impact on structures.

- Geometry of the building can be inserted with coordinates or transferred from the Revit working space (Plane of the building in Dynamo space must be reconstructed using the intersection of building with terrain surface).

- Parameters that are analyzed for the building are – vertical displacement, which is taken equal to the vertical deformation of terrain under the net of the building plane, and angle of inclination which taken from the difference of vertical displacements. Classification of damage is done using the method applied by INFRATRANSPORTI.TO S. R. L. for the project of Second Line of Metro in Turin.

The technical implemental background of the code is relying on analyzed geometry complexity increasing:

1. Basic module (Point). Input requires only coordinate of the point, algorithm of the program finds the corresponding point on tunnel alignment, which is responsible for the inserted point displacements and the value of displacement as the consequence of earthworks is automatically calculated, using regression models and automatic distance identification.
2. Profile analysis module (Line). If user is interested in settlement distribution along the line, with an input of coordinates of start and end of the line, the output in the form of settlement on every point of the line can be taken as an output (level of discretization is also an input). The same methodology works also with curves, inputting the coordinates of inner points of the curve to correctly insert its shape (if the curve can be imagined as curvilinear function, input coordinates must be minimum and maximum points of the function).
3. Plane (3D). Requires polygon coordinates input or transfer, the plane is constructed and discretized automatically, using the level of discretization as a user input. Analysis of deformation are done according to the coordinates of points on the net of the plane.
4. Risk analysis module (Assessment Core). For an imported object (e.g., foundation), it automatically applies a grid, calculates displacements at all nodes, determines all skew angles, and outputs the final critical values: maximum displacement and maximum deviation angle.

Key advantages and novelty of the developed method:

- Full automation: Dynamo calculates distances, depths and constructions based on a coordinate model.

- Flexibility and integration: Supports data input from Revit, Excel or manually.

- Spatial clarity: Visualization of deformations in 3D and on any horizontal cross-sections.

- Practical and regulatory focus: Direct output of parameters for damage assessment in accordance with standards.

- Complete BIM contour: Export of results (geometry in Revit, tables in Excel).

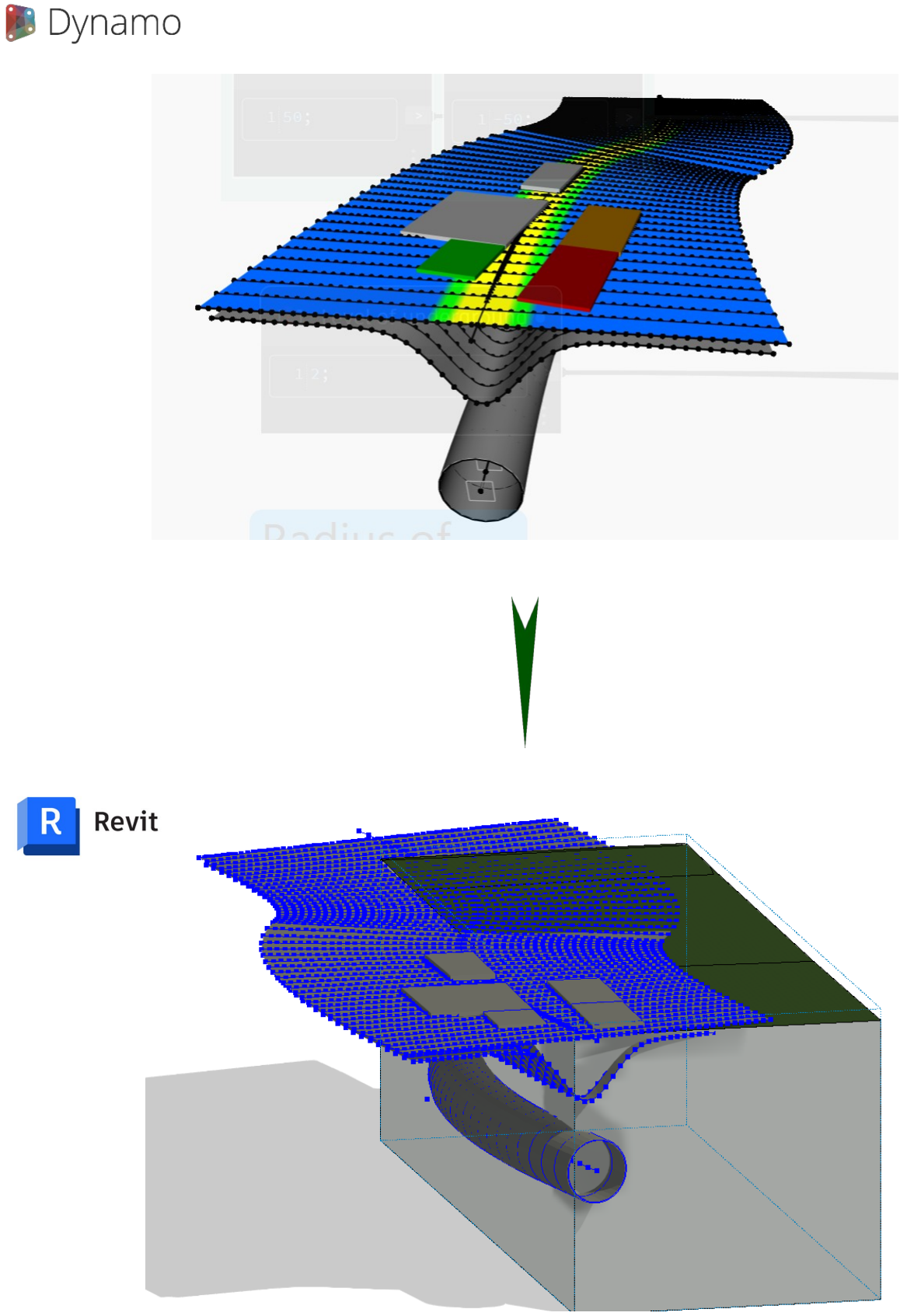

Figure 7.1. Dynamo parametric model to AutoDesk Revit export

The methodology was then extended to include buildings. Building geometries were imported as solid bodies, maintaining consistency within the global coordinate system. Using geometric proximity operations, horizontal distance to the tunnel alignment and local tunnel depth were automatically identified for each relevant point. Two computational strategies were developed: a detailed approach based on dense surface discretization and a simplified approach based on discretization of the most critical building edges. The simplified method significantly reduced computational demand while preserving accuracy for typical geometric configurations encountered in the case study.

One of the most important verification steps of the developed methodology was performed through a comparative analysis of the overestimation percentages obtained from different assessment approaches. For a group of reference buildings analyzed by INFRATRASPORTI.TO S.R.L., empirical methods were compared with results derived from Finite Element Method (FEM) analyses. The buildings used for this comparison were PAPN03, PAPN18, PNCA41, PNCA43, RM02, and CAMO15, which were selected within an approximate 1 km range from the analyzed tunnel segment in order to ensure comparable geotechnical conditions and soil characteristics. The results of this comparison showed that empirical procedures overestimate maximum settlement by approximately 99.5% and maximum inclination angle by about 144% on average when compared with FEM simulations.

A parallel comparison was then performed between the empirical results provided by the company and the results obtained through the BIM-based parametric modelling workflow developed in Autodesk Dynamo for the buildings located within the analyzed tunnel segment, namely PNCA06, PNCA07, PNCA09, PNCA10, PNCA11, PNCA12, PNCA13, PNCA14, PNCA15, PNCA16, PNCA17, PNCA18, PNCA19, and PNCA20. In this case, empirical methods overestimated maximum settlement by an average of approximately 104.2% and maximum inclination angle by 133.8%. The strong correspondence between these two sets of overestimation percentages demonstrates that the results obtained through the BIM-based computational approach reproduce the same behavioral trends observed when empirical methods are compared with FEM simulations. This agreement confirms that the developed BIM-based methodology implemented in Dynamo is capable of producing reliable and technically consistent predictions of ground settlement and building deformation.

An additional important validation of the developed parametric model was performed through systematic variation of key input parameters. These tests included modifications of the tunnel radius, as well as changes in the horizontal and vertical alignment of the tunnel path. The objective of these simulations was to evaluate whether the model responds consistently to geometric and positional changes of the tunnel and whether the resulting settlement distribution follows the expected theoretical behavior. The performed tests confirmed that variations in tunnel radius directly influence the maximum settlement and the width of the settlement basin, in accordance with established theoretical principles of tunnelling-induced ground deformation. Similarly, modifications of the tunnel alignment demonstrated that the maximum settlement consistently follows the tunnel axis, while the generated settlement profiles remain smooth and physically consistent along all cross-sections.

These input variation analyses demonstrate that the developed parametric model not only produces realistic results for the case study geometry but also behaves robustly and predictably when key design parameters are modified, confirming its applicability for the analysis of tunnels with different geometries and spatial configurations.

In conclusion, the research presented in this thesis demonstrates the development and application of a dynamic BIM-based parametric model designed to support the analysis of tunnelling-induced ground deformation in urban environments. The model was created with two principal objectives. The first objective was to simulate the behavior of the soil mass during tunnel excavation, generating detailed geometrical outputs such as the tunnel model, original terrain surface, and the resulting deformed terrain representing the settlement basin. These geometrical results can be directly transferred from the computational environment implemented in Autodesk Dynamo to Autodesk Revit and further exported to CAD platforms, enabling clear visualization of the deformation processes through planimetric views, elevations, and cross-sections, as well as their integration into engineering documentation.

The second objective of the developed model was to provide automated numerical evaluation of the impact of tunnelling on surrounding buildings. Within the computational workflow, the position of each building relative to the tunnel axis is determined automatically, allowing the model to estimate the corresponding settlement distribution beneath the building foundations. Based on this information, the system calculates the maximum settlement values and the maximum inclination (distortion) angles for each analyzed structure, producing structured numerical outputs together with the corresponding damage classification categories. These results are automatically organized and exported to Microsoft Excel, providing a clear and efficient framework for result interpretation and documentation.

Through this combination of geometrical simulation and automated numerical assessment, the developed BIM-based workflow demonstrates the capability to evaluate tunnelling-induced ground deformation and its influence on nearby structures in an efficient and technically consistent manner. The performed verification procedures confirm that the model produces reliable predictions while significantly simplifying the analysis process compared to traditional numerical approaches. As a result, the proposed methodology represents a practical and flexible tool for the preliminary assessment of tunnelling impacts on urban infrastructure, supporting engineers in the planning and design stages of underground construction projects.

References

1. Addenbrooke T. I. (1996). *Numerical analysis of tunnelling in stiff clay,* Ph.D. thesis, Imperial College, University of London. pp. 693–712.

2. Attewell, P. B., Yeates, J., and Selby, A. R. (1986). *Soil movements induced by tunnelling and their effects on pipelines and structures,* Blackie & Son Ltd., London.

3. Boscardin, M. D., & Cording, E. J. (1989). *Building response to excavation-induced settlement,* Journal of Geotech. Engineering, pp. 1–21.

4. Burland JB., Wroth CP. (1974). *Settlement of buildings and associated damage,* in Proc. of Conference "Settlement of Structures", London. pp. 611–654.

5. Burland, J. B., Broms, B. B., & de Mello V.F.B. (1977). *Behavior of foundations and structures,* in Proc of International Conference of Soil Mechanics and Foundation Engineering, Tokio, ASCE, pp. 495–546.

6. Burland, J. B. (1995). *Assessment of risk of damage to buildings due to tunnelling and excavation,* Invited Special Lecture. In: 1st Int. Conf. on Earthquake Geotech. Engineering, IS Tokyo '95.

7. Fabozzi S., Biancardo S. A., Veropalumbo R., Biotta E. (2021). *I-BIM approach for geotechnical and numerical modelling of conventional tunnel excavation*", Tunneling and Underground Space Technology, 108, pp. 3-13.

8. Franzius JN. (2003). *Behavior of buildings due to tunnel induced subsidence*, PhD Thesis, Imperial College of Science Technology and Medicine, London.

9. INFRATRASPORTI.TO S.R.L Published documents concerning Second Metro Line in Turin on website: http://geoportale.comune.torino.it/web/linea-2-della-metropolitana-torinese-progetto-definitivo

10. Namazi E. and Mohamad H. (2013). *Assessment of Building Damage Induced by Three-Dimensional Ground Movements*, Journal of Geotechnical and Geoenvironmental Engineering, Vol. 139, No. 4, pp. 608–618.

11. Nemorini F. (2010). *Modellazione Numerica di Gallerie Metropolitane*, Master degree thesis at University of Parma. pp. 69-90.

12. O'Reilly MP., New BM. (1982). *Settlements above tunnels in U.K. - their magnitude and prediction*, in, Tunneling '82. pp. 173-181.

13. Peck RB. (1969). *Deep excavations and tunneling in soft ground. State of the art report,* in Proc of 7th International Conference on Soil Mechanics and Foundation Engineering, Mexico City, pp. 225-290, 1969.

14. Schmidt B. (1969). *Prediction of settlements due to tunneling in soil: three case histories*, in Proc. of 2nd Rapid Excavation Tunneling Conference, San Francisco, CA, pp. 801-812.

15. Tang, D. K. W., Lee, K. M., & Ng, C. W. W. (2000). *Stress paths around a 3-D numerically simulated NATM tunnel in stiff clay,* chapter in Geotechnical Aspects of Underground Construction in Soft Ground, pp. 443–449.

16. Taylor, R. N. (1995). *Underground construction in soft ground,* Tunnelling in soft ground in the UK. pp. 123–126.

List of software applied for project development:

1. Autodesk (2023). *Autodesk Revit 2023*. Autodesk, Inc.

2. Autodesk (2023). *Dynamo (Version 2.13, integrated with Revit 2023)*. Autodesk, Inc.

3. Autodesk (2025). *AutoCAD 2025*. Autodesk, Inc.

Attachments

1. Code for classification of buildings damage degree according to maximum settlement along the building

```
// Input parameters

Smax = s;

VulIN = V;



// Damage classification based on maximum settlement

Damageclass =

(VulIN <= 20 && Smax < 10) ? "VULNERABILITY: IRRELEVANT / DAMAGE GRADE: VERY SLIGHT" :

(VulIN <= 20 && Smax >= 10 && Smax < 50) ? "VULNERABILITY: IRRELEVANT / DAMAGE GRADE: SLIGHT" :

(VulIN <= 20 && Smax >= 50 && Smax < 75) ? "VULNERABILITY: IRRELEVANT / DAMAGE GRADE: MODERATE" :

(VulIN <= 20 && Smax >= 75) ? "VULNERABILITY: IRRELEVANT / DAMAGE GRADE: VERY SEVERE" :



(VulIN > 20 && VulIN <= 40 && Smax < 8) ? "VULNERABILITY: LOW / DAMAGE GRADE: VERY SLIGHT" :

(VulIN > 20 && VulIN <= 40 && Smax >= 8 && Smax < 40) ? "VULNERABILITY: LOW / DAMAGE GRADE: SLIGHT" :

(VulIN > 20 && VulIN <= 40 && Smax >= 40 && Smax < 60) ? "VULNERABILITY: LOW / DAMAGE GRADE: MODERATE" :

(VulIN > 20 && VulIN <= 40 && Smax >= 60) ? "VULNERABILITY: LOW / DAMAGE GRADE: VERY SEVERE" :

(VulIN > 40 && VulIN <= 60 && Smax < 6.7) ? "VULNERABILITY: MEDIUM / DAMAGE GRADE: VERY SLIGHT" :

(VulIN > 40 && VulIN <= 60 && Smax >= 6.7 && Smax < 33.3) ? "VULNERABILITY: MEDIUM / DAMAGE GRADE: SLIGHT" :

(VulIN > 40 && VulIN <= 60 && Smax >= 33.3 && Smax < 50) ? "VULNERABILITY: MEDIUM / DAMAGE GRADE: MODERATE" :

(VulIN > 40 && VulIN <= 60 && Smax >= 50) ? "VULNERABILITY: MEDIUM / DAMAGE GRADE: VERY SEVERE"
:
```

```
(VulIN > 60 && VulIN <= 80 && Smax < 5.7) ? "VULNERABILITY: HIGH / DAMAGE GRADE: VERY SLIGHT" :

(VulIN > 60 && VulIN <= 80 && Smax >= 5.7 && Smax < 28.6) ? "VULNERABILITY: HIGH / DAMAGE GRADE: SLIGHT" :

(VulIN > 60 && VulIN <= 80 && Smax >= 28.6 && Smax < 42.9) ? "VULNERABILITY: HIGH / DAMAGE GRADE: MODERATE" :

(VulIN > 60 && VulIN <= 80 && Smax >= 42.9) ? "VULNERABILITY: HIGH / DAMAGE GRADE: VERY SEVERE" :



(VulIN > 80 && VulIN <= 100 && Smax < 5) ? "VULNERABILITY: VERY HIGH / DAMAGE GRADE: VERY SLIGHT" :

(VulIN > 80 && VulIN <= 100 && Smax >= 5 && Smax < 25) ? "VULNERABILITY: VERY HIGH / DAMAGE GRADE: SLIGHT" :

(VulIN > 80 && VulIN <= 100 && Smax >= 25 && Smax < 37.5) ? "VULNERABILITY: VERY HIGH / DAMAGE GRADE: MODERATE" :

(VulIN > 80 && VulIN <= 100 && Smax >= 37.5) ? "VULNERABILITY: VERY HIGH / DAMAGE GRADE: VERY SEVERE" :

"NOT APPLICABLE – CHECK INPUT DATA";
```

2. Code for classification of buildings damage degree according to maximum distortion angle along the building

```
// Input parameters

AngINC = beta;

VulIN = V;



// Damage classification based on angular distortion

Damageclass =

(VulIN <= 20 && AngINC < 0.002) ? "VULNERABILITY: IRRELEVANT / DAMAGE GRADE: VERY SLIGHT" :

(VulIN <= 20 && AngINC >= 0.002 && AngINC < 0.005) ? "VULNERABILITY: IRRELEVANT / DAMAGE GRADE: SLIGHT" :
```

(VulIN <= 20 && AngINC >= 0.005 && AngINC < 0.02) ? "VULNERABILITY: IRRELEVANT / DAMAGE GRADE: MODERATE" :

(VulIN <= 20 && AngINC >= 0.02) ? "VULNERABILITY: IRRELEVANT / DAMAGE GRADE: VERY SEVERE" :

(VulIN > 20 && VulIN <= 40 && AngINC < 0.0016) ? "VULNERABILITY: LOW / DAMAGE GRADE: VERY SLIGHT" :

(VulIN > 20 && VulIN <= 40 && AngINC >= 0.0016 && AngINC < 0.004) ? "VULNERABILITY: LOW / DAMAGE GRADE: SLIGHT" :

(VulIN > 20 && VulIN <= 40 && AngINC >= 0.004 && AngINC < 0.016) ? "VULNERABILITY: LOW / DAMAGE GRADE: MODERATE" :

(VulIN > 20 && VulIN <= 40 && AngINC >= 0.016) ? "VULNERABILITY: LOW / DAMAGE GRADE: VERY SEVERE" :

(VulIN > 40 && VulIN <= 60 && AngINC < 0.0013) ? "VULNERABILITY: MEDIUM / DAMAGE GRADE: VERY SLIGHT" :

(VulIN > 40 && VulIN <= 60 && AngINC >= 0.0013 && AngINC < 0.0033) ? "VULNERABILITY: MEDIUM / DAMAGE GRADE: SLIGHT" :

(VulIN > 40 && VulIN <= 60 && AngINC >= 0.0033 && AngINC < 0.013) ? "VULNERABILITY: MEDIUM / DAMAGE GRADE: MODERATE" :

(VulIN > 40 && VulIN <= 60 && AngINC >= 0.013) ? "VULNERABILITY: MEDIUM / DAMAGE GRADE: VERY SEVERE" :

(VulIN > 60 && VulIN <= 80 && AngINC < 0.0012) ? "VULNERABILITY: HIGH / DAMAGE GRADE: VERY SLIGHT" :

(VulIN > 60 && VulIN <= 80 && AngINC >= 0.0012 && AngINC < 0.0028) ? "VULNERABILITY: HIGH / DAMAGE GRADE: SLIGHT" :

(VulIN > 60 && VulIN <= 80 && AngINC >= 0.0028 && AngINC < 0.0114) ? "VULNERABILITY: HIGH / DAMAGE GRADE: MODERATE" :

(VulIN > 60 && VulIN <= 80 && AngINC >= 0.0114) ? "VULNERABILITY: HIGH / DAMAGE GRADE: VERY SEVERE" :

(VulIN > 80 && VulIN <= 100 && AngINC < 0.001) ? "VULNERABILITY: VERY HIGH / DAMAGE GRADE: VERY

```
SLIGHT" :

(VulIN > 80 && VulIN <= 100 && AngINC >= 0.001 && AngINC < 0.0025) ? "VULNERABILITY: VERY HIGH / DAMAGE GRADE: SLIGHT" :

(VulIN > 80 && VulIN <= 100 && AngINC >= 0.0025 && AngINC < 0.01) ? "VULNERABILITY: VERY HIGH / DAMAGE GRADE: MODERATE" :

(VulIN > 80 && VulIN <= 100 && AngINC >= 0.01) ? "VULNERABILITY: VERY HIGH / DAMAGE GRADE: VERY SEVERE" :

"NOT APPLICABLE – CHECK INPUT DATA";
```

3. Code to colour the terrain plate according to the settlement distribution

```
// Settlement value

z_val = -(Zi - dz - z);

// Color classification

color = (z_val < -25) ? Color.ByARGB(255,100,0,0) :

        (z_val >= -25 && z_val < -20) ? Color.ByARGB(255,255,0,0) :

        (z_val >= -20 && z_val < -15) ? Color.ByARGB(255,255,165,0) :

        (z_val >= -15 && z_val < -10) ? Color.ByARGB(255,255,255,0) :

        (z_val >= -10 && z_val < -5)  ? Color.ByARGB(255,0,255,0) :

                                        Color.ByARGB(255,0,100,255);
```